On the functional morphology and locomotion of the two-toed sloth (*Choloepus didactylus*, Xenarthra)

Dissertation zur Erlangung des akademischen Grades
Doctor rerum naturalium (Dr. rer. nat.)

Vorgelegt dem Rat der Biologisch-Pharmazeutischen Fakultät der Friedrich-Schiller- Universität Jena am 14.06.2010 von John A. Nyakatura (1. Staatsexamen für das Lehramt an Gymnasien) geboren am 19.09.1979 in Merseburg.

Gutachter:
Prof. Dr. Martin S. Fischer (Friedrich-Schiller-Universität Jena, Germany)
Prof. Dr. David R. Carrier (University of Utah, Salt Lake City, USA)
Prof. Dr. Sergio F. Vizcaìno (Universidad Nacional de La Plata, Argentina)

Datum der öffentlichen Disputation: 08.11.2010.

ACKNOWLEDGEMENTS

First and foremost I thank my supervisor Prof. Dr. M.S. Fischer for giving me the opportunity to do research on these fascinating animals.

This dissertation would not have been possible without the constant help of my colleagues. In particular I am indebted to my fellow PhD candidates, some of which - of course - already earned their degrees. I am grateful for the many enlightening discussions and practical support. I have listed the detailed acknowledgements at the end of each chapter.

Last but not least I want to thank my family for the encouragement and support to commence and finish this project.

“Of all mammals the sloths have probably the strangest mode of progression.”

Ruth A. Miller, anatomist (1935)

CONTENTS

- Chapter 1 -

GENERAL INTRODUCTION

The new framework for the investigation of the evolution of quadrupedal suspensory locomotion in sloths

Long before Ruth Miller stated "of all mammals the sloths probably have the strangest mode of progression" in 1935, the quadrupedal suspensory locomotion of sloths drew the interest of anatomists of the 18th and 19th century. Georges Cuvier (1798) early analyzed the anatomy of sloths in comparison to other mammals and grouped them with anteaters, armadillos, pangolins and the aardvark. Drawing on Cuvier's early work, others soon followed (Humphry, 1869; Mackintosh, 1873, 1874; Flower, 1882; Lucae, 1882; Windle and Parsons, 1899; Meincke, 1911).

Almost 30 years ago Frank Mendel published a series of papers that discuss different aspects of the functional anatomy of sloths in the context of 'upside down' posture and locomotion (Mendel, 1979, 1981a, 1981b, 1981c, 1985a, 1985b). Making use of the classic morphological approach he mostly deduced function from morphology, but also studied aspects of the locomotion of these American mammals *in vivo*. In his published findings he exquisitely and aptly describes the functional anatomy of the appendages (hands and feet) in two-toed sloths and his publications will remain a key reference for years to come.

It was a long held belief that there is a phylogenetic division between extant 'tree sloths' and extinct 'ground sloths'. After all, it was Sir Richard Owen himself who coined the term Gravigrada for 'ground sloths' to clearly distinguish them from the Tardigrada ('tree sloths') (Owen, 1842). But recent molecular phylogenetic studies that also include ancient DNA from fossil skin and dung remnants (Höss et al., 1996; Greenwood et al., 2001; Poinar et al., 2003) as well as phylogenetic studies based on morphologic comparison of extinct and extant sloth species (Gaudin, 2004; Pujos et al., 2007) suggest that modern sloths are only distantly related. It is thereby proposed that the three-toed sloth (*Bradypus*) is the sister taxon to all other known sloths (Gaudin, 2004; Fig. 1-1) and is not closely related to two-toed sloths (*Choloepus*). This hypothesis was first postulated by Patterson and Pascual at the 16th International Zoological Congress in 1963 (cited in Webb, 1985). Taking into account that no known fossil has been interpreted to have been suspensory (Webb, 1985; White, 1993;

McDonald and De Iuliis, 2008), it is parsimonious to assume a convergent evolution of the characteristic posture and locomotion of modern sloths.

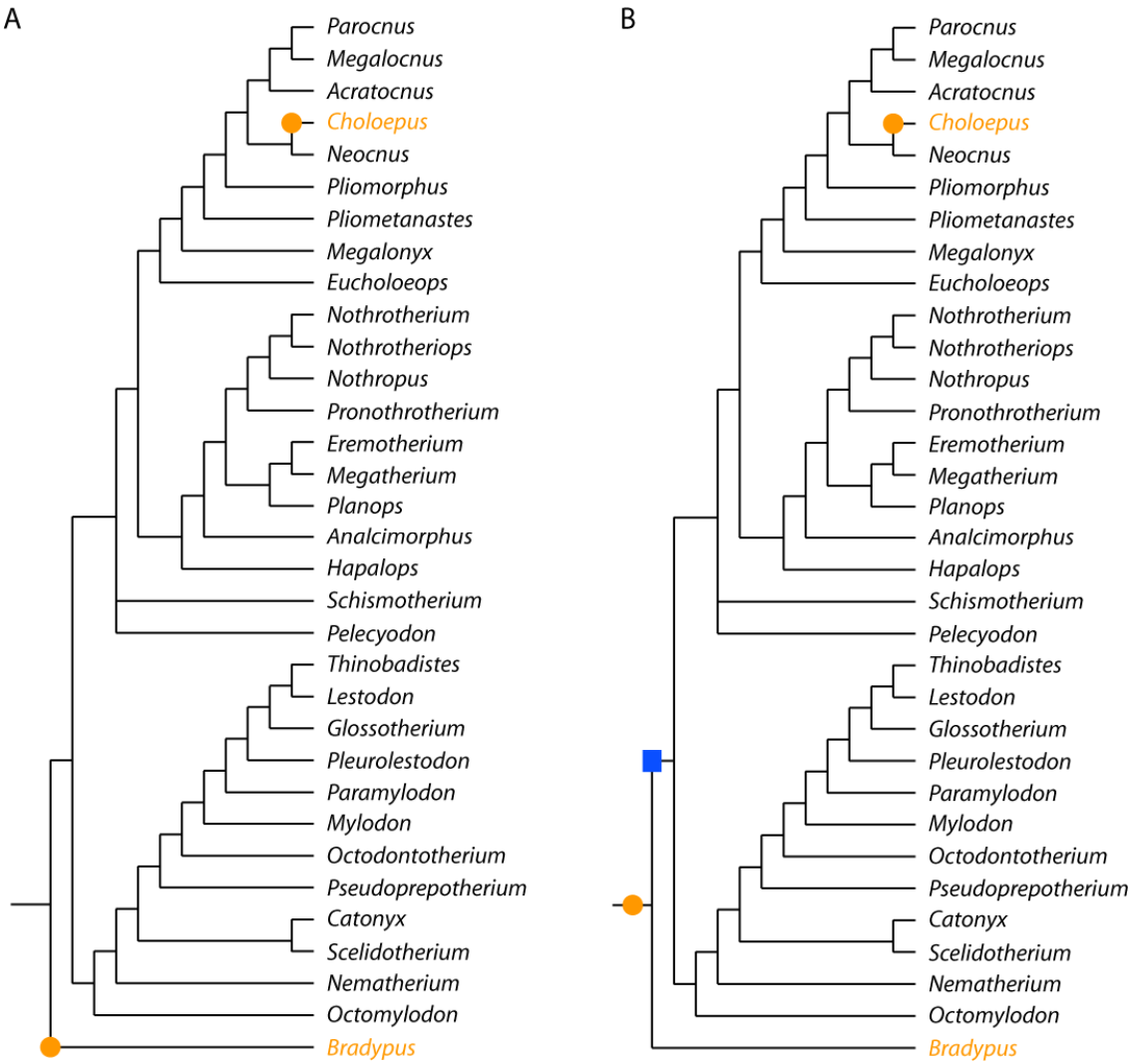

Fig. 1-1: Convergent evolution of suspensory quadrupedal posture and locomotion in sloths. Only orange genera are not extinct. No known fossil has been interpreted to have been suspensory. Orange circles depict the evolution of suspensory quadrupedal posture and locomotion; blue squares depict the loss of suspensory quadrupedal posture and locomotion. Scenario A requires just two evolutionary changes of the orientation of the body in regard of the force of gravity, whereas scenario B requires three. Both scenarios imply a convergent evolution of quadrupedal suspensory locomotion. Cladogram from Gaudin (2004).

These findings prompted Gaudin to call the obligatory suspensory posture and locomotion of both modern sloth genera "one of the most striking examples of convergent evolution known among mammals" (Gaudin, 2004). In light of this new phylogenetic framework previous work on sloth anatomy is even more appreciable. But questions remain to be answered, especially since most authors have hitherto concentrated on the more obvious characteristics of the appendages forming hook-like

claws (Jouffroy et al., 1962, Meincke, 1911, Mendel, 1981a, 1981b). In contrast to this, Fischer and co-workers have shown that it is the proximal limb elements that contribute the most to displacements of the hands and feet (Fischer et al., 2002; Fischer and Blickhan, 2006). The morphological adaptations of more proximal limb elements and differences to pronograde mammals in the kinematical pattern that are associated with the 'upside-down' posture and locomotion are poorly understood. An in-depth analysis of the locomotion and functional morphology in sloths offers the chance to better understand the convergent evolution of this peculiar posture and locomotion.

Analysis of a 'natural experiment'

Sloths, as the only extant example of true obligatory quadrupedal 'upside-down' posture and locomotion, also provide a 'natural experiment' to analyze the influence of gravity on the musculo-skeletal apparatus in mammals (Fig. 1-2). The kinematic pattern of limb movement has been shown to be highly conservative in quadruped therian mammals (Gasc, 2001; Fischer et al., 2002). It is not known to what extent kinematics are influenced by upside-down orientation of the body. Moreover, inverse orientation of the body towards the force of gravity suggests a series of related changes of the musculature with 'anti-gravity' functions that must have ramifications also for the pattern of neuromuscular control. However, comprehensive analysis of sloth locomotion and functional morphology to identify conservative traits and functional specializations in this context is lacking.

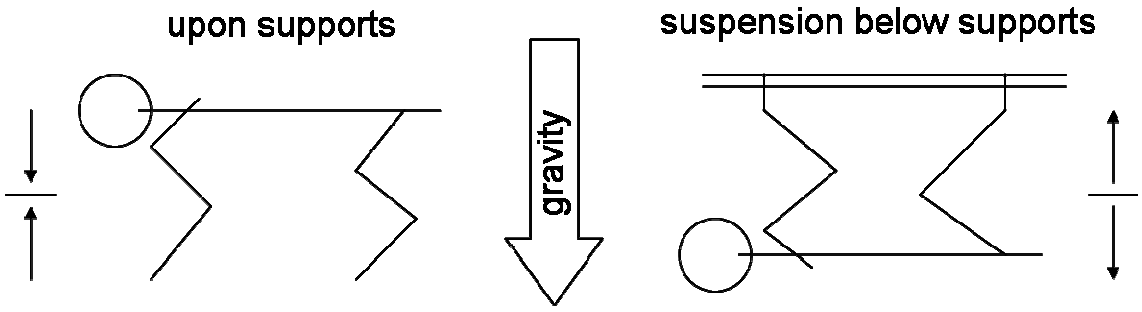

Fig. 1-2: The orientation of the body in relation to the gravity vector. When standing upon supports gravity provokes moments that flex the limb joints and extensors need to counteract flexion induced by gravity. When suspended below supports gravity provokes moments that extend limb joints and flexors can be hypothesized to counteract extension induced by gravity.

Investigating the form-function interface in an evolutionary context

Adaptation is a core concept in evolutionary argumentation (Bock, 1980).

According to Sudhaus (2006) there are different fields in morphological research that complement each other with regard to the proximate, ultimate or historic questions they try to answer. The author sees functional morphology to investigate proximate conditions and continues to state that to this end functional adaptations must be shown in the interaction of all parts in organismic constructions. This approach is in contrast to the ultimate conditions that were aspired to be identified in the so called 'adaptionist program' (e.g. Mayr, 1983), i.e. specific selective forces as causes for the evolution of observable adaptations. The adaptionist program has been heavily critized, most prominently by Gould and Lewontin (1979). Similar to these authors but earlier, Seilacher (1970) showed that any biological structure is not only determined by its adaptation to an (often largely) hypothetic biological role, but also by structural constraints (the main point of critique by Gould and Lewontin, 1979) and of course its evolutionary history. In short, the existence of form does not prove purpose (Nielsen, 2009). In addition, Gould and Lewontin (1979) argued that subdivision and separate analysis of morphological traits has led to an analytical 'atomization' of biological organisms, which restrained researchers from accounting for the premise that the concept of fitness is only attributable to whole individuals.

As a consequence authors became more hesitant to speculate on adaptive stories (Nielsen, 2009). Since then more emphasis has been laid on placing morphofunctional investigations onto a sound phylogenetic basis to be able to account for the evolutionary inheritance of structures. It has been argued that morphofunctional analyses should be connected to behavioral and ecologic studies that investigate the biological role of proposed adaptations by evaluating overall performance in the natural setting to account for the fact that selective forces can only act on the whole organism (ecological morphology, see Bock, 1980; Reilly and Wainwright, 1994). The analysis of the form-function interface can thus be argued to be consisting of three necessary analytical levels. First, potential morphological key innovations are identified usually by deducing possible function from classic morphological analysis. Second, after identification of a possible key innovation, whole-animal performance experiments should be undertaken in lab-based studies (Reilly and Wainwright, 1994).

Finally, field studies should complement and validate the laboratory based whole-animal performance experiments (e.g., Nyakatura and Heymann, 2010). However, the sequence of these analytical levels is interchangeable. For example, Schön Ybarra and Schön (1987) took field observations as the starting point for their morphological analyses on the primate locomotor apparatus. Moreover, the separate levels often represent individual studies and can therefore be conducted at different times and even by different authors.

The 'cladogenesis', i.e. the mere branching pattern of a phylogenetic hypothesis, can be distinguished from the 'anagenesis'. The latter is the processes between the nodes of a branching pattern (Fig. 1-3). While functional morphology can only contribute little to the pattern (but see Lauder, 1981), it is argued here that it can be helpful to reconstruct the process. Only evolutionary interpretation of the transformations and structural change between two adjacent nodes of a branching pattern make evolution comprehensible from a retrospective instead of a teleologic perspective (Sudhaus, 2006). For example, the evolutionary interpretation of the anagenesis needs to show how a certain structural change 'canalizes' or even determines the subsequent structural change (Sudhaus, 2006). An understanding of the morphofunction and biological role of a structure is a fundamental asset for this endeavor. Moreover, whereas apomorphies are in the centre of attention for phylogenetic reconstruction, convergent evolution offers a means to gain insight into the adaptive significance of a structure via functional analysis. In the case of convergent evolution of a trait, adaptive significance of this trait is implied. In other words, in convergent traits the existence of form renders purpose the most likely explanation.

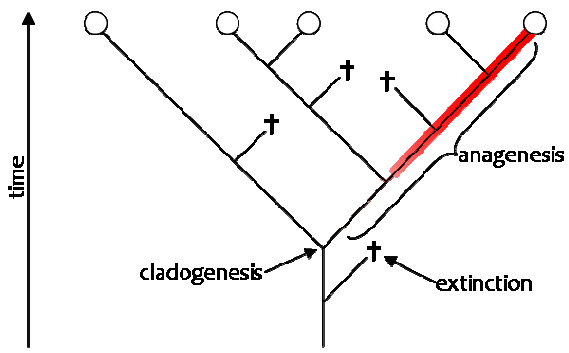

Figure 1-3: The processes of phylogeny. Modified from Sudhaus (2006). Within a cladogramm only an understanding of the 'anagenesis' makes evolution comprehensible from a retrospective perspective.

Aims and outline of the dissertation

This dissertation project was undertaken to improve the understanding of the functional morphology of the musculo-skeletal apparatus and the obligatory quadrupedal suspensory locomotion of the two-toed sloth. This knowledge can contribute to our understanding of (i) the convergent evolution of obligatory suspensory posture and locomotion in the two extant sloth genera and (ii), more generally, the influence of the gravitational force on the mammalian musculo-skeletal apparatus.

The author of this dissertation is acutely aware that it would have been preferable to undertake a comparative approach that would also include the three-toed sloth (*Bradypus* sp.) in the analysis. Unfortunately *Bradypus* cannot be kept in Europe, because of its very specific food requirements (basically one single plant: *Cercropia* sp.), which is restricted to Latin America (Superina et al., 2008). It was thus impossible to analyze the locomotion of three-toed sloths and the experimental analysis was restricted to *C. didactylus.* Analysis of both sloth genera was only possible on the anatomical level in dissections of specimens of both genera. The comparison of the anatomy of *Bradypus* and *Choloepus* with detailed knowledge of locomotor characteristics of the latter facilitates an evaluation of the functional morphology of *Bradypus* as well. In an effort to extend Mendel's investigation on the functional morphology of the distal limbs (Mendel, 1979; 1981a; 1981b; 1985), this dissertation lays emphasis on the functional morphology of the proximal limbs, the pectoral and pelvic girdles, and the body axis.

This is a cumulative dissertation. Each of the following 5 chapters was written to stand on its own as an independent publication. Some redundancy, for example in the methods sections, is unavoidable.

Chapter 2 is an in-depth analysis of overall locomotor characteristics in the two toed sloth. Unrestrained and steady-state locomotion are compared to infer speed related aspects of quadrupedal suspensory locomotion in two-toed sloths. Interlimb coordination, spatio-temporal gait parameters and limb kinematics are analyzed. The study represents a base-line study for the following chapters.

In Chapter 3 kinematic and morphological characteristics of the shoulder girdle are interpreted regarding their role during quadrupedal suspensory locomotion of *C.*

didactylus. 'Scientific rotoscoping' (SR) is used to investigate shoulder kinematics three-dimensionally (3D). SR is a new, non-invasive approach that combines high-speed x-ray videography and 3D reconstruction of skeletal elements (via CT bone scans) to visualize and measure 3D kinematics of skeletal structures.

Based on the 3D shoulder motion analysis, the muscular topography at the pectoral girdle is compared in *Bradypus* and *Choloepus* in Chapter 4. Extrinsic forelimb musculature topography is discussed in the context of the two main functions during locomotion for *C. didactylus*: (i) to protract and retract the forelimb and (ii) to suspend the weight of the thorax between both forelimbs. Then, the muscular topography is compared in both genera to identify possible convergent morphological solutions to the problems presented by the adoption of 'upside-down' posture and locomotion.

Chapter 5 then focuses on the functional morphology of the thoraco-lumbar spine and 3D intervertebral movements during locomotion that result in complex pelvic displacements and also influence the 3D kinematics of the femur. To achieve this, again SR was used.

Chapter 6 uses a biomechanical investigation for the functional interpretation of characteristics of the musculo-skeletal apparatus. Based on realistic parameterization of the sloth body, a mechanical link model was built and an inverse dynamic analysis was conducted to calculate limb joint torques and support reaction forces.

The individual contributions (chapters 2 to 6) are followed by a synopsis to summarize the evidence gathered and to formulate the conclusions of this dissertation (chapter 7).

Several methodical approaches were used to gain insight into the functional morphology of sloths. On the level of anatomical description macroscopic and also microscopic analysis was used. Skeletal morphology and the muscular topography of the shoulder of both sloth genera was formally described to facilitate morphofunctional interpretation of the locomotion analysis data and also to document differences between both extant genera. The sterno-clavicular articulation of *C. didactylus* was histologically stained to evaluate its characteristics and role during 'upside down' locomotion. The fascicle architecture of the epaxial muscles of *C. didactylus* was reconstructed to facilitate in-depth interpretation of the 3D locomotion analysis data. On the experimental level the locomotion of *C. didactylus* was also

analyzed with complementary techniques. First, standard light high-speed videos were used to assess spatio-temporal gait parameters and interlimb coordination. Second, a large dataset of biplanar high-speed x-ray videos was used to assess speed-related effects in intralimb kinematics. Third, SR was used to analyze the 3D excursions of the shoulder, pelvis and intervertebral movements. Finally, an inverse dynamics analysis was conducted to calculate moments acting on the limb joints during locomotion and to calculate substrate reaction forces that occur during locomotion of live sloths.

Hence, in this dissertation both inductive and hypothesis-driven reasoning was used. Instead of formulating overly simplified 'hypotheses' as starting points prior to initial investigation or – even worse – simply pretending to strictly conform to an hypothetico-deductive approach ("Here is the evidence, now what is the hypothesis?" Kell and Oliver, 2003), the investigation started with an interesting question (what are the consequences of upside down locomotion in sloths on the functional morphology of the locomotor apparatus?) and the results were compared to the data available for pronograde quadrupedal mammals in the literature. Thus, although being largely descriptive in nature, the initial investigation (chapter 2) was by no means the proverbial 'fishing experiment'. The extensive in-depth analysis of the locomotion allowed the formulation of more fine-grained expectations in the subsequent investigations (chapters 3 to 6).

OVERVIEW OF MANUSCRIPTS

Chapter 2

John A. Nyakatura, Alexander Petrovitch & Martin S. Fischer: Limb kinematics during locomotion in the two-toed sloth (*Choloepus didactylus*, Xenarthra) and its implications for the evolution of the sloth locomotor apparatus.

Zoology 113, 221-234.

JAN and MSF conceived of the study and contributed to the final manuscript. JAN took care of and trained the animals, designed and conducted the steady-state locomotion experiment and the standard light motion analysis, analyzed and interpreted all data, and drafted the manuscript. All authors conducted unrestrained locomotion experiment. MSF designed unrestrained locomotion experiment.

Chapter 3

John A. Nyakatura & Martin S. Fischer: Three-dimensional kinematic analysis of the pectoral girdle during upside-down locomotion of two-toed sloths (*Choloepus didactylus*, Xenarthra).

Frontiers in Zoology 7, Art. No. 21

JAN took care of and trained the animals, visited the museum collections, conducted all experiments, reconstructed bone models from CT scans, performed XROMM analysis, and drafted the manuscript. JAN and MSF conceived of the study, designed the experiments, dissected the cadavers, interpreted the data, and contributed to the final manuscript.

Chapter 4

John A. Nyakatura & Martin S. Fischer: Functional morphology of the muscular sling at the pectoral girdle in tree sloths: convergent morphological solutions to new functional demands?

Manuscript submitted to *Journal of Anatomy*.

JAN dissected the *Bradypus* specimen, and drafted the manuscript. JAN and MSF conceived of the study, dissected the *Choloepus* specimen, interpreted the data, and contributed to the final manuscript.

Chapter 5

John A. Nyakatura & Martin S. Fischer: Functional morphology and three-dimensional kinematics of the thoraco-lumbar spine of the two-toed sloth (*Choloepus didactylus*, Xenarthra).

Journal of Experimental Biology 213, 4278-4290.

JAN conceived of the study, took care of and trained the animals, designed and conducted all experiments, performed XROMM analysis, dissected the animals, and drafted the manuscript. JAN and MSF interpreted the data and contributed to the final manuscript.

Chapter 6

John A. Nyakatura & Emanuel Andrada: Inverse dynamic analysis aids interpretation of functional limb morphology and locomotor strategy of two toed sloths.

Manuscript to be submitted.

JAN conceived of the study, took care of and trained the animals, assessed body segment parameters, performed the x-ray motion analysis. EA conducted the inverse dynamic analysis. JAN and EA interpreted the data and contributed equally to the final manuscript.

I have read the authors' contributions stated above and confirm their correctness

Prof. Dr. Martin S. Fischer (supervisor)

- Chapter 2 -

Limb kinematics during locomotion in the two-toed sloth (*Choloepus didactylus*, Xenarthra) and its implications for the evolution of the sloth locomotor apparatus

John A. Nyakatura, Alexander Petrovitch & Martin S. Fischer

Abstract

To gain insight to the function of the extant sloth locomotor mode and its evolution, we conducted a detailed videoradiographic analysis of two-toed sloth locomotion (Xenarthra: *Choloepus didactylus*). Both unrestrained as well as steady-state locomotion was analysed. Spatio-temporal gait parameters, data on interlimb coordination, and limb kinematics are reported. Two-toed sloths displayed great variability in spatio-temporal gait parameters over the observed range of speed. They increase speed by decreasing durations of contact and swing phases, as well as by increasing step length. Gait utilization also varies with no strict gait sequence or interlimb timing evident in slow movements, but a tendency to employ diagonal sequence, diagonal couplet gaits in fast movements. In contrast, limb kinematics were highly conserved with respect to 'normal' pronograde locomotion. Limb element and joint angles at touch down and lift off, element and joint excursions, and contribution to body progression of individual elements are similar to those reported for non-cursorial mammals of small to medium size. Hands and feet are specialized to maintain firm connection to supports, and do not contribute to step length or progression. In so doing, the tarsometatarsus lost its role as an individual propulsive element during the evolution of suspensory locomotion. Conservative kinematic behaviour of the remaining limb elements does not preclude that muscle recruitment and neuromuscular control for limb pro- and retraction are also conserved. The observed kinematic patterns of two-toed sloths improve our understanding of the convergent evolution of quadrupedal suspensory posture and locomotion in the two extant sloth lineages.

INTRODUCTION

Basic kinematic patterns for fore- and hindlimb movements during symmetrical and asymmetrical quadrupedal locomotion have been published for a broad sample of mammals (e.g. Muybridge, 1887; Manter, 1938; Hildebrand, 1966; Miller and van der Meché, 1975; Hildebrand, 1977; Jenkins and Weijs, 1979; Goslow et al., 1981; Vilensky and Larson, 1989; Gasc, 1993; Fischer, 1994; Rocha-Barbosa et al., 1996; Robert et al., 1999; Schmitt, 1999; Fischer et al., 2002; Schmidt, 2005; Hutchinson et al., 2007; Day and Jayne, 2007; Schmidt, 2008). In principle, these patterns are independent of phylogenetic position, habitat, or anatomical variations from the 'standard mammal' (e.g., reduction or loss of digits or clavicle, presence or absence of long tails). In contrast to the sprawled limb configuration of reptiles and early mammals, which consists of only two propulsive elements (stylopodium and zeugopodium), the therian limb configuration comprises three propulsive elements and one contact element. A proximal element (scapula) was added to the forelimbs, and a distal element (tarsometatarsus) emerged as an individual propulsive element in the hindlimbs (Jenkins and Weijs, 1979; Kuznetsov, 1985, Fischer and Witte, 1998). In symmetrical gaits more than half of a limb's propulsive moment is produced by retraction of proximal elements (i.e., scapulae and femora). The theoretical prediction of an energy saving, self-stabilizing, three-segmented limb in zig-zag configuration with proximal and distal elements operating in matched motion (pantograph behaviour) throughout stance phase is largely fulfilled by therian mammals (Kuznetsov, 1995; Seyfarth et al., 2001; Hackert et al, 2006; Fischer and Blickhan, 2006). Proximal pivots operate at the same height, whereas distal joints predominantly adjust functional limb length to accommodate uneven supports (Fischer et al., 2002). To determine how widespread and adaptive these basic patterns are, non-quadrupeds and/or non-terrestrial species require investigation. This paper presents spatio-temporal gait characteristics and data on inter- and intralimb coordination for two-toed sloths (Xenarthra: *Choloepus didactylus*, Linné 1758) during quadrupedal suspensory locomotion.

Sloth anatomy has been studied extensively (Lucae, 1882; Wislocki, 1928; Britton, 1941; Jouffroy et al., 1962; Goffart, 1971; Mendel, 1979, 1981a, b, 1985a). However, with the exception of publications by Mendel concentrating on the autopodia (Mendel, 1981c, 1985b), locomotion-related hypotheses drawn from these descriptions have

rarely been tested experimentally. To date, no comprehensive analysis of spatio-temporal or kinematic data of sloth locomotor performance exists. For quadrupedal suspensory locomotion and postures to be energy efficient, a suite of related morphological adaptations were necessary. Two-toed sloths, unable to lift their trunks from the ground for extended time (Beebe, 1926; Britton, 1941; Mendel, 1981c), evolved hook-like autopodia as well as other adaptations of the musculoskeletal apparatus, especially of limb morphology (Lucae, 1882; Strauss and Wislocki, 1932; Miller, 1935; Jouffroy et al., 1962; Mendel, 1979; Mendel, 1981a, b; Mendel, 1985a). These include distal insertions of certain muscles (e.g. *m. brachioradialis* and *m. biceps femoris*) that morphologically maintain flexion of the limbs requiring activity of the extensors to overcome (Mendel, 1985a), and thus no activity of the flexors against the action of gravity to maintain a flexed limb posture. The morphological adaptations for a sloth-like posture and locomotion are, therefore, profound, a fact which is reflected by the minimal convergent evolution of this posture in other mammalian lineages, despite its benefits. Only extant lorises are able to move in a suspended quadrupedal posture similar to those of sloths (Ishida et al, 1990; Jouffroy and Petter, 1990; Jouffroy and Stern, 1990), although members of the subfossil strepsirhine primate family Palaeopropithecidae are argued to have had sloth-like quadrupedal suspensory postures (Jungers et al., 1991; Jungers et al., 1997).

Recent morphological (Gaudin, 2004; Pujos et al. 2007; Gaudin and McDonald, 2008) and molecular (Höss et al., 1996; Delsuc et al., 2001; Greenwood et al., 2001; Poinar, 2003, Delsuc and Douzery, 2008) analyses suggest that two- and three-toed sloths (genus *Bradypus*) are only distantly related, a hypothesis first put forward by Patterson and Pascual cited in Webb (Webb, 1985a). Hence their similar quadrupedal suspensory postures resulted from convergent evolution. *Bradypus* is argued to be either the sister group to all other extinct and extant sloths (Gaudin and McDonald, 2008) or, according to most molecular phylogenies, to be associated with the extinct megatherid sloths (Höss et al., 1996, Greenwood et al., 2001). *Choloepus* is regarded as a member of the Megalonychidae, a group comprised primarily of extinct ‘ground sloths’ from North America (McDonald and DeIuliis, 2008). Whatever the case, it is likely that suspensory quadrupedalism evolved independently in the lines leading to extant sloths.

The aims of this paper are to: (1) provide a detailed description of *Choloepus* locomotor kinematics in order to understand whether, and if so, how the quadrupedal suspensory locomotion of two-toed sloths deviates from the basic limb kinematics of therian mammals besides being inverted, (2) contribute to the understanding of the convergent evolution of suspensory posture and locomotion of sloths, and (3) provide a baseline study for further investigations of the musculoskeletal system of sloths.

MATERIALS AND METHODS

Study design and study subjects

We conducted two basic locomotion analyses. First, we analysed the unrestrained locomotion (1) of two-toed sloths to gauge speed-related aspects of spatio-temporal and kinematic parameters, and to determine a suitable speed range for a detailed kinematic analysis in the subsequent steady-state locomotion analysis (2). In both basic analyses we used high-speed standard light videography and videoradiography (see below). As an additional heuristic tool we developed an animated 3D model based on computer tomography reconstruction and kinematic data from videoradiography which made whole body skeletal motions visible from any desired perspective (Fischer et al., 2010).

(1) Unrestrained locomotion was filmed (a) using a PHOTRON Fastcam™-X 1024PCI (VKT GmbH, Germany) during daily habituation to assess spatio-temporal gait parameters and interlimb coordination and (b) using a biplane x-ray facility at the Klinik für Interventionelle und Diagnostische Radiologie of the university hospitals of Friedrich-Schiller-Universität Jena, Germany to assess speed-dependent effects of intralimb kinematics. During daily habituation sloths were filmed as they moved freely along a horizontal wooden pole 4.2 m long and 40 mm in diameter. Mendel (1981a, b) speculated that sloth locomotion was most efficient on supports of about this diameter. Locomotion was recorded at 125 frames per second (fps). The camera was positioned perpendicular to the direction of travel. Videoradiographic recordings from the lateral and dorso-ventral perspective were made at 30 fps as the sloths passed 40 cm and 28cm image intensifiers, respectively, at their own preferred speeds. Because the animals were large relative to the size of the image intensifiers, only parts of a limb moving through its step cycle could be recorded. However, we recorded sufficient

trials to obtain at least 30 shots of individual joints and elements at instants of touch down, mid-contact, lift off, and mid-swing to assess speed-related kinematic effects.

(2) In the steady-state locomotion analysis spatio-temporal gait parameters, interlimb coordination data, and intralimb coordination data were recorded simultaneously. We used the recently established high-speed videoradiography facility of our institute. The digital system is based on the high-end x-ray device Neurostar™ (Siemens AG, Germany), which we, in collaboration with Siemens, adjusted to our needs. It allows synchronous biplane videoradiographic recordings on two 40 cm image intensifiers and the recording of two additional synchronous standard light high-speed cameras. Sloth locomotion was recorded at 300 fps using maximum resolution (1536*1024 pixels). To ensure steady-state locomotion sloths were trained to move along a motorized 4 m long 'treadpole', the equivalent to an arboreal treadmill. The speed of the 'treadpole' was continually adjusted to keep the sloths in front of the image intensifiers for as long as possible. That is, 'treadpole' speed was adjusted to that preferred by the animals. Subsequently, only trials with speeds between 0.2 and 0.3 m/sec were analysed. Trials which were slower or faster than this were discarded, as were trials in which the subjects obviously braked or accelerated. The selected speed range (1) enabled sloths to stride uniformly and (2) was regarded to yield uniform kinematics upon analysis of the unrestrained locomotion analysis. Keeping the animals in front of the two image intensifiers with help of the 'treadpole' allowed us to simultaneously record the movements of the skeletal elements from dorsoventral and lateral perspectives. Videoradiographic recordings were made at 55 to 75 kV and 28 to 75 mA depending on thickness of the body region of interest and body properties of the subjects. Parallax was corrected by calibration of the recordings before data analysis. In addition to these 'anatomical close-ups', we used the synchronous standard light high-speed recordings to assess spatio-temporal gait parameters and interlimb coordination of the steady-state analysis. To this end one of the standard light cameras was positioned perpendicular to the 'treadpole'.

Three of four adult subjects available for the study were successfully trained to move on the different experimental setups. The training period necessary for the animals to get accustomed to the setups varied between subjects but generally was longest for the 'treadpole' setup (up to six months). Subject 1 (female, 7.3 kg, 84 cm snout vent

length (svl)) was wild caught and purchased from International Zoo Services. Subjects 2 (female, 10.6 kg, 87 cm svl) and 3 (male, 6.5 kg, 78 cm svl) were kindly loaned from Zoo Dortmund, Germany. All subjects appeared to be healthy with no abnormalities. The animals were cared for in accordance with the recommendations of Superina et al. (2008), and in strict adherence to German animal welfare regulations. All experiments were registered with the Committee for Animal Protection of the State of Thuringia, Germany. Unfortunately, subject 1 died unexpectedly of intestinal obstruction before the concluding steady-state locomotion analysis.

Analysed parameters

The following spatio-temporal gait parameters were calculated from high-speed video data: Step length (distance between the lift off and touch down positions of a limb measured at the distal phalangeal joint of the anterior phalange), stride duration (duration from touch down to subsequent touch down of a reference hindlimb), contact duration and swing duration. In unrestrained trials speed was measured by the distance the tip of the nose travelled during one stride and will be reported in meters per second (m/s). In steady-state trials 'treadpole' speed was additionally accounted for.

Interlimb coordination was analysed using the gait formula introduced by Hildebrand (1966). This formula comprises two dimensions. The first, diagonality (syn. limb phase, *D*) is the percentage of the stride interval a forefoot lags behind the touch down of the ipsilateral hindfoot. The second is duty factor (syn. relative stance phase duration, *S*), the percentage of the stride interval that a foot is in contact with the support. *D* facilitates the quantitative discrimination of diagonal sequences (DS; $D > 0.5$; footfall pattern: right hind (rh), left front (lf), left hind (lh), right front (rf)), lateral sequences (LS; $D < 0.5$; rh, rf, lh, lf), and allows further classification of gaits with help of video analysis (cf. Cartmill et al., 2002; Nyakatura et al., 2008): In a trot ($D \sim 0.5$) diagonal limbs have simultaneous swing and stance phases. Because two limbs will never swing perfectly in phase in a natural environment we concede slight deviations to an ideal trot (i.e., $0.45 < D < 0.55$). In diagonal couplet (DC) gaits, either in LS or DS, the swing and contact phase of diagonal limbs is closely related in time. Therefore DC gaits resemble a trot. Single foot (SF) gaits, again either in LS or DS, are characterized by

approximately even spaced footfalls in time. Whereas diagonality reflects spatial temporal coordination of the four limbs during locomotion, the duty factor provides information about the speed. Hildebrand (1966) defined running by a value for *S* of less than 0.5.

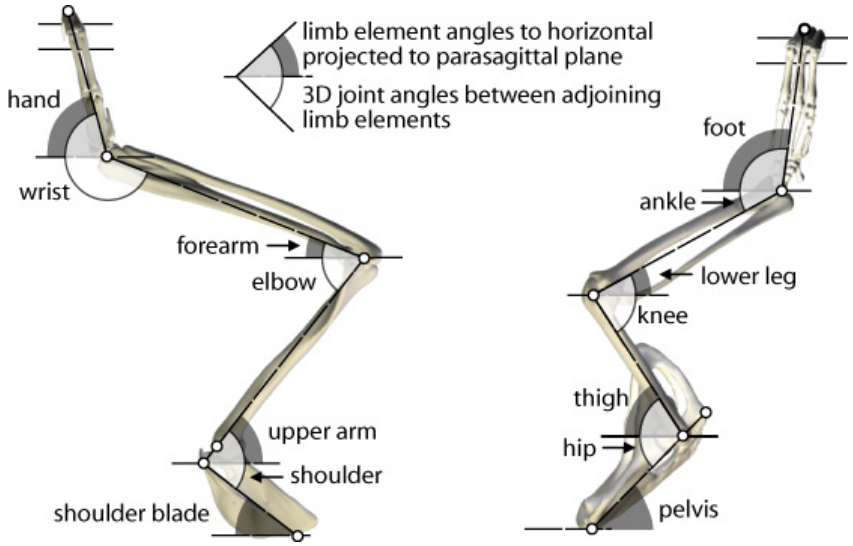

Fig. 2-1: Skeletal landmarks and calculated limb element and joint angles from the videoradiography locomotion analysis.

Anatomically defined limb joint angles were measured on the flexor sides of each joint, and limb element angles relative to the horizontal. Landmarks, joint angles, and element angles used for the kinematic analysis are shown in Fig. 2-1. Limb element angles were projected onto a parasagittal plane. Limb movements are not restricted to the parasagittal plane and since 2D approaches tend to overestimate elbow and knee angles if limbs are significantly out of plane (Stevens et al., 2006) we here report 3D joint angles obtained from biplanar videoradiographic analysis. Ongoing studies aim to quantify 3D excursions of skeletal elements during sloth locomotion to gain insight to their ability to navigate the complex 3D habitat. However, since 3D limb element data would not permit a comparison with existing 2D data from other mammals it would be beyond the scope of this article to include it here and will be presented elsewhere. Moreover, for the quantification of a limb element's contribution to stride length (see below) only displacements in the direction of travelling, i.e. the parasaggital plane, matter. Effective angular displacement (*EAD*), coefficient of stance phase (*CSP* - referred to in this publication as coefficient of contact phase to account for the

suspensory posture of sloths), and contribution of individual limb elements to step length were calculated following previously published methods (Fischer and Lehmann, 1998; Fischer et al., 2002). *EAD* is the difference between joint angles at touch down and lift off. The ratio of *EAD* to maximum joint excursion amplitudes during the contact phase gives the *CSP*, a measure of the role of a joint in adjusting functional limb length and thus for the contribution of a joint to limb compliance. The lower the *CSP* of a particular joint, the higher its yield during weight bearing. To assess how much the excursion of a limb element contributes to body propulsion or step length, the 'overlay method' (Fischer and Lehmann, 1998) was employed. This method considers that only angular movement of a limb element within its proximal adjacent joint and its pivot height determine its contribution to propulsion. Only for the most proximal limb element, the amplitude of excursion results exclusively from the actual motion of the element about its pivot. The amplitude of all more distal elements is a product of both their own actual motion and the passive displacement generated by the motion of the more proximal elements. The 'overlay method' can dissociate these two components of amplitude by overlaying the proximal element onto the next configuration (i.e. the next frame), without changing angles in the more distal joints. The difference between the horizontal excursion of a finger or toe tip at instant i (frame 1) and at instant i+1 (frame 2) is the horizontal distance caused by the movement of the element in question. The absolute contribution of each element to step length is given as the summation of all single-frame calculations. The contribution of the remaining elements to forward motion is calculated in the same way, except that the angular movement achieved by sagittal rotation of the more proximal elements is subtracted. Because no whole limb videoradiographic recordings were possible in this study, we used mean values instead of entire individual trials.

Data analysis

All videos were analysed using Simi® Motion 3D 7.5 motion analysis software (SIMI Reality Motion Systems GmbH, Unterschleissheim, Germany). After calibration of either 2D or 3D space the software can be used to obtain spatio-temporal gait parameters and data on interlimb coordination. In addition the software calculates intralimb kinematic data from manually digitized ('clicked') landmarks. High sampling

rates, ease of visualizing skeletal landmarks in videoradiographs, and relatively large skeletal elements fostered comparable accurate measurements. To test for accuracy, we determined the shoulder joint angle of the same trial at touch down on ten days of data analysis and found minimal deviation (mean touch down frame: 708.3 ± 0.95 (± s.d.) i.e., roughly ± 1/300 s; mean touch down angle: 114.345 ± 0.45°). To reflect this slight inaccuracy of measurement we decided to report element and joint angles as well as standard deviations rounded to full degrees. Data were exported to Microsoft Excel® and SPSS® for further analysis. To describe the curvilinear relationships of different gait parameters as a function of speed we performed a curve fitting estimation (Sokal and Rohlf, 1985) and tested ten mathematical models in SPSS (linear, logarithmic, inverse, quadratic, cubic, power, compound, S-curve, growth and exponential) in each parameter for fore- and hindlimbs, respectively. The model that yielded the highest coefficient of determination (r^2) will be reported. The relationship between intralimb kinematics and speed will be depicted by linear least squares regression lines in graphs.

RESULTS

Spatio-temporal gait parameters

Data for spatio-temporal gait parameters are reported in table 1. Contact phase duration varied considerably, ranging from 0.68 s to 17.44 s. (Fig. 2-2). On average, contact phase lasted twice as long as swing phase, which ranged from 0.19s to 4.54 s. Step length ranged from 0.21 m to 0.83 m.

Table 2-1: Spatio-temporal gait parameters of unrestrained and steady-state ('treadpole') locomotion.

	N	Contact duration (mean in sec ± s.d.)	Swing duration (mean in sec ± s.d.)	Stride length (mean in m ± s.d.)
Unrestrained locomotion (all trials)				
forelimb	205	2.57 ± 2.50	1.16 ± 0.48	0.59 ± 0.12
hindlimb	205	2.28 ± 2.27	1.33 ± 0.66	0.60 ± 0.13
Unrestrained locomotion (0.2 – 0.3 m/sec)				
forelimb	93	1.55 ± 0.33	1.02 ± 0.26	0.62 ± 0.10
hindlimb	93	1.32 ± 0.21	1.11 ± 0.31	0.63 ± 0.09
Steady-state locomotion (0.2 – 0.3 m/sec)				
forelimb	32	1.50 ± 0.20	0.84 ± 0.20	0.59 ± 0.05
hindlimb	32	1.66 ± 0.25	0.67 ± 0.15	0.60 ± 0.05

Speed-related aspects of spatio-temporal gait parameters. Mammals can increase velocity by increasing step length, stride frequency, or both. Stride frequency is the inverse of stride duration, which is determined by adding contact duration and swing duration. In fast mammalian locomotion, especially in asymmetrical gaits, an aerial phase is often introduced. The deliberate suspensory quadrupedalism of two- and three-toed sloths is limited to symmetrical gaits and aerial phases were never observed (Mendel, 1981c; Mendel, 1985b; this study). The velocity of two-toed sloth locomotion ranged from 0.02 m/sec to 0.47 m/sec. We found the relationship between contact phase and speed best described by a power function in the forelimbs and by an inverse model in the hindlimbs. Swing duration can be approximated as a function of speed with quadratic and cubic polynomial regressions, respectively (Fig. 2-2). Step length proved to be mathematically best approximated by power functions for both, fore- and hindlimbs. The analysis of unrestrained locomotion revealed that strategies to increase speed gradually change from slower to faster locomotion in sloths. In slower trials, contact duration and, to a lesser extent, swing duration decrease strongly with increasing speed, with step length only moderately increasing (Fig. 2-2). When increasing from moderate to higher speeds, a decrease in phase durations and an increase in step length contribute equally to increasing speed.

Comparison between unrestrained and steady-state locomotion. Spatio-temporal gait parameters during unrestrained and steady-state locomotion analyses followed the same basic pattern when the speed range of the steady-state analysis is considered (Fig. 2-2). However, as an artefact of the steady-state analysis on the motorized 'treadpole', we did document differences in hindlimb parameters. While the mean hindlimb contact duration was shorter than forelimb contact in unrestrained locomotion trials, it was the other way around in our steady-state analysis, resulting from longer hindlimb contact durations on the 'treadpole' (Table 2-1). In unrestrained locomotion, mean hindlimb swing phase was longer in duration than forelimb swing phase, whereas it was vice versa in the steady-state trials. This effect can be attributed to shorter overall hindlimb swing durations on the motorized 'treadpole' than during unrestrained locomotion (Table 2-1). For all spatio-temporal gait parameters we obtained lower standard deviations, i.e., higher uniformity, for steady-state trials. The

mean stride duration of in steady-state trials was 3.08 s, with a mean contact phase duration of 2.278 ± 0.09 s, and a mean swing phase duration of 0.792 ± 0.03 s.

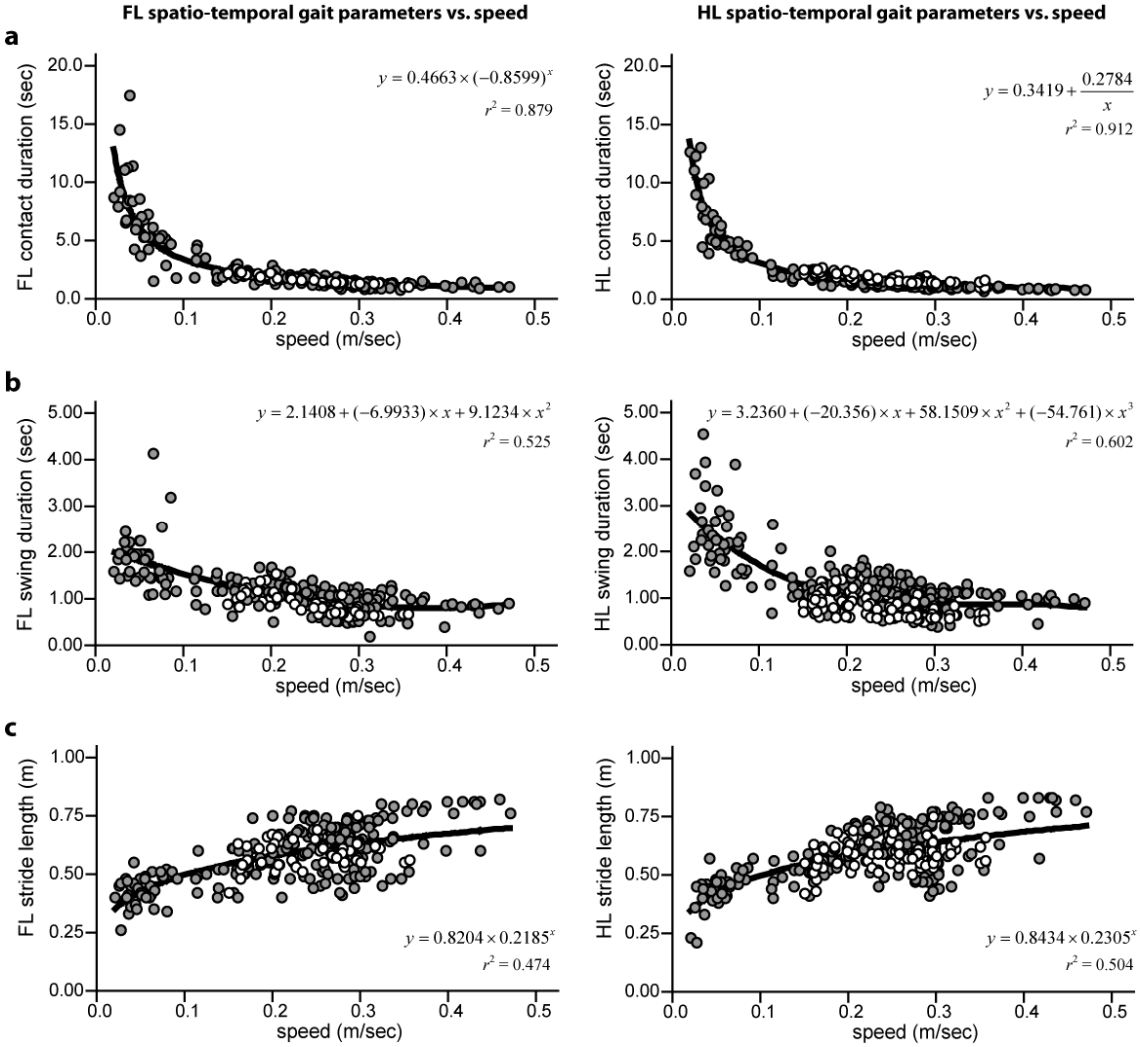

Fig. 2-2: Spatio-temporal gait parameters (*y*) as a function of speed (*x*). Left side: Forelimb (FL); right side: hindlimb (HL). a: contact duration vs. speed; b: swing duration vs. speed; c: step length vs. speed. Grey: unrestrained locomotion trials; white: steady-state 'treadpole' trials. Model for best fit curvilinear regression and coefficient of determination (r^2) provided in each graph.

Interlimb coordination

Two-toed sloth locomotion is characterised by a remarkable level of variability in interlimb timing, so various lateral sequence and diagonal sequence gaits were observed (Fig. 2-3). This is reflected in the wide range of values for diagonality ($0.17 < D < 0.80$; n = 195). The best fit curve estimation reveals that diagonality tends to be higher during faster sloth locomotion (i.e., when *D* is small) and DS gaits are utilized at a higher rate. Moreover, the variability of *D* decreases when *S* approximates 0.5 as can

be seen from the graph (Fig. 2-3). The duty factor quantifies the sloths' obvious inability to employ aerial phases during locomotion (range from *S* = 0.51 to *S* = 0.89). In faster trials, however, it was often close to 0.5 and the bilateral support of a limb pair was brief (Fig. 2-3).

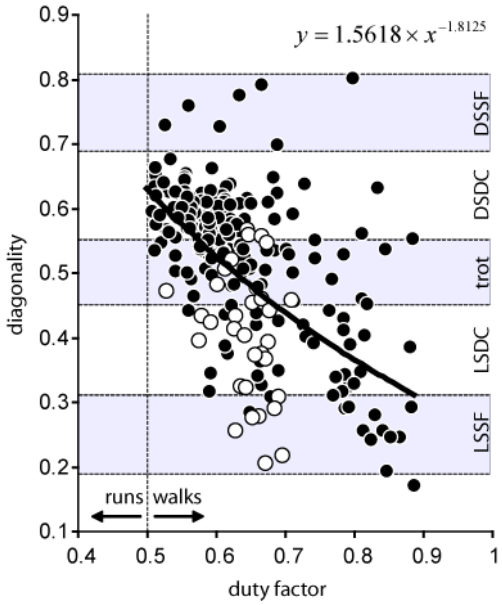

Fig. 2-3: Modified Hildebrand diagram of diagonality plotted against duty factor. Black: unrestrained locomotion trials; white: steady-state 'treadpole' trials. LSSF: lateral sequence, single foot gait; LSDC: lateral sequence, diagonal couplet gait; DSDC: diagonal sequence, diagonal couplet gait; DSSF: diagonal sequence diagonal couplet gait. Model for best fit curvilinear regression indicates that diagonality tends to be higher in faster locomotion. For explanation of gaits see text. Note that in fastest trials (duty factor < 0.55) almost exclusively DS gaits are utilized.

Intralimb coordination

Speed-related aspects of intralimb coordination. Figures 2-4 and 2-5 illustrate the relationship between speed and particular fore- and hindlimb kinematic parameters. In unrestrained locomotion, forelimb movement is almost independent of speed, as indicated by the regression lines of the touch down and lift off angles as well as of the angles at mid-contact and mid-swing for each limb element and joint. The touch down angles of the upper arm and shoulder joint increase with increasing speed, and become less variable, accompanied by a slight decrease in the scapular angle relative to horizontal. Hands are approximately perpendicular to supports throughout contact phase, and wrist excursions are not speed-related. During slow progression two-toed sloths often assume a more crouched position with their noses close to supports, a locomotor posture we term 'exploratory gait'. This posture results predominantly from

pronounced flexion of shoulders and elbows (Fig. 2-5, 2-6) with a corresponding negatively inclined upper arm. This gait is further characterised by more variable spatio-temporal parameters and interlimb coordination and by halting and deliberate steps. The greater touch down angles of shoulders in faster trials, termed 'travelling gait', result in more protracted and extended arms and lead to increased step lengths (Fig. 2-8). However, these 'gaits' are qualitative descriptions of the two ends of a spectrum rather than hard definitions, because transition from one 'gait' to the other is fluent.

Movement of hindlimbs is more uniform than that of forelimbs, as illustrated in figures 4 and 5. Angles of distal hindlimb elements and joints in particular hardly change with speed. Increased step lengths in faster trials result mainly from increased retraction of femora and increased hip extension. The crouched posture of the forelimbs in 'exploratory gaits' is not paralleled in the hindlimbs. As a result, whole body posture is tapered in 'exploratory gaits' and more rectangular when 'travelling' (Figs. 2-6, 2-8).

Limb kinematics during steady-state locomotion. The speed range in the steady-state analysis fell within the observed speed range of the unrestrained videoradiographic analysis. The absence of dramatic speed-related effects over a wide range of speeds observed in unrestrained locomotion trials allowed us to combine kinematic data of different body regions from the narrow speed range of the 'treadpole' trials in the steady-state locomotion analysis. The sloths displayed only the faster 'travelling gait' during steady-state locomotion.

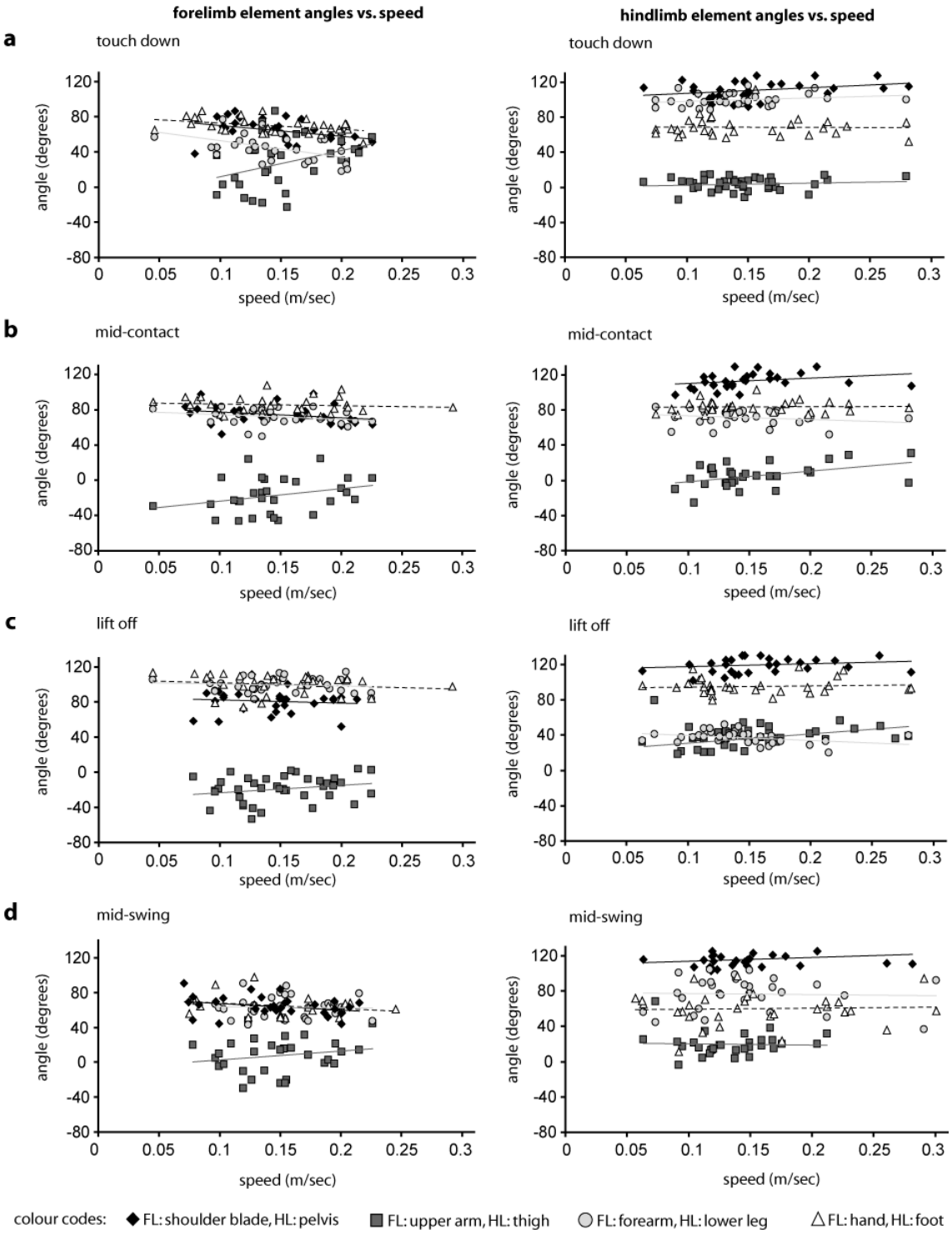

Fig. 2-4: Limb element angles plotted versus speed. Data for all trials of unrestrained videoradiographic locomotion analysis. Left: forelimb; right: hindlimb. a: touch down; b: mid-contact; c: lift off; d: mid-swing. Least squares linear regression lines are depicted for each segment for analysed instants of the step cycle.

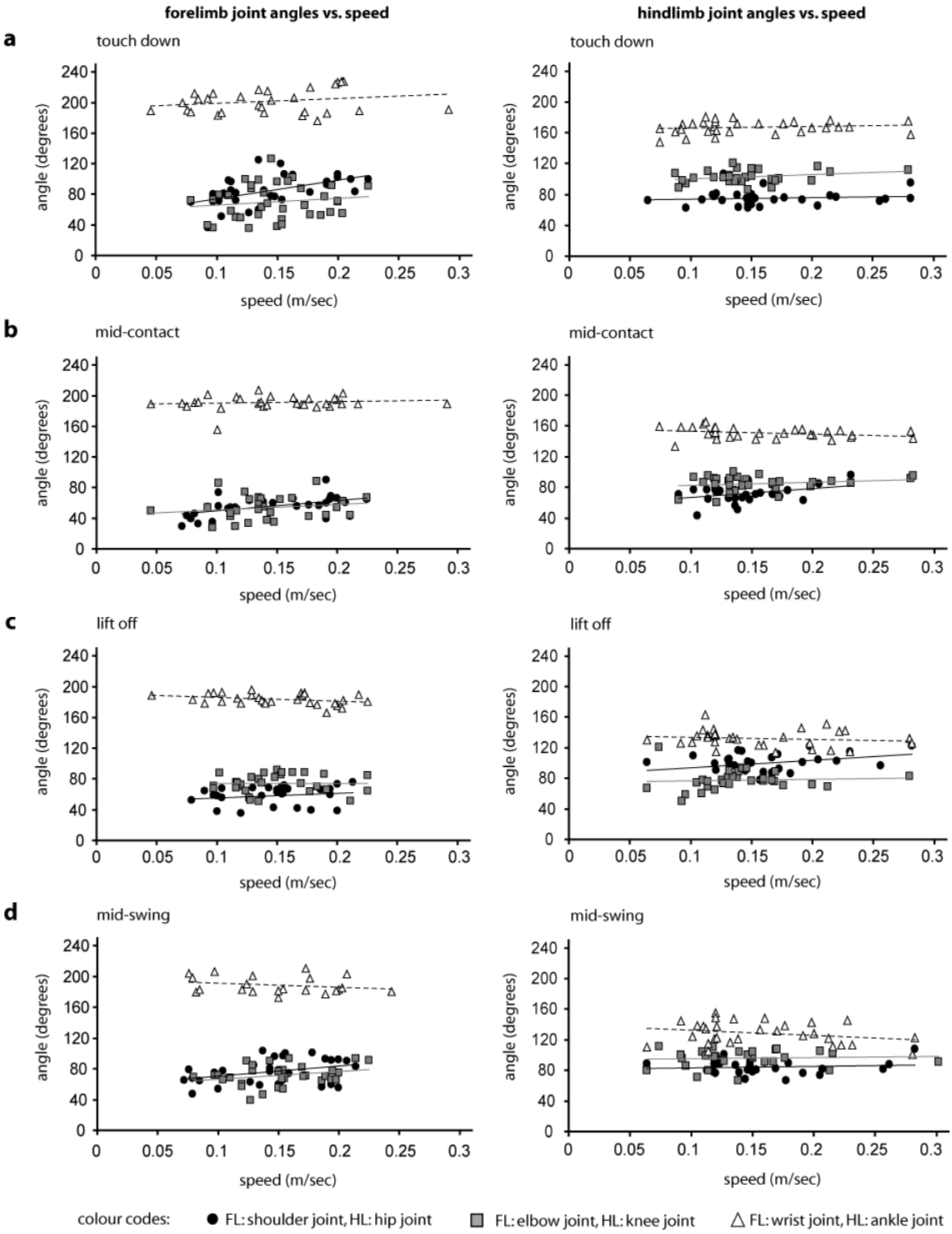

Fig. 2-5: Joint angles plotted versus speed. Data for all trials of unrestrained videoradiographic locomotion analysis. Left: forelimb, right: hindlimb. a: touch down; b: mid-contact; c: lift off; d: mid-swing. Least squares linear regression lines are depicted for each joint for analysed instants of the step cycle.

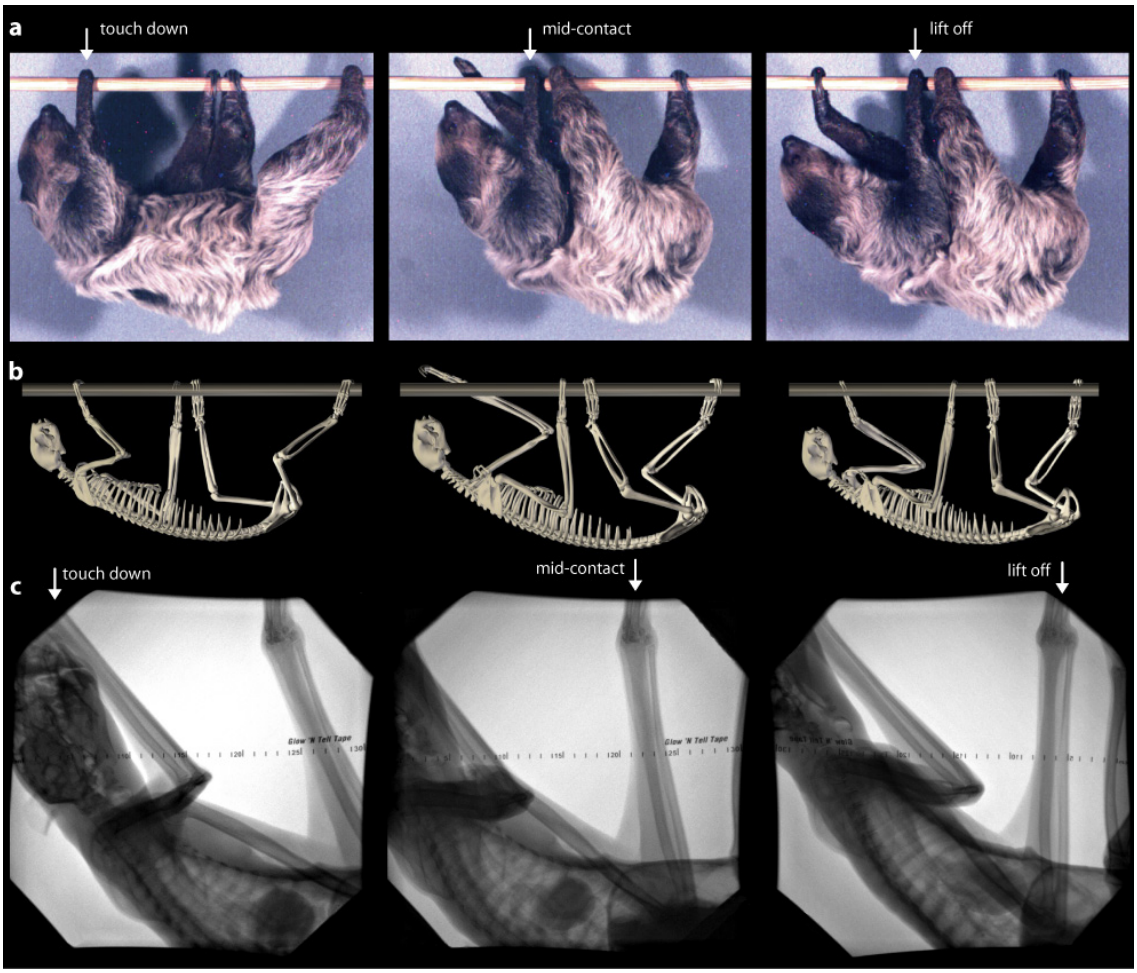

Fig. 2-6: Representative frames from standard light high-speed video, animation, and videoradiography of forelimb kinematics in the 'exploratory gait'. a: high speed video; b: animation composed of several videoradiographic trials covering different areas of the body makes whole body skeletal movements visible; c: videoradiographs to demonstrate scapular and humeral retraction in the parasagittal plane during contact phase. Note the 'crouched' posture due to retracted scapula (almost vertical position of spina scapulae in touch down position), strong shoulder joint and elbow flexion.

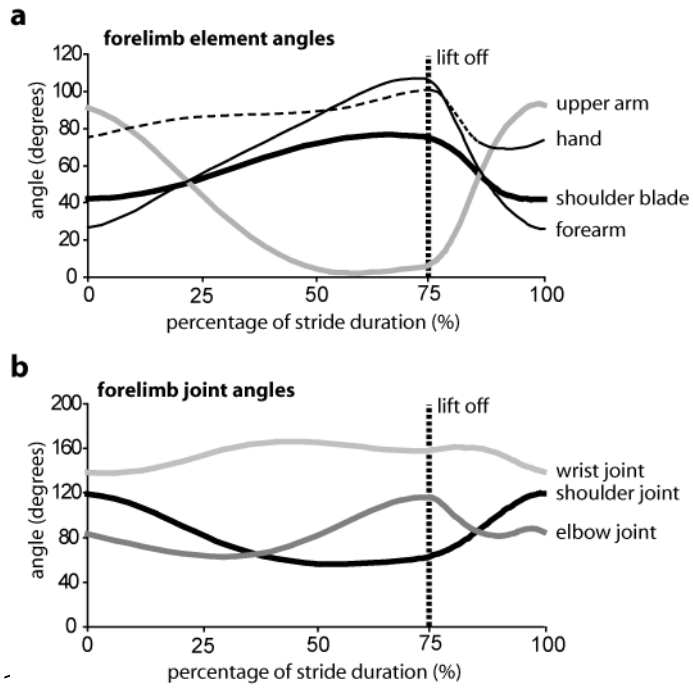

Fig. 2-7: Mean values of forelimb element angular excursions in 'travelling gait' (steady-state locomotion analysis). a: forelimb element angles; b: forelimb joint angles.

Limb displacements mainly consist of retraction during contact phase and protraction during swing phase. Retraction of forelimbs starts immediately before touch down at 96% of the previous cycle (scapular and arm retraction; Fig. 2-7). At forelimb touch down, scapulae have a mean angle of 42 ± 5°. From this oblique position they rotate caudally and reach a mean lift off angle of 76 ± 4°. Scapular craniocaudal rotation alone contributes about 50% of step length due to its position at the proximal pivot of the limb, which, as an instantaneous centre, is located close to the vertebral border (Table 2-2). Upper arms are nearly vertical at touch down, and subsequently retract to nearly horizontal during contact phase. This movement is completed by about 60% of contact phase, and there is no more motion in the shoulder joint until lift off (Fig. 2-7, 2-8). The high excursion amplitude of arms results in a 72% contribution to step length. Forearms have a mean angle of 27 ± 11° at forelimb touch down. Retraction during contact leads to a mean lift off angle of 107 ± 5°. Most of this high excursion results from passive displacement of forearms by movements of more proximal elements. Due to flexion of elbows, the motion of forearms actually shortens step lengths, especially in the first part of contact phase before elbows are extended (Fig. 2-10). Thus, forearms have an overall negative contribution to step length. Because hands are held perpendicular to supports, they too do not contribute positively to step length.

The negative values of distal elements are compensated for mainly by upper arms (Fig. 2-10, Table 2-2).

Table 2-2: Kinematic parameters of limb element and joint angles. Note that for distal elements and joints it was not possible to obtain the amplitude for an entire stride cycle due to the size restriction of the x-ray image intensifier (depicted by *). In place of these values, mean amplitudes for distal elements are reported.

	Touch down angle (degrees)			Mid-contact angle (degrees)			Lift off angle (degrees)			Amplitude contact phase (degrees)	Contribution to step length (%)	*EAD*	*CSP*
	mean	range	N	mean	range	N	mean	range	N	mean	mean	mean	mean
Forelimb elements													
Shoulder blade	42 (± 5)	33 - 52	20	59 (± 7)	53 - 74	20	76 (± 4)	74 - 85	20	41.5	49.8	-	-
Upper arm	91 (± 10)	75 - 108	20	27 (± 16)	7 - 45	20	5 (± 9)	-4 - 20	20	98.1	72.4	-	-
Forearm	27 (± 11)	12 - 39	33*	65 (± 7)	52 - 77	31*	107 (± 5)	104 - 119	36*	92.3	-1.5	-	-
Hand	75 (± 4)	69 - 78	40*	87 (± 2)	81 - 93	40*	100 (± 6)	94 - 107	40*	36.8	-20.7	-	-
Forelimb joints													
Shoulder	119 (± 13)	101 - 148	20	67 (± 12)	53 - 85	20	61 (± 11)	45 - 76	20	75.1	-	58.3	0.78
Elbow	83 (± 8)	76 - 97	37*	65 (± 11)	49 - 82	32*	116 (± 11)	111 - 135	34*	52.6	-	32.4	0.62
Wrist	138 (± 10)	123 - 158	35*	162 (± 3)	148 - 169	40*	157 (± 7)	145 - 163	33*	28.1	-	18.9	0.67
Hindlimb elements													
Pelvis	47 (± 6)	40 - 50	20	42 (± 4)	35 -47	20	45 (± 4)	38 - 50	20	8.5	8.4	-	-
Thigh	37 (± 5)	23 - 47	20	55 (± 6)	43 - 63	20	103 (± 6)	96 - 112	20	75.7	134.8	-	-
Lower leg	94 (± 13)	75 - 108	40*	64 (± 7)	45 - 73	38*	41 (± 10)	28 - 48	40*	53.4	-17.8	-	-
Foot	73 (± 5)	57 - 78	36*	87 (± 3)	82 - 91	35*	88 (± 4)	77 - 100	34*	17.8	-25.4	-	-
Hindlimb joints													
Hip	64 (± 8)	51 - 71	20	91 (± 4)	84 - 99	20	127 (± 6)	121 - 130	20	65.4	-	62.7	0.96
Knee	111 (± 6)	104 - 122	38*	92 (± 9)	80 - 109	40*	127 (± 11)	86 - 138	40*	47.5	-	16.9	0.36
Ankle	171 (± 6)	156 - 184	35*	140 (± 7)	128 - 154	33*	142 (± 7)	125 - 156	37*	37.3	-	29.2	0.78

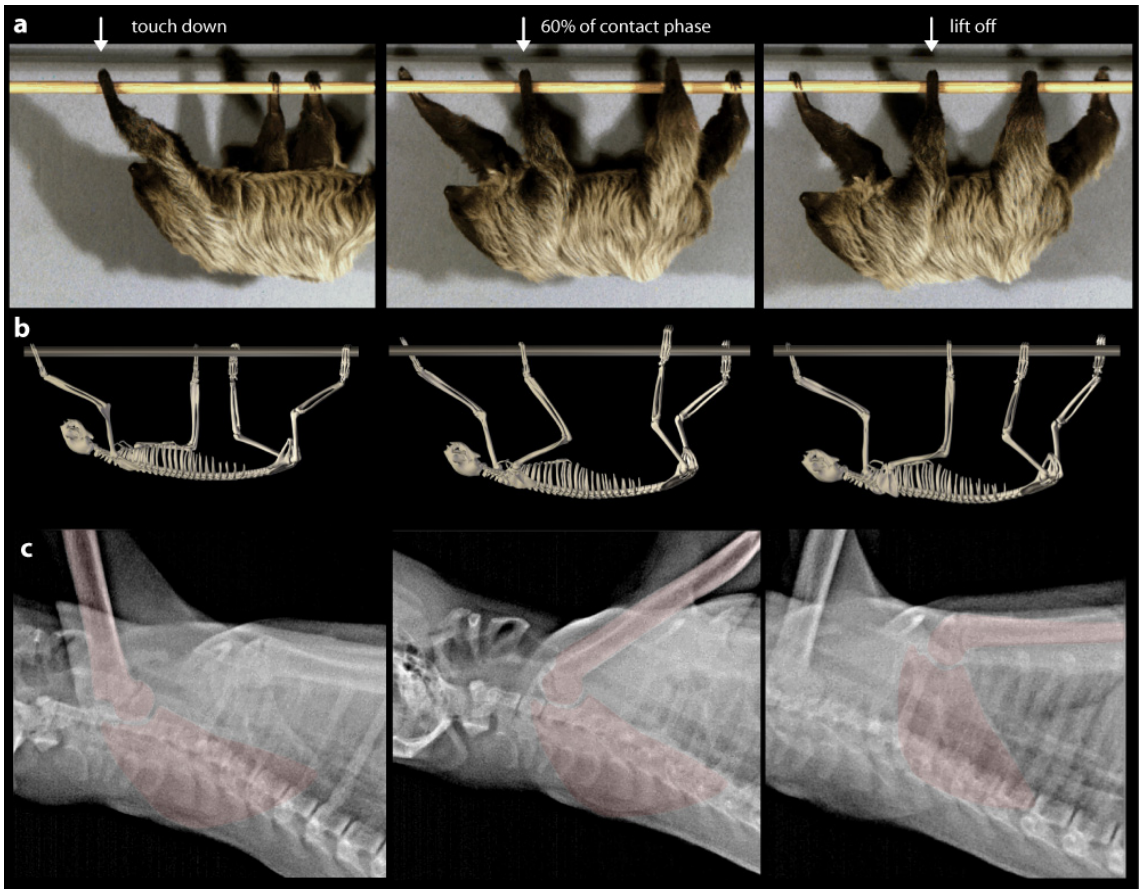

Fig. 2-8: Representative frames from standard light high-speed video, animation, and videoradiography of proximal forelimb kinematics in the 'travelling gait'. a: high speed video; b: animation composed of several trials makes whole body skeletal movements visible; c: videoradiographs to demonstrate scapular and humeral retraction in the parasagittal plane during contact phase. Left column: right forelimb touch down; middle column: flexion of shoulder joint is completed at about 60% of contact phase; right column: right forelimb lift off. Note that after completion of shoulder joint flexion scapular retraction continues until lift off. Overall mobility of the pectoral girdle is indicated by the position of the highlighted shoulder joint in comparison to the contralateral shoulder joint. Hands and feet are held approximately perpendicular to the support throughout contact phase.

Forelimb joint excursions reflect the role of forelimb elements in contributing to step length. Shoulder joints are extended to almost 120 ± 13° on average at forelimb touch down, and are subsequently flexed to a mean lift off angle of 61 ± 11° (Fig. 2-7). However, flexion of this joint is completed by about 60% of contact phase, and further retraction of arms is implemented exclusively by scapular retraction. At 0.78 the coefficient of contact phase of the shoulder joint reveals its predominant role for progression (Table 2-2). More distal forelimb joints have lower CSP values, indicating their predominant role in adjusting functional limb length.

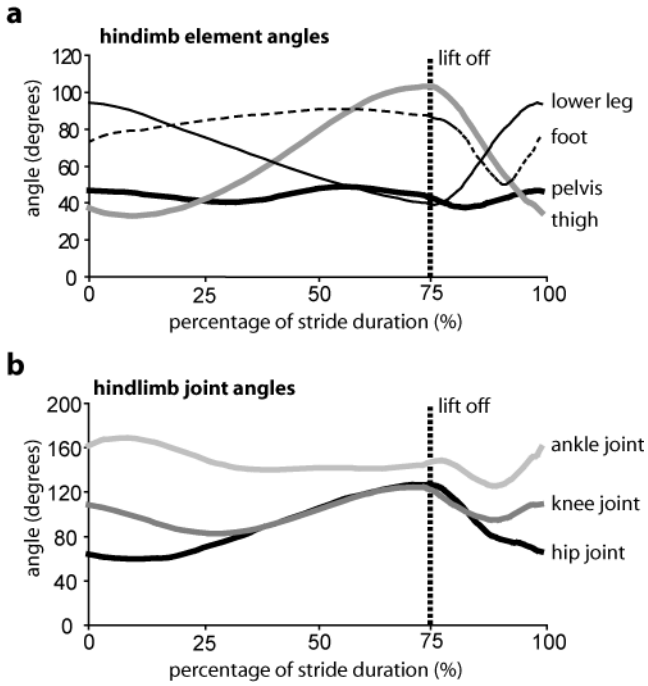

Fig. 2-9: Mean values of hindlimb element angular excursions in 'travelling gait' (steady-state locomotion analysis).

Pelvic displacements result solely from additive intervertebral movements. 'Pelvic movements' consisting of lateral bending, tilting and sagittal bending (Jenkins and Camazine, 1977; Schilling and Fischer, 1999) result in craniad and caudad translation of the hip joints which is relevant in body progression. The course of pelvic motion is always influenced by movements of both hindlimbs. We thus observed biphasic movements during contact phases of each limb (Fig. 2-9). At touch down of a considered hindlimb the pelvis is protracted. Retraction then lasts until the contralateral hindlimb lifts off the support. This is followed by a new cycle of pelvic protraction until the contralateral hindlimb touches down and another retraction lasts until lift off of the considered hindlimb. Sagittal pelvic movements contribute about 8-9% of step length mainly through craniad translation of hip joints (Fig. 2-10; Table 2-2). Femora have a mean touch down angle of 37 ± 5°. During contact phase femora are retracted to a mean lift off angle of 103 ± 6°. This high excursion contributes more than 130% to step length, i.e., it compensates for the de facto negative influence of the more distal elements (Fig. 2-10). Lower legs have a mean angle of 94 ± 13° at hindlimb touch down and 41 ± 10° at lift off. Calculated contribution to step length is -17%. Like the hands, feet are held at approximately 90° throughout contact phase (Fig. 2-9). This

precludes positive contribution to step length reflected by its mathematical contribution of -25%.

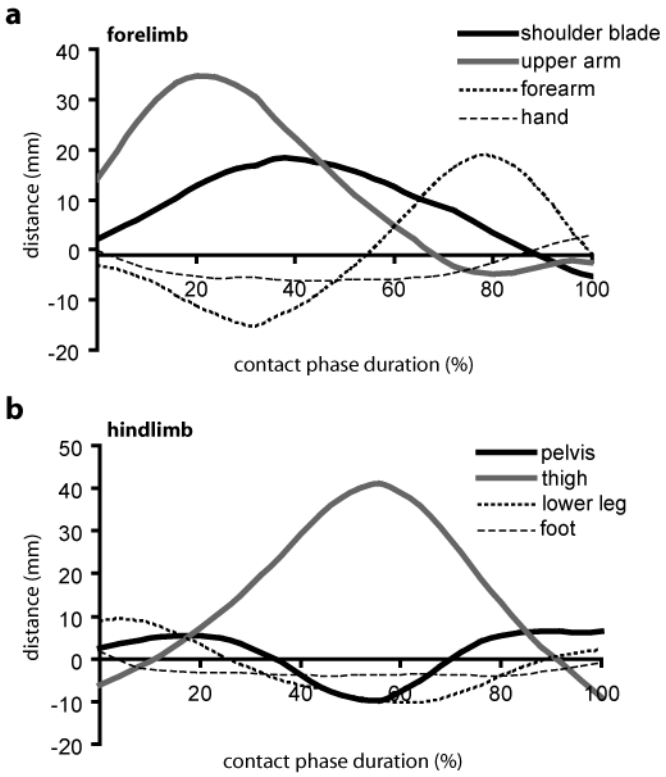

Fig. 2-10: Absolute contribution to step length as distance travelled by a: forelimb elements and b: hindlimb elements as a result of extension of the proximal adjoining joint plotted against percentage of contact phase duration ('travelling gait' of steady-state locomotion analysis).

Angular excursion of the hips reflects the dominant role of the femora for generating step length. At touch down, hip joints have a mean angle of 64 ± 8° and are subsequently extended to 127 ± 6° until lift off (Fig. 2-9). The joint's CSP value is 0.96 (Table 2-2), i.e., almost the entire hip excursion is used for progression. Knees have similar angles at touch down and lift off (110° vs. 127°), and thus the mean excursion of 17° during contact phase, reflected by a CSP value of just 0.36, contributes little to propulsion. Ankles, like wrists, serve to position feet perpendicular to supports and facilitate movements of the limb out of the parasagittal plane. Its relatively high value of CSP reflects its limited role in contributing to limb compliance.

DISCUSSION

Speed-related aspects of two-toed sloth locomotion

Previous studies on various mammalian taxa have shown that mammals generally increase velocity within symmetrical gaits by increasing stride frequency (mainly by reducing contact phase), and often, to a lesser extent, by extending step length on terrestrial and arboreal supports (e.g. Howell, 1944; Hildebrand, 1966; Goslow et al., 1973; Alexander, 1981; Vilensky, 1983; Heglund and Taylor, 1988; Demes et al., 1990; Cartmill et al., 2002; Schmidt, 2008). However, Pennycuick (1975) reported that several ungulates increased velocity by extending step length while maintaining constant stride frequency. Swing duration is generally regarded to be more constant (Goslow et al., 1973), but a significant reduction of swing phase has recently been documented in mice (Herbin et al., 2004), dogs (Maes et al., 2008), horses (Robilliard et al., 2007), and elephants (Hutchinson et al., 2006). In our study two-toed sloths displayed every possible strategy for increasing speed (fastest trials being over 20 times faster than slowest trials). Decrease of contact and swing durations was more important for increasing speed during slower progression, but in order to increase relatively fast progression extending step length became similarly important. Our observations concur with those of Demes and colleagues (Demes et al., 1990) who note that lorises increase tempo of limb protraction during swing phase and are thus able to increase speed without shortening support phase. This may be related to similar deliberate locomotor behaviour and the avoidance of aerial phases in lorises (Jouffroy and Petter, 1990; Demes et al., 1990) and sloths. In the fastest trials observed duty factor of sloths was only slightly above 0.5. Further reduction of contact phase with constant swing duration would result in an aerial phase, and yet further increase in speed via temporal parameters is possible only by reducing swing phase as well.

Unlike the highly variable spatio-temporal gait parameters, intralimb coordination was not related to speed (with exceptions relating to an increase in stride length, see below). Independence of intralimb coordination and speed within symmetrical gaits was also observed in small mammals (Fischer et al., 2002), dogs (Maes et al., 2008), and quadrupedal primates (Courtine et al., 2005; Schmidt, 2008). Extended stride length, i.e., the increase of total limb angular excursion, in faster sloth trials results from increased protraction of proximal elements in forelimbs, and increased retraction

of thighs in hindlimbs. In 'exploratory gaits' noses are drawn close to supports by a combination of scapular retraction, strong shoulder flexion, and increased elbow flexion. Steps are short and arms are not protracted beyond heads. Obviously, forelimb configuration during 'exploratory gaits' is more of an accommodation to a crouched body posture than to locomotion. However, not all of the slowest trials are 'exploratory'. Some slow trials were similar to faster trials in terms of intralimb coordination.

Interlimb coordination and arboreal locomotion

Arboreal mammals usually utilize diagonal couplet gaits, often in combination with diagonal sequence (syn. 'forward cross type') footfall patterns during locomotion on small diameter supports (relative to thorax diameter). This distinct locomotor pattern was first documented for primates by Muybridge (1887) and scientifically described by Hildebrand (1966, 1967) and Tomita (1967). Later it was also found to pertain to arboreal australodelphid marsupials (*Trichosurus vulpecula*: Goldfinch and Molnar, 1978; Nyakatura et al., 2007), arboreal didelphid marsupials (*Dromiciops australis*: Pridmore, 1994 and *Caluromys philander*: Schmitt and Lemelin, 2002), and an arboreal carnivore (*Potos flavus*: Lemelin et al., 2007). Slow lorises (*Nycticebus coucang)* have also been found, although not exclusively, to use this DSDC gait during level upside down locomotion (Jouffroy and Petter, 1990). The convergent evolution of DSDC gaits by a variety of distantly related forms implies adaptive significance. It has been convincingly argued that diagonal coupling (DC) of limbs is more stable on slender supports, because (1) the simultaneous swing of diagonal fore- and hindlimbs reduces craniocaudal torsional moments and (2) diagonal limbs exert opposing mediolateral substrate reaction forces during contact phase and thus stabilize the trunk above the support via lateral compensating movements (Cartmill, 1985; Preuschoft, 2002; Lammers and Gauntner, 2008; Schmidt, 2008). The convergent utilization of diagonal sequences (DS) in combination with DC in distantly related taxa is less well understood. Recent results from studies on primate locomotion are inconsistent with previously proposed biomechanical hypotheses such as the 'polygon support model' (Young et al., 2007) and other potential advantages on small branches (Wallace and Demes, 2008) that try to explain DS gaits. The possibility of ipsilateral limb interference additionally

poses a potential drawback of a diagonal gait sequence pattern, especially for relatively long limbed arboreal species (Hildebrand, 1967; Cartmill et al., 2002; Wallace and Demes, 2008). During slower trials the sloths often were observed to overstride, i.e., placing an ipsilateral hindlimb craniad to a forelimb. The slowness of sloth progression can in part be attributed to the frequent need to 'sort out' interfering limbs. However, in contrast to pronograde aboreal mammals this behaviour can be assumed to be less problematic in an intrinsically stable suspensory posture, in which toppling from the branch is impossible. Still, overstriding was not observed in faster trials thereby reducing the time needed to 'sort out' the limbs, instead the sloths increased total angular excursion by protracting forelimbs further and increasing retraction of the hindlimbs.

One hypothesis for the occurrence of DSDC gaits in arboreal mammals is that this gait sequence combines advantages shared with other gaits in terms of (1) security at touch down (Cartmill et al., 2002, 2007; Shapiro and Raichlen, 2007; but see Wallace and Demes, 2008) and (2) minimization of ipsilateral bipedal support (Cartmill et al., 2002). Although this explanation does not explicitly incorporate dynamic stability of faster locomotion, static stability probably plays a role in sloth locomotion. While toppling from branches is of no concern to sloths, security at touch down of limbs on untested supports is of paramount importance for these cautious animals during movement under terminal branches. With regard to habitat characteristics and utilization, it is hypothesized that DSDC gaits enable animals to draw back if branches break or crack, because a hindlimb is always placed near the centre of mass *before* the diagonal forelimb touches down (Cartmill et al., 2002). It is surprising, therefore, that two-toed sloths do not restrict their locomotion to diagonal sequence gaits, especially during 'exploratory gait'. Instead, we observed a wide range of gaits from LSSF to DSSF, as did Mendel (1981c) in a study of two-toed sloth locomotion on variously inclined supports. During 'exploratory gait' interlimb coordination was more variable than during 'travelling gait'. Moreover, diagonal sequence gaits were most common in fast 'travelling gait', during which supports were never 'tested' by nose before touch down. Similar plasticity in interlimb coordination was also found in three-toed sloths (Mendel, 1985b), in upside down locomotion of slow lorises (Jouffroy and Petter, 1990), and in diverse primates when challenged with more complex experimental setups (Rollinson

and Martin, 1981; Vilensky et al., 1994; Stevens, 2003; Nyakatura et al., 2008; Higurashi et al., 2009). Flexibility in gait sequence pattern is proposed to be used to accommodate different challenges of the three-dimensional arboreal habitat (Stevens, 2006). An explanation for the observed plasticity in sloths might be that in 'exploratory gait', which is marked by a extended period of bilateral forelimb support after touch down, two-toed sloths do not protract their arms as far as they do during 'travelling gait' (relationship of speed and step length). Because of this the amount of weight transferred on a forelimb right after touch down can be assumed to be less than during faster locomotion. As a result in slower locomotion the importance of interlimb timing for security at touch down and thus the necessity of a DS may be reduced. Additionally, by 'nose- checking' supports in 'exploratory gait' two-toed sloths might collect important information on support security before touch down. In contrast, two-toed sloth locomotion in 'travelling gait' is marked by longer steps and only short overlaps in forelimb support. It seems then that only during these faster modes two-toed sloths favour DSDC gaits as suggested by Cartmill et al. (2002). Under natural conditions two-toed sloths may use fast 'travelling gaits' only in emergencies, e.g., escaping predators. Selection of DSDC gaits under these conditions seems plausible, as it provides more security when 'nose-checking' is not possible and more weight is transferred onto a forelimb directly after touch down. An analysis of the relationship of bilateral forelimb support, forelimb weight transfer, step length and interlimb timing could further improve our understanding of DSDC gaits in pronograde arboreal mammals.

Conserved kinematics and consequences of limb morphology peculiar to sloths

Despite adoption of an upside down posture, with concomitant inverse influence of gravity during locomotion, overall kinematic patterns, especially of the forelimbs, of two-toed sloth locomotion are remarkably similar to pronograde mammals. As has been shown for a broad sample of systematically, ecologically, and anatomically diverse small mammals, (reviewed by Fischer et al., 2002; detailed kinematic analyses cited therein), two-toed sloths also progress primarily by retracting the most proximal elements of fore- and hindlimbs. Proximal pivots operate at the same distance from supports (in 'travelling gait'), and more distal joints contribute little or nothing to step

length. Scapulae and forearms of two-toed sloths move in matched motion across the observed speed range. Kinematic values such as scapular touch down and lift off angles and excursions are highly similar to those reported for pronograde locomotion (Jenkins and Weijs, 1979; Fischer et al., 2002; Rocha-Barbosa et al., 2005), and are especially close to terrestrial mammals of similar size. Mean amplitude of scapular retraction is 34° in two-toed sloths, 35° in dogs, 41° in goats and cats, and 28° in vervet monkeys (Boczek-Fucke et al., 1996; Whitehead and Larson, 1994; Fischer and Blickhan, 2006). Also, scapular rotation contribution to step length (50%) is well within the range of pronograde locomotion (Fischer et al., 2002). This is surprising because scapulae of *Choloepus* are short relative to other forelimb elements when compared to the forelimb element proportions reported for 189 mammalian species (Schmidt and Fischer, 2009). Indeed, proportions of the three propulsive forelimb segments from proximal to distal measured in 3 specimens of *C. didactylus* were 17/38/45 compared to 28/37/35 of similar sized mammals. Its displacive effect on the more distal elements is thus limited. We attribute the nevertheless high importance of the scapula for the generation of step length to the negative influence of hands on step length (see below), which in turn increases the importance of the remaining elements. Similarly, kinematics of arm, elbow and forearm are strikingly similar to those of pronograde small mammals (Jenkins and Weijs, 1979; Fischer et al., 2002; Rocha-Barbosa et al., 2005), rhesus monkeys (Courtine et al., 2005), small arboreal primates (Schmidt, 2008), and dogs (Goslow et al., 1981). Two-toed sloth forelimb proportions resemble those of primates, especially those of advanced climbers such as lorises and colobines (Schmidt, 2008). Relatively small scapulae in combination with rounded rib cages, common to many highly arboreal primates as well as sloths, may facilitate arm abduction, which is presumably advantageous in arboreal environments. Schmidt and Krause (in press) point out that three dimensional scapular mobility guided by the clavicle in contrast to a restriction to parasagittal movement in aclaviculate mammals is a means to abduct the forelimb if movement in the glenohumeral joint is limited to the scapular plane. A three dimensional analysis of sloth proximal forelimb motion is needed to determine the amount of abduction realised by either lateral glenohumeral joint mobility, as proposed by Mendel (1985a), or by scapular abduction.

Although sloth kinematics are similar to the basic therian pattern in many regards, they also differ. The most obvious difference is the loss of a propulsive element from the hindlimbs, because the tarsometatarsus can no longer be regarded as a functionally individual element in the sense of Kuznetsov (1985) and Fischer (1994). The foot is syndactylous to distal interphalangeal joints with metatarsophalangeal (MTP) joints usually maintained in neutral positions (Mendel, 1981a). Ankle joints are usually flexed 90°, so that the feet are aligned parallel to the long axes of the lower legs (Mendel, 1981a). Furthermore, there is extensive inversion at talar-navicular joints, which rotate volar pads toward supports (Mendel, 1981a). But, this inversion of feet rotates the planes of motion of the MTP joints' out of the parasagittal plane, rendering them ineffective for locomotion. Similarly, volar surfaces of hands are rotated towards supports (Mendel, 1981b) with analogous consequences for the planes of motion of metacarpophalangeal (MCP) joints relative to direction of progression. Although occasional movements in MCP joints of hands (Mendel, 1981c) and MTP joints of feet (Mendel, 1981a) are observed, they are usually small (in neutral position in 61% of observations), and functionally linked to clamping on supports of different diameters, according to Mendel. Our kinematic data quantitatively demonstrate that both hands and feet of two-toed sloths are absolved from their normal roles in contributing to progression, and are used solely for the purposes of effectively clamping supports between claws and volar pads (as deduced from morphology by Mendel, 1981c). To this end, hands and feet must always be held more or less perpendicular to supports, and thus, they can not contribute positively to body progression.

This effective loss of a functional limb element may also explain the pronounced contribution of upper arms and thighs to progression in two-toed sloths when compared to pronograde locomotion, despite the fact that angular excursions of the proximal elements are so similar to those in other previously studied mammals. The unparalleled importance of arms for generation of step length (Fischer et al., 2002) can likely be attributed to a combination of two factors. The first is the negative influence of distal elements, especially hands, leading to the mathematical emphasis of contributions of proximal elements. The second is the comparably short scapulae, which, if longer, certainly would have an even more pronounced impact on step

length, because equal angular excursion has a greater displacive effect on adjoining distal elements, if the element is relatively longer. Similarly in the hindlimbs contribution to step length is pronounced in the proximal elements (thighs), although angular displacements are again similar to those seen in standard pronograde locomotion (Goslow et al., 1973; Fischer et al., 2002; Rocha-Barbosa et al., 2005; Schmidt, 2005). The mathematical contribution of thighs to step length is 135%, negating the negative effects of lower legs (-18%), and feet (-25%). Pelvic displacements in the parasagittal plane additionally contribute over 8% to step length. Contributions to step length of a single hindlimb element of over 100% have also been documented for thighs of goats (Fischer and Blickhan, 2006), and values of over 90% are quite common in different taxa (e.g., *Monodelphis domestica* (Marsupialia): 93%, *Microcebus murinus* (Primates): 93%, *Saimiri sciureus* (Primates): 91% (Fischer et al., 2002, Fischer and Blickhan, 2006)).

Upside down locomotion of slow lorises is characterized by reciprocal activity patterns of limb flexors and extensors (Jouffroy and Stern, 1990). The authors were also able to dissociate antigravity function from propulsive function in limb muscle activation by comparing pronograde and upside down locomotion in their EMG study. In light of conserved kinematic patterns during upside down locomotion in slow lorises (Jouffroy and Petter, 1990) and sloths (present study), we assume that the same muscles responsible for pro- and retraction of proximal limb elements in pronograde mammals are also responsible for these tasks in inverted orientation to the support. However, antigravity function and forelimb retraction are sometimes peformed by identical muscles (e.g., *m. pectoralis*) of the 'muscular sling' of mammals that suspends thorax between forelimbs (Jenkins and Weijs, 1979). On the other hand, no activity was observed during stance phase in the main forelimb retractors (*m. pectoralis profundus* and *m. latissimus dorsi*) in recent studies of eight primate species (Larson and Stern, 2007), and dogs moving at a constant trot (Carrier et al., 2006; Carrier et al., 2008). Similarly, the reported patterns for hindlimb retractor muscle recruitment are not consistent in species studied so far. There are two recognized patterns (Schilling et al., 2009): In cats and rats, hip extensors are active throughout hindlimb stance until lift off (Rasmussen et al., 1978; Nicolopoulos-Stournaras and Iles, 1984), whereas, in horses and trotting dogs, recruitment of hip extensors is limited to late swing and early

stance phases (Robert et al., 1999; Schilling et al., 2009). Reduced retractor muscle recruitment throughout stance in forelimbs, and in the second half of hindlimb stance is tentatively suggested to be specializations for endurance running (Carrier et al., 2008; Schilling et al., 2009), so this pattern would then not be expected in sloths. These nonuniform results make it difficult to link observed kinematics of skeletal limb elements to retractor muscle recruitment. Nevertheless there is no substantive difference between intralimb coordination in pronograde and upside down locomotion and conserved recruitment patterns cannot be precluded. Ultimately, only EMG of fore- and hindlimb pro- and retractor muscles can elucidate this issue conclusively. The conserved limb configuration, with its three propulsive elements sensu Kuznetsov (1985) and Fischer (1994) in sloth forelimbs during locomotion despite the necessary reciprocity of activation patterns in flexors and extensors and profound anatomical modifications (cf. Mendel, 1985) raises further questions as to why the zig-zag configuration of the limb and intralimb coordination are maintained. Mechanical self stability, as suggested for pronograde locomotion (Seyfarth et al., 2001), seems an unlikely explanation this phenomenon in upside down posture and deliberate locomotion.

Convergent evolution of quadrupedal suspensory locomotion in two- and three-toed sloths

The peculiar suspensory locomotion of both extant sloth lineages has been termed ‘one of the most striking examples of convergent evolution known among mammals’ (Gaudin, 2004). Divergence of the two modern lineages may date back 21 ± 3 Myr (Delsuc and Douzery, 2008) or as far as 25 Myr (Sarich, 1985). Morphological adaptations to suspensory quadrupedalism shared by two- and three toed sloths include modification of hands and feet to relatively rigid hooks, maximized mobility at nearly all joints proximal to midcarpal and transverse tarsal joints, and emphasis on powerful limb flexion (Engelmann, 1985; Mendel, 1985a). In light of our new data, we hypothesize from descriptions of three-toed sloth locomotion (Mendel, 1985b) that it will not deviate substantially from the basic therian pattern of limb kinematics, either. Assuming that adaptations necessary to enable limb pro- and retraction during suspensory quadrupedalism are comparably minor, then independent parallel

evolution of this locomotor mode and posture in two- and three-toed sloths seems less implausible, especially if autopodia were already preadapted in the last common ancestor. For example, the propulsive role of the tarsometatarsus element was probably reduced in the last common ancestor of Pilosa (anteaters and sloths), because modern anteaters as well as fossil sloths are/were plantigrade (McDonald et al., 2008) or exhibit modifications of plantigrady ('pedolateral' feet cf. McDonald, 2007). Neural constraints on evolutionary transformation of limbs, as well as conservatism in rhythmogenic spinal centers have been proposed (Jenkins and Goslow, 1983; Cheng et al., 1998). Convergent patterns of two-toed and three-toed sloth limb pro- and retraction, despite upside down postures, may present an additional example for such neural constraints. What ever the case, the evolutionary changes in neuromuscular control involved in the reciprocal antigravity functions of flexor and extensor muscles in both sloth lineages demand attention in future studies.

Conclusions

Two-toed sloths display a considerable range of speeds, variable spatio-temporal gait parameters, and different gaits. But intralimb coordination is fairly uniform and resembles data reported for pronograde mammals, especially in the forelimbs. Even in this peculiar inverted locomotor mode the conserved intralimb coordination is remarkably unchanged, and therefore does not preclude similarly conserved recruitment of extrinsic fore- and hindlimb retractor muscles and control. However, suspension of the thorax between the forelimbs, as well as all anti-gravity work within the limbs, must be solved differently in sloths because of the inverse influence of gravity. This is the framework for ongoing research into sloth muscular properties.

As a direct consequence of the suspensory quadrupedal posture of two-toed sloths there is little to no movement in the MCP and MTP joints of hands and feet, respectively, and the plane of movement of these joints is rotated 90 degrees away from the direction of progression, and toward supports. These adaptations have differing effects on the kinematics of fore- and hindlimbs. Whereas forelimb kinematics remain unchanged from those of pronograde mammals, those for hindlimbs are obviously different. It may be that morphological adaptations of sloth autopodia to suspensory postures effect hindlimb kinematics more profoundly than

forelimbs, because hands contribute relatively little to progression even in pronograde mammals (Fischer et al., 2002). In contrast, the tarsometatarsus, which became a separate functional element within feet in the course of therian evolution, is (re)integrated into largely immobile feet in the two sloth lineages, thereby removing one propulsive element from the sloth hindlimb.

Although our understanding of sloth functional morphology remains incomplete, the present study supports the hypothesis that evolutionary changes related to limb pro- and retraction, and linked properties of neuromuscular control, were rather minor. Accordingly, convergent evolution from terrestrial or (semi)arboreal ancestors (White, 1993) in the two extant sloth lineages is not as dramatic a notion as it may seem on the exclusive basis of morphological similarity and extensive separate evolutionary histories.

ACKNOWLEDGEMENTS

We are indebted to Elke Woker (animal keeping), Lydia Wagner and Rommy Petersohn (assistance during data aquisition), and Katrin Dix (assistance with data analysis). Ilona Schappert (Zoo Dortmund, Germany) kindly provided the sloths Evita and Julius. Richard Kraft (Zoologische Staatssammlung München, Germany) generously contributed skeletal material. Manuela Schmidt, Alexander Stößel, and Frank C. Mendel were the authors of helpful comments and provided insightful criticism of earlier versions of this manuscript. Two anonymous reviewers' comments greatly enhanced clearity of the manuscript. Lucy Cathrow thoroughly edited the language. The study was supported by the German research foundation (grant to MS Fischer: DFG Fi 410/11-1).

- Chapter 3 -

Three-dimensional kinematic analysis of the pectoral girdle during upside-down locomotion of two-toed sloths (*Choloepus didactylus*, Linné 1758)

John A. Nyakatura & Martin S. Fischer

Abstract

Background: Theria (marsupials and placental mammals) are characterized by a highly mobile pectoral girdle in which the scapula has been shown to be an important propulsive element during locomotion. Shoulder function and kinematics are highly conservative during locomotion within quadrupedal therian mammals. In order to gain insight into the functional morphology and evolution of the pectoral girdle of the two-toed sloth we here analyze the anatomy and the three-dimensional (3D) pattern of shoulder kinematics during quadrupedal suspensory ('upside-down') locomotion.

Methods: We use scientific rotoscoping, a new, non-invasive, markerless approach for x-ray reconstruction of moving morphology (XROMM), to quantify *in vivo* the 3D movements of all constituent skeletal elements of the shoulder girdle. Additionally we use histologic staining to analyze the configuration of the sterno-clavicular articulation (SCA).

Results: Despite the inverse orientation towards gravity, sloths display a 3D kinematic pattern and an orientation of the scapula relative to the thorax similar to pronograde claviculate mammalian species that differs from that of aclaviculate as well as brachiating mammals. Reduction of the relative length of the scapula alters its displacing effect on limb excursions. The configuration of the SCA maximizes mobility at this joint and demonstrates a tensile loading regime between thorax and limbs.

Conclusions: The morphological characteristics of the scapula and the SCA allow maximal mobility of the forelimb to facilitate effective locomotion within a discontinuous habitat. These evolutionary changes associated with the adoption of the suspensory posture emphasized humeral influence on forelimb motion, but allowed the retention of the plesiomorphic 3D kinematic pattern.

BACKGROUND

In therian mammals (i.e., marsupials and placental mammals) the shoulder girdle is mobilized when compared to monotremes and other amniotes (Eaton jr., 1944). The coracoids are reduced and the scapula became an important propulsive element in the forelimb (Kuznetsov, 1985; Fischer, 1994; Gasc, 2001). It has been shown that both forelimb kinematics (Fischer et al., 2002) and the relative proportions of propulsive elements are rather conservative in quadrupedal therian mammals (Schmidt & Fischer, 2009) – observations that have been attributed to biomechanical constraints of limb configuration (see review in Fischer & Blickhan, 2006).

In 1935 the functional anatomist Ruth Miller wrote "of all mammals the sloths have probably the strangest mode of progression" (Miller, 1935). Due to their characteristic 'upside-down' posture and locomotion these animals represent interesting 'natural experiments' to study functional implications of the inverse body orientation with regard to the force of gravity. Unlike in 'normal', pronograde locomotion, a tensile loading regime acts within the limbs rather than a compressive one (Patel & Carlson, 2008), and flexors are required to counteract the gravity-induced extension of the limbs (Mendel, 1985a). Many morphological peculiarities of the limbs were stringently interpreted as adaptations to facilitate the upside-down posture and locomotion of sloths. For example, the anatomy of the main flexor muscles of the limbs (m. brachioradialis and m. biceps femoris) have largely advantageous moment arms on the joints they span to flex the forelimb against gravity-induced extension (Mendel, 1979).

Earlier studies on sloth functional anatomy concentrated on the skeletal and muscular adaptations of the distal limbs to suspensory posture (Miller, 1935; Mendel, 1979; 1981a; 1985a) or more general aspects of the overall locomotor pattern (Mendel, 1981b; 1985b; Nyakatura et al., 2010), and there is considerably less data available for the interpretation of possible functional aspects of peculiarities of the proximal limbs and their connection to the axial skeleton, i.e., the pectoral and pelvic girdles. The gravity vector has fundamental relevance for the connection between the limbs and the thorax. Extrinsic forelimb musculature acting on the pectoral girdle not only protracts and retracts the forelimb but also functions to suspend the weight of the thorax in mammals (Davis, 1949; Carrier et al., 2006).

In claviculate mammals the clavicle is the only remaining skeletal connection of the forelimbs to the thorax (Eaton jr., 1944). Although in both extant sloth genera a clavicle is developed, it has an unusual articulation to the sternum (manubrium sterni), because the articulating faces are lacking (e.g., Lucae, 1882). The sterno-clavicular articulation (SCA) is described as either cartilaginous (Lucae, 1882) or ligamentous (Miller, 1935; Mendel, 1985a). Whatever the configuration of the SCA, a functional significance is implied, as authors point out the extraordinary mobility of the clavicle at this joint (Lucae, 1882; Miller, 1935; Mendel, 1985a).

We present a precise reconstruction of the three-dimensional (3D) *in vivo* motion of skeletal structures of the pectoral girdle to gain insight into the function of the pectoral girdle in two-toed sloths (Xenarthra: *Choloepus didactylus*, Linné 1758) and the evolutionary changes of shoulder function associated with the adoption of the suspensory quadrupedal posture and locomotion. The data were obtained using 'scientific rotoscoping' (SR) (Gatesy et al., 2010), a markerless, non-invasive approach for x-ray reconstruction of moving morphology (XROMM) (Brainerd et al., 2010). This technique combines synchronous biplane high-speed x-ray video and x-ray computed tomography scans to visualize and measure three-dimensional motions of the pectoral girdle usually hidden under integument, muscles and other tissue (Fig. 3-1). Thanks to this new approach we are able to report six degrees of freedom (DOF) data for all constituent skeletal elements of the pectoral girdle in sloths and test for the significance of different aspects of the movement of individual skeletal elements in 'virtual experiments'. Additionally, the SCA is examined using histochemical methods to aid functional interpretation of its configuration. Morphological and kinematic changes that are associated with the adoption of the suspensory quadrupedal locomotion during the evolution of modern sloths will be discussed. Analysis of the functional morphology of the pectoral girdle in sloths may yield insights into constraints and flexibility of the mammalian shoulder girdle to functional demands.

METHODS

Anatomical investigation

No sloths were sacrificed for this study. All procedures and animal care were carried out in compliance with the animal welfare regulations of the state of Thuringia,

Germany. Two frozen specimens of adult female *C. didactylus* from zoos in Paris, France, and Dresden, Germany were donated to us. The skin was removed and the subjects were formalin fixed. Prior to histological staining, tissue from the sterno-clavicular articulation (SCA) was prepared from one of the donated specimens by first removing all muscular connections from the clavicle and manubrium sterni and subsequently cutting through the midpoint of the clavicle and the middle of the manubrium sterni. Bone remnants were carefully removed *ex situ* and connective tissue from the articulation was embedded in paraffin before being sectioned with a Microm™ HM360 microtome (10µm sections). Serial sections from medial to lateral were produced and histological properties were analyzed using differential staining methods (Hämalaun-Eosin (HE), Azan, and Masson-Goldner) on consecutive sections.

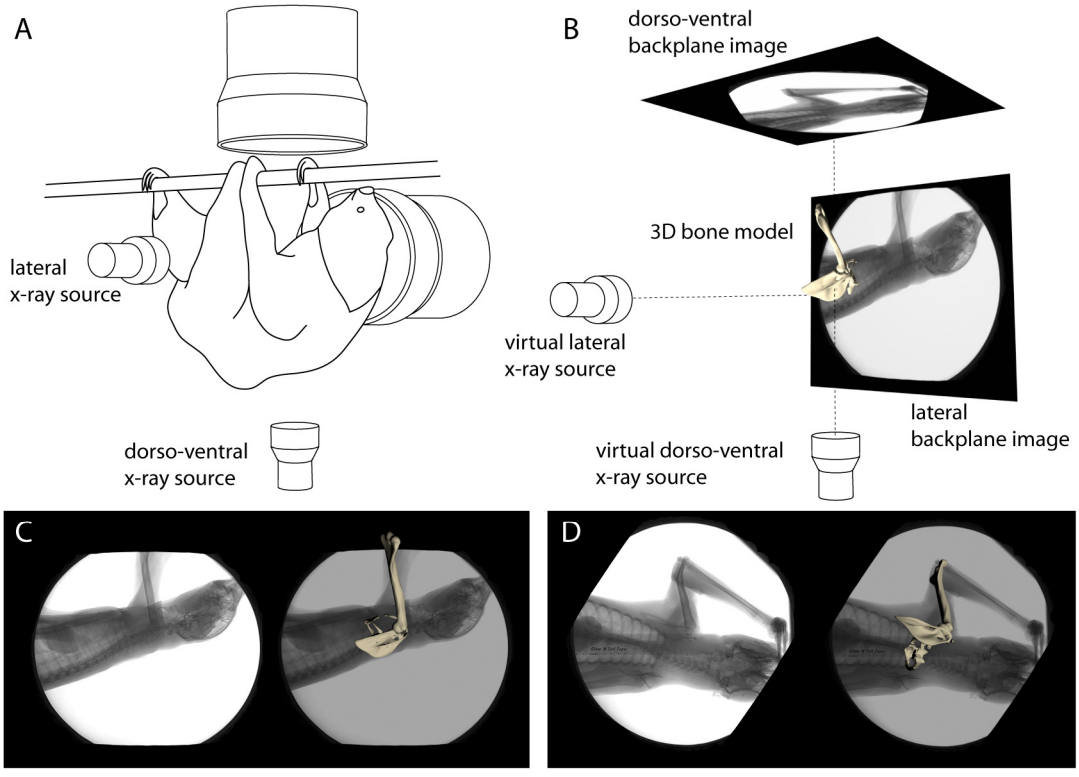

Fig. 3-1: Scientific rotoscoping [20]. The experimental setup for synchronous high-speed x-ray video recording (A) is virtually re-created within animation software (B). X-ray videos are loaded into the backplane as image sequence planes. A 3D bone model is positioned to match the x-ray shadow in both the lateral (C) and dorso-ventral (D) backplane for the entire image sequence. Six DOF (degrees of freedom, i.e., translations and rotations about anatomically defined coordinate systems - see methods) are exported for all constituent skeletal elements of the shoulder girdle.

In order to rule out the possibility that we were studying morphological extremes in two animals used for the locomotion analysis, we additionally measured skeletal properties in the few available adult (fused epiphyses of long bones) *C. didactylus* individuals obtained from German museum collections (Museum f. Naturkunde, Berlin; Zoologisches Museum, Hamburg). We found our experimental subjects to lie mostly within one standard deviation of the anatomical variability of the small sample (Table 3-1).

Biplane high-speed x-ray motion analysis: experimental setup

X-ray videos of two adult *C. didactylus* of different weights and sex were recorded. Neither the female (10.6 kg, 87 cm snout vent length) nor the male (6.5 kg, 78 cm svl) displayed any physical and behavioral peculiarities. X-rays were taken synchronously from the dorso-ventral and letero-lateral projections during steady-state locomotion (Fig. 1). Subjects were trained to move along a motor-driven 'treadpole' (4000 x 40 mm), which permitted the x-ray recording of several consecutive strides in a trial. Stride cycles were treated as independent events. Between 0.2 m/sec and 0.3 m/sec locomotion of two-toed sloths has been shown to be relatively uniform (Nyakatura et al., 2010). All slower and faster trials were discarded for the present study and only strides with symmetry values (i.e., the percentage of a given limb cycle that the contralateral limb touches down) between 0.4 and 0.6 were analyzed for the sake of uniformity. We used the Student's t-test for independent samples (analyses carried out in SPSS™ 12.0) to test whether both individuals differed significantly in regard of gait parameters in different strides (sample size n = 14 and n = 18, respectively; Table 3-2). Intra-individual variability of gait parameters appeared to be so distinct that inter-individual differences carried no weight. Based on the observation of statistically insignificant differences between subjects in stride length, swing phase duration and contact phase duration, as well as scapula touch down angle projected to the parasagittal plane (i.e., the 2D angle obtained from the latero-lateral projection) and the qualitative comparison of inter- and intra-individual variability (Table 2), stride cycles from both experimental individuals were subsequently pooled. 10 steady-state stride cycles in each study subject were analyzed. All trials were time normalized to 50 points over the contact phase and swing phase, respectively, to facilitate compilation

of multiple trials so that the mean and standard deviation of the kinematic curves could be determined.

Table 3-1: Comparative measurements of pectoral girdle elements. Scapula length is measured as distance from angulus inferior to acromio-clavicular joint; spina scapulae length is measured along spina scapulae from vertebral border to glenoid cavity. Hand length is measured from wrist joint to distal interphalangeal joint. All values are reported in cm. MfN: Museum für Naturkunde Berlin; ZMH: Zoologisches Museum Hamburg; x: missing data due to incompleteness of museum material. *: measurements of XROMM study animals retrieved from x-ray images.

Specimen	scapula length	spina scapulae l.	humerus length	clavicle length	ulna length	hand length
Museum material						
C. didactylus (MfN 102636)	8.98	5.74	14.06	4.64	17.02	x
C. didactylus (ZMH 1507)	7.32	5.18	12.94	3.80	13.91	8.81
C. didactylus (ZMH 1506)	7.25	4.45	11.75	3.21	14.42	x
Dissected specimens						
C. didactylus	8.68	5.73	15.7	4.52	19.4	10.01
C. didactylus	7.71	5.24	14.58	4.2	17.38	9.2
Study animals*						
C. didactylus (male)	7.7	5.0	13.2	3.6	15.2	9.0
C. didactylus [female)	8.2	5.8	15.9	4.6	19.4	9.8
Mean (± s.d.)	7.98 (± 0.67)	5.31 (± 0.49)	14.02 (± 1.51)	4.08 (± 0.56)	16.68 (± 2.25)	9.37 (± 0.52)

Both 40 cm diameter image intensifiers were equipped with a Visario Speedcam™ (Weinberger GmbH, Erlangen, Germany) and recorded at a resolution of 1.536 x 1.024 pixels and a speed of 300 frames per second (fps). A calibration object (20 x 12 x 12 cm) with metal beads inserted at 1 cm distances was used to calibrate the 3D space covered by both x-ray devices for subsequent analysis using 11 parameter direct linear transformation (DLT; necessary Matlab™ files available at www.xromm.org) (Brainerd et al., 2010).

Table 3-2: Intra-individual differences and inter-individual variability of gait parameters. The Student's t-test for independent samples was used to test for significant differences in intra-individual variability of gait parameters. *: significant differences when $p \leq 0.05$, n.s.: not significant.

	Individual 1 (mean ± s.d.)	Individual 2 (mean ± s.d.)	Comparison of intra-individual variability (p-value*)	Both individuals pooled (mean ± s.d.)
Stride length (in cm)	57.4 ± 4.8 (n = 18)	60.4 ± 4.9 (n = 14)	0.098 n.s.	58.9 ± 5.0 (n = 32)
Forelimb swing phase duration (in sec)	0.81 ± 0.1 (n = 18)	0.88 ± 0.3 (n = 14)	0.316 n.s.	0.84 ± 0.2 (n = 32)
Forelimb contact phase duration (in sec)	1.47 ± 0.2 (n = 18)	1.52 ± 0.2 (n = 14)	0.541 n.s.	1.50 ± 0.2 (n = 32)
Scapula touch down angle (in degree)	43.7 ± 5.5 (n = 10)	40.4 ± 4.9 (n = 10)	0.174 n.s.	42.0 ± 5.3 (n = 20)

X-ray reconstruction of moving morphology (XROMM)

Scans of disarticulated skeletal elements were taken using a GE Lightspeed™ 16 CT scanner at the Zentralklinik, Bad Berka, Germany, at 120 kV and 150 mA. Voxel size of the scan was 0.47815 mm with a slice thickness of 0.625 mm. To reconstruct bone models raw data was surface rendered in Imaris™ 6.4 and converted into .obj file format using customized software (by H. Stark available at www.stark-jena.de). Models were imported into Maya™ 8.0 and hierarchically connected via virtual joints to form a digital marionette (Gatesy et al., 2010). In order to avoid possible harm of the valuable zoo animals from anesthesia a different skeleton was scanned and then scaled to match the size of the experimental subjects by using the scale tool in Maya™ and the calibrated x-ray references in the backplane.

Distortion of all x-ray recordings was corrected using a reference grid (see Brainerd et al., 2010). In Maya™ virtual dorso-ventral and letero-lateral cameras were created and their relative position in virtual 3D space calibrated so that they imitated the actual x-ray sources (necessary Matlab™ and Maya™ embedded language files available at www.xromm.org) (Fig. 3-1). The un-distorted x-ray image sequences from both projections were put in the backplane of the recreated x-ray cameras. Subsequently

the digital marionette was posed to match both x-ray references frame for frame in an iterative process. After a trial had been approximated satisfactorily, rotations and translations of each element were exported into Microsoft™ Excel.

Motions are reported relative to hierarchically higher ordered skeletal elements (Table 3-3). Right handed anatomical coordinate systems were implemented at the center of rotation of each element (Fig. 3-2). Translations were set to zero at the instant of touch down.

During SR the digital marionette was then positioned to match the x-ray shadow of both projections for every fifths frame. After a trial had been completed the three rotations representing the movement of a bone relative to the higher ordered skeletal element were exported into Microsoft™ Excel.

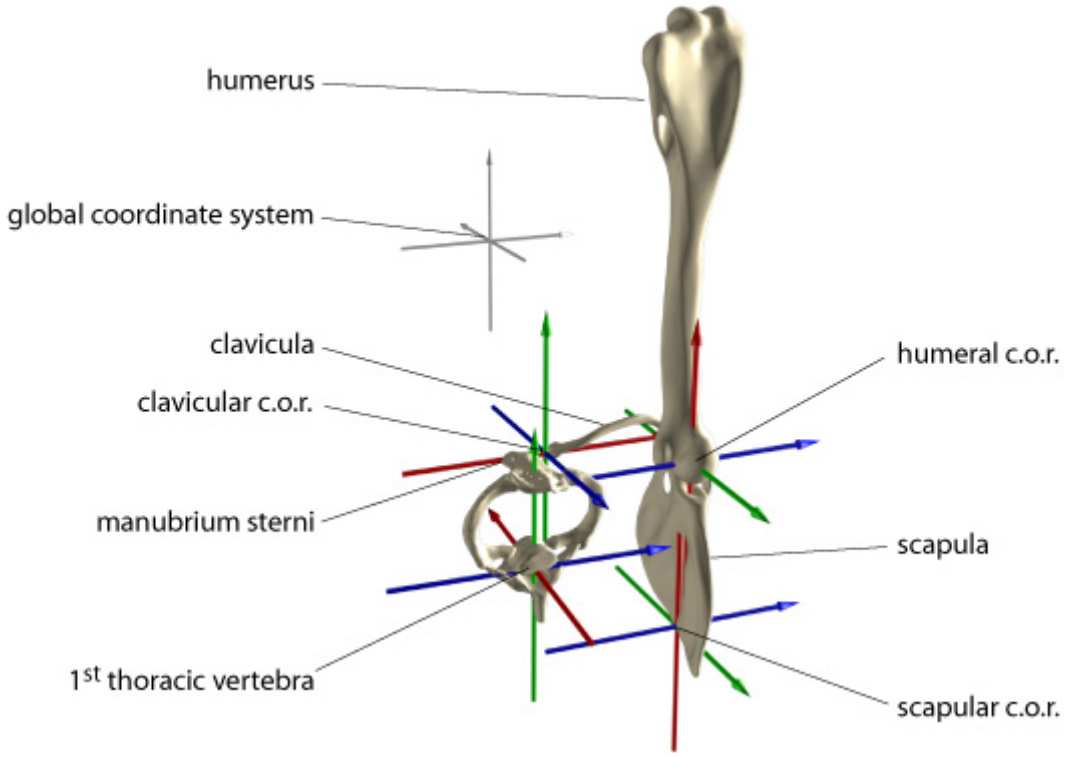

Fig. 3-2: Anatomical coordinate systems and zero-positions of rotations are used to quantify three-dimensional kinematics of the pectoral girdle. The anatomical coordinate systems were placed in the center of rotation (c.o.r.) of the proximally adjacent joint (in case of 1st thoracic vertebra into the center of the vertebral body; in case of scapula we approximated the instantaneous c.o.r. at the vertebral border of the scapula at the extension of the spina scapulae). *X*-axes (red) were set to represent the long axis of elements. *Z*-axes (blue) were oriented to represent the most distinct motion of the bone of interest. *Y*-axes (green) were orthogonal to the other two axes. For zero-points of rotations the anatomical axes were aligned according to the global coordinate system (unnatural pose). Motions of hierarchically higher elements have displacing effect for all lower ranked elements, i.e., motions of humerus are reported relative to scapula, scapular and clavicular motion relative to 1st thoracic vertebra, 1st thoracic vertebra motion relative to global reference.

In SR, accuracy and repeatability depends on many factors, including the quality of calibration, the visibility of skeletal structures on the x-ray references, the temporal resolution of reference x-ray videos, and on the effort of the investigator. Due to the unequal shape and thickness of the structures studied, there is not one value that can represent the accuracy of all measurements. General accuracy for optimal conditions was measured by comparing the known opening of a vernier caliper (150 mm) to the measured opening following the approach used in this study. We determined an opening of 150.704 mm; i.e., a deviation of less then one millimeter. To assess repeatability we determined the scapular lift off position of a single trial on ten consecutive days of data analysis and found only small deviations (mean ± s.d.): lift off frame 708.3 ± 0.95 (i.e., s.d. is less than 1 frame or 1/300 sec); trans x -0.43 cm (± 0.13); trans y -0.83 cm (± 0.12); trans z 0.17 cm (± 0.12); rot x -18° (± 0.76); rot y -18° (± 0.24); rot z 38° (± 0.16). Due to these deviations we report all kinematic data rounded to the closest tenth of a cm and degree, respectively.

Quantification of displacing effects of individual elements

One of the merits of the XROMM approach to kinematic analysis is that it allows 'virtual experiments' with the animated 3D reconstruction. Here, we quantify the displacing effects of individual elements of a joint chain by turning off its movements either by 'muting' all translations and rotations or by 'muting' only specific rotations. With XROMM it is possible, for example, to turn off abduction and adduction of a bone relative to its defined anatomical coordinate system. The displacing effect of the motion of an element can then be assessed by comparing the displacement of normal movements at the most distal point of the joint chain to the displacement of the most distal point in the joint chain obtained in the 'virtual experiment', with aspects of the motion turned off. In this study we assess the displacing effects of aspects of scapular and humeral motion on the displacement of the elbow. The displacement of the elbow is obtained relative to the first thoracic vertebra. We subsequently turned off total scapular motion (all translations and rotations), total humeral motion, scapular rotation along its long axis, scapular abduction/adduction, and humeral abduction/adduction from the scapular plane. In each of these experiments motion was turned off in the moment of touch down; i.e., initial position of the elbow is the

same in each case but displacement is altered during the course of the 'virtual' contact phase and subsequent swing phase. Three dimensional trajectories of the elbow are reported and total deviations among the 'virtual experiments' can thus be compared.

RESULTS

Skeletal anatomy of pectoral girdle

The thorax of *C. didactylus* has 23 to 24 ribs, of which 12 are connected to the sternum (Flower, 1882). In cranial direction the thorax tapers considerably. The SCA allows virtually all degrees of freedom, when the clavicle is stripped of attaching muscles (Mendel, 1985). The internally curved clavicle articulates to the scapula in a small notch at the widely flared acromial process. Fused to the coracoid process, the acromion forms an arch that is extended cranially beyond the humeral head. It provides prominent attachment sites for the m. trapezius, m. subclavius, and m. deltoideus. When compared to forelimb intralimb proportions reported for large dataset of mammalian species (Schmidt and Fischer, 2009), the relative length of the scapula of *C. didactylus* (expressed as percentage of sum of scapula, upper arm and lower arm lengths) is very short [21% instead of ca. 30%; cf. 6]. The scapula is thin and the spina scapulae does not reach the vertebral border. The caudal border is characterized by a broad attachment site for the well developed m. teres major. The gleno-humeral joint is marked by a shallow fossa glenoidalis and round humeral head. There is a considerable incongruity between both articulating surfaces.

Table 3-3 (opposite page): Anatomical coordinate systems used for the kinematic analysis. Right handed coordinate systems are used for each joint with the *x*-axis oriented along the long axis of the bone of interest, *z*-axis always oriented to represent the most distinct motion of this bone, and *y-axis* orthogonal to both other axes (see Fig. 2). The anatomical coordinate systems are placed directly where the motion takes place, i.e. in the joint, and are fixed to the proximally adjoining bone. This means that motion of the bone of interest is reported relative to the proximally adjoining bone. Motion of the 1st order hierarchy bone (1st thoracic vertebra) is reported relative to a global coordinate system with positive *x* in direction of movement, positive *y* towards dorso-ventral image intensifier (ventral to the animal), and positive *z* to animal's left. + = positive rotation about respective axis; - = negative rotation about respective axis.

Joint/element (hierarchy)	Anatomical meaning of rotation about axis	Zero-point for rotations
Global coordinate system (top)		
x-axis	-	-
y-axis	-	-
z-axis	-	-
1st thoracic vertebra (1st order)		
x-axis	Long axis rotation of vertebral column (roll)	Aligned to global *x*
y-axis	Lateral undulation of vertebral column (yaw, +: undulation to the right)	Aligned to global *y*
z-axis	Pitch of vertebral column (+: decrease of head-support distance)	Aligned to global *z*
Scapular center of rotation/scapula (2nd order)		
x-axis	Inward (+) /outward (-) rotation about long axis of scapula	Scapula is not rotated (long axis of scapula parallel to thoracic *y*-axis)
y-axis	Abduction (-) /adduction (+) of scapula (yaw)	Scapula is not abducted
z-axis	Protraction (-) /retraction (+) of scapula (pitch)	Scapula is vertical (in perfect dorso-ventral orientation)
Glenohumeral joint/humerus (3rd order)		
x-axis	Long axis rotation of humerus (roll, +: outward rotation)	Humerus is not rotated (epicondyles aligned in frontal plane)
y-axis	Humeral abduction (-) /adduction (+) from scapular plane (yaw)	Humerus is in scapular plane
z-axis	Humeral protraction (-) /retraction (+) (flexion in glenohumeral joint, pitch)	Humerus is orientated vertical (long axis parallel to scapula long axis)
Sterno-clavicular joint/ clavicle (2nd order)		
x-axis	Rotation about long axis of clavicle (+: caudal rotation)	The curvature of the clavicle is pointing ventral
y-axis	Anterior (+) /posterior (-) displacement of acromio-clavicular joint relative to manubrium sterni	Clavicle is pointing lateral and forms 90° angle to long axis and *y*-axis of the 1st thoracic vertebra
z-axis	Dorso (-) /ventral (+) displacements of acromio-clavicular joint relative to manubrium sterni	Clavicle is pointing lateral and forms 90° angle to long axis and *y*-axis of the 1st thoracic vertebra

Histologic properties of the SCA

Serial cross sections and differential staining of the SCA from proximal to distal revealed a homogenous fibrous composition of the structure (Fig 3-3). No elastic or reticular fibers are evident, as they would have stained orange-red in Azan staining and light green in Masson-Goldner staining. Also, there is no cartilage or fibrocartilage within the SCA, as it would have stained blue in the HE staining. Additionally, there is little intercellular substance (violet in HE staining) apart from the intercellular collagen. Thus the SCA can be identified as dense connective tissue containing irregular arranged collagen fiber bundles. There was no synovial cavity found.

Thorax movements

During quadrupedal suspensory locomotion in sloths, the thorax experiences side to side displacement over the course of a step cycle (translation along *z*-axis in Fig 3-4A). In combination with the tapered shape of the rib cage, this movement leads to the approximate alignment of the thoracic wall with the parasagittal plane at the moment of forelimb lift off at the same body side. Rotation about the *y*-axis indicates that during contact of a forelimb the long axis of the 1st thoracic vertebra first points towards the contralateral side and then rotates to face the ipsilateral body side at lift off. We documented almost no rotation about the long axis and a relatively constant pitch towards the support in the 1st thoracic vertebra (Table 3-4).

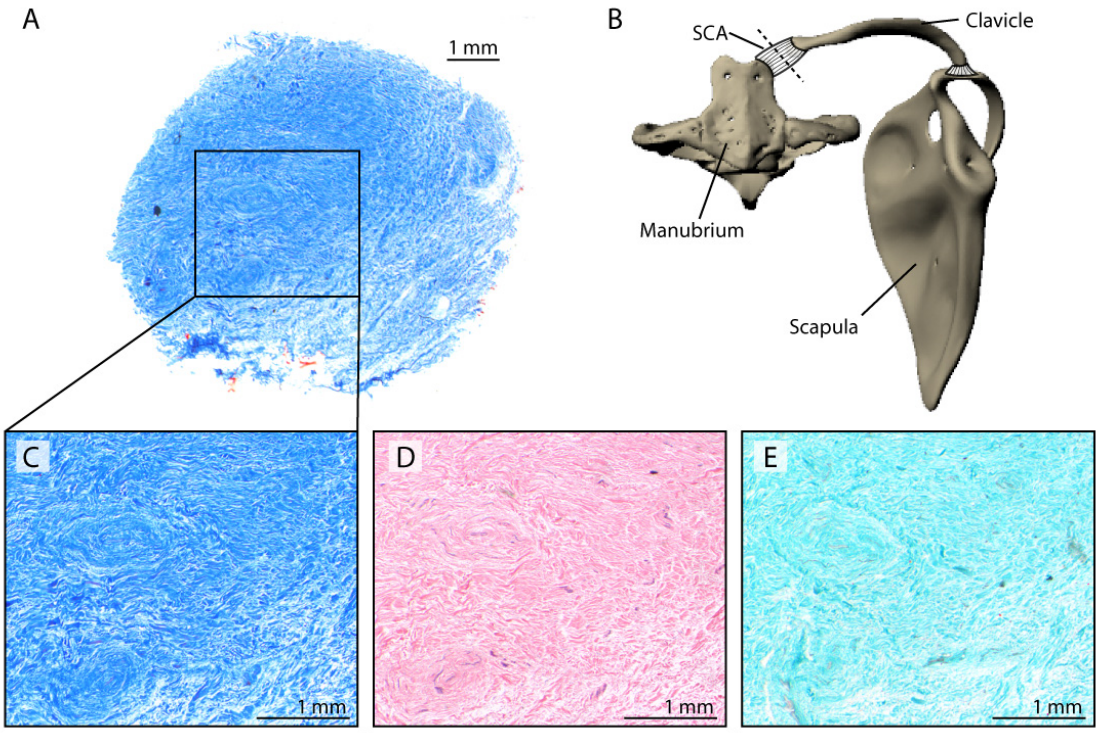

Fig. 3-3: Histological properties of the sterno-clavicular articulation (SCA). A: Overview of representative cross section, B: illustration of manubrium sterni (ventral aspect), clavicle, scapula, and position of the representative cross section through the SCA (dotted line), C-E enlarged insets of A stained differently on subsequent sections. Panels A and C stained with Azan, D stained with HE, E stained following Masson-Goldner protocol. The articulation comprises solely irregular fibrous connective tissue. Neither elastic fibers nor cartilage or muscle tissue are evident. The collagen fibers do not form regular parallel bundles. No synovial cavity is present.

Three dimensional movements of the scapula

Movements of the shoulder blade follow the morphology of the thorax and are confined by the clavicle (Fig. 3-5). The center of rotation of scapular protraction and retraction is positioned at the vertebral border of the scapula. We documented slight translations of the center of rotation in the second half of the contact phase (Fig. 3-4B), the most prominent being a caudal translation along the thoracic wall with a maximum of about 0.8 cm on average (Table 3-4). At the same time the center of rotation is translated laterally and ventrally.

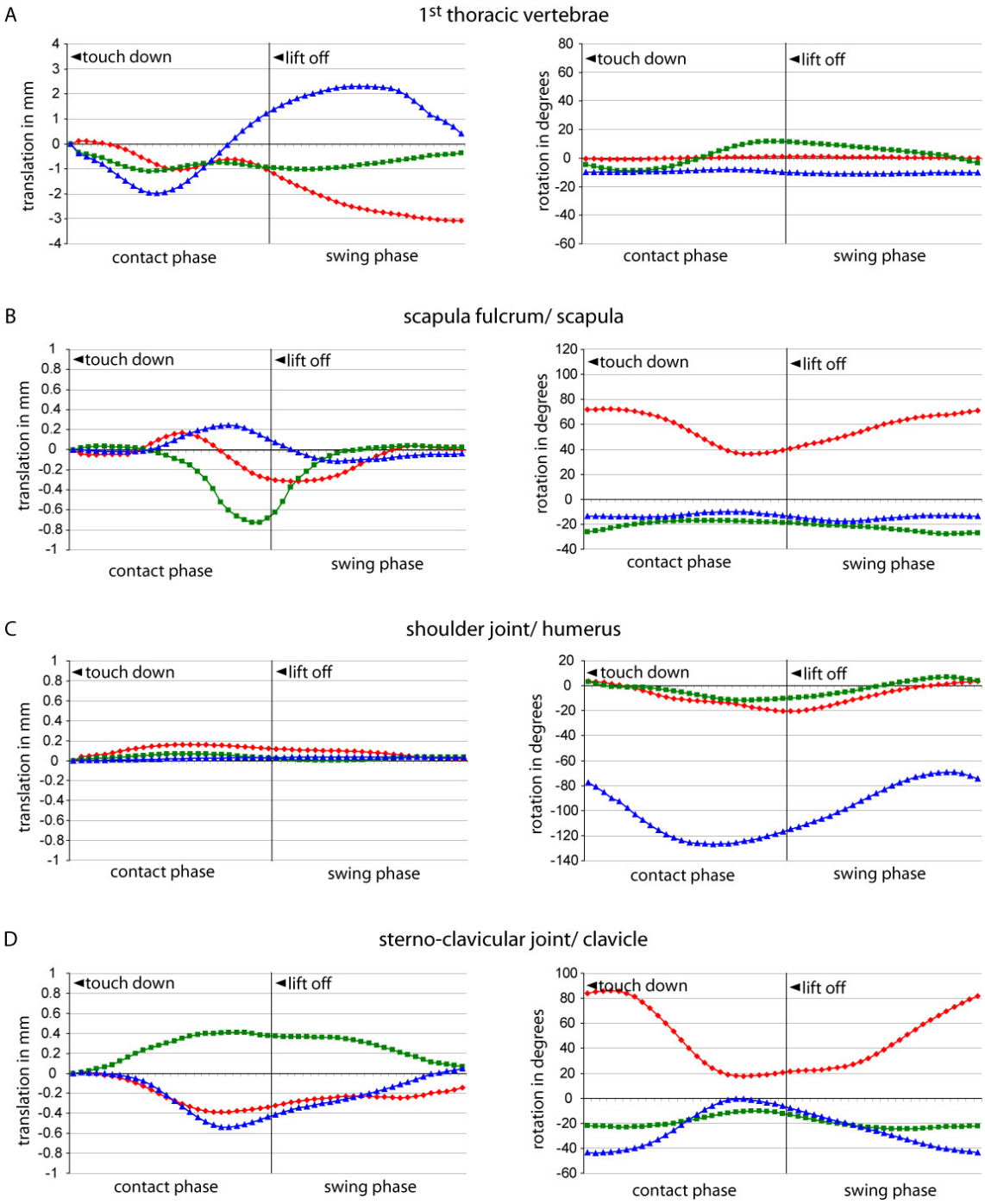

Fig. 3-4: Mean 3D kinematics of the pectoral girdle over a step cycle (n = 20). A: 1st thoracic vertebra; B: scapular center of rotation/ scapula; C: shoulder joint/ humerus; D: sterno-clavicular joint/ clavicle. Translations shown left, rotations right. Translations and rotations about *x*-axes are red, translations about *y*-axes are green, translations and rotations about *z*-axes are blue. The anatomical significance of these motions is detailed in Table 3 and Fig. 2.

At initial contact the scapula is positioned cranially and dorsally (Fig. 3-5). It is almost maximally protracted (rotated about the *z*-axis 72° from vertical), rotated inward to about 26° and mean net abduction is -14° (i.e. the shoulder joint is positioned more medial than the scapular center of rotation). After about 30% of the contact phase,

scapular retraction, i.e., rotation about the *z*-axis (Fig. 3-4B), sets in. During retraction the scapula glides around the rounded thorax and the degree of scapular rotation about the long axis decreases to a minimum of about 18° shortly before lift off. The negative abduction, on the other hand, remains relatively constant. At maximum retraction the long axis of the scapula is orientated 39° from vertical (36° maximum amplitude; Table 3-4). The laterally displaced tapered thorax almost positions the scapula into the parasagittal plane, but it is still rotated inwards (about its long axis) at lift off. The ventro-caudal movement of the glenoid during the contact phase describes a semi-circle, with its distance to the sternum kept relatively constant by the clavicle. At lift-off the glenoid fossa faces ventral. Scapula protraction starts shortly before lift-off and full protraction is reached shortly before the limb touches down again.

Movements in the gleno-humeral joint

Only minimal translations of less than two millimeters are observed in the gleno-humeral joint (Fig. 3-4C) - minute motions which are only slightly above our estimated analytical grade of repeatability. During the initial third of the contact phase, when there is little scapula movement, the upper arm is retracted exclusively via flexion in the gleno-humeral joint (rotation about *z*-axis Fig. 3-4C, Fig. 3-5). Flexion starts immediately before touch down from maximal extension (approx. -70° from long axis of scapula), and full flexion (approx. -125° from long axis of scapula) is reached shortly after mid contact. In the second half of the contact phase the gleno-humeral joint extends slowly and continues this extension for most of the swing phase until it reaches full extension again. During steady-state locomotion in *C. didactylus*, humeral abduction from the scapular plane is moderate (maximal amplitude during contact approx. 13°).

Table 3-4: Six DOF data for the elements of the pectoral girdle. All translations were set to zero at the instant of touch down. Translations are reported in cm, rotations in degrees.

	Touch down (± s.d.)	Lift off (± s.d.)	Contact amplitude	Maximal amplitude
1st thoracic vertebra				
x-axis translation	0	-1.0 (± 2.1)	1.0	3.2
y-axis translation	0	-0.9 (± 0.9)	0.9	1.1
z-axis translation	0	1.2 (± 1.7)	1.2	4.3
x-axis rotation	-0.4 (± 3.5)	1.0 (± 4.0)	1.4	1.9
y-axis rotation	-4.6 (± 6.2)	11.5 (± 5.7)	16.2	20.5
z-axis rotation	-10.1 (± 4.0)	-9.8 (± 2.6)	0.3	3.0
Scapula center of rotation/scapula				
x-axis translation	0	-0.3 (± 0.2)	0.3	0.5
y-axis translation	0	-0.7 (± 0.1)	0.7	0.8
z-axis translation	0	0.1 (± 0.3)	0.1	0.4
x-axis rotation	-26.3 (± 8.1)	-18.6 (± 9.2)	7.7	10.7
y-axis rotation	-13.5 (± 3.2)	-13.1 (± 5.0)	0.4	7.6
z-axis rotation	71.7 (± 12.9)	39.3 (± 8.7)	32.4	35.9
Shoulder joint/humerus				
x-axis translation	0	0.1 (± 0.1)	0.1	0.2
y-axis translation	0	0.0 (± 0.1)	0.0	0.1
z-axis translation	0	0.0 (± 0.1)	0.0	0.0
x-axis rotation	3.3 (± 7.2)	-20.3 (± 4.6)	23.6	23.8
y-axis rotation	2.9 (± 1.2)	-10.4 (± 6.2)	13.3	18.7
z-axis rotation	-77.4 (± 11.4)	-117.1 (± 18.2)	39.7	57.7
Sterno-clavicular joint/clavicle				
x-axis translation	0	-0.3 (± 0.2)	0.3	0.4
y-axis translation	0	0.4 (± 0.2)	0.4	0.4
z-axis translation	0	-0.4 ± (0.2)	0.4	0.6
x-axis rotation	83.8 (± 16.4)	20.6 (± 21.1)	63.2	68.2
y-axis rotation	-22.0 (± 2.4)	-9.0 (± 1.3)	13.0	19.6
z-axis rotation	-43.7 (± 8.0)	-6.2 (± 7.7)	37.5	43.3

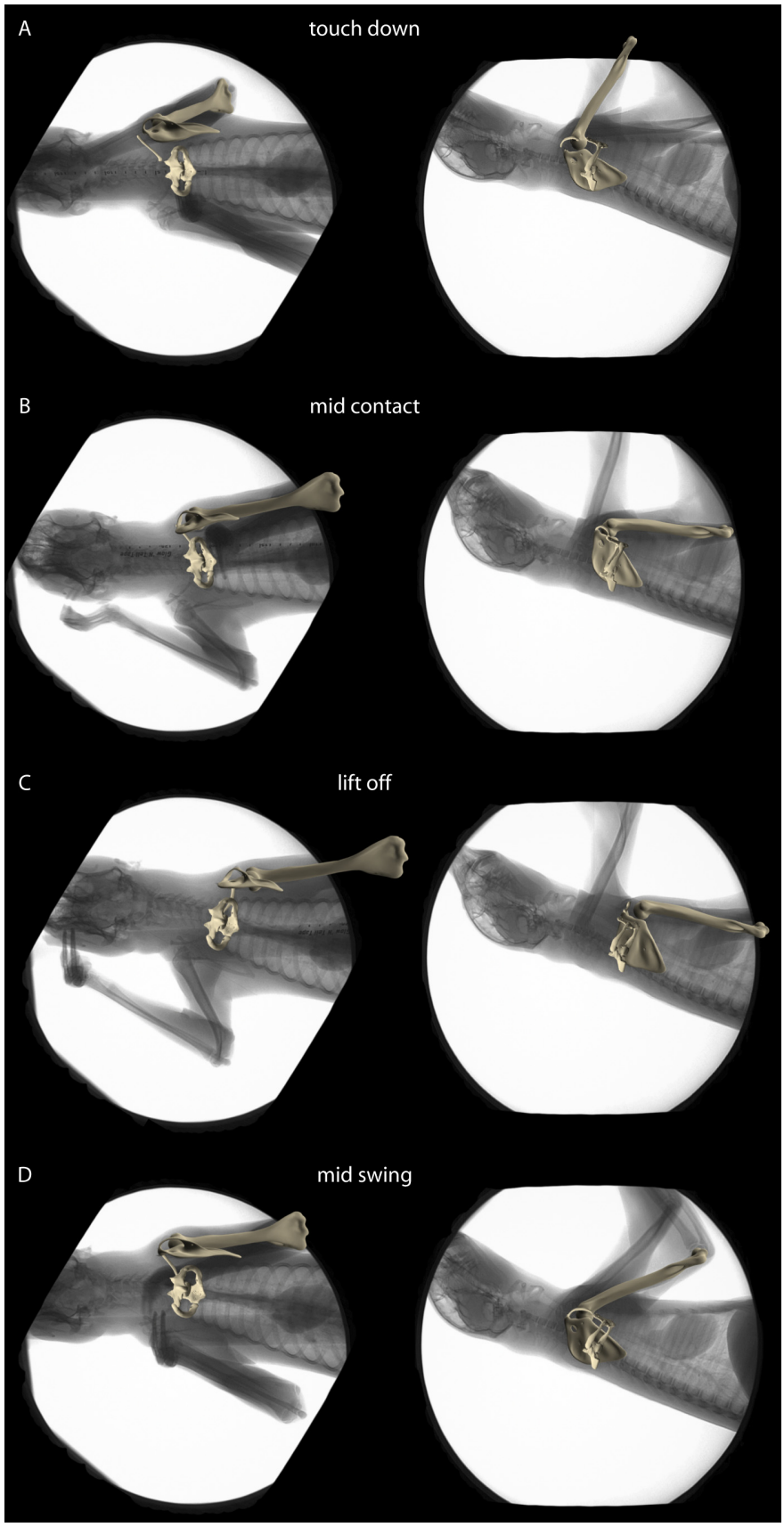

Fig. 3-5: Representative frames of instants of (A) touch down, (B) mid contact, (C) lift off, and (D) mid swing. X-ray image with bone model posed to match the x-ray shadow is shown for the dorso-ventral projection and the latero-lateral projection.

Movements of the clavicle

The sternal end of the clavicle translates up to 0.6 cm relative to the manubrium sterni (Table 3-2, Fig. 3-4D). These movements are facilitated by the connective tissue making up the sterno-clavicular articulation (SCA) (Fig. 3-3). At touch down, the clavicle is rotated approximately 84° about its long axis (rotation about *x*-axis in Fig. 3-4D) and protracted by about 22° (indicated by a negative value for rotation about *y*-axis). The acromio-clavicular joint is positioned more dorsal than the manubrium sterni (44° rotation about *z*-axis). During limb retraction rotation about the long axis decreases to about 20° and the clavicle is both retracted and depressed so that at lift off, the acromio-clavicular joint and the SCA are at the same height. It is noteworthy that caudal displacement of the acromio-clavicular joint is achieved not only by rotation about the *y*-axis, but also by the pronounced rotation about the long axis of the curved clavicle.

3D displacement of the elbow: effects of scapular and humeral motion

The displacement of the elbow is governed by both scapular and humeral motions, i.e., trajectories of elbow displacement differ markedly if scapular or humeral motion is 'muted' (Fig. 3-6A,D). Normal locomotion has a medio-lateral amplitude of displacement of the elbow of 2.5 cm relative to the 1st thoracic vertebra (Table 3-5, Fig. 3-6B). The amplitude of medio-lateral displacement is just 1.7 cm if all humeral translations and rotations in the gleno-humeral joint are turned off. The amplitude remains at 2.5 if scapular motion is turned off completely in the 'virtual experiment', however both the maximum and the minimum increase. The 'muting' of scapular abduction/adduction has almost no effect on elbow displacement as these movements are rather minor (Table 3-5; Fig. 3-6D). The turning off of scapular as well as humeral rotation about their repective long axes both increases the amplitude of medio-lateral displacement of the elbow to 3.1 cm. This means that the rotation about the long axis in the scapula and humeral abduction/adduction partly offset each other and observed medio-lateral displacement of the elbow is smaller (Fig. 3-6E). In sum, total abduction of the arm is determined by the combination of the scapula's position relative to the rounded rib cage (i.e., scapular rotation about the long axis and scapular protraction and retraction) and humeral abduction from the scapular plane.

Cranio-caudal displacement of the elbow relative to first thoracic vertebra is predominantly achieved by humeral retraction in the gleno-humeral joint (a decrease in cranio-caudal displacement from 14.4 cm to 9.0 cm if humeral motion is turned off). Scapular retraction also contributes to the amplitude of elbow displacement as the amplitude decreases to 10.6 cm if scapula motion is 'muted' virtually in the 3D animated reconstruction (Fig. 3-6C). Scapular abduction/adduction and scapular rotation about its long axis has only little influence on the cranio-caudal amplitude of the 3D trajectory of displacement of the elbow (Table 3-5). Turning off humeral abduction/adduction slightly increases the cranio-caudal amplitude of elbow displacement.

Dorso-ventral displacement of the elbow is largely determined by humeral retraction (Table 3-5) with only little influence of the scapula. However, as evident in the graph (Fig. 6B) only the combination of both movements effectively displaces the elbow in dorso-ventral direction. Scapular abduction/adduction as well as rotation about its long axis again has very limited influence on the displacement of the elbow. The amplitude of dorso-ventral displacement is slightly reduced if humeral abduction/adduction is 'muted' in our 'virtual experiment' (from 10.3 cm to 9.4 cm).

DISCUSSION

Significance of scapular motion

Humeral retraction has been shown to be responsible for over 70% of stride length in two-toed sloths (Nyakatura et al., 2010). Accordingly, most of the cranio-caudal displacement of the elbow observed in this study is generated by retraction of the humerus in the gleno-humeral joint. However, despite emphasized influence of humeral motion to the displacement of the hand, the overall pattern of forelimb movement is very similar to pronograde mammals: forelimb movement in sloths takes place at the most proximal pivot possible through the fixing of distal limb joints and retraction of the scapula as the most proximal element (Nyakatura et al., 2010).

Scapula movement has been demonstrated via x-ray motion analysis to be an important aspect of forelimb kinematics during quadrupedalism in therian mammals (Jenkins, 1974; Whitehead and Larson, 1994; Fischer, 1994; Fischer et al., 2002; Fischer and Blickhan, 2006). The six DOF of scapular motion quantified here correspond to

previous qualitative descriptions of three dimensional scapular movement in claviculate arboreal and terrestrial pronograde therian mammals (Table 3-6), but differ from the 3D data quantified in walking cats and the qualitative description of shoulder movements in brachiating spider monkeys (Jenkins et al., 1978; Boczek-Funke et al., 1996). Whereas in the aclaviculate cat there is an effective rotation about the scapular long axis of less than 2° (Boczek-Funke et al., 1996), rotation about the long axis of the scapula during the contact phase of sloths has an approximate 8° amplitude (Table 4). The observation of movements that are largely restricted to the parasagittal plane in aclaviculate mammals is also in line with results from an analysis of rats with excised clavicles (Jenkins, 1974). But the scapula, as in the cat, remains slightly abducted throughout the stride cycle in the sloth and has only a small amplitude during the contact phase (less than 1°; Table 3-4). Motions of the shoulder blade during quadrupedal suspensory locomotion of the sloth are also in stark contrast to the motions described for brachiating spider monkeys (Jenkins et al., 1978). Spider monkeys maintain the scapula in a distinct dorsal orientation and the fossa glenoidalis faces cranially throughout the contact of the limb (Jenkins et al., 1978). In similar fashion as in the claviculate pronograde species investigated (Jenkins and Weijs, 1979; Schmidt and Krause, in press), a relatively round thorax permits the scapula in the two-toed sloth to effectively slide dorsally during forelimb protraction from it's almost parasagittal orientation at lift off. This is accomplished via a combination of protraction, long-axis rotation and abduction/adduction. The more dorsal orientation of the scapula at touch down inevitably results in a more laterally facing fossa glenoidalis. The orientation of the scapula at touch down has an abducting effect on the whole forelimb. This indicates that, despite the adoption of obligatory quadrupedal suspensory locomotion, the basic kinematics of the scapula remained practically unchanged. The only striking differences are that scapular retraction sets in later in the contact phase and the initial period is marked by humeral retraction alone in sloths.

Overall mobility of the shoulder in mammals results always from a combination of mobility in the gleno-humeral joint and mobility of the pectoral girdle, which is determined by the shape of thorax, relative position of the scapula, and configuration of the clavicle (Chan, 2007a). However, mobility may not be confused with in vivo

movement during linear locomotion, which should only represent a fracture of overall mobility.

Table 3-5: Mean maximal and minimal 3D displacements of the elbow relative to the 1st thoracic vertebra during normal locomotion and 'virtual experiments' to assess the displacing effect of the motion of the scapula and humerus. All values are reported in cm. Amplitude is also expressed relatively in percent of total forelimb length (% tll; average length in both individuals: 49.2 cm incl. scapula).

	Max	Min	Amplitude	% tll
I. medio-lateral displacement				
Normal locomotion (mean)	8.3	5.9	2.5	5.1
Without total humeral motion	8.7	7.0	1.7	3.5
Without total scapular motion	8.9	6.4	2.5	5.1
Without scapular abduction/adduction	8.3	5.9	2.5	5.1
Without scapular long-axis rotation	9.1	6.0	3.1	6.3
Without humeral abduction/adduction	8.7	5.5	3.1	6.3
II. cranio-caudal displacement				
Normal locomotion (mean)	11.7	-2.8	14.4	29.3
Without total humeral motion	6.0	-3.0	9.0	18.3
Without total scapular motion	7.8	-2.8	10.6	21.5
Without scapular abduction/adduction	11.6	-2.9	14.6	29.7
Without scapular long-axis rotation	11.4	-2.8	14.2	28.9
Without humeral abduction/adduction	12.2	-2.9	15.2	30.1
III. dorso-ventral displacement				
Normal locomotion (mean)	15.7	5.4	10.3	20.9
Without total humeral motion	15.9	14.5	1.4	2.8
Without total scapular motion	15.6	9.4	6.2	12.6
Without scapular abduction/adduction	15.7	5.3	10.4	21.1
Without scapular long-axis rotation	15.8	5.0	10.9	22.2
Without humeral abduction/adduction	15.2	5.7	9.4	19.1

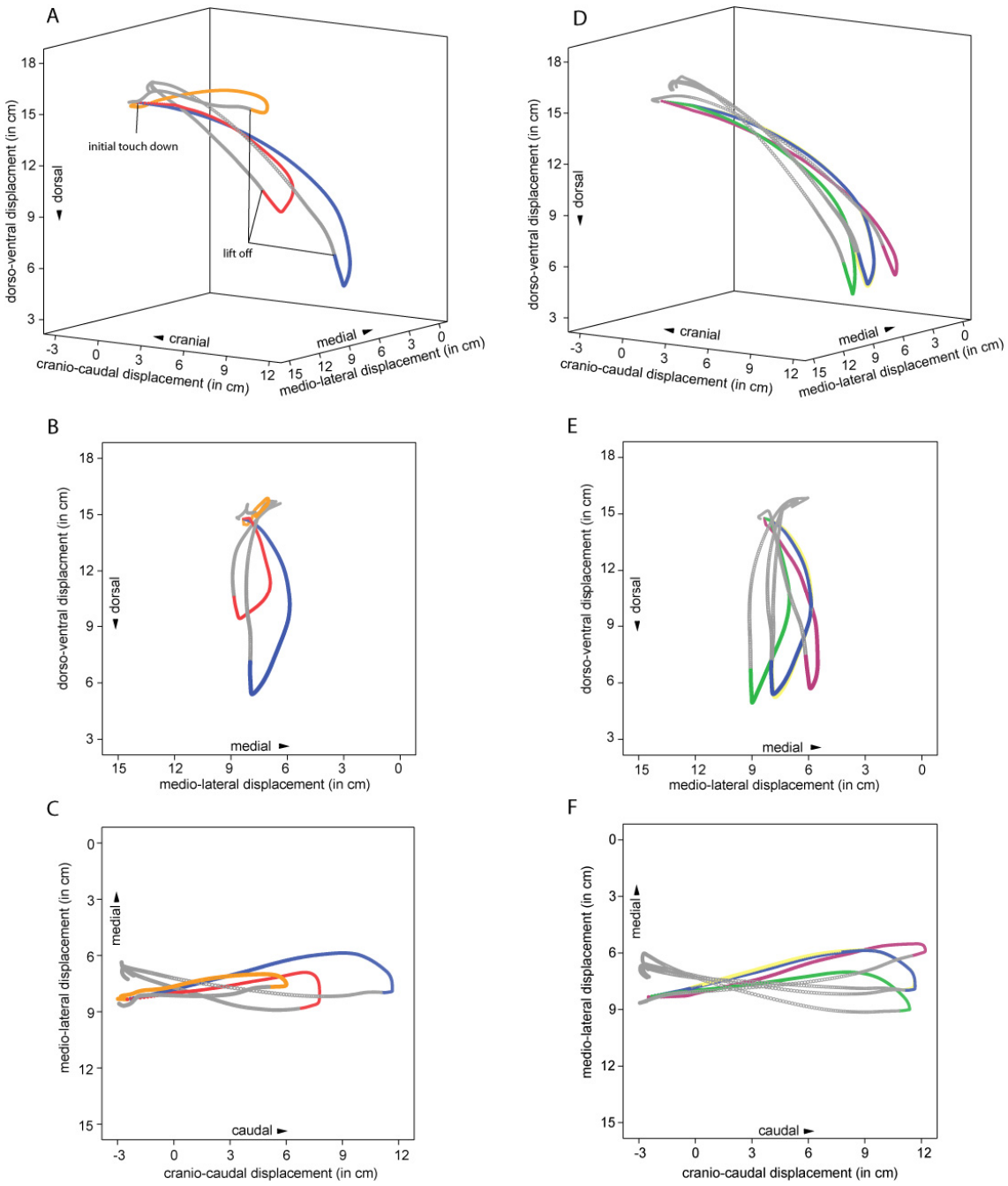

Fig. 3-6: 3D displacement of the right elbow and the influence of scapular and humeral motion. A, D: 3D trajectories of the elbow shown for normal locomotion (blue), without humeral motion (orange), without scapular motion (red), without scapular abduction/adduction (yellow – almost completely covered by blue trajectory, i.e. almost identical), without scapular rotation along its long axis (green), and without humeral abduction from the scapular plane (purple). Swing phases are shown in gray. B, E: depict a 2D projection of the trajectory onto the transversal plane as seen from caudal. C, F: 2-D projection of the trajectory onto the frontal plane as seen from ventral.

When thorax width is compared to the dataset of different primate taxa analyzed by Kagaya et al. (2008), the sloth has a smaller width (log thoracic width 1,63 mm; log body mass 0.93 kg; cf. Kagaya et al., 2008). The small diameter and rounded shape of the thorax of sloths emphasizes the 3D excursions of the comparably small scapula during forelimb protraction. Based on x-ray motion analysis, abduction generated from scapular movement seems to be emphasized in the investigated small quadrupedal primates that likely resemble the ancestral anatomical condition regarding the shape of the thorax and the position of the scapula (Schmidt and Krause, 2007). Nevertheless, overall great mobility of the pectoral girdle as well as great mobility in the gleno-humeral joint, probably used in non-locomotor behavior, has been shown for a large dataset of primates (Chan, 2007a; 2007b). The combination of a small scapula and a rounded, small-diameter thorax of sloths represents a solution to the functional demand of extensive forelimb mobility in the arboreal context. Additionally, configuration of the shoulder joint may permit extensive medio-lateral excursions of the limb by abduction of the humerus from the scapular plane as present in most Anthropoidea during locomotion (Schmidt and Schilling, 2007). Although limb abduction during quadrupedal suspensory locomotion of sloths is small, considering the morphological and kinematic data presented here we suggest that in sloths both modes are present (i.e., abduction via scapular movements and via humeral abduction from the scapular plane). Forelimb abduction in early contact phase is accomplished by a combination of an inward rotation of the scapula along its long axis with a simultaneous cranial displacement of the gleno-humeral joint by protraction of scapula. At this time the humerus remains approximately in the scapular plane. During the later contact phase outward rotation of the scapula along its long axis adducts the elbow. This adduction is offset by humeral abduction from the scapular plane, which displaces the elbow lateral (please compare green and purple trajectories in Fig. 3-6). The resulting trajectory is has a small medio-leteral amplitude. Interestingly, the combination of a small scapula and a rounded thorax is also present in Loridae (Strauss and Wislocki, 1932; Schmidt, 2008), i.e., in other deliberate arboreal species unable to jump and with the need for increased forelimb mobility, especially for bridging, due to the discontinuous nature of their arboreal substrates.

In terrestrial quadruped therian mammals the scapula usually dominates forelimb propulsion and, especially in cursorial species, limb movement is restricted more or less to the parasagittal plane, with the scapula orientated lateral to the thoracic wall (Fischer and Blickhan, 2006). A relatively short scapula on the one hand decreases its effect in displacing distal elements of the limb in cranio-caudal direction, but on the other hand facilitates more pronounced 3D motions along the thoracic wall (e.g., from the lateral, retracted orientation at lift off to the more dorsal, protracted position at touch down). The relatively short scapula thus facilitates displacements of the limb in the medio-lateral direction through 3D displacements of the limb provoked by marked 3D motions relative to the thorax.

In this context it is important to note that the scapula, as a newly propulsive skeletal element added proximally to the forelimb in therian mammals, has an independent developmental program from the serially homologous elements of the fore- and hindlimbs (stylopod, zeugopod, and autopod) (Huang et al., 2000; Schmidt and Fischer, 2009). Variation of overall configuration and relative proportions of the serially homologous elements in the fore- and hindlimbs might be constrained by shared developmental programs (Schmidt and Fischer, 2009), but – thanks to its individual developmental program – morphology of the scapula can probably evolve more freely according to demands that act specifically on the forelimbs. Accordingly, the scapula has been found to be the most variable element in both fore- and hindlimbs (Schmidt and Fischer, 2009).

Clavicular motion

The clavicle guides all scapular movements along the thoracic wall(Jenkins, 1974). With the distancebetween sternum and acromion kept relatively constant by the clavicle, the trajectory ofthe gleno-humeral joint of the sloth describes an arch during the contact phase of a stridecycle. The same phenomenon has been described qualitatively for other claviculate therian mammals (rat: Jenkins, 1974; opossum: Jenkins and Weijs, 1979; small quadrupedal primates Schmidt and Krause, in press). Voisin argued that the internal curvature of the clavicle of gibbons (*Hylobates*) and spider monkeys (*Ateles*) facilitates this bone's function as a crank during arm flexion and helps the glenoid cavity of the scapula to effectively rotate cranially (Voisin, 2006).

The author further proposes that internal curvature of the clavicle may be linked to suspensory postures in these primates (Voisin, 2006). The strong internal curvature of the clavicle in sloths supports this notion.

In pronograde mammals the clavicle is thought to function as a 'spoke' and a 'strut' (Jenkins, 1974) and thus to transmit compressive forces between the limb and the trunk. The causal theory of histogenesis put forward by Pauwels (1960) predicts that connective tissue differentiates according to its loading regime. Under compressive loads fibrocartilage differentiates within tendons and ligaments (Benjamin and Ralphs, 1994). The absence of fibrocartilage in the SCA in two-toed sloths demonstrates that not only does tensile loading act on the distal limbs (Patel and Carlson, 2008), but that tension is also transferred to the thorax (Fig. 3-4). Collagen fibers are differentiated in the SCA of *C. didactylus* in the same way as Pauwels (1960) predicts for a tensile loading regime. It is intriguing to hypothesize that ossification remains incomplete at the sternal end of the clavicle (a bone that is part of the dermal skeleton) during ontogeny because of the lack of a specific stimulus (here compressive load) to differentiate an articulating face towards the manubrium sterni. A SCA composed of irregular dense fibrous connective tissue not only provides passive stability against translations and rotations (Ralphs and Benjamin, 1994) but complies with the added demand for increased pectoral girdle mobility in a discontinuous habitat. The absence of elastic fibers negates the possibility of elastic energy storage, although the sternal end of the clavicle translates as far as 0.8 cm cranial from its lift off position. In armadillos and the tamandua the clavicula does not articulate directly with the manubrium sterni either, and the SCA is made up of fibrous connective tissue here too (Miles, 1941; Taylor, 1978). However, it is not known whether fibrocartilage tissue differentiates as an adaptation to compressive load in these species. A comparative study in Xenarthra would yield further insights into the evolution of this interesting trait.

Summary and conclusion

The adoption of deliberate, non-agile locomotion within a discontinuous habitat made 3D limb excursions necessary, e.g., to facilitate bridging of gaps between branches or to reach for food. Sloths accomplish increased forelimb mobility through a

Table 3-6: Published data on scapular movements in mammals. Quantification of 3D motion is rare. Please note that the scapular protraction and retraction of the two-toed sloth is very similar to quadrupedal mammals of similar weight. All weights according to Apfelbach and Grzimek (1997). *:determined from figure 3 in Rocha-Barbosa et al. 1996); **: determined from figure 2 in Whitehead and Larson (1994); ***:when projected into the parasagittal plane as in Nyakatura et al. (2010); ****: during brachiation

Species	Weight	Mean amplitude of protraction/retraction during contact phase	Data on 3D motion	References
Monodelphis domestica (Didelphidae)	0.05 – 0.075 kg	59°		[5]
Microcebus murinus (Primates)	0.05 – 0.1 kg	48°±6°	Qualitative description	[5,34, 37]
Tupaia glis (Scandentia)	0.05 – 0.180 kg	59°		[5, 38]
Dasyuroides byrnei (Dasyuridae)	0.1 – 0.12 kg	44°		[5]
Rattus norvegicus (Rodentia)	0.14 – 0.4 kg	60°		[5, 23]
Saguinus Oedipus (Primates)	0.35 – 0.45 kg	49°±6°	Qualitative description	[32, 37]
Galea musteloides (Rodentia)	0.4 – 0.5 kg	60°		[5]
Cavia porcellus (Rodentia)	0.6 – 1.0 kg	57° *		[39]
Saimiri scuireus (Primates)	0.365 – 1.135 kg	55°±4°	Qualitative description	[37, 40]
Procavia capensis (Hyracoidea)	1.8 - 5.4 kg	53°		[3, 5]
Eulemur fulvus (Primates)	≈ 3.0 kg	51°±9°	Qualitative description	[34, 37, 41]
Didelphis virginiana (Didelphidae)	2.0 – 5.5 kg	40°	Qualitative description	[28]
Cercopithecus aethiops (Primates)	2.5 – 6 kg	28° **		[24]
Felis catus f. domestica (Carnivora)	3.0 – 8.0 kg	41°	3D movements quantified	[25, 41]
Choloepus didactylus (Xenarthra)	4.0 – 10.0 kg	32° (34° ***)	3D movements quantified (6 DOF)	[16], this study
Ateles geoffroyi/ Ateles paniscus (Primates)	7.5 -8.4 kg / 7.75 – 9.5 kg	15° ****	Qualitative description	[26]
Canis lupus f. familiaris (Carnivora)	15 – 80 kg	35°±4°		[7]
Capra hircus (Artiodactyla)	25 – 70 kg	41°±7°		[7]
Equus przewalski f. caballus (Perissodactyla)	≈ 350 kg	25°±5°		[7]
Loxodonta africana (Proboscidea)	3500 – 7000 kg	15°±5°		[7]

combination of three morphological specializations, whereas the overall 3D kinematic pattern of the pectoral girdle remains remarkably unchanged, when compared to pronograde quadruped therians with developed clavicles (Jenkins, 1974; Jenkins and Weijs, 1979; Schmidt and Krause, in press). Morphological specializations at the pectoral girdle for 3D limb excursions are i) a relatively short scapula in combination with a round, small diameter thorax, ii) maximized mobility at the SCA, and iii) an internally curved clavicle that allows effective cranial displacement of the shoulder.

Results of this study somewhat contradict Miller's (1935) notion that sloths may have the strangest mode of progression amongst mammals. In the two-toed sloth morphological specializations facilitate pronounced forelimb mobility necessary in the discontinuous 3D habitat. But, increased forelimb mobility through morphological specialization at the same time allowed the retention of the plesiomorphic kinematic pattern.

ACKNOWLEDGEMENTS

The authors acknowledge that this study would not have been possible without the hugely informative XROMM course held by the developers EL Brainerd, SM Gatesy and others at Brown University, RI, USA in August 2009. We thank R. Petersohn for technical assistance and the curators of the museums for access to their collections. Dirk Arnold assisted the preparation of the specimens. CT scans were generously provided by Alexander Petrovitch. Heiko Stark developed helpful software. Sabine Moritz and Alexander Stössel were the authors of insightful critique of the manuscript. Lucy Cathrow thoroughly edited the language of the final draft. The manuscript profited from the helpful comments of five anonymous referees. Supported by the German Science Foundation (DFG Fi 410/11-1 to MSF).

- Chapter 4 -

Functional morphology of the muscular sling at the pectoral girdle in tree sloths: convergent morphological solutions to new functional demands?

John A. Nyakatura & Martin S. Fischer

Abstract

Recent phylogenetic analyses imply a dipyhly of tree sloths and a convergent evolution of the obligatory suspensory locomotion. In mammals the extrinsic shoulder musculature is forming a muscular sling. The muscular sling has two major functions: suspension of the weight of the thorax between the forelimbs and movement of the proximal forelimb elements during locomotion. Due to the inverse orientation of the body in regard to the gravitational force, the muscular sling as configured in pronograde mammals is unsuited to suspend the weight of the thorax in sloths. We here review the muscular topography of the shoulder in *Choloepus didactylus* and *Bradypus variegatus* in the light of presumably convergent evolution to adapt to the altered functional demands of the inverse orientation of the body. In a second step we venture to deduce the effect of the shoulder musculature of *C. didactylus* during locomotion based on the published 3D kinematics. Finally, we assess likely convergences in the muscular topography of both extant sloth lineages. Muscular topography of the shoulder in *C. didactylus* is altered from the plesiomorphic condition of pronograde mammals, whereas the shoulder in *B. variegatus* more closely resembles the general pattern. Overall kinematics as well as the muscles suitable for pro- and retraction of the forelimb was found to be largely comparable to pronograde mammals in *C. didactylus*. We conclude that most of the peculiar topography of extrinsic forelimb musculature can be attributed to the inverse orientation of the body. These characteristics are very similar in both genera and we found only details were different morphological solutions evolved to satisfy the new functional demands. We suggest that the long common phylogeny canalized the spectrum of possible solutions, and digging adaptations of early xenarthrans posed morphological constraints that likened suspensory postures. The data of this study, including muscle maps, will be helpful to infer locomotor characteristics of fossil sloths.

INTRODUCTION

Recent morphological and molecular phylogenetic studies point to a long history of independent evolution of the two lines leading to extant tree sloths and only a distant relationship between the two remaining extant genera *Choloepus* and *Bradypus* (Höss et al., 1996; Delsuc et al., 2001; Greenwood et al., 2001; Poinar, 2003; Gaudin, 2004; Pujos, 2007). Some of the molecular phylogenetic studies even make use of ancient DNA recovered from extinct forms (Höss et al., 1996; Greenwood et al., 2001; Poinar et al., 2003). Morphological and phylogenetic studies imply a convergent evolution of the quadrupedal suspensory posture and locomotion of modern sloths (Gaudin, 2004; Gaudin and McDonald, 2008).

In comparison to monotremes, the therian pectoral girdle is not rigid but extensively mobilized. A mobile and often even completely reduced clavicle represents the only remaining skeletal connection between the thorax and the forelimbs (e.g., Eaton, 1944). Hence, the extrinsic shoulder musculature has to fulfill two important roles during locomotion: a) suspend the weight of the thorax between the forelimbs and b) move the skeletal elements of the proximal forelimbs (i.e., scapula and humerus) (e.g. Jenkins and Weijs, 1979; Carrier et al., 2006). In pronograde therian mammals the former is achieved by the extrinsic shoulder musculature forming a 'musclular sling' (Davis, 1949), which is composed of three primary muscles: The m. rhomboideus, the m. serratus ventralis and the m. pectoralis. Specifically the m. serratus ventralis thoracis has been deduced from its attachment sites and orientation to predominantly or even entirely being responsible for the support of body mass at the forelimbs. This hypothesis has been experimentally validated in an EMG study on trotting dogs (Carrier et al., 2006), i.e., in an aclaviculate mammal adapted for sustained running. However, because of the lines of action of the muscles forming the muscular sling, these muscles are at least partly unsuited to support body mass at the forelimbs in the quadrupedal suspensory posture of sloths unless profound morphological changes would have taken place during the evolution of modern sloths (Fig. 4-1).

Furthermore, whereas in aclaviculate mammals movements of the scapula are mostly restricted to the parasagittal plane, scapular movements are much more complex in claviculate therians (Jenkins, 1974; Schmidt, 2002; Nyakatura and Fischer, 2010). The orientation of the proximal forelimb elements relative to the thorax changes

considerably during the contact phase of a limb. Thus different muscles of the 'muscular sling' could be suitable to support body weight at the forelimbs at different instants of the contact phase. Since sloths have highly mobile forelimbs similar to primates (Grand, 1972; Mendel, 1985), the three-dimensional kinematic data of the shoulder region of sloths from high-speed x-ray recordings (Nyakatura et al., 2010; Nyakatura and Fischer, 2010) provide an adequate basis to investigate the muscular topography of two toed sloths (Xenarthra: *Choloepus didactylus*, Linné 1758) in order to improve our understanding of the function of the 'muscular sling' in sloths.

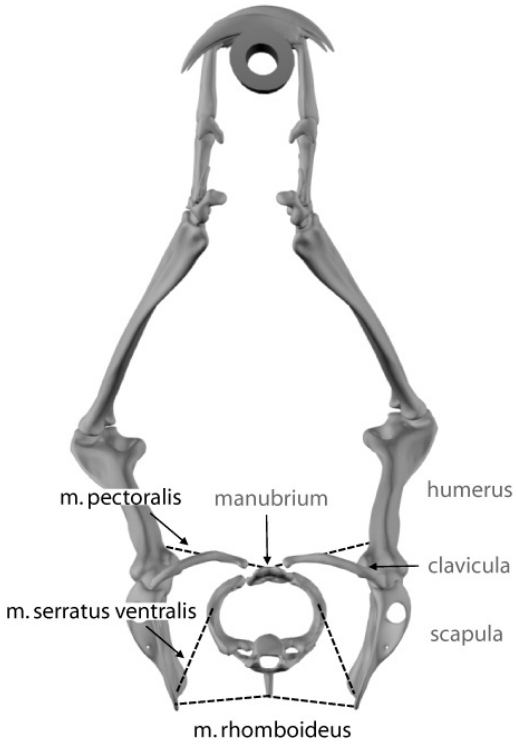

Fig. 4-1: Frontal view of the orientation of the limbs in relation to the thorax in *C. didactylus* reconstructed after x-ray images. Dotted lines represent primary muscles of the 'muscular sling' in the pectoral girdle of a generalized pronograde therian mammal. Only the first thoracic vertebra, rib, and the frontal part of the manubrium sterni are shown. There are no articulating surfaces in the sternoclavicular joint (see text). M. serratus ventralis and m. rhomboideus are unsuited to suspend the thorax between the limbs of *C. didactylus*.

Descriptions of the myology of the shoulder in two-toed sloths and three-toed sloths are often contradictory or incomplete and thus we find it necessary to review, confirm and extend available anatomical description of the shoulder girdle.

In this publication we chose to use a three step approach. First, we want to document myological topography of the extrinsic and intrinsic shoulder musculature of *C.*

didactylus and *B. variegatus* and identify similarities and differences. Second, we want to use the *in vivo* three-dimensional (3D) kinematic data of skeletal shoulder elements during steady-state locomotion of *C. didactylus* to interpret the myology regarding its role in weight suspension of the thorax and movement of the proximal skeletal elements of the forelimbs. And finally, we want to identify possible convergent solutions to the functional demands in regard of the generation of propulsion and weight bearing at the shoulder in the two distantly related modern sloth lineages.

Obviously this study would greatly benefit if the motion analysis could have been performed for both genera. But, *Bradypus* is not held captive in Europe and was not available for the x-ray motion analysis. Since the three *C. didactylus* individuals used the *in vivo* motion analysis (Nyakatura et al., 2010; Nyakatura and Fischer, 2010) were valuable loans from the Dortmund Zoo, invasive EMG recordings were not aspired in this study. Hence, no direct evidence for muscle function is available. By integration of the detailed anatomical investigation with the high resolution 3D kinematics we gather indirect evidence to deduce the effect of muscles during locomotion. This means, we here venture a step of plausibility to address the question which muscles are adequate to fulfill the two primary roles of the extrinsic shoulder musculature during quadrupedal suspensory locomotion in *C. didactylus* during the course of a step cycle.

MATERIALS AND METHODS

All the experiments and procedures were registered with the Committee for Animal Protection of the State of Thuringia, Germany, and were conducted in accordance with its guidelines (Reg.-Nr.: 02-08/04).

Myological preparation

No sloths were sacrificed for this study. We received two frozen carcasses of adult female *C. didactylus* from zoos in Paris, France, and Dresden, Germany, respectively. Both specimens died a natural death and were available for the anatomical investigation. The subjects were formalin fixated after skin was removed. The specimen of *Bradypus* is from the anatomical collection of the Phyletisches Museum Jena (Mam 3842) and was conserved in alcohol. Unfortunately the species name of the specimen as well as its place and date of origin has not been documented, but the

specimen was undoubtedly determined as *B. variegatus* according to the identification key of Wetzel (1985). We carefully documented the different stages of the dissection with photographs and drawings. Muscles were identified using the criterion of innervation following nomenclature of Evans (1993) and according to earlier publications of myological description (*C. didactylus*: Humphry, 1869; Mackintosh, 1874; Lucae, 1882; Windle and Parsons, 1899; Miller, 1935; Mendel, 1985; *B. variegatus*: Humphry, 1869; Mackintosh, 1873; Windle and Parsons, 1899; Meincke, 1911; Miller, 1935).

X-ray motion analysis

The experimental setup for the high-speed x-ray motion analysis and the methodology of the x-ray reconstruction of moving morphology approach (XROMM; Brainerd et al., 2010) has been described extensively in previous publications (Nyakatura et al., 2010; Nyakatura and Fischer,2010). In short, three *C. didactylus* were trained to move along a simulated branch (wooden pole 4m long; 40mm in diameter) at their preferred speeds using positive motivation *via* food rewards. Locomotion was filmed with two synchronized high-speed x-ray cameras and an additional standard light camera (also synchronized) filming the scene at 300 frames per second. The two x-ray cameras were oriented at the dorso-ventral and the lateral perspective and the covered 3D space was calibrated with a 20cm x 12cm calibration object that has metal beads inserted at regular intervals. To obtain three dimensional kinematic data two subjects were trained to move along a motorized version of the simulated branch. We made use of the non-invasive, markerless XROMM method termed ‘scientific rotoscoping’ (Gatesy et al., 2010). This method combines reconstructions of skeletal elements from CT bone scans and the high-speed x-ray videos to realistically animate and measure the kinematics of internal skeletal structures. Quantitative date is available in previous publications (Nyakatura et al., 2010; Nyakatura and Fischer, 2010). We here will use qualitative description of the occurring movements based on the data of these studies.

RESULTS

Morphology

We here describe the morphology of the pectoral girdle in *C. didactylus* and compare it to *B. variegatus.* Often we found published literature incomplete or contradictory. In these cases we report opposing views.

Skeletal anatomy of pectoral girdle

The thorax of *C. didactylus* has 23-24 ribs, of which 12 are connected directly to the sternum. In craniad direction the thorax tapers considerably. The well developed clavicle does not have an articulating facet on its sternal end. Rather, the sterno-clavicular joint is composed of connective tissue between clavicle and manubrium sterni (see below). As described earlier this joint allows virtually all degrees of freedom, when the clavicle is stripped of attaching muscles (Mendel, 1985). The slightly curved clavicle articulates to the scapula in a small notch at the widely flared acromial process. Fused to the coracoid process the acromion forms an arch that is extended craniad beyond the humeral head. It provides prominent attachment sites for the m. trapezius, m. subclavius, and m. deltoideus. The scapula is thin and the spina scapulae is short and does not reach the vertebral border. The caudal border is characterized by a broad attachment site for the well developed m. teres major. The scapula is comparable small (Nyakatura and Fischer, 2010). The gleno-humeral joint is marked by a shallow fossa glenoidalis and round humeral head. There is a considerable incongruity between both articulating surfaces.

The thorax of *B. variegatus* has 14 ribs, of which 11 to 12 are connected directly to the sternum. As in *C. didactylus* the thorax of *B. variegatus* tapers considerably in cranial direction. The clavicle is rudimentary and covers only half of the distance from the acromion to the manubrium, and, as in *C. didactylus*, is connected to it by a ligament. In contrast to *C. didactylus* the coracoid process is not fused to the acromion in *B. variegatus*. Instead, another ligament connects the ends of these to bony elements (coraco-acromial ligament). The scapula of *B. variegatus* is comparable to that of *C. didactylus* in that it is also comparable small, the spina does not quite extend to the vertebral border, and there is a prominent attachment site of the m. teres major. As in *C. didactylus* there is considerable incongruity between the articulating surfaces of the fossa glenoidalis and the humeral head.

Extrinsic shoulder musculature

In *C. didactylus* the m. trapezius originates along the middle line of the neck between the occiput and an aponeurosis at the eights thoracic spine. The cervical and thoracic portions can be separated due to a large intramuscular hiatus of the dorsal fascia in the area dorsal to the fossa infraspinata of the scapula. M. trapezius pars thoracis inserts via the dorsal fascia along the proximal spina scapulae and parts of the margo dorsalis of the scapula, whereas the pars cervicis inserts along the whole length of the short spina scapulae, the flared acromion and dorso-lateral surface of the clavicle (Fig. 2).

In accordance to the description of Windle and Parsons (1899), the m. trapezius of *B. variegatus* in our specimen has similar topography as described here for *C. didactylus*, but does not reach the occiput. A cervical portion can also be distinguished from a thoracic one by a large intra-muscular hiatus. The muscle's origin extends from the lower five cervical spines to the sixth thoracic spine and it inserts along the whole length of the spina scapulae, the coraco-acromial ligamentum and the cranial aspect of the short clavicle. In contrast, Miller (1935) found no cervical portion in her specimen. In accordance with the specimen studied by Mackintosh (1973) and Windle and Parsons (1899), we found the most anterior fibers to continue into the clavicular head of the m. deltoideus (see below).

In *C. didactylus* m. rhomboideus is divisible into two parts. M. rhomboideus major arises from the last cervical and first three thoracic vertebrae. It inserts along the whole margo vertebralis of the scapula and is made up by parallel fibers that span the length of the muscle (Fig. 2). Anterior to this muscle we find a thin occipital portion (m. rhomboideus capitis) that was also present in the specimens studied by Lucae (1882) and Windle and Parsons (1899). It has its origin at the occiput and inserts at the superior angle of the shoulder blade. A third distinct portion under the m. rhomboideus major as described by Mackintosh (1874) is not found in our individuals in agreement with Lucae (1882).

In our specimen of B. variegates no occipital portion of the m. rhomboideus is present. This is in line with the findings of Mackintosh (1873) and Windle and Parsons (1899).

In *C. didactylus* m. latissimus dorsi (Fig. 5) arises from the fourth to seventh thoracic vertebrae, from the eleventh to fifteenth ribs, and from the fascia lumbodorsalis. The

muscle runs over the ventral border of the scapula and the long fibers converge towards the insertion. The attachment is on the medial side of the proximal humerus in a broad tendon distal to the tuberculum minus and medial to the well separated attachment site of the m. teres major (Fig. 3).

Similarly, the m. latissimus dorsi of our *B. variegatus* has its origin from the posterior half of the thoracic spines, the fascia lumbodorsalis and the fifth to twelfth ribs. It attaches to its common site at the medial side of the proximal humerus. As in *C. didactylus* the attachment is via a broad tendon, which is separated from the fleshy insertion of the m. teres major.

In *C. didactylus*, proximal to the insertion of the m. latissimus dorsi its fibers are inseparable from those of the m. dorso-epitrochlearis (Fig. 4-5). This comparable large parallel fibered muscle runs medially alongside the much more slender caput longum of m. triceps brachii on the dorsal side of the upper arm and inserts on the epicondylus medialis into the anterior ridge of the supracondyloid foramen. Due to its fleshy origin from the m. latissimus dorsi this muscle was identified as m. latissimus dorsi pars brachialis by Lucae (1882) and m. latissimo-olecranalis by Windle and Parsons (1899). However, it is innervated by nervus radialis and can thus be hypothesized to be a derivate of the m. triceps brachii.

The same muscle is, though present, much more slender in *B. variegatus*. As there is no supracondyloid foramen the muscle inserts at the supracondylar ridge. Our specimen is in line with that of Meincke (1911), but in contrast Mackintosh (1874) notes that the muscle takes origin at the triceps.

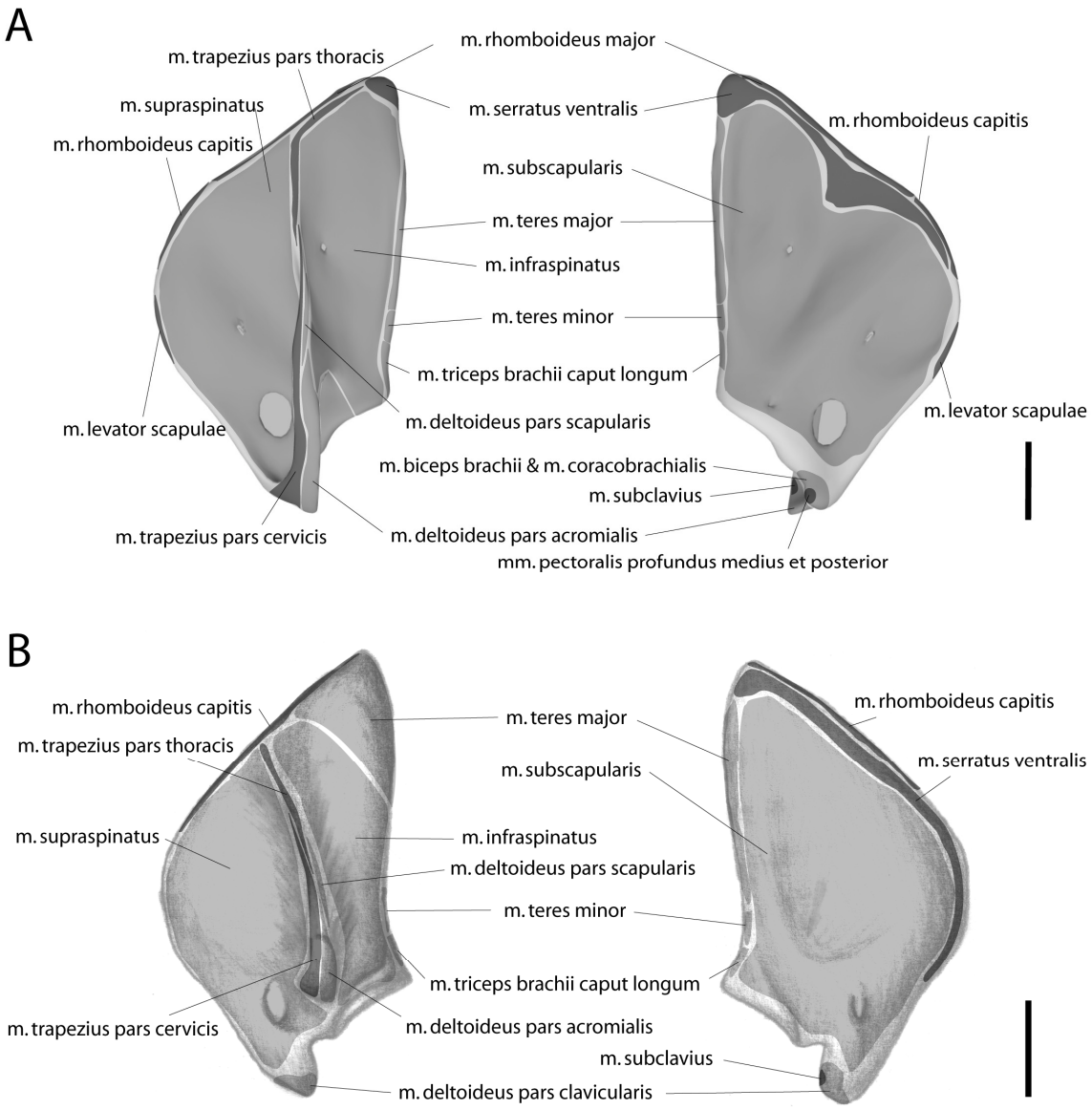

Fig. 4-2: Muscle maps of the shoulder musculature attaching to the scapula. A: *C. didactylus*; B: *B. variegatus*; left: lateral aspect of a left scapula; right: medial aspect of a left scapula. Dark grey: attachment areas of extrinsic shoulder musculature; light grey: attachment areas of intrinsic shoulder musculature. Scale bar = 2 cm. Further explanations see text.

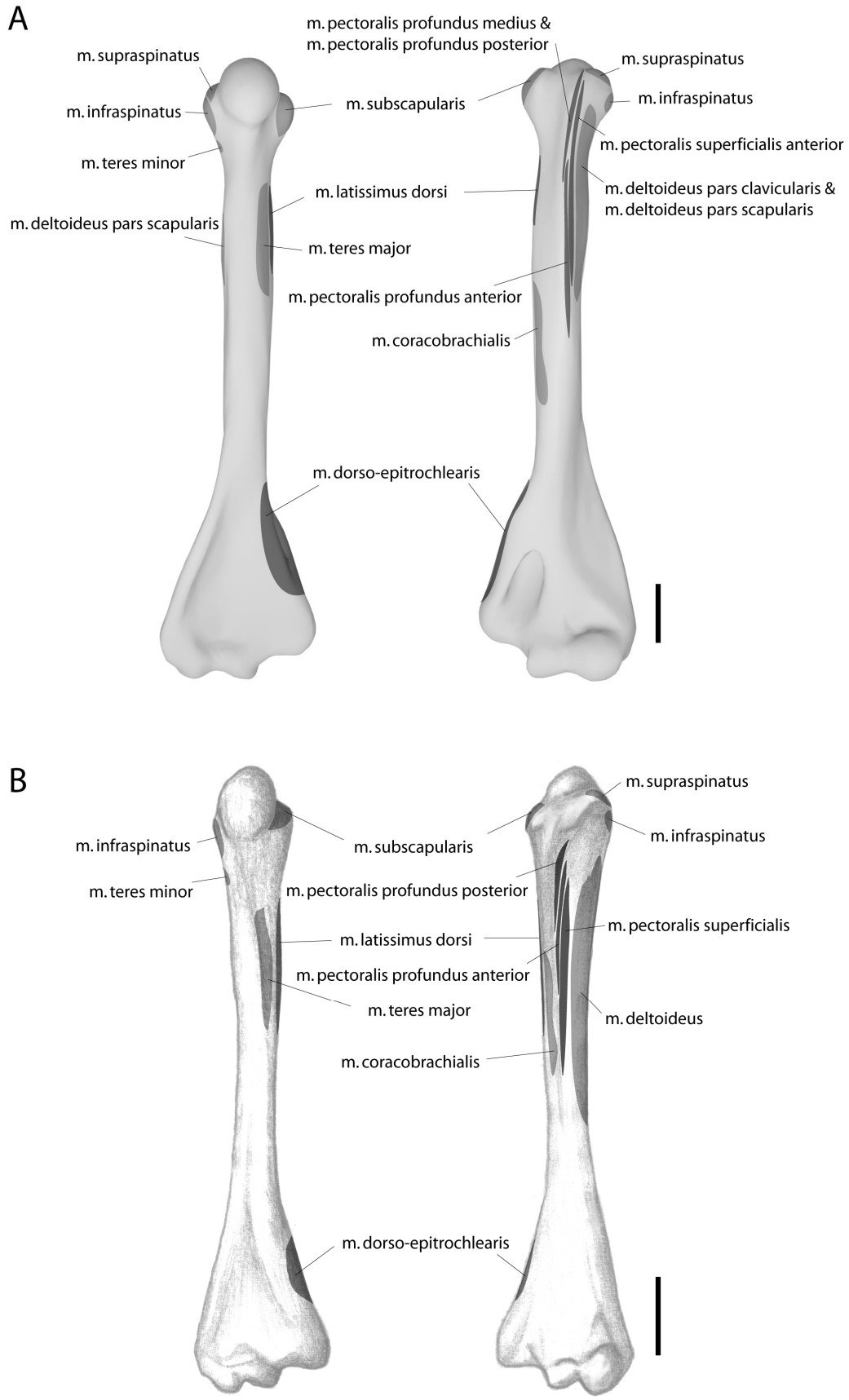

Fig. 4-3: Muscle maps of shoulder muscles attaching to the humerus. A: *C. didactylus*; B: *B. variegatus*; left: caudal aspect; right: cranial aspect. Dark grey: extrinsic shoulder musculature; light grey: intrinsic shoulder musculature. Scale bar = 2 cm. Further explanations see text.

The m. pectoralis - complex in *C. didactylus* is characterized by a complicated architecture (Fig. 4-5). We find five clearly separated portions all innervated by branches of n. pectoralis. Superficially m. pectoralis superficialis anterior arises from the cranial tip of the manubrium sterni and m. pectoralis superficialis posterior originates adjacent to the first slightly more caudal from the manubrium sterni and most cranial sternum. The former inserts in a short broad tendon on the tuberculum majus and along the proximal part of the pectoral crest of the humerus directly underneath the clavicular part of the m. deltoideus (Fig. 4-3). It was termed m. pectoralis minor by Lucae (1882), but m. pectoralis major by Miller (1935) and was not described by Mackintosh (1874). M. pectoralis superficialis posterior, composed of long parallel fibers, runs medially down the upper arm and eventually forms a common tendon with the m. deltoideus pars acromialis. This tendon subsequently joins the anterior belly of m. biceps brachii and inserts on the tuberositas of the proximal radius (Fig. 4-4). This superficial portion of the m. pectoralis was identified in all earlier descriptions and has also been termed gladiolar head or bicipital head of m. pectoralis by Mendel (1985) and Mackintosh (1874), respectively. We here refer to the general terminology used by Evans (1993). Beneath the m. pectoralis superficialis we find three layered portions of the m. pectoralis profundus in agreement with the observation of Miller (1935). The most superficial of which, the m. pectoralis profundus anterior, originates underneath the m. pectoralis superficialis posterior on the manubrium sterni and cranial sternum and attaches to the pectoral crest under m. pectoralis superficialis anterior, but extending more distally (to about half the length of the humerus). Its fibers are aligned in parallel. The m. pectoralis profundus medius has the broadest area of origin (the whole length of the sternum), its cranial origin lies underneath the origin of m. pectoralis profundus anterior, and its fibers converge distally. The muscle attaches more proximal then the previous with a short broad tendon on the proximal pectoral crest and the tuberculum majus of the humerus, on the shoulder joint capsule underneath the m. pectoralis superficialis anterior, and at the processus coracoideus of the scapula (Figs. 4-2, 4-3). The deepest layer, the m. pectoralis profundus posterior, arises from the eighth to eleventh rib, runs as a slender muscle underneath m. pectoralis profundus medius and joins its inserting tendon on the proximal side. The three parts of the m. pectoralis profundus have different

orientations, from approximately medio-lateral (m. pectoralis profundus anterior) to almost cranio-caudal (m. pectoralis profundus posterior).

In *Bradypus* the pectoralis is less complex. In our specimen we discerned three portions. Superficially the m. pectoralis superficialis originates from the whole length of the sternum including the manubrium. The fibers of this relatively flat sheet converge and insert along the pectoral crest at the proximal half of the humerus. It is important to note that although no insertion at the forearm is present as described above for *C. didactylus,* the m. pectoralis superficialis exchanges some fibers with anterior belly of the m. biceps brachii. M. pectoralis profundus comprises of two portions in *B. variegatus*. Cranially the m. pectoralis profundus anterior originates at the manubrium and attaches deep to the superficial sheet at the proximal pectoral crest. The m. pectoralis profundus posterior (named m. pectoralis quartus by Mackintosh, 1873 and Meincke, 1911) arises from the sixth to tenth ribs laterally from the m. pectoralis profundus anterior, but ventral to the m. lattisimus dorsi. In contrast to Humphry (1869) we did not find it originating from the m. rectus abdominis. It attaches proximal and deep to the other pectoral portions at the tuberculum majus of the humerus and the shoulder joint capsule. As in *C. didactylus* the portion that arises most caudally has the most proximal insertion.

In *C. didactylus* the m. serratus ventralis can be differentiated into a cervical and a thoracic part. The cervical part's origin extends from the third to seventh (and final) cervical transverse processes, whereas the thoracic part arises from the first eight ribs. Both parts insert on the margo vertebralis of the scapula. Or results correspond to Windle and Parsons (1899), but a cervical part was not found in the specimen of Miller (1935).

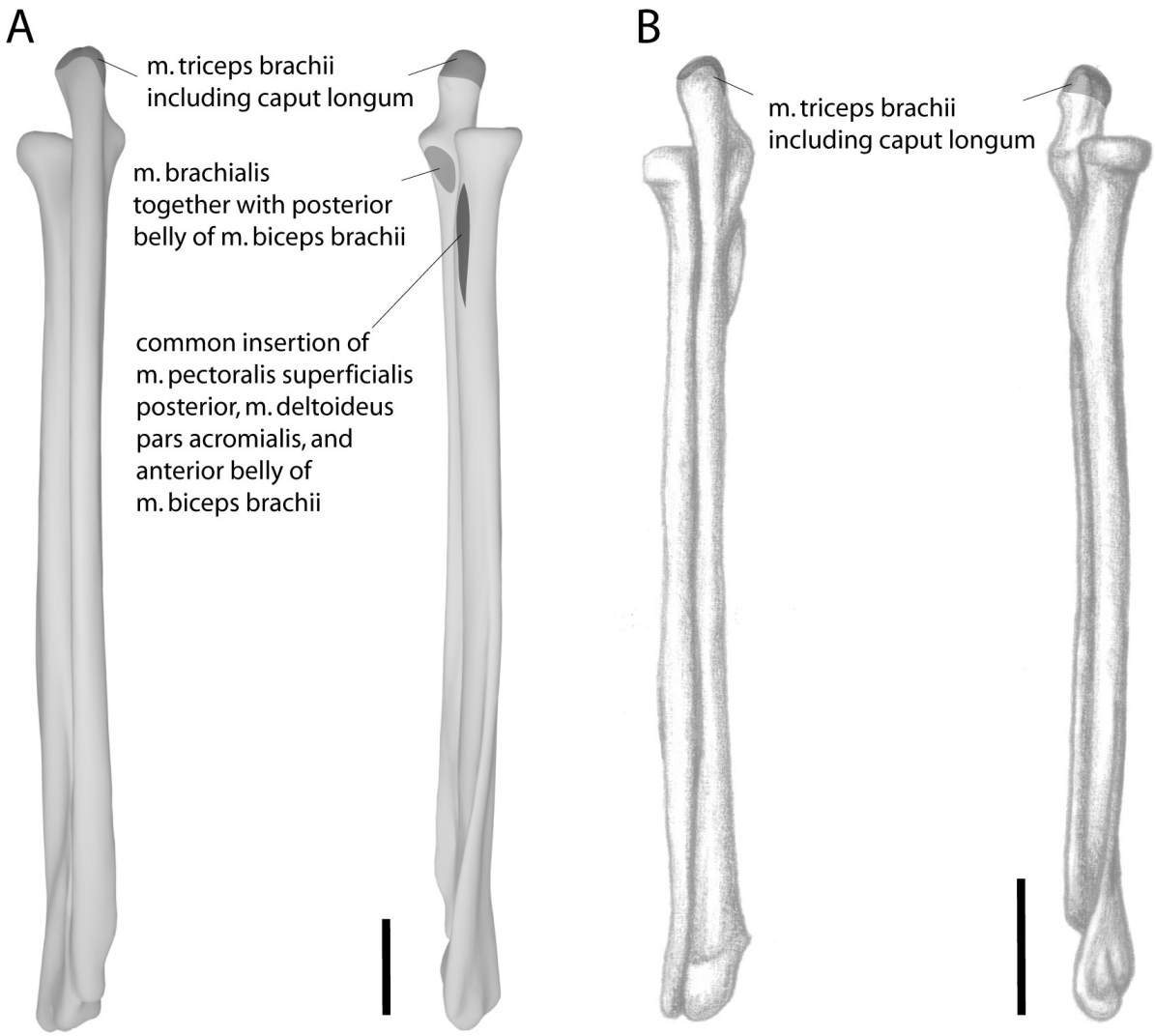

Fig. 4-4: Muscle maps of shoulder muscles attaching to the forearm. A: *C. didactylus*; B: *B. variegatus*; left: caudal aspect; right: cranial aspect. Dark grey: extrinsic shoulder musculature; light grey: intrinsic shoulder musculature. Scale bar = 2 cm. Further explanations see text.

In *B. variegatus* the m. serratus ventralis can also be differentiated into a cervical and a thoracic part. The cervical part however is only weakly developed and has its origin at the transversal processes of the three most caudal cervical vertebrae. The thoracic part arises from the first eight ribs as in *C. didactlus*. Both parts attach to the whole length of the vertebral border of the scapula. Miller (1935) did not mention a cervical part in the description of her specimen.

M. levator scapulae is a thin slender muscle that arises from the processus mastoideus and attaches to the margo cranialis of the scapula in *C. didactylus* (Fig. 2).

We did not find a corresponding muscle in *B. variegatus* in accordance with the earlier studies (Mackintosh, 1873; Windle and Parsons, 1899; Miller, 1935)

In *C. didactylus* a slender m. subclavius originates on the sternal end of the first rib and attaches to the inner border of the acromio-clavicular joint (Fig. 4-2).

The muscle is also present in *B. variegatus*. It has the same origin, but inserts at the coracoid process and at the under side of the clavicle.

M. sternomastoideus and m. cleidomastoideus attach to the processus mastoideus and expand to the sterno-clavicular articulation and the clavicle, respectively, in *C. didactylus* (Fig. 4-5).

We did not find these muscles separated in our specimen of *B. variegatus*. The muscle exchanges some fibers with the m. pectoralis superficialis. We could not determine the attachment site of the muscle due to damage of the specimen.

Intrinsic shoulder musculature

Although it was found to be restricted to its clavicular origin by Miller (1935), we find m. deltoideus separable into the usual three parts in *C. didactylus* in agreement with Mackintosh (1874) and Lucae (1882): partes clavicularis, acromialis, and scapularis. Whereas the clavicular and scapular parts have the common attachment sites at the deltoid crest of the humerus (Fig. 4-3) the m. deltoideus acromialis forms a common tendon with the m. pectoralis superficialis posterior and more distally joins the anterior belly of m. biceps brachii to have a common insertion on the radius (Fig. 4-4).

In *B. variegatus* the m. deltoideus is more difficult to be distinguished in the three parts arising from the spina scapulae, the acromion, and from the clavicle and coraco-acromial ligament, respectively. The most anterior fibers of the clavicular part continue into the cervical part of the m. trapezius. These were recognized as m. cephalo-humeral by Windle and Parsons (1899) and have also been described by Mackintosh (1873) and Meincke (1911). It is important to note that the acromial part of the m. deltoideus exchanges fibers with anterior belly of the m. biceps brachii.

In *C. didactylus* the m. supraspinatus arises from the fossa supraspinata and attaches to the tuberculum majus. M. infraspinatus originates from the fossa infraspinata and the spina scapulae and inserts distally adjacent to the aforementioned muscle on the tuberculum majus of the humerus as well (Figs. 4-2, 4-3). M. subscapularis, arising from the fossa subscapularis of the scapula, attaches to the tuberculum minus.

Mackintosh (1874) noted that its weight is about the same the combined weight of m. supraspinatus and m. infraspinatus (Figs. 4-2, 4-3).

These muscles are also present in a similar manner in *B. variegatus*.

In *C. didactylus* the m. biceps brachii arises in a single long flat tendon from the processus coracoideus of the scapula and splits into an anterior and a posterior belly (Fig. 4-5). The anterior belly joins the common tendon of m. deltoideus and m. pectoralis superficialis posterior and attaches to the tuberositas on the proximal radius (Fig. 4-4). The posterior belly fuses with m. brachialis and attaches to the ulna (Fig. 4-4).

In *B. variegatus* no coracoidal head is present and the origin is only on the humerus. We include it here, because the m. pectoralis superficialis and the m. deltoideus pars acromialis both exchange fibers with the anterior belly, which inserts on the inner side of the forearm at the ulna.

M. teres major is relatively large in *C. didactylus*, arises at the margo caudalis of the scapula, and inserts on the crista tuberculi minoris medial to the attachment site of m. latissimus dorsi (Fig. 4-3).

In *B. variegatus* this muscle is even more prominent. It not only has its origin on the margo caudalis of the scapula, but also on the posterior fossa infraspinata. As in *C. didactylus* it inserts on the crista tuberculi minoris medial to the latissimus dorsi.

M. teres minor was recognized by neither Mackintosh (1874) and Lucae (1882) nor Miller (1935) in *C. didactylus*, and was suggested to be fused to m. infraspinatus (Mackintosh, 1874). However, we find this small muscle arising from the distal margo caudalis of the scapula innervated by n. axillaris. It runs medial the long head of m. triceps brachii and inserts distal to m. infraspinatus on the tuberculum majus of the humerus (Fig. 4-3).

It is also found in our specimen of *B. variegatus* in accordance to Meincke (1911) and Miller (1935), although it was not mentioned by Mackintosh (1873).

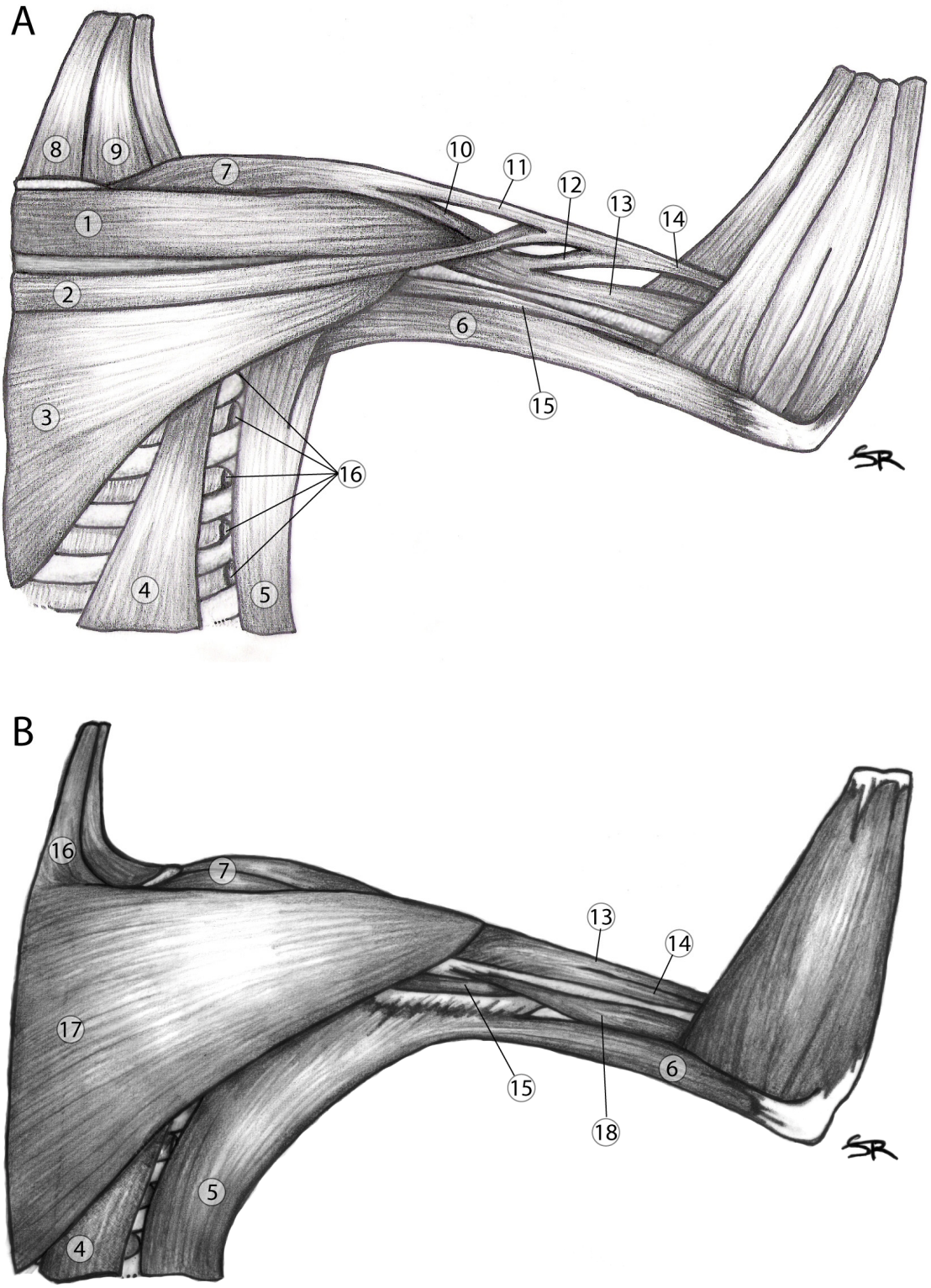

Fig. 4-5: Superficial muscles of the shoulder region of *C. didactylus* (A) and *B. variegatus* (B). Ventral aspect. 1: M. pectoralis superficialis anterior; 2: M. pectoralis superficialis posterior; 3: M. pectoralis profundus medius; 4: M. pectoralis profundus posterior; 5: M. latissimus dorsi; 6: M. dorso-epitrochlearis; 7: M. deltoideus; 8: M. sternomastoideus; 9: M. cleidomastoideus; 10: M. deltoideus pars clavicularis; 11: M. deltoideus pars acromialis; 12: M. biceps brachii anterior belly; 13: M. biceps brachii caudal belly; 14: Common tendon of 2, 11, 12; 15: M. coracobrachialis; 16: M. serratus ventralis.; 17: M. pectoralis superficialis; 18: M. triceps brachii caput mediale.

Caput longum of m. triceps brachii of *C. didactylus* as well as *B. variegatus* originates on the distal margo caudalis of the scapula adjacent the origin of m. teres minor (Fig. 4-2). It runs laterally to the m. latissimus dorsi and m. dorso-epitrochlearis into a common strong fascia with the medial and lateral head, which both originate from the humerus, respectively. The fascia attaches to the short olecranon (Fig. 4-4, 4-6).

In *C. didactylus* m. coracobrachialis maintains its usual attachment sites on the coracoid and the humerus (Figs. 4-2, 4-3). A second distinct portion as mentioned by Lucae (1882) is not present in our specimens in accordance to findings of Humphry (1869), Mackintosh (1874), and Miller (1935). The presence and sites of origin and attachment are also found in our specimen of *B. variegatus*.

3-D kinematics of the shoulder in C. didactylus

In depth quantification of the 3D kinematics at the shoulder are presented elsewhere (Nyakatura and Fischer, 2010). We here provide just a qualitative description of the movements as a basis for the discussion of the effect individual muscles might have during locomotion.

At touch down of a forelimb the scapula is protracted and pulled dorsad so that it lies dorsally on the thorax with the glenoid fossa facing towards the ear (Fig. 4-7). The shoulder joint is lower than the sternum (i.e., further away from the support). It is extended and the humerus is thus protracted. However, humeral retraction started briefly prior to touch down. The clavicle is rotated cranially and at the same time pointing somewhat dorsally.

During the first half of contact phase mainly the humeral retraction occurs, while the scapula approximately remains at its position of initial contact. Humeral retraction is completed by 60% of the contact phase. In the second half of the contact phase scapula retraction is the predominant motion, whereas the shoulder joints remains flexed at approximately 80 to 90°. Scapular retraction positions the shoulder joint at the same height as the sternum at lift off or even higher (i.e., closer to the support). Additionally, there is a small translation of the scapula along the thoracic wall facilitated by a ligamentous connection of the clavicle to the sternum. The clavicle points laterally at lift off forming approximately an angle of 90° to the sagittal plane. The glenoid fossa faces ventrad at lift off.

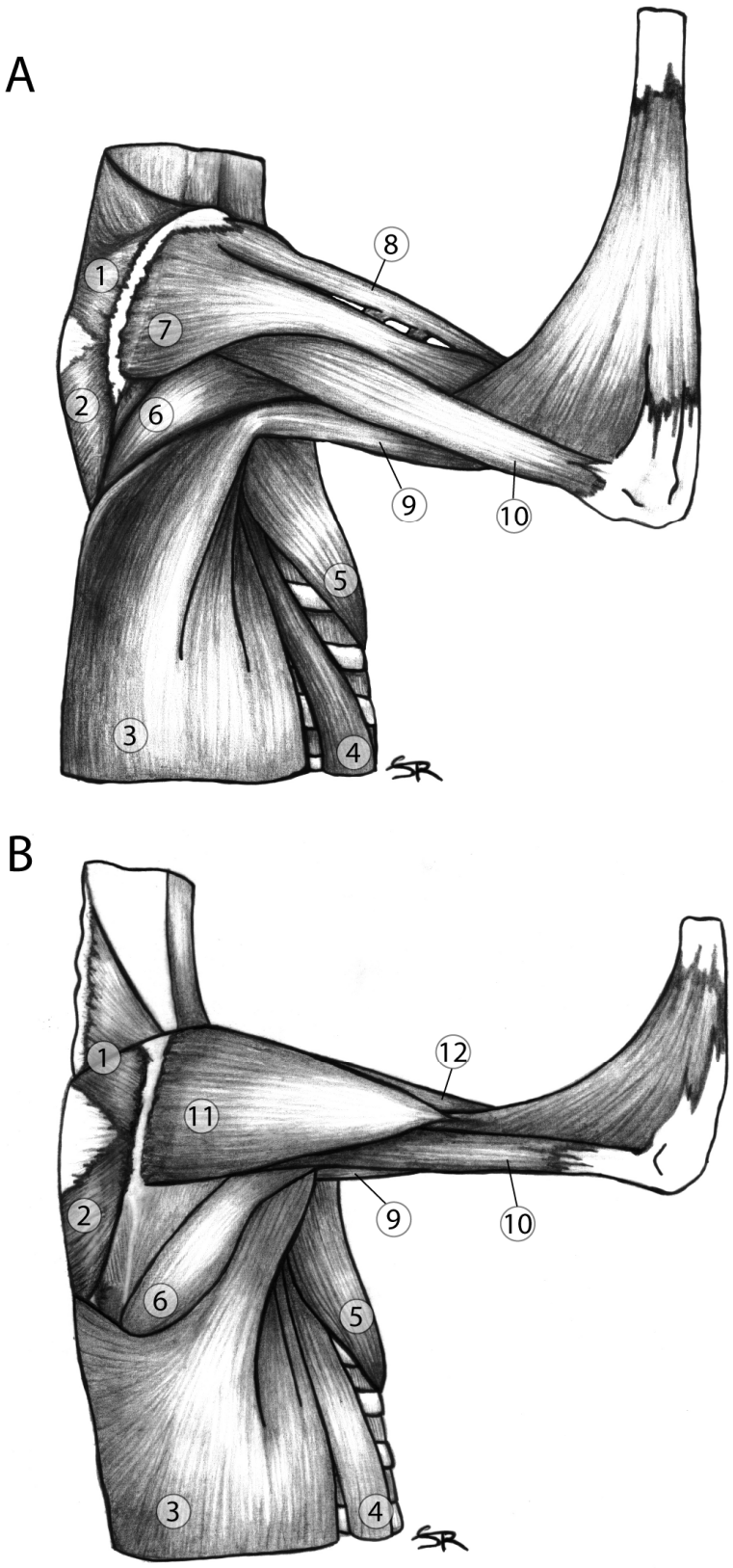

Fig. 4-6: Superficial muscles of the shoulder region of *C. didactylus* (A) and *B. variegatus* (B). Lateral aspect. 1: M. trapezius pars cervicis; 2: M. trapezius thoracis; 3: M. latissimus dorsi; 4: M. pectoralis profundus posterior; 5: M. pectoralis superficialis; 6: M. teres major; 7: M. deltoideus pars scapularis; 8: M. deltoideus pars acromialis; 9: M. dorso-epitrochlearis; 10: M. triceps brachii caput longum; 11: M. deltoideus; 12: M. biceps brachii.

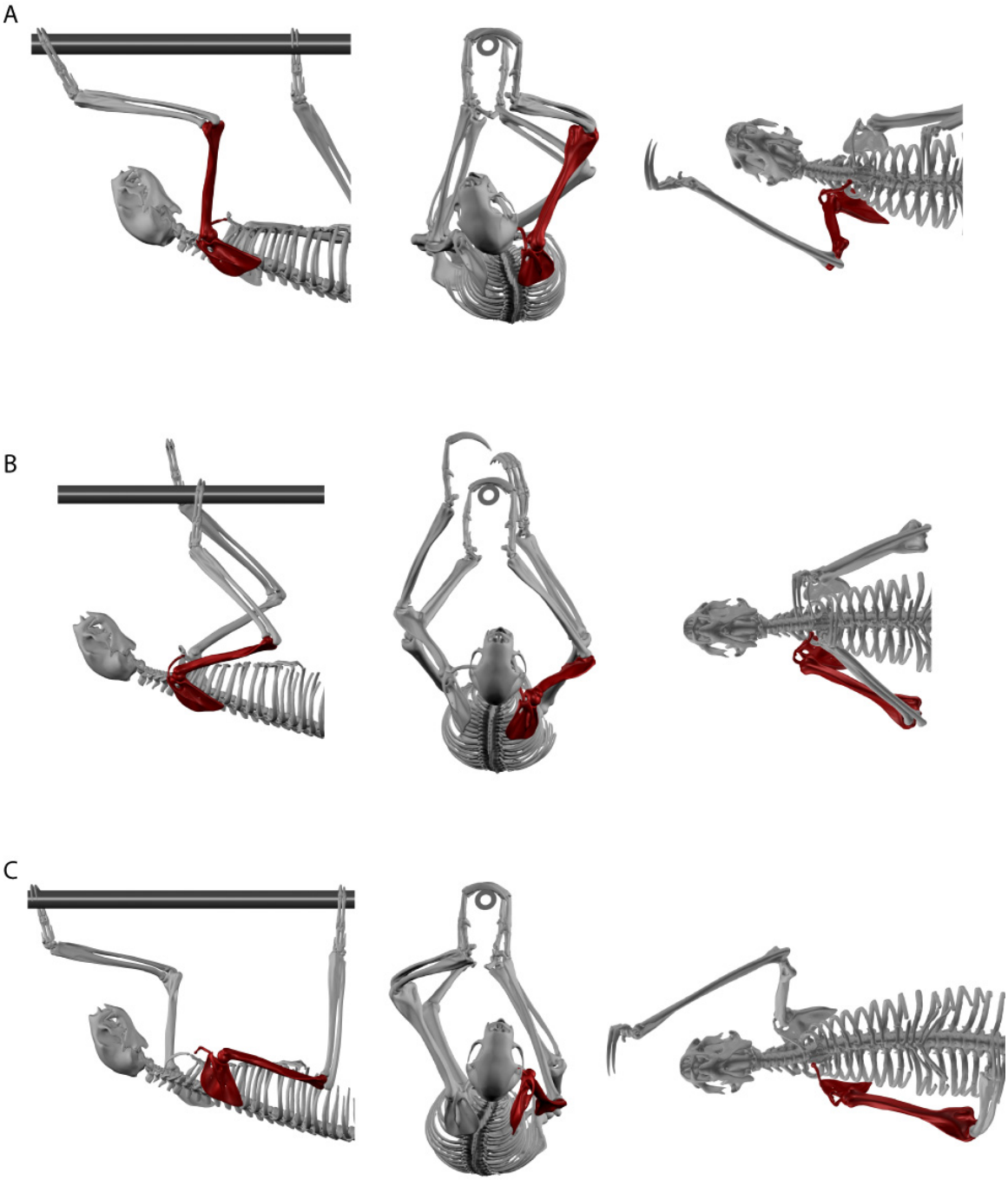

Fig. 4-7: 3D kinematics of the shoulder region in sloths animated according to high-speed x-ray recordings in lateral, frontal and ventral view. A: touch down; B: mid-contact; C: lift off. Further explanations see text.

DISCUSSION

Shoulder muscle function in weight support

Due to the inverse orientation of the body in regard of the gravitational force during locomotion the m. serratus ventralis and the m. rhomboideus (except for a short period prior to lift off) are unsuited to support weight at the forelimbs in *C. didactylus*.

The ability of other muscles to fulfill this role greatly depends on the orientation of the forelimb at different instants of the contact phase. At touch down the fossa glenoidalis has a dorsal position in relation to the manubrium sterni and the upper arm is orientated nearly vertical. The scapula is pulled dorsal by the cervical m. trapezius and m. rhomboideus. Weight transmission to the limb after touch down leads to moments that tend to extend the elbow and shoulder joints. Intrinsic limb musculature is primed for powerful flexion of the shoulder and elbow joints to counteract gravity induced extension (Mendel, 1985). However, in early contact phase the extrinsic shoulder muscles m. pectoralis superficialis posterior and m. dorso-epitrochlearis are best suited to support the weight of the thorax at the forelimbs. Both muscles are characterized by long parallel fibers and have a nearly vertical orientation at this instant of the step cycle. The 'anti-extensors' mm. teres major and dorso-epitrochlearis have paramount responsibility to counteract extension at the shoulder joint. These muscles likely are the functional analogues of suspenory quadrupedalism to 'anti-flexor' muscles such as the long head of m. triceps brachii in pronograde mammals considering the importance to maintain the zig-zag configuration of the leg for locomotion (Goslow et al., 1981; Fischer and Blickhan, 2006). M. trapezius also has the orientation necessary for effective weight transmission between limb and thorax (i.e., its insertion is more ventral than its origin) in the sloth. Later in contact phase the glenoid cavity is moved ventro-caudad and m. pectoralis superficialis posterior and m. dorso-epitrochlearis become more and more unsuited to suspend the weight of the thorax at the forelimbs due to progessive humeral retraction at the shoulder joint. Due to the scapular retraction the shoulder joint is positioned ventrad to the sternum in late contact phase and now the m. pectoralis superficialis anterior is best suited for the task of weight support. M. trapezius and prior to lift off also m. rhomboideus major have suitable orientations to fulfill this role, too.

The effect of shoulder muscles during quadrupedal suspensory locomotion of *C. didactylus*

Our preferred approach to experimentally investigate the functional morphology of the locomotor apparatus is an integration of anatomical data, kinematic data and electromyographic (EMG) data (Fischer, 1999, Scholle et al., 2001). EMG might

represent the best way to analyze *in vivo* muscle function. But, based on the high resolution 3-D data available for the study at hand and our in-depth analysis of shoulder muscle topography as well as facing the impossibility to get access to EMG-recordings in sloths, we venture to deduce the effect of shoulder muscles during steady-state quadrupedal suspensory locomotion of *C. didactylus*. As the muscular action is deduced from muscle topography and kinematics and is not directly observed, we prefer to refer to its *effect* rather than its *activity* (Fischer, 1998).

Recruitment of different muscles at the shoulder region during quadrupedal locomotion is well studied in aclaviculate mammals like cats (e.g. English, 1978) and dogs (e.g. Tokuriki 1973a, b, 1974; Carrier et al., 2006, 2008), in which shoulder movements are largely confined to the parasagittal plane (Boczek-Funcke et al., 1996). EMG data for selected muscles acting on the pectoral girdle of claviculate arboreal quadrupedal primates is also published for four lemurid species, spider monkeys, howling monkeys, and woolly monkeys, as well as for the more terrestrial vervets and patas monkeys (Stern et al., 1980; Konstant et al., 1982; Larson and Stern, 1989; Schmitt et al., 1994; Larson and Stern, 2007). Jenkins and Weijs (1979) comprehensively studied the functional morphology of the claviculate Virginia opossum. We will here discuss these data in context of the observed kinematics and muscular morphology of *C. didactylus*.

In *C. didactylus* early contact phase requires a constant position of the scapula. The mm. rhomboideus capitis et major, levator scapulae, and the cervical part of m. trapezius are suitable to pull the trunk and thereby keep the scapula in the protracted dorsal position during early contact phase. Data for the cranial m. trapezius in spider monkeys during quadrupedal locomotion (Konstant et al., 1982), which have a generally more dorsal orientation of the scapula (Jenkins et al., 1978), was observed to be consistent with a function as assumed for *C. didactylus*.

Flexion in the gleno-humeral joint during early contact is likely realized by the strong m. teres major and M. dorso-epitrochlearis. The long head of m. triceps brachii also contributes to shoulder joint flexion, especially if the elbow joint angle is held constant against gravity induced extension (see below). M. latissimus dorsi and m. pectoralis have an orientation suitable for humeral retraction. Because of a more distal insertion on the pectoral crest of the humerus, m. pectoralis superficialis anterior (but not m.

pectoralis superficialis posterior) is better suited to retract the humerus in early contact phase then m. pectoralis profundus. Larson and Stern (2007) did record only minimal activation by the mm. latissimus dorsi et pectoralis and concluded that these muscles have a reduced role in body progression due to a functional differentiation between fore- and hindlimbs in primates. In contrast, in spider, woolly, and howling monkeys the cranial m. pectoralis 'fires' throughout contact phase during pronograde quadrupedalism, whereas the caudal m. pectoralis is active in the first half of contact phase (Stern et al., 1980). Both parts were found by these authors to be propulsive. Mm. latissimus dorsi et pectoralis are also recruited almost throughout contact phase in the opossum (Jenkins and Weijs, 1979). We assume the m. pectoralis superficialis anterior and especially the mm. latissimus dorsi et dorso-epitrochlearis to effectively retract the humerus given the importance of humeral retraction for sloth forelimb stride length (Nyakatura et al., 2010). As previously proposed by Fischer (1998) for the hyrax, the combined effect of mm. supraspinatus, infraspinatus et subscapularis presumably guides humeral retraction at the gleno-humeral joint in the scapular plane and minimizes humeral abduction. Synchronous activation of these three muscles in the opossum during contact phase (Jenkins and Weijs, 1979) as well as synchronous recruitment of mm. supraspinatus et infraspinatus in vervets (Larson and Stern, 1989) seems to corroborate this notion.

With increasing gleno-humeral flexion the different portions of m. pectoralis become unsuited to further retract the forelimb at the humerus. Since the portion that originates most caudally (m. pectoralis profundus posterior) attaches most proximally at the shoulder, it is suitable to continue forelimb retraction until lift-off. After gleno-humeral flexion has ceased, m. pectoralis profundus medius et posterior as well as m. latissimus dorsi further retract the limb in the second half of forelimb contact. The semi-circular motion described by the glenoid cavity also leads to a more ventral position of the glenoid at lift off, i.e., this movement could be mostly passive by making use of the inverse orientation of the body to gravity. The mode of progression during contact phase would thus be a pull due to humeral retraction in the first half of contact and a mainly passive scapular retraction in the second half of contact provoked by gravity pulling at the trunk.

This pattern would be consistent with the anterior/posterior directed substrate reaction forces measured during upside down locomotion of Loris (Ishida et al., 1990). These authors showed that during upside down locomotion of Loris the limbs exert a pulling force in the first half of contact phase in contrast to the pushing force usually obtained in the second half of stance of pronograde quadrupedalism (Ishida et al., 1990). In this scenario it would be necessary to maintain the scapular pivot at a relatively constant position. Although Schmitt et al. (1994) did not find the m. serratus ventralis involved in scapular rotation in vervets, English (1978) and Jenkins and Weijs (1979) postulated that this task is realized by the combined effect of the cervical part of m. trapezius, which attaches ventral to the scapular pivot, and the cervical part of m. serratus ventralis, which attaches dorsal to it. Both muscles are suited to maintain the scapular pivot at its position during ventro-caudad displacement of the fossa glenoidalis by counteracting the forelimb retractors (cf. Fischer, 1998).

After lift off the scapula is protracted and the gleno-humeral joint continues to extend. In contrast to pronograde locomotion the limb does not need to be flexed in the gleno-humeral and elbow joints (to be lifted of the ground), but is extended to protract the hand above the support. Effective scapular protractors are the cervical part of m. trapezius, m. levator scapulae and m. rhomboideus capitis. m. cleidomastoideus is also suitable to protract the shoulder as long as the head is stabilized in its position by coactivation of other neck muscles. In early swing phase additionally the m. pectoralis superficialis anterior could also effectively protract the shoulder due to the transversal orientation of the muscle and the shoulder's position caudal to the manubrium sterni at this instant of the step cycle. Thus, the m. pectoralis superficialis anterior probably contributes to pro- *and* retraction depending on the position of the limb as was also inferred from the recruitment patterns of the m. pectoralis superficialis transversus in trotting dogs (Carrier et al., 2006). Action of the m. pectoralis superficialis posterior, m. deltoideus acromialis, and m. biceps brachii, which all insert in a common tendon on the forearm protracts the whole limb and extends the glenohumeral joint at early swing phase. During forelimb protraction the scapular pivot is stabilized by the thoracic parts of m. trapezius and m. serratus ventralis. The m. subclavius was found to decelerate the protraction of the limb prior to touch down in quadrupedal locomotion

of spider monkeys (Konstant et al., 1982). We deduce a similar effect of this muscle in *C. didactylus* due to the comparable topography and kinematics.

Convergent morphological solutions to new functional demands

When modern tree sloths adopted the entirely aboreal lifestyle they adapted to the necessity of locomotion on supports that have a small diameter relative to the thorax by evolving the typical upside-down posture and locomotion. But, the inverse orientation of the body with regard to gravity is associated with new functional demands posed on the locomotor apparatus. If the proposed convergent evolution of upside-down posture in both extant sloth lineages (Gaudin, 2004) has lead to any morphological adaptations, these should be present in both lineages. A clear indication of convergent evolution would be a morphologically different solution to the same problem posed by the new functional demand (here the inverse orientation of the body in regard of the force of gravity). However, the phylogenetic heritage of a structure tends to canalize the possible spectrum of solutions to problems posed by changing functional demands (e.g., Sudhaus, 2006). Hence, the more distantly related and, thereby, the less phylogenetic heritage is shared, the more different solutions to changing functional demands can be expected to be realized by evolution.

The adoption of quadrupedal suspensory locomotion of *C. didactylus* has been shown to be characterized by a plesiomorphic pattern of forelimb protraction and retraction and only some small scaled morphological changes that are probably related to the orientation of the body towards the force of gravity. These include the strong flexor groups of the limbs (Mendel, 1985), and as shown above, the topography of the m. pectoralis superficialis posterior, the topography of the acromial head of m. deltoideus, the small serratus ventralis, as well as the distal insertion of the pectoralis superficialis anterior. The fact that most of the named convergences are less pronounced in *Bradypus* might be attributed to its postural behavior, which is less dominated by suspension (e.g. Goffart, 1971).

These characterisitics of the shoulder are all also found in *Bradypus*, and thus it remains unclear whether these characteristics are simply homoplasic.

Only morphological details were identified here that might represent different morphological solutions to the new functional demands posed by the adoption of

upside-down orientation of the body during locomotion. Although the pectoralis is not as complex in *Bradypus*, it may be suited to fulfill the tasks deduced for this muscle complex in *Choloepus* from the x-ray motion analysis and analysis of the muscular topography, but morphologically different. Namely, due to the fibers that the m. pectoralis superficialis exchanges with the m. biceps brachii, it should also be helpful to carry the weight of the thorax at touch-down of the forelimb. This also applies for the acromial head of m. deltoideus, which also sends some of its fibers into the m. biceps brachii, but again in a different way as shown for *C. didactylus*.

Another example probably is the m. dorso-epitrochlearis. We deduced its effect to be similar to that of the m. teres major (mainly to flex the shoulder joint). Both muscles are well developed in *Choloepus* and *Bradypus*. However, whereas in *Choloepus* both muscles are of approximately the same size, in *Bradypus* the m. teres major is even more prominent and is much larger than the m. dorso-epitrochlearis. That means, that in both genera the shoulder flexor group is strong, but it is realized in a slightly different way.

Conclusions

The adoption of the suspensory posture and locomotion of *C. didactylus* had differing effects regarding the main functional demands of the pectoral girdle – weight support and limb protraction and retraction. The similar kinematic pattern of the pectoral girdle renders major evolutionary changes in modes of limb protraction and retraction during adoption of obligatory quadrupedal suspensory posture and related muscular topography unnecessary. This furthermore reduced the need for new patterns of neural control and renders the convergent evolution in the different sloth genera as proposed by phylogenetic analysis less improbable.

The peculiar shoulder morphology of *C. didactylus* is thus likely related to the functional demand of weight bearing at the forelimbs in regard of the inverse orientation of the body to the gravitational force. Comparable characteristics are not as clearly present in *B. variegatus.*

In sum, many characteristics of the muscular topography seem to be related to the inverse orientation of the body in regard of the force of gravity, but only few are realized in a morphologically different way in both species analyzed. This may be

because of relatively close phylogenetic relationship and long common phylogenetic history that may have canalized the possible spectrum of solutions to changed functional demands realized during the evolution of this peculiar locomotor behavior. We suggest that digging adaptations (for example strong limb retractors, long claws) in the common evolutionary history, as proposed for early Xenarthrans, had the effect of posing morphological constraints and canalized evolution to convergently realize suspensory postures. In this context it is important to note that the tiny anteater (*Cyclopes*) is also capable of suspensory locomotion.

ACKNOWLEDGEMENTS

The authors wish to thank I. Schappert of the Zoo Dortmund who kindly provided the sloths Julius and Evita. D. Arnold, with whom it was a pleasure to work, provided practical help with the identification of muscles using the criterion of innervation. Sandy Reinhard skillfully prepared figures 5 and 6.

- Chapter 5 -

Functional morphology and three-dimensional kinematics of the thoraco-lumbar region of the spine of the two-toed sloth

John A. Nyakatura & Martin S. Fischer

Abstract

Given the importance of thoraco-lumbar spine movements for the locomotion of mammals it surprises that in vivo three dimensional (3D) data on intervertebral movements of the mammalian thoraco-lumbar vertebral column during symmetrical gaits is limited to horses and dogs. To test whether similar kinematic patterns as published for these species are also present during an aberrant mode of quadrupedalism, we quantified thoraco-lumbar intervertebral movements, resulting pelvic displacements, and relative femoral movements during trot-like steady state suspensory quadrupedal locomotion of the two-toed sloth (*Choloepus didactylus*, Xenarthra). Scientific rotoscoping, a new non-invasive approach that combines synchronous biplanar high speed x-ray videos and reconstruction of skeletal elements from CT bone scans was used to quantify 3D kinematics. Analysis of vertebral anatomy and epaxial muscle fascicle architecture suggests that the thoraco-lumbar spine is well suited to produce lateral bending and long-axis rotation, but limits powerful sagittal extension. Sloths exhibit complex 3D movements in the thoraco-lumbar spine that are comparable to other arboreal quadrupedal mammals. Monophasic lateral bending and long-axis rotation, biphasic sagittal bending, and maximal amplitude of sagittal bending at the lumbo-sacral joint were also found in other quadruped mammals and may represent general aspects of mammalian symmetric gaits. Maximal amplitude of lateral bending and long-axis rotation vary in regard to the vertebral level. A cranio-caudal pattern of maximal angular deflections of the spine is suggested to result from out of phase movement of diagonal fore- and hindlimbs in other walking gaits, because it is not evident in trot-like locomotion. The analysis also illustrates the difficulties that arise when lumbar mobility is deduced from intervertebral joint morphology alone.

INTRODUCTION

Movements of the vertebral column are of fundamental significance for the locomotion of vertebrates. During symmetrical gaits monophasic lateral bending of the vertebral column is the most substantial movement (Shapiro et al., 2001), whereas biphasic sagittal bending is less pronounced (Schilling and Fischer, 1999; Faber et al., 2000; Ritter et al., 2001; Licka et al., 2001). Additionally, axial rotation about the long-axis of the spine is more pronounced in symmetrical gaits in comparison to asymmetrical gaits (Faber et al., 2000). During symmetrical gaits the pelvis is thus displaced three dimensionally (3D) (cf. Jenkins and Camazine, 1977).

Considering the importance of these 3D axial movements for mammalian symmetrical gaits it is surprising that to date kinematic data on the body axis is limited. While published quantifications of 3D pelvic displacements during symmetric mammalian quadrupedalism are scant (Jenkins and Camazine; 1977; Schilling and Fischer, 1999; Wennerstrand et al., 2004; Schmidt, 2005) the associated minute intervertebral movements are even less investigated. Due to the difficult observation of these movements, necessary 3D in vivo data of intervertebral movements has only been published for horses (Haussler et al., 2001) and single intervertebral joints of dogs (Wood et al., 1992; Schendel et al., 1995), i.e. for highly cursorial mammals adapted for sustained running. Moreover, these few studies used invasive instrumentation of the vertebrae analyzed.

In kinematic studies on back movements of horses using a slow lateral sequence walk, a phase shift of maximal intervertebral lateral bending was observed to occur earlier between the lumbar vertebrae than between the more craniad thoracic intervertebral joints, whereas in a trotting gait this shift was not evident (Faber et al., 2000; Haussler et al., 2001). Accordingly, Schilling and Carrier documented sequential electromyographical (EMG) activation patterns of the back muscles during walking and gallop, but synchronized activity during trot in dogs (Schilling and Carrier, 2010). The authors concluded that cranio-caudal EMG patterns of dogs are consistent with a traveling wave of trunk bending in walking gaits and with a standing wave of trunk bending in trot (Schilling and Carrier, 2010). Thus, kinematic data and EMG data imply a close relationship between specific footfall pattern and 3D motions of the vertebral column during symmetric gaits.

Furthermore, published studies on 3D axial movement of quadrupedal mammals showed that there are regional differences in the magnitude and pattern of the three axial rotations (lateral bending about a dorso-ventral axis, sagittal bending about a latero-lateral axis, and long-axis rotation about a longitudinal axis) (Haussler et al., 2001). Effort has been made to deduce intervertebral mobility from the morphology of the vertebrae (e.g. Slijper, 1946; Boszczyk et al., 2001), but only a fraction of possible in vitro mobility of the musculo-skeletal system should be expected during cyclic locomotion (Fischer, 1998), and, in at least one available example of experimental in vivo motion analysis observed movements were greater than expected based on the articular features (Haussler et al., 2001).

To test whether published patterns of 3D throaco-lumbar intervertebral movements are also present in the sloth, we here present an in vivo analysis of suspensory quadrupedal locomotion in the two-toed sloth (Xenarthra: *Choloepus didactylus*, Linné 1758). If previously published patterns on 3D axial movement during symmetric mammalian quadrupedalism are also present in this contrasting type of symmetric locomotor behavior it is likely to represent a more general pattern. Based on the available data on horses and dogs the following movements in the thoraco-lumbar spine are expected during suspensory quadrupedalism of the two-toed sloth.

1. Lateral bending (LB) is monophasic and maxima to either side are associated with touch down events of the hindlimbs.
2. Sagittal bending (SB) is biphasic and maxima of flexion are associated with touch down events of both hindlimbs, whereas minima occur at instances of hindlimb lift off.
3. Long-axis rotation (LAR) is monophasic and maximal rotations towards one body side are associated with touch down of the ipsilateral hindlimb, whereas minima occur at lift off of ipsilateral hindlimbs.
4. Amplitudes of intervertebral angular deflections are highest at the lumbo-sacral joint.
5. Due to the trot-like footfall pattern that sloths utilize during steady state locomotion (Nyakatura et al., 2010) no cranio-caudal phase shift is expected for the timing of maximal amplitudes of intervertebral angular deflection.

Additionally, 3D movements of the axial skeleton and according displacements of the pelvis have a displacing effect on the pivot of the femur (cf. Jenkins and Camazine, 1977). 3D femoral movements relative to the pelvis are seldom quantified (but see Rubenson et al., 2008; Kubo), because an anatomical coordinate system at the hip joint is necessary to obtain this data. On the other hand kinematic data on femoral movement is often used to interpret for example EMG data of limb muscles. In this publication we quantify thoraco-lumbar movement, pelvic displacement, and femoral movement relative to the perlvis.

To achieve in vivo 3D analysis we used 'scientific rotoscoping' (SR) (Gatesy et al., 2010), a new, non-invasive, marker-less XROMM approach ('X-ray Reconstruction Of Moving Morphology': Brainerd et al., 2010) that combines synchronous biplanar high-speed x-ray videography and 3D reconstruction of skeletal elements from computed tomography (CT) bone scans (Fig. 5-1). The kinematic results will be discussed in relation to the skeletal anatomy and characteristics of the epaxial musculature of the thoraco-lumbar vertebral spine.

MATERIALS AND METHODS

All experiments and procedures were registered with the Committee for Animal Protection of the State of Thuringia, Germany, and were conducted in accordance with its guidelines (Reg.-Nr.: 02-08/04).

Anatomical investigation

Anatomical investigation was undertaken on a female cadaver of *C. didactylus* donated by the zoo Dresden (Germany). After dissection to study the epaxial muscular topography the cadaver was macerated and the vertebrae of the thoraco-lumbar spine were photographed to document intervertebral joint configuration of the two-toed sloth. We here adopt the anatomical nomenclature of the Federative Committee on Anatomical Terminology (FCAT; 2008)

The subjects used for the anatomical investigation and the motion analysis (see below) have been used in previous studies and have been shown to not have uncharacteristic morphologies. Rather morphometric parameters were within one standard deviation

of a larger sample that was composed of museum material (Nyakatura and Fischer, 2010).

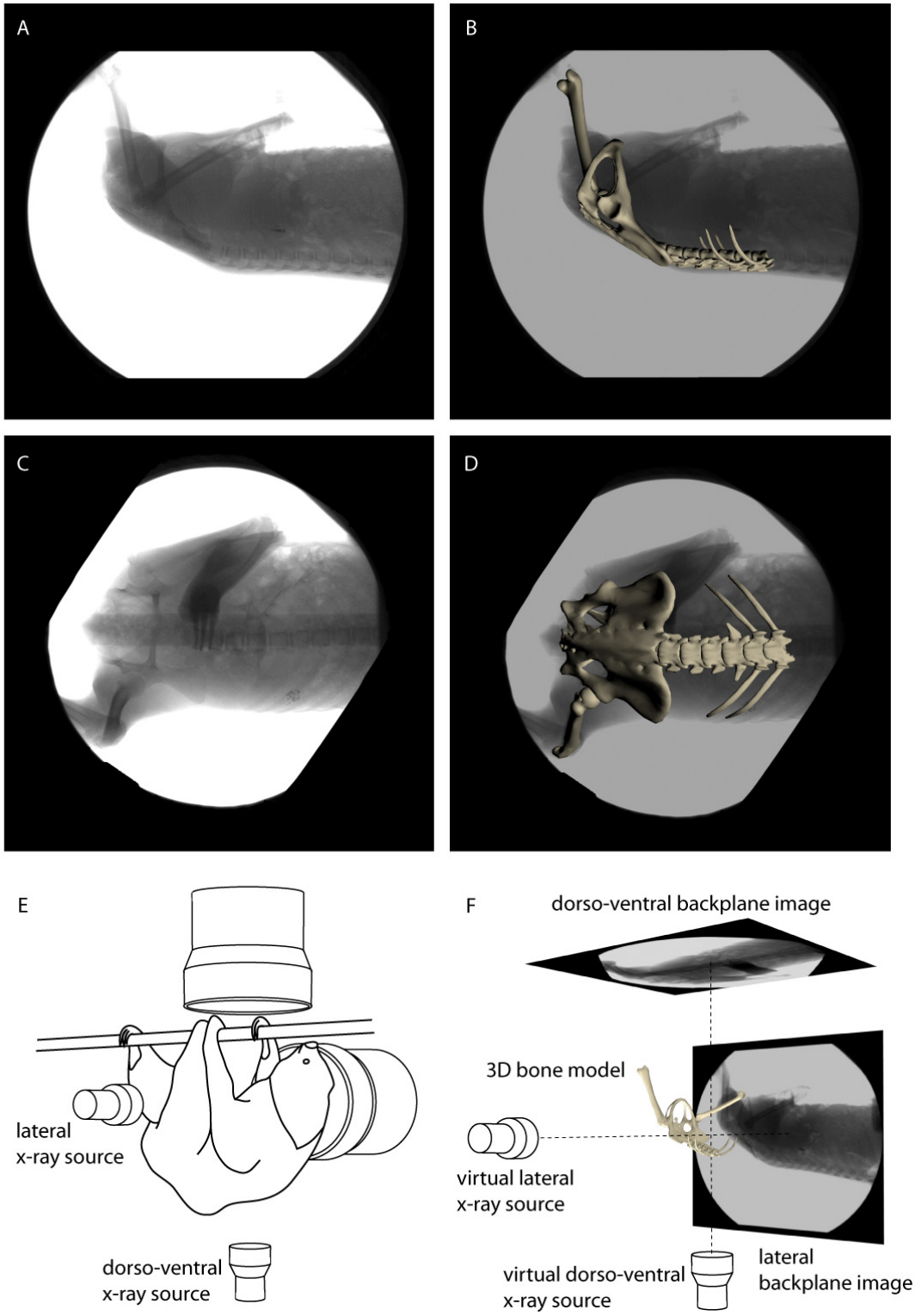

Fig. 5-1: 'Scientific rotoscoping' (Gatesy et al. 2010). A virtual marionette is posed to match the x-ray shadow of synchronously recorded latero-lateral (A, B) and dorso-ventral (C, D) x-ray videos. To achieve this, the experimental setup (E) is 3D calibrated and virtually recreated within 3D software Maya (F). For further explanation see text.

Experimental setup for biplanar high-speed x-ray video recordings

The experimental setup for obtaining synchronous biplanar x-ray videos was described in detail in a previous publication (Nyakatura et al., 2010). Briefly, we recorded synchronous, digital high-speed x-ray videos from the dorso-ventral and latero-lateral projections during steady-state locomotion in two individuals (Fig. 5-1). Both 40 cm diameter image intensifiers were equipped with a Visario Speedcam™ (Weinberger GmbH, Erlangen, Germany) and recorded at a resolution of 1.536 x 1.024 pixels and a framerate of 300 frames per second. Distortion of x-ray images was corrected with help of a Matlab™ workflow developed by the XROMM group (Brown University, Providence, Rhode Island, USA). Images were undistorted by recording the x-ray image of a standardized perforated metal grid and subsequently using the idealized geometry of the perforations to undistort all frames of the x-ray videos (Brainerd et al., 2010).

A calibration object made of acrylic glass (20 x 12 x 12 cm) with metal spheres inserted at 1 cm distances was also recorded in the same experimental setup. We used 16 of these spheres that needed to be identified on both recorded projections to calibrate the 3D space covered by both x-ray devices using a 11 parameter direct linear transformation Matlab™ program (DLT; necessary Matlab™ files available at www.xromm.org) also developed by the XROMM group at Brown University (Brainerd et al., 2010).

Neither the female [10.6 kg, 87 cm length (measured from anterior tip of nose to ischium)] nor the male (6.5 kg, 78 cm) displayed any peculiarities. To foster the recording of several consecutive strides the sloths were trained to move along a motor-driven 'treadpole' (4.000 x 40 mm) in front of the image intensifiers. All trials slower than 0.2 m/sec and faster than 0.3 m/sec were discarded and only strides with symmetry values (i.e., the percentage of a given hindlimb cycle at the instant of contralateral hindlimb touch down) between 0.4 and 0.6 were analyzed for the sake of uniformity of trials. Prior to pooling of data from both individuals, intra-individual variability of gait parameters (stride length, swing duration, contact duration and touch-down angle of the femur) and inter-individual differences of gait parameters were compared. Large intra-individual differences made inter-individual differences insignificant and hence data from both individuals could be pooled (Table 5-1). 10 steady-state trials in each study subject were analyzed. All trials were time normalized

to 50 points over the contact phase and swing phase, respectively, to facilitate compilation of multiple trials so that the mean and standard deviation of the kinematic curves could be determined.

Table 5-1: Interindividual differences compared to intraindividual variability of gait parameters. No statistically significant differences were observed and subsequently all trials were pooled and analyzed together. *: significant differences when $p \leq 0.05$, n.s.: not significant.

	Male individual (mean ± s.d.)	Female individual (mean ± s.d.)	Both individuals (mean ± s.d.)	Comparison between individuals (p-value*)
Stride length (in cm)	58.8 ± 5.0 (n = 18)	60.2 ± 5.9 (n = 14)	59.5 ± 5.3 (n = 32)	0.480 n.s.
Hindlimb swing phase duration (in sec)	0.65 ± 0.2 (n = 18)	0.7 ± 0.1 (n = 14)	0.67 ± 0.2 (n = 32)	0.407 n.s.
Hindlimb contact phase duration (in sec)	1.62 ± 0.3 (n = 18)	1.68 ± 0.2 (n = 14)	1.66 ± 0.2 (n = 32)	0.702 n.s.
Femur touch down angle (in degree)	39.0 ± 5.1 (n = 10)	34.7 ± 5.2 (n = 10)	36.9 ± 5.4 (n = 20)	0.077 n.s.

X-ray reconstruction of moving morphology (XROMM)

CT scans of disarticulated skeletal elements were performed using a GE Lightspeed 16 CT scanner at the Zentralklinik, Bad Berka, Germany, at 120 kV and 150 mA. To reconstruct bone models raw data was surface rendered in Imaris™ 6.4 and converted into .obj file format using customized software (by H. Stark available at www.stark-jena.de). Models were imported into Maya™ 8.0 and hierarchically connected via virtual joints to form a digital marionette. To prevent the living animals from potential damage of anesthesia a different skeleton was scanned and then scaled to match the size of the living subjects via reference x-ray images (cf. Gatesy et al., 2010).

In Maya™ virtual dorso-ventral and latero-lateral oriented cameras were created and their relative position in virtual 3D space was calibrated so that they imitated the actual x-ray sources (necessary Maya™ embedded language files available at www.xromm.org) (Fig. 5-1).

If in the hierarchical joint chain a higher ordered skeletal element is moved, all lower ranked skeletal elements are passively displaced. Motions of skeletal elements are reported relative to higher ordered skeletal elements in the hierarchical joint chain (Table 5-2). Displacement of the pelvis (top rank in hierarchy) is reported relative to a global coordinate system with positive *x* in direction of movement, positive *y* ventral, and positive *z* to animal's left. Right handed anatomical coordinate systems were implemented at the pelvis and at the pivot of the femur, as well as at the six most

caudal presacral joints (in the center of the intervertebral discs). The anatomical coordinate systems are implemented for each joint with the *x*-axis oriented along the long axis of the bone, of which the movement is measured and the *z*-axis oriented to reflect its main axis of rotation. Zero-positions of rotations are unnatural, but idealistic positions aligned to the global coordinate system (Table 5-2). We were forced to restrict the analysis to the six most caudal presacral vertebrae, because of the limited size of the visible field of both x-ray cameras. Intervertebral movements are reported by describing motion of a craniad vertebra relative to the vertebra immediately caudad (cf. Haussler et al., 2001). Although 3D kinematics always consist of three rotations (about the *x*-, *y*-, and *z*-axis) and three translations (along the *x*-, *y*-, and *z*-axis), translations between vertebrae, in the lumbo-sacral joint and in the hip joint were found to be very small (less than our analytical accuracy, see below) and are therefore neglected in this study.

During SR the digital marionette was then positioned to match the x-ray shadow of both projections for every fifths frame. After a trial had been completed the three rotations representing the movement of a bone relative to the higher ordered skeletal element were exported into Microsoft™ Excel.

SR is an iterative process and quality largely depends on the effort of the investigator, but also on the accuracy of the 3D representation of the experimental scene within Maya™ and repeatability of measurements. Accuracy and repeatability are determined by the quality of undistortion, calibration, visibility of the skeletal structures on the x-ray images, and framerate of the x-ray videos used. Due to the unequal shape and thickness of the studied structures no one value can represent the accuracy of all measurements. General accuracy for optimal conditions was measured by comparing the known opening of a vernier caliper (150 mm) to the measured opening following the approach used in this study. We determined the opening to be 150.705 mm within Maya™; i.e., a deviation of less then one millimeter. To assess repeatability the femoral orientation relative to the pelvis and rotations at the lumbo-sacral joint at lift off in a single trial were determined on five consecutive days of data analysis and only small deviations (mean±s.d.) were found. Lift off frame: 153.3 ± 0.75 (i.e., s.d. is less than 1/300 sec). Femoral orientation (rotations relative to the zero-point of measurement): rot x -28.3 ± 1.45°; rot y -33.0 ± 0.84°; rot z -62.2 ± 0.46°. Rotations at the lumbo-sacral

joint: LB -2.3 ± 0.21°; SB 18.3 ± 0.34°; LAR 0.9 ± 0.87°. To account for this inaccuracy we decided to report values rounded to full degrees. This also means that minute movements of less than one degree were not reliably measured. Because especially AR in intervertebral joints was very difficult to detect we only measured LAR of intervertebral joints at touch down, lift off, mid contact and mid swing of each limb (i.e., 8 measurements during a stride cycle) to reveal the minute motions between these instances. Then, Maya™ uses a spline-curve estimate to connect the measured instances (cf. Gatesy et al., 2010).

Table 2: Anatomical coordinate systems used for the kinematic analysis. Confer figure 2. Right handed coordinate systems are implemented for each joint with the *x*-axis oriented along the long axis of adjacent bone and z-axis always oriented to represent the most distinct motion of adjacent bone. Global coordinate system with positive *x* in direction of movement, positive *y* towards dorso-ventral image intensifier, and positive *z* to animal's left.

Joint/element (hierarchy)	Anatomical significance of rotation about axis	Zero-point for rotations
Global coordinate system (top)		
x-axis	-	-
y-axis	-	-
z-axis	-	-
Pelvis (1st order)		
x-axis	Long-axis rotation of pelvis (roll)	Aligned to global *x*
y-axis	Lateral displacement of pelvis (yaw)	Aligned to global *y*
z-axis	Sagittal protraction/retraction of pelvis (pitch)	Aligned to global *z*
Femoral pivot/femur (2nd grade)		
x-axis	Long axis rotation of the femur	Femur is not rotated (lateral and medial condyles aligned to global *y*-axis)
y-axis	Abduction relative to the pelvis	Femur is not abducted
z-axis	Pro- and retraction relative to the pelvis	Femur is parallel to global *x*-axis
Pre-sacral joints/3rd lumbar to 21st thoracal vertebrae (2nd to 7th order)		
x-axis	Long-axis rotation about long axis of the spine (negative rotation decreases the distance from reference hip joint to support)	Vertebrae are not rotated
y-axis	Lateral bending (negative towards body side of reference hindlimb)	Vertebrae are orientated along the long axis of spine (global *x*)
z-axis	Sagittal bending (degree of flexion from zero point)	Vertebrae are orientated along global z

Quantifying the displacing effect of pelvic movements on the trajectory of the knee

Pelvic displacements contribute to step length in symmetrical gaits. XROMM provides the possibility to quantify the contribution of pelvic displacements to overall 3D displacement of the limb. To accomplish this we conducted 'virtual experiments' and turned off ('muted') the motion of the pelvis or only specific aspects of the motion [i.e., either pelvic tilt (roll), pelvic protraction/retraction (pitch), or pelvic lateral displacement (yaw)] in the animated trials. The displacing effect of specific motions of

the pelvis was then assessed by comparison of the knee trajectory of the virtual experiment with the knee trajectory of normal locomotion.

RESULTS

Skeletal anatomy of the thoraco-lumbar spine and pelvic region

Xenarthra are characterized inter alia by additional ('xenarthrous') intervertebral articulations in the postdiaphragmatic spine formed between enlarged met- and anapophyses (Flower, 1882; see Gaudin and McDonald, 2008 for a recent review of xenarthran morphology). However, in extant sloths the anapophyses are only weakly developed (Gaudin and McDonald, 2008) and are not visible in *Choloepus* (Kraft, 1995). *C. didactylus* usually has 23 thoracic and 3 lumbar vertebrae (Buchholtz and Stepien, 2009). In all Xenarthra the ischium is fused to the anterior caudal vertebrae. Thus, the pelvis has two rigid articulations to the vertebral column that prohibit any motion of the pelvis relative to the spine: the sacro-iliacic joint and the sacro-ischiadic joint. Our dissected specimen and our live subjects did not differ from these general characteristics.

In *C. didactylus* the thoraco-lumbar spine has exceptionally short spinal processes that point caudad (Fig. 5-2). Anterior zygapophyses of the thoracic vertebrae are oriented to face dorsad, whereas those of the last thoracic vertebra and all lumbar vertebrae embrace the posterior zygapophysis of the previous vertebra and have a more medial (parasagittal) orientation. I.e., TH22 has horizontal anterior, but parasagittal posterior zygapophyses and is thus termed the diaphragmatic vertebra (Slijper, 1946). Parasagittal facetation of the zygapophyses is also present at the lumbo-sacral joint. The posterior zygapophyses and the lamina arcus vertebrae of the thoraco-lumbar spine form a relatively flat surface that protrudes caudad into the space between the medially facing anterior zygapophyses of the subsequent vertebra. Configuration of the lumbar vertebrae can be compared to roofing tiles. X-ray images of maximal sagittal extension by manipulation of a cadaver revealed that no hyperextension is possible at the thoraco-lumbar spine.

Morphological characteristics of the epaxial musculature at the thoraco-lumbar spine

The m. iliocostalis, m. longissimus dorsi and the transversospinal system are easily to discern in the sloth due to different orientation of fascicles or fascia separating these muscles. In total, the epaxial musculature is remarkably thin. The m. iliocostalis for example only consists of two to three layers of fascicles. A strong fascia thoracolumbalis covers the fascicles of the epaxial muscles.

In the thoraco-lumbar region the fascicles of the m. iliocostalis lumborum originate from the crista iliaca, from the lamina superficialis of the fascia thoracolumbalis and from an aponeurosis that separates the muscle medially from the m. longissimus dorsi. The fascicles of the lumbar portion of the m. iliocostalis attach to the three most caudal thoracic vertebrae or to the lamina profunda of the fascia thoracolumbalis that connects the crista iliaca, the processus costales of the lumbar vertebrae, and the most caudal ribs and extends ventral to the epaxial muscles.

In the lumbar region the m. longissimus dorsi originates at the fascia thoracolumbalis and medially from the fascia that separates this muscle from the transversospinal system. It inserts on the lamina profunda of the fascia thoracolumbalis and to the aponeurosis that separates m. iliocostalis from this muscle. Moreover, at the thorax, the fascicles attach on the dorsal surface of the ribs proximal to the m. iliocostalis. Fascicle length at the lumbar spine is much more variable than at the thorax, where individual fascicles almost exclusively span two vertebral levels.

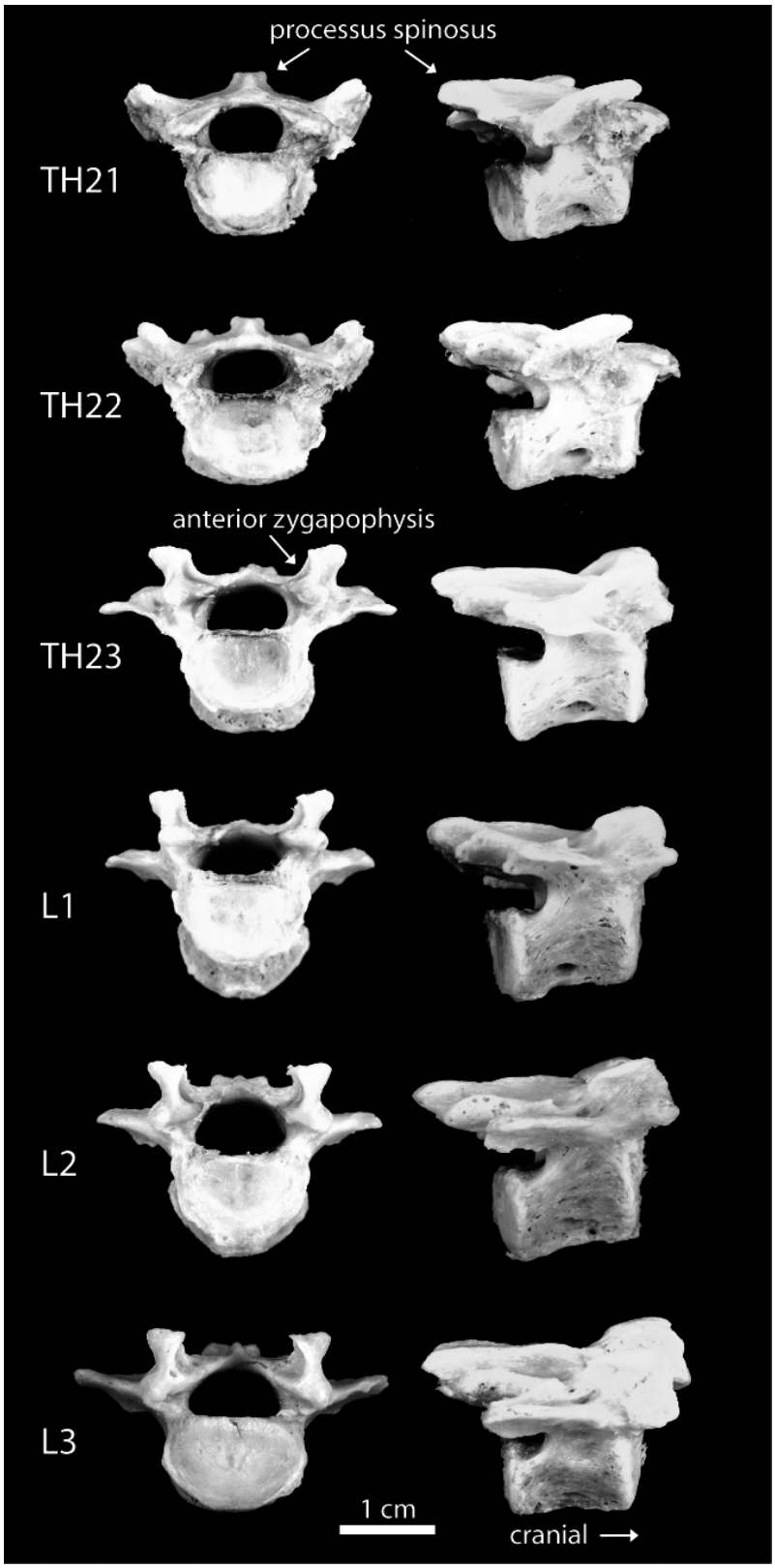

Fig. 5-2: Photographs of the 6 most caudal presacral vertebrae. Left: cranial aspect; right: lateral aspect. Please note the approximately horizontal articular facets at the anterior zygapophyses of vertebrae TH21 and TH22, and approximately parasagittal articular facets in the anterior zygapophyses of the last 4 presacral vertebrae. Please also note the very low processus spinosi.

An attribution of individual fascicles to the separate muscles that make up the transversopinal system was not aspired here because no intramuscular aponeuroses that separate the different muscles were observed. In the lumbar region fascicles of the transversopinal system originate from the fascia thoracolumbalis, the intramuscular aponeurosis that separates this muscle from the m. longissimus, the medial crista iliaca, and the dorsal surface of the sacrum and lumbar vertebrae. The fascicles attach to the remarkably short processus spinosi, the lamina arcus vertebrae of the lumbar and thoracic spine, and the processus costales. But, it is important to point out that the general orientation of most fascicles is cranio-medial instead of cranio-lateral. Fascicle lengths of the transversopinal system are very variable reflecting its composition of different muscles. Lengths vary from fascicles that span only one vertebral level (e.g. mm. rotatores breves) to fascicles that span the complete lumbar spine and directly attach to thoracic vertebrae (m. semispinalis, m. multifidus).

Characteristics of steady-state locomotion in the sloth

Interlimb coordination and spatio-temporal gait parameters of unrestrained and steady-state locomotion of the two-toed sloth were reported in an earlier publication (Nyakatura et al., 2010). Characteristics of steady-state ('treadpole') locomotion are only briefly summarized here. Analysis of steady-state locomotion was restricted from 0.2 to 0.3 m/sec. At this speed range limb kinematics and spatio-temporal gait parameters were relatively uniform and the sloths utilized trot-like diagonal couplets gaits (diagonal fore- and hindlimbs are moved nearly synchronously). The average stride cycle of the hindlimbs during a steady-state trial lasted 2.34 ± 0.4 sec (mean ± s.d.; n = 32). Contact ended after 1.66 ± 0.25 sec (or 71% of the stride cycle) and stride length was 0.60 ± 0.05 m. On average, touch-down events of hindlimbs were nearly symmetric in analyzed trials with the contralateral hindlimb touching down at 49±4 % of the reference hindlimbs' stride cycle. In this study we assume symmetric touch down events. In sum, during an average hindlimb stride cycle there is first a phase of bilateral support (until lift off of the contralateral hind at the 21% mark), followed by unilateral support (until touch down of the contralateral hind at the 50% mark), again followed by bilateral support (until lift off of the reference hind at the 71% mark), and

a final unilateral support phase of the contralateral hind (until touch down of the reference hind at the 100% mark).

Intervertebral angular movements of the thoraco-lumbar spine during locomotion

Lateral bending. LB movement patterns obtained for the six presacral intervertebral joints were monophasic over the course of a step cycle (Fig. 5-3). At touch down of a hindlimb additive intervertebral movement bent the thoraco-lumbar spine towards the regarded hindlimb's body side (negative values for LB; Table 5-3). At touch down of the contralateral hindlimb the thoraco-lumbar spine is bent maximally towards the opposing body side (positive values for LB; Fig. 5-3). Amplitudes of LB increased from the lumbo-sacral joint to the 3rd presacral joint at which the greatest amplitude was observed and then decreased gradually in the more craniad intervertebral joints (Fig. 5-4). At the 6th presacral joint only minimal LB movements (less than 1° to either side) occur and detection of such minute movements is not reliable with the non-invasive approach used in this study, because the amplitudes are within one standard deviation of data acquisition. None of the six presacral joints analyzed had maximal amplitudes greater than 7° on average. No cranio-caudal pattern was observed for the timing of extreme angular displacements of individual intervertebral joints as extreme LB was reached approximately at touch-down of either limb (Table 5-4) and the instant of the stride cycle in which the extreme was reached varied between trials. Moreover, phases of bilateral hindlimb support were marked by comparatively little LB movements (Fig. 5-3).

Table 5-3: Mean intervertebral angles and pelvic displacements (average rounded to full degrees) at touch down and lift off of reference hindlimb.

	LB		SB		LAR	
	Touch down angle (°) ± s.d.	Lift off angle (°) ± s.d.	Touch down angle (°± s.d.)	Lift off angle (°± s.d.)	Touch down angle (°± s.d.)	Lift off angle (°± s.d.)
6th PSJ	-1 ± 1	0 ± 1	1 ± 1	1 ± 0	0 ± 1	0 ± 0
5th PSJ	-2 ± 1	1 ± 1	1 ± 1	1 ± 1	-2 ± 1	0 ± 1
4th PSJ	-2 ± 1	1 ± 2	4 ± 2	3 ± 1	-4 ± 3	2 ± 2
3rd PSJ	-3 ± 1	3 ± 0	5 ± 2	4 ± 1	-3 ± 3	1 ± 1
2nd PSJ	-3 ± 1	1 ± 1	10 ±1	9 ± 2	-1 ± 2	1 ± 1
LS joint	-1 ± 1	0 ± 1	19 ± 3	15 ± 2	-1 ± 1	1 ± 1
Pelvic displacement	-14 ± 4	9 ± 4	41 ± 9	33 ± 6	-13 ± 4	6 ± 3

Sagittal bending. SB movements measured in the six presacral intervertebral joints were biphasic over the course of a step cycle (Fig. 5-3). At touch-down of either hindlimb the thoraco-lumbar spine is maximally flexed (higher values for SB; Table 5-3). Minima are associated with instants of lift off of a hindlimb, but on average these minima occur slightly after the lift off event of either hindlimb (Table 5-4). SB amplitudes were highest at the lumbo-sacral joint and decreased gradually in craniad direction, although we observed slightly higher SB movements at the 4th presacral joint than in the 3rd presacral joint (Fig. 5-4). Again no clear cranio-caudal pattern was observed for the timing of extreme angular displacements of individual intervertebral joints during an average stride cycle (Table 5-4).

Long-axis rotation. LAR movement patterns of vertebrae at the six analyzed presacral joints were monophasic (Fig. 5-3). Clockwise rotation along the long axis of the vertebral column is maximal approximately at the instant of touch down of the left hindlimb (negative values for AR; Table 5-3). After touch down of the left hindlimb counterclockwise LAR set in. It was at its maximum approximately at the instant of contralateral hindlimb touch down. Then again clockwise rotation set in. Amplitudes of intervertebral LAR increase until the 4th presacral joint. At this joint the maximal mean amplitude of 7° was observed (Fig. 5-4). Intervertebral angular amplitudes during a stride cycle were much smaller at the 5th presacral joint and to small to be reliably detected at the 6th presacral joint. As for the LB and SB movement patterns we did not observe a temporal cranio-caudal pattern of intervertebral LAR (Table 5-4).

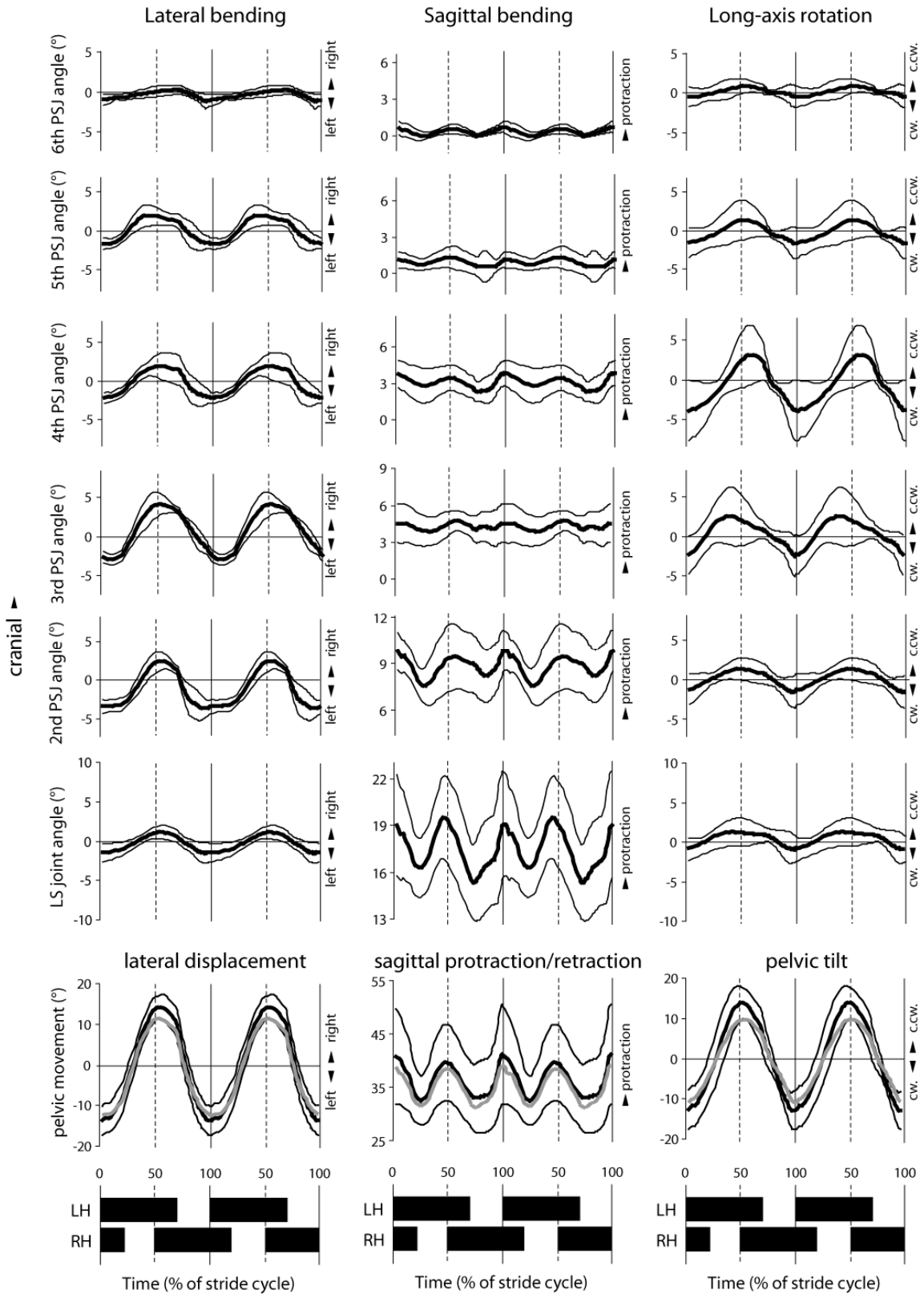

Fig. 5-3: Average angular intervertebral movements and pelvic displacements (+/- s.d.; n = 20) relative to two consecutive average stride cycles. LS: lumbo-sacral joint; PSJ: presacral joint; cw: clockwise; c.cw.:counterclockwise; grey: addition of presacral intervertebral movements. Timing of contact phases (black boxes) and swing phases (white space between boxes) during two mean stride cycles of the left hindlimb (LH) and right hindlimb (RH).

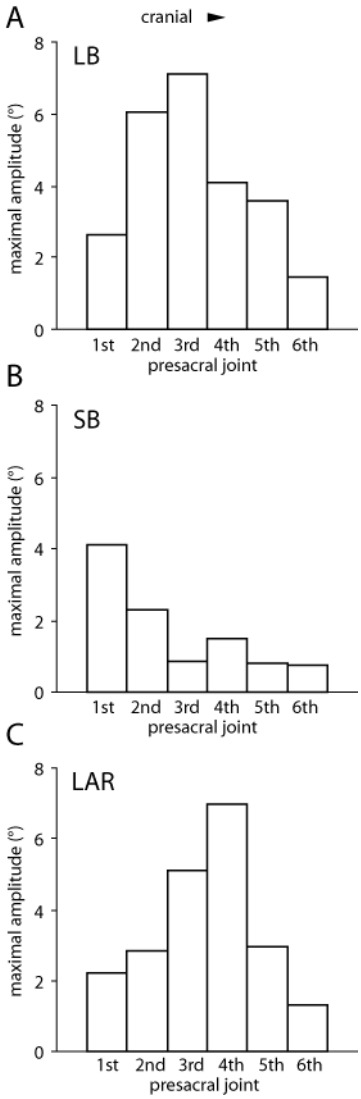

Fig. 5-4: Maximal mean amplitudes of intervertebral movements for individual intervertebral joints over the course of a reference hindlimb's stride cycle (n = 20). A: lateral bending; B: sagittal bending; C: long-axis rotation.

Table 5-4: Percentage of stride cycle that maximum and minimum angular displacements (average rounded to full percent) follow touch down of reference hindlimb. *: The 1st maximum of sagittal bending movement is associated with the touch down of the contralateral hindlimb. The 2nd maximum is associated with touch down of the reference hindlimb. In some cases it is reached after touch down (early in respect to reference contact phase).

	LB			SB			LAR	
	max (%) ± s.d.	min	1st max*	max (%) ± s.d.	min	1st max*
6th PSJ	68 ± 4	95 ± 3	51 ± 3	68 ± 4	95 ± 3	51 ± 3
5th PSJ	45 ± 4	3 ± 6	51 ± 5	45 ± 4	3 ± 6	51 ± 5
4th PSJ	54 ± 6	3 ± 4	51 ± 5	54 ± 6	3 ± 4	51 ± 5
3rd PSJ	54± 5	8 ± 5	60 ± 5	5 4± 5	8 ± 5	60 ± 5
2nd PSJ	56 ± 6	85 ± 5	53 ± 4	56 ± 6	85 ± 5	53 ± 4
LS joint	56 ± 4	95 ± 5	45 ± 3	56 ± 4	95 ± 5	45 ± 3
Pelvis	56 ± 8	100 ± 6	48 ± 5	56 ± 8	100 ± 6	48 ± 5

Resulting pelvic displacements

The small intervertebral angular movements are associated with pelvic displacements (Fig. 5-3). Hence, likewise to the intervertebral joint movement LB and LAR were monophasic, whereas SB was biphasic. Mean amplitudes of 28°, 9°, and 27° occur for lateral displacement and sagittal retroversion/anteversion and LAR respectively. Most of observed pelvic displacement can directly be attributed to the summation of intervertebral movements measured at the thoraco-lumbar spine. The summation of LB movements of the six presacral joints analyzed accounted for 85.2% of the observed mean amplitude of lateral pelvic displacement. Likewise SB movements in the thoraco-lumbar spine accounted for 90.8% the observed maximal amplitude of sagittal displacements of the pelvis. Summed up LAR movements of the six most caudal presacral joints accounted for 77.2% of LAR observed in the pelvis.

Over the course of reference hindlimb's stride cycle the pelvis is displaced in such a way that at touch down the pelvis is maximally displaced towards the ipsilateral side, is maximally protracted in its sagittal plane and is rotated so that the ipsilateral hip joint is placed closer to the support. At contralateral lift off the pelvis is maximally retracted in its sagittal plane, but lateral displacement remains close to the value of ipsilateral touch down. Little lateral displacement results in a position of the hip joint directly under the foothold when the pelvis is progressed under the foot during ipsilateral contact phase. During contralateral swing the pelvis is displaced laterally and rotated about its long axis towards the contralateral body side, again protracted in its sagittal plane. Apart from the protraction, the pelvis approximately maintains this orientation until ipsilateral lift off. During ipsilateral swing phase the pelvis swings and rotates back to the body side of the hindlimb in swing phase.

Femoral movements relative to the pelvis

Femoral movements consist of pro- and retraction, ab- and adduction, and rotation about its long axis. These movements are determined relative to the pelvis with use of an anatomical coordinate system placed at the hip joint. At touch down the femur is retracted approximately 60° (Fig 5-5A) from the position parallel to the pelvic long axis used as the zero point for femoral rotations (Table 5-2). During the initial third of

contact phase no significant retraction is observed but during the last two thirds of contact the femur is continuously retracted to about 120° until lift off. During swing phase the femur is protracted again. The mean amplitude of femoral pro- and retraction is 57° over the stride cycle.

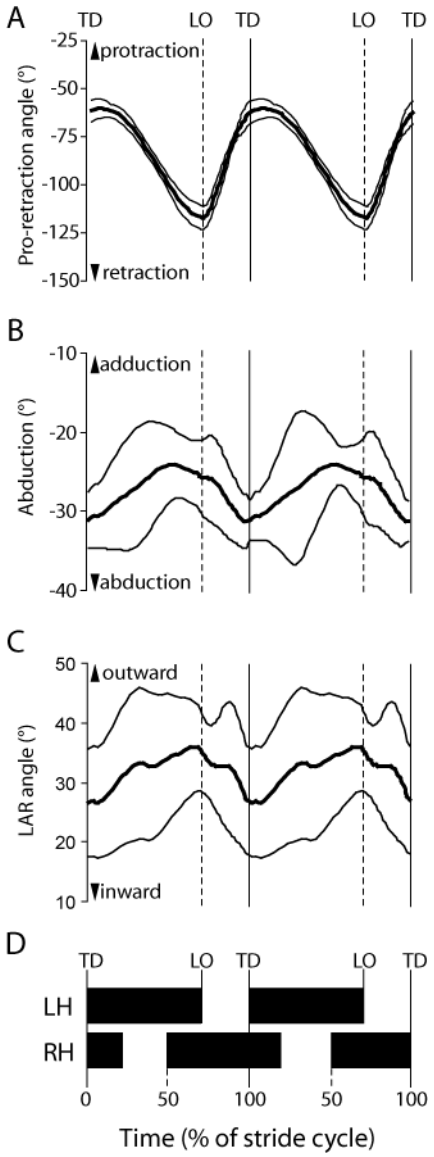

Fig 5-5: Average angular rotations at the femoral fulcrum (+/- s.d.; n = 20) relative to two consecutive average stride cycles. A: femoral pro- and retraction; B: femoral abduction, C: femoral long-axis rotation.

In contrast, the degree of abduction was clearly influenced by the pelvic orientations at touch down of both hindlimbs (Fig. 5-5B). Relative to the pelvis the femur is abducted by 31° on average (-31° rotation about the y-axis of anatomical coordinate system placed at the femoral pivot). During contact phase abduction decreases and reaches a minimum at the instant of contralateral touch down (ca. -25°). Abduction

then increases again until completion of the ipsilateral contact phase and throughout the ipsilateral swing phase. It reaches a maximum at touch down of the ipsilateral hindlimb. Overall amplitude of abduction/adduction was 7° on average.

The cranial surface of the femur is rotated outward about its longaxis throughout the stride cycle (Fig. 5-5C). This outward rotation increases from touch down to lift off by about 8° on average. After reaching its maximum at lift off outward rotation of the femoral longaxis decreases again and reaches its minimum shortly prior to touch down. We determined mean overall amplitude of longaxis rotation to be 7°.

Influence of pelvic displacements on the trajectory of the knee

During normal locomotion knee displacement has an average medio-lateral amplitude of 3.9 cm (Fig. 5-6). If all of the pelvic rotations are turned off, medio-lateral displacement increases to 5.7 cm. Specifically pelvic roll has a drastic influence on medio-lateral displacement, as it increases to over 8 cm if pelvic roll is 'muted' in the virtual experiment. In sum pelvic rotations over the course of the stride cycle facilitate a relatively linear retraction of the knee, without extensive medio-lateral excursions.

During normal locomotion the knee has an amplitude of about 23.5 cm cranio-caudal displacement. If all pelvic rotations are turned off this value decreases to less than 14 cm. Pelvic roll, yaw, and pitch all contribute similarly to the cranio-caudal displacement of the knee, with the biggest influence having pelvic pitch (Fig. 5-6).

The amplitude of dorso-ventral displacement of the knee over the course of a stride cycle is about 5.1 cm. If pelvic rotations are 'muted' this value decreases slightly. It is interesting to note that 'muting' of pelvic roll actually increases dorso-ventral displacement of the knee, but this effect is contradicted by the effect of pelvic yaw and pelvic pitch.

DISCUSSION

Morphology of the thoraco-lumbar spine in relation to observed motions

The order Xenarthra is characterized by xenarthrous articulations in the thoraco-lumbar spine that have been argued to restrict LAR of the vertebral column (Kraft, 1995; Endo et al., 2009). Although this argumentation might be incorrect since Gaudin and Biewener (1992) found no significant differences to opossums when subjecting the

thoraco-lumbar spine of an armadillo to torsion and ventral bending, two-toed sloths do not have distinct xenarthrous articulations (Kraft, 1995). The parasagittal orientation of the articulating planes at the anterior zygapophyses of the lumbar vertebrae and last thoracic vertebra present in the sloth are also found in other species including humans and have also been argued to restrict extensive LAR and LB (see Rockwell et al., 1938; Boszczyk et al., 2001; Benninger et al., 2006). As shown here for the sloth small additive intervertebral motions can result in considerable long-axis rotation and lateral displacement of the pelvis even with this configuration of the zygapophyses. Pridmore (1992) also found LB in the postdiaphragmatic spine (i.e., between those vertebrae with parasagittal facetation of the zygapophyses) to be similar to that of the prediaphragmatic spine (vertebrae with horizontal zygapophysal facetation) in a cineradiographic study on LB in *Monodelphis* (Marsupialia). Available cineradiographic data of symmetrical gaits of mammals hence does not clearly reflect the differences in mobility that might be deduced from the articular features.

According to Slijper (1946) long spinal processes result in advantageous lever arms for muscles that sagittally extend the vertebral column. Therefore, this feature is often found in species that are able to gallop at high velocities and display powerful sagittal extension (Slijper, 1946). The two-toed sloth has very short spinal processes and correspondingly only a thin layer of muscle.

Moreover, Slijper (1946) claims that cranially directed spinal processes are better suited to extend the spine in the sagittal plane, whereas caudally directed spinal processes are favorable for LAR *via* the mm. rotatores and effective LB. Curtis (1995) accordingly observed caudally directed spinal processes in slow Loris (*Nycticebus coucang*), a species that is also unable to gallop and is characterized by extensive LB during locomotion (Demes et al., 1990).

Since sloths are not displaying asymmetrical gaits (Mendel, 1981; Nyakatura et al., 2010), the combination of a reduction of the overall muscle mass of the epaxial musculature, and reduced height of the spinal processes that are caudally directed is thus in accordance with expectations based on previous findings.

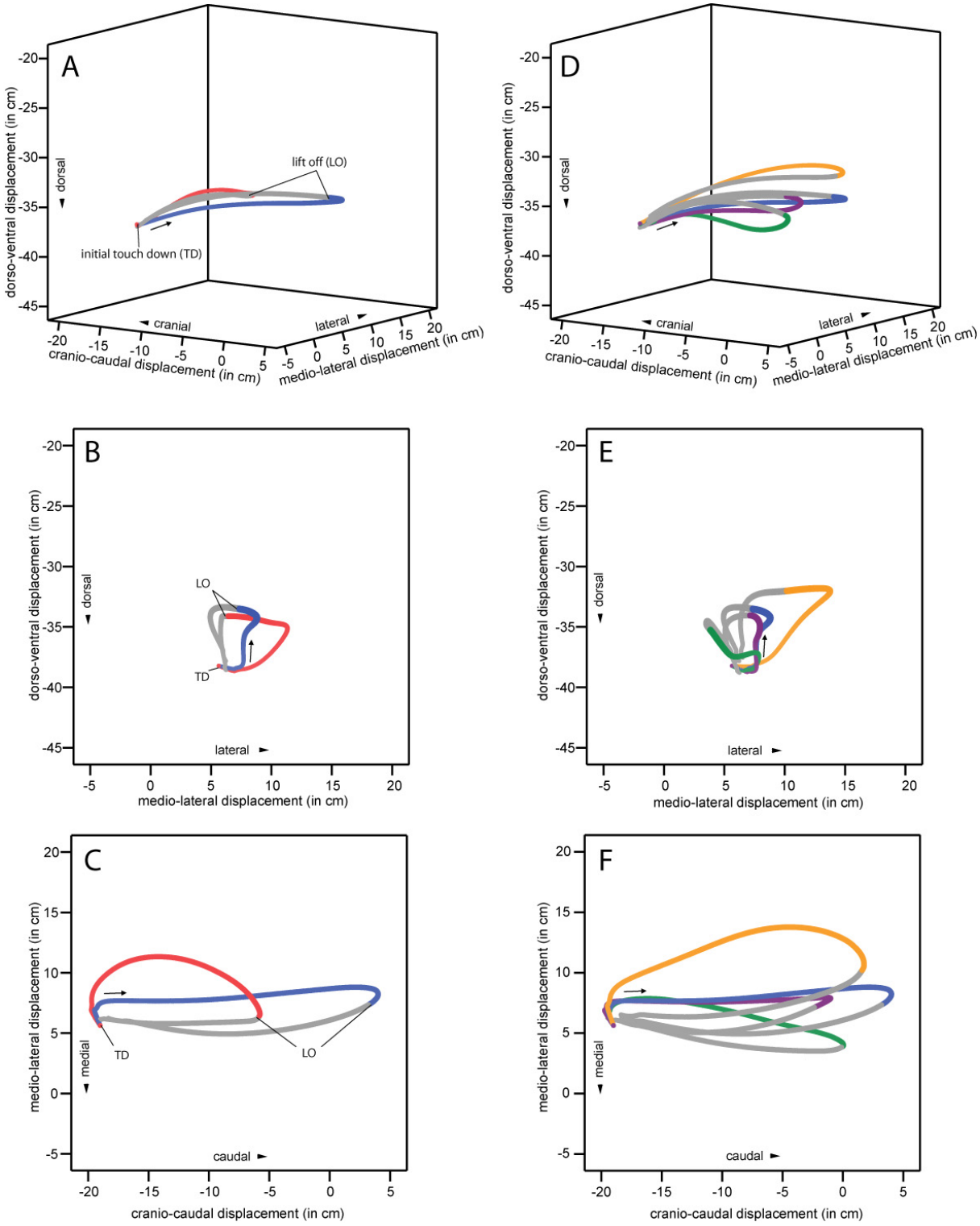

Fig 6: Trajectories of the right knee and the influence of pelvic rotations. Blue: normal locomotion; red: all pelvic rotations turned off; yellow: pelvic roll turned off; green: pelvic yaw turned off; purple: pelvic pitch turned off; grey: swing phases. A, D: 3D trajectories; B, E: trajectories seen from caudal; C, F: trajectories seen from ventral. The small arrow indicates the direction of knee displacement.

3D thoraco-lumbar spine movements and pelvic displacements

3D thoraco-lumbar spine movements mostly were in accordance with our expectations based on published data on symmetric gaits of other mammalian quadrupeds.

LB of the thoraco-lumbar spine and associated pelvic lateral displacements were monophasic. The maximal pelvic displacement to either side was reached approximately at the touch-down of a hindlimb. This pattern was also observed in *Monodelphis* (Pridmore, 1992), tree-shrews (Schilling and Fischer, 1999), different primate species (Shapiro et al., 2001; Schmidt, 2005), three carnivoran species (Jenkins and Camazine, 1977), and horses (Faber et al., 2000). Between touch down of a reference hindlimb and contralateral hindlimb touch down LB of the pelvis had an amplitude of 28°. It is tempting to hypothesize that pronounced lateral displacements of the pelvis are related to arboreal locomotion, where hindlimbs need to be placed on supports that are smaller in diameter than the pelvis. But available data of pelvic displacements due to LB of the spine in other species does not support this notion. Although similar lateral pelvic displacement was found in six strepsirrhine primate species (between 14° in *Loris tardigradus* and 37° in *Nycticebus coucang*) studied by Shapiro et al. (2001), values for more terrestrial species vary between 8° in tree-shrews (Schilling and Fischer, 1999) and 30-40° in *Monodelphis* (Pridmore, 1992). In their x-ray study on carnivoran pelvic displacements Jenkins and Camazine (1977) observed just 13.5°, 10.4° and 7.8° in raccoons, foxes and cats, respectively and van de Graaff et al. (1982) observed a LB amplitude of 20° in the terrestrial skunk (*Mephitis mephitis*). Probably cursorial adaptations with a pronounced restriction to parasagittal limb excursions are generally accompanied by relatively low values of LB in the spine (cf. Jenkins and Camazine, 1977), but this does not explain the very low value found in the tree-shrew.

Intervertebral SB and the resulting displacement of the pelvis was biphasic and maxima of flexion were associated with touch down events of the hindlimbs, whereas minima occurred at instances of hindlimb lift off. This pattern was also observed in horses (Faber et al., 2000; Haussler et al., 2001), dogs (Ritter et al., 2001), nine species of small quadrupedal mammals (Rocha Barbosa et al., 1996; Fischer et al., 2002) and seems to be a general characteristic of symmetric gaits of mammals. Maximal overall amplitude of the resulting pelvic movements of just 9° is comparable to values for the

eight small mammalian species studied by Fischer et al. (2002) that ranged from 7° in rats to 17° in kowaris and the guinea pig (16°) studied by Rocha-Barbosa et al. (1996). Resulting rotation about the long-axis of the pelvis was monophasic as expected. Rotations to either side were maximal (and reduced the distance from the hip joint to the support) at hindlimb touch down. Similar movement was described by Jenkins and Camazine (1977). A later study by Schilling and Fischer (1999) found maximal amplitudes of LAR of the pelvis in the tree-shrew to be approximately 5°. Wennerstrand et al. (2004) observed mean LAR of 6° in the pelvis of sport horses. In the present study a much larger amplitude of 27° for LAR of the sloth pelvis was measured. Schmidt (2005) qualitatively states that extensive LB and twisting movements of the lumbar spine occur during symmetric quadrupedalism of four small arboreal primate species, but no quantitative data is provided. Clearly more comparative data is needed to identify the conditions that influence the 3D movements of the thoraco-lumbar region of the mammalian spine and resulting pelvic displacements during symmetrical gaits.

Amplitudes of intervertebral angular deflections

In vitro studies show regional differences of intervertebral mobility (Yamamoto et al., 1989; Gaudin and Biewener, 1992; Fischer, 1994; Benninger et al., 2004). Studies on in vivo pelvic displacements alone cannot account for differences of mean angular deflection between individual intervertebral joints. Since during cyclic symmetric locomotion only a fraction of maximal mobility is used (e.g. Fischer, 1998) we cannot directly compare our in vivo data with in vitro data. Most published in vivo quantifications of regional differences of movements of the thoraco-lumbar spine averaged angular displacement over several vertebrae (Kafkafi and Golani, 1998; Faber et al., 2000; Shapiro et al., 2001; Wennerstrand et al., 2004; Gradner et al., 2007).

We expected the greatest amplitudes of individual presacral motion of LB, SB and LAR to be in the lumbo-sacral joint. This expectation was based on results of the sole study, from Haussler et al. (2001) that analyzed more than one individual presacral joint in vivo during symmetric locomotion of a mammal (horse). They made use of an invasive method [similar to that of Wood et al. (1992) and Schendel et al. (1995)] with a transducer fixed firmly on pins that were implanted on the vertebral bodies and

protruded out of the skin to directly measure the movement between the instrumented vertebrae during locomotion. In our analysis of sloth locomotion the position of maximal magnitude of intervertebral angular movement differs along the spine for the three rotations. This is accordance with in vitro data of humans (Yamamoto et al., 1989) and dogs (Benninger et al., 2004).

In contrast to in vivo data from Haussler et al. (2001) for the horse, in the present study we documented the highest magnitude of intervertebral LB motion (approx. 7°) to be at the 3rd most caudal presacral joint. Benninger et al. (2004) determined the greatest amplitude to occur at the 4th most caudal presacral joint. Faber et al. (2000) found the region of most pronounced angular LB movement in horses during slow walking to be between vertebral level of TH13 and TH17 (approx. 4.3°; i.e. an average of approx. 1.1° per joint). Considering the amplitudes of individual intervertebral LB, similar values as in the sloth can be expected for the lumbar spine of the six strepsirrhine primate species analyzed by Shapiro et al. (2001) that accounted for lateral displacement of the pelvis of up to 37°.

In trot-like sloth locomotion greater amplitudes of SB in individual presacral joints were observed in increasingly caudal intervertebral joints with the greatest magnitude occurring at the lumbo-sacral joint. This result is in accordance with data from horses (Haussler et al., 2001; Wennerstrand et al., 2004), dogs (Benninger et al., 2004), and humans (Yamamoto et al., 1989).

In disagreement to horses (Haussler et al., 2001), in sloths the maximal magnitude of LAR occurred at the 4th most caudal presacral joint. The in vitro study on the lumbar spine of dogs revealed the greatest mobility for LAR at the lumbo-sacral joint, but similar values at the 4th most caudal prescaral joint as well (Benninger et al., 2004). Yamamoto et al. (1989) found the greatest range of motion in vitro in the 3rd and 4th most caudal presacral joints of humans.

In sum, all studies that investigated 3D intervertebral movements in the lumbar spine found the greatest range of motion of SB to occur at the lumbo-sacral joint, whereas the vertebral level of maximal SB and LAR differs among the species analyzed so far. Again, more comparative in vivo data of intervertebral angular motion is needed to evaluate this observation.

Timing of maximal intervertebral angular deflections

Available data suggests that the presence of a cranio-caudal pattern of maximal angular deflections of the spine is depending on the gait sequence pattern. Kafkafi and Golani (1998) and Faber et al. (2000) found that a traveling wave best describes spinal lateral movements during (lateral sequence) walking of ferrets and horses, respectively. In the argumentation of Faber et al. (2000) the observed temporal cranio-caudal pattern of maximal intervertebral angular deflection offsets the phase differences between hindlimbs and forelimbs which are regarded to act as a pivot point. Thus, in trot-like gaits no temporal cranio-caudal pattern of maximal intervertebral angular deflection should be present, because diagonal fore- and hindlimbs are moved approximately synchronously and no phase differences between diagonal fore- and hindlimbs occur (further characterized by a standing wave of lateral spinal bending). Accordingly, a standing wave of lateral vertebral bending with nodes at the pectoral and pelvic girdle was observed in walking trots of salamanders (Frolich and Biewener, 1992; Ashley-Ross, 1994) and lizards (Reilly and Delancey, 1997). In line with this notion, no cranio-caudal pattern of maximal angular deflections was observed in the thoraco-lumbar spine of sloths during trot-like locomotion in this study and was also not observed in trotting horses (Haussler et al., 2001).

Moreover, this hypothesis on the relationship between gait sequence pattern and an occurrence of a cranio-caudal pattern of maximal angular deflections is in line with published data on epaxial muscle activation. The cranio-caudal activation pattern of the epaxial muscles is consistent with a standing wave during trotting of dogs and might represent a plesiomorphic pattern, due to the comparable diagonal touch down and lift off events of the limbs also present in salamanders and lizards (Schilling and Carrier, 2010).

3D femoral movements relative to the pelvis

Whereas maxima and minima of protraction and retraction as well as LAR of the femur were occurring approximately at touch down and lift off events of the hindlimb regarded, abduction and adduction was clearly influenced by the pelvic position. Abduction was lowest in the moment of contralateral hindlimb touch down, when the pelvis is maximally displaced and rotated (about its long axis) to the contralateral side,

before abduction increases again prior to lift off. At contralateral hindlimb touch down the ipsilateral hip joint (hindlimb pivot) is routed directly underneath the foot as the body is progressed under the support. Jenkins and Camazine (1977) observed a different pattern in their study of three carnivoran species, but recognized that femoral abduction during contact phase and lateral displacement of the pelvis are interrelated components. In these terrestrial species femoral abduction was at a minimum at touch down and increased until lift off. Unfortunately the authors do not exactly state femoral movements during the short bipedal hindlimb support of the walking gaits studied. It can be assumed that quadrupedal mammals during arboreal locomotion, when forced to place their limbs on supports smaller than the diameter of their torso, exhibit more pronounced abduction/adduction movements over the course of a stride cycle than terrestrial ones. However, again more comparative data is necessary to evaluate this hypothesis.

Kinematic studies of pelvic displacement during symmetric mammalian gaits have shown that the pelvis is displaced three-dimensionally (Jenkins and Camazine, 1977). Combined analysis of pelvic and femoral movements in the sloth shows that the knee trajectory results from displacements of the pelvis and motions of the femur relative to it that include long-axis rotation and adduction/abduction. To assess femoral motion relative to the pelvis anatomical coordinate systems are necessary (e.g. Rubenson et al., 2007). Importantly, the observable trajectory of the knee and distal limb is almost linear during the contact phase of the sloth (cf. Fig. 5-6C). The 3D kinematic data presented here thus hints at a more complex muscular activity underlying femoral movement than might be deduced from the rather linear trajectory of the knee alone. If this also applies to other mammalian species, 3D kinematic analyses should be helpful when interpreting EMG data or substrate reaction forces to infer limb function.

Conclusions

Short, caudally pointed spinal processes and a thin epaxial muscle layer suggest that the thoraco-lumbar spine in sloths is not favorable for powerful extension in the sagittal plane, but likely facilitates LB and LAR movements. The kinematic data does not reflect differences in intervertebral mobility that could be deduced from the

configuration of the zygapophyses alone. 3D in vivo kinematics of angular motion in the six most caudal presacral joints, resulting pelvic displacements and relative femoral movements were in accordance with some expectations that were based on the scant 3D data available from previous publications. Due to consistency of the pattern for thoraco-lumbar LB (monophasic) and SB (biphasic) as well as LAR (monophasic) in diverse mammalian quadrupeds, these patterns can be assumed to be part of a general pattern in mammalian symmetric gaits. In contrast to the only comparable in vivo data from horses maximal angular deflections of LB and LAR did not occur at the lumbo-sacral joint. In accordance to the other species investigated in trot-like symmetrical gaits of sloths no cranio-caudal pattern of maximal angular deflection is observed. Therefore, we hypothesize that a temporal cranio-caudal pattern of maximal intervertebral angular deflections is only be present when fore- and hindlimbs move out of phase and spinal movement is best described with a traveling wave. It remains to be determined *via* EMG data on the epaxial muscles of the sloth whether pelvic displacements are the consequence of active bending of the spine or the result of passive motion induced by the action of extrinsic hindlimb muscles as proposed for more dynamic trotting of dogs (Schilling and Carrier, 2009). More generally, perhaps this relationship between active bending and passive displacement depends on the speed of mammalian symmetrical locomotion. Femoral protraction and retraction as well as long axis rotation was governed by the leg's stride cycle, whereas abduction was interrelated to lateral displacement of the pelvis. Both, displacement of the pelvis as well as movements of the femur are complex. Quantification of these 3D movements might facilitate more differentiated inference of hindlimb muscle function from EMG or substrate reaction force data. In arboreal species more pronounced movements of the thoraco-lumbar spine likely facilitate efficient retraction of the hindlimb during contact phase while the foot is placed closer the sagittal plane on narrow supports. More comparative data is necessary to further elucidate the spatial and temporal patterns of intervertebral movements of the mammalian spine during symmetric gaits.

ACKNOWLEDGEMENTS

Without the XROMM short course in August 2009 held by the developers of the method at Brown University, Providence (RI), USA, this study would not have been possible. A. Petrovitch provided access to the medical CT scanner. I. Shappert generously provided the sloths Julius and Evita as a loan from Zoo Dortmund, Germany. E. Woker helped with animal keeping. R. Kraft of the Bayrische Staatssammlung Munich, Germany granted access to the museum collection. R. Petersohn and L. Wagner helped with the experiments. H. Stark developed the software that was used to convert file formats of different 3D softwares. N. Schilling formulated helpful critique on an earlier version of the manuscript. The study was financially supported by the DFG (grant to M. S. Fischer: DFG Fi 410/11-1).

- Chapter 6 -

Inverse dynamic analysis aids interpretation of functional limb morphology and locomotor strategy of two toed sloths

John A. Nyakatura & Emanuel Andrada

Abstract

Sloths are morphologically specialized in suspensory quadrupedal locomotion and posture. During steady-state locomotion they utilize a trot-like gait sequence pattern. To gain insight into this locomotor mode and the functional morphology of the sloth locomotor apparatus and to test whether sloth locomotion can be described by simple connected pendulum mechanics, we analyzed the mechanics of sloth locomotion. No simple pendular mechanics were present. Subsequently, we built a mechanical link model to enable us to carry out an inverse dynamic analysis. The model integrates the body segment parameters and was driven by the kinematics obtained from one sloth. The analysis allowed us to estimate limb joint torques and substrate reaction forces during the contact phase. The previously hypothesized "anti-gravity role" of limb joint flexor muscles was confirmed. We identified the peculiar topography of the m. pectoralis superficialis posterior to facilitate acceleration of the lower arm during locomotion. The effective generation of moments in the wrist is only possible with simultaneous scapular retraction. This is effected mainly via the plesiomorphic pattern for forelimb retraction also present in pronograde mammals. The model indicates a pulling effect of the forelimbs to generate propulsion. Sloths seem to actively reduce the dynamical forces that are transmitted onto the support. We conclude that these findings reflect the need to reduce the risk of breaking supports, because if the support breaks this species is unlikely to be able to react quickly enough to prevent potentially lethal falls. Furthermore, this locomotor strategy may be facilitated by the species' reliance on a ubiquitous food resource.

INTRODUCTION

No other mammals are as restricted to suspensory posture and locomotion as extant sloths. Sloths possess a suite of morphological distinctions, such as hook-like appendages, that permit effective arboreal locomotion under superstrates that are small relative to the trunk (e.g. Miller, 1935; Vassal et al., 1962). However, modern tree sloths are very clumsy on the ground (Mendel, 1981b). In the arboreal setting, the suspensory posture of sloths extends the feeding sphere (Grand, 1972) and at the same time avoids the need to balance on small, flexible supports (Cartmill, 1985).

The biological role and morphological consequences of suspensory postures have received considerable research interest in the past with regard to brachiating primates, i.e. gibbons, siamangs, orang utans and atelines (Ashton and Oxnard, 1964; Fleagle, 1974, 1976; Jungers and Stern, 1981; Turnquist et al., 1999). Long forelimbs, the architecture of the pectoral girdle (with maximized mobility at the shoulder joint) and the morphology of muscles that flex the fingers are all interpreted as adaptations to brachiation, especially in the gibbons and siamangs. Preuschoft and Demes cite elongated forelimbs, passive muscles that support body weight at the elbow and shoulder via elastic tension so as to remove the need for muscular activity during passive hanging, and strong finger flexors that are able to flex the fingers against the pull of the body weight as prerequisites for suspensory posture and locomotion (Preuschoft and Demes, 1984). It is therefore not surprising that these features also evolved convergently in quadrupedal suspensory two-toed sloths (Xenarthra: *Choloepus didactylus*, Linné 1758). Sloths clearly have elongated limbs (Strauss and Wislocki, 1932). The forelimb appendage is characterized by a strong m. flexor digitorum profundus that inserts to the distal phalanges (which bear the large claws) and flexes the distal interphalangeal joint to form an effective hook-like hand (Mendel, 1981a). A similar configuration is also present in the hindlimbs (see Mendel, 1981b). Moreover, sloths have impressive mobility at the shoulder joint and also have muscles with long tendinous insertions that span the elbow and knee joints and are argued to maintain passive flexion in these joints with minimal muscular activity via elastic tension (Mendel, 1985).

A recent analysis of sloth locomotion revealed speed-related effects in kinematics (Nyakatura et al., 2010). When moving steadily on a ‘treadpole’ (see below), sloths

consistently have relatively extended limbs and also use trot-like gaits (i.e., diagonal fore- and hindlimbs touch down and lift off at the same time). Taking the morphological convergences to brachiators into account, we initially hypothesized that these behavioral adjustments are made to make use of passive pendular mechanics comparable to a connected simple pendulum that swings in phase (Fig. 6-1A-C). Biomechanical studies demonstrate that effective pendular mechanics are used in slow 'continuous contact' forelimb brachiation in primates (Kummer, 1970; Fleagle, 1974; Preuschoft and Demes, 1984; Swartz, 1989, Turnquist et al., 1999; Chang et al., 2000). With the exception of anatomical investigations and locomotor analyses by Mendel that focused on specific aspects of the wrist, hands and feet (Mendel, 1979, 1981a, 1981b, 1985), hardly any research has been done into the functional morphology and, in particular, the biomechanics of the extant sloth locomotor apparatus.

It has been hypothesized that during suspensory locomotion, flexors need to counteract the gravity-induced extension of the limbs (Mendel, 1985; Nyakatura et al., 2010). Morphological features such as the long tendinous insertions of the elbow and knee flexors described above are consistent with this premise. We therefore expected the torques acting on the limb joints during locomotion to reflect this biomechanical demand.

If simple pendular mechanics apply during steady-state trot-like locomotion, there should be a cyclic exchange between potential and kinetic energy. This exchange will then be reflected in the support reaction forces (SRFs). Specifically, we expected a dynamic fluctuation in the vertical SRF component (Fig. 6-1D). A propulsive impulse was expected to be exerted in the first half of the contact phase and a breaking impulse in the second half of the contact phase (Fig. 6-1E). However, analysis of the swing frequency and the vertical oscillation of the approximated center of mass (CoM) in the sloth demonstrate that these parameters do not match values predicted for a simple connected pendulum. Hence, simple pendular mechanics are unlikely to apply in sloths (Table 6-1).

Table 6-1: Trot-like locomotion in sloths cannot be approximated by a simple connected pendulum. Please note that vertical CoM fluctuation is less than half of the predicted value and swing frequency is approximately 1.5 times as long. *: the simple model accounted for total weight, limb weight and length of pendulum, i.e. initial functional limb length.

	CoM vertical amplitude	Duration of contact phase (swing frequency)
Connected pendulum 4-bar mechanism*	> 5.0 cm	0.97 sec
Live sloth (sloth A)	2.03 cm	1.47 sec

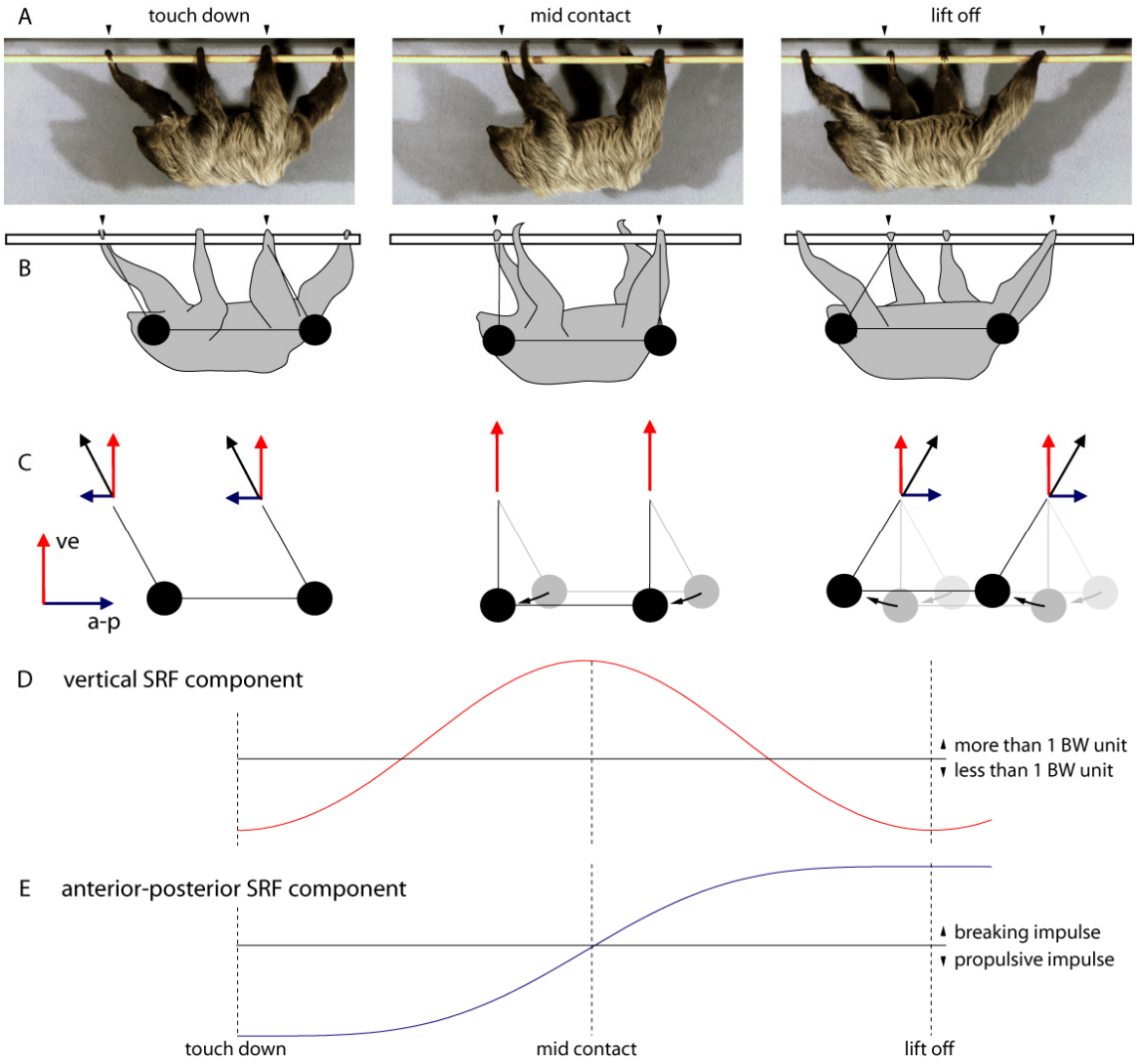

Fig. 6-1: The initial hypothesis that the musculo-skeletal apparatus acts as a simple connected pendulum during steady-state trot-like locomotion in sloths. A: Representative frames of a steady-state locomotor trial of *C. didactylus*; B: In trotting gaits the body of the sloth is connected to the support by diagonal limbs that enter swing phase and contact phase simultaneously, C: schematic representation of a simple connected pendulum swinging in phase and associated SRF. D: Vertical component (ve) of SRF exerted on the support during the motion of a connected pendulum. E: Anterior-posterior (a-p) directed component of SRF during the motion of a connected pendulum.

In order to gain further insights into the musculo-skeletal function of the two toed sloth, we developed a mechanical segment link model that integrated the body parameters of one 'target' sloth and was driven by the kinematics obtained in an earlier x-ray motion analysis of the 'target' animal (Nyakatura et al., 2010). The mechanical link model was then used to mathematically determine the moments acting on individual limb joints of the target during a contact phase. Furthermore, we also used the model to calculate the support reaction forces (SRFs) that can be expected in live sloths. The data we obtained is used in our interpretation of the functional characteristics of the sloth locomotor apparatus and the sloth's locomotor strategy.

MATERIAL AND METHODS

Kinematic analysis and assessment of body parameters

The characteristics of sloth steady-state locomotion and speed-related effects are documented in detail in Nyakatura et al. (2010) and will only briefly be summarized here. The kinematic data used as the 'target' in this study were taken from the earlier publication and represent a subset of the larger dataset already published; only the steady-state locomotion data of one sloth (sloth A: the 'target' of our model) was used here. To achieve steady-state locomotion the sloth was trained to move along a motorized 'treadpole' (4m long, 40mm diameter), the arboreal equivalent of a treadmill, in front of high-speed x-ray cameras (for details of experimental design and setup see Nyakatura et al., 2010).

Sloth A was weighed and the lengths of limb elements were measured from calibrated x-ray video frames. To protect the live animal (a kind loan from Dortmund Zoo, Germany) from the possible risks of anesthesia, we used a fresh cadaver of a different *C. didactylus* specimen (sloth B) to assess the weights of the individual limb elements of sloth A. The mass of the individual limb elements (relative to total weight) of sloth B was linearly scaled to the size and total weight of sloth A (our 'target', Table 6-2) to closely approximate body segment parameters.

Table 2: Body parameters of sloth A (our 'target'), body mass = 6500g. J: mass moment of inertia about the CoM; L: distance between proximal and distal joint. The position of the CoM is relative to the proximal joint. HAT: trunk + neck + head + swinging extremities.

	Mass (g)	J (g cm²)	L (cm)	CoM (%)
Hand	124	798	10.3	45
Lower arm	234	11645	19.1	47.6
Upper arm	234	4809	16.2	46
Scapula	58	534	8	50
Foot	131	632	11.5	49
Lower leg	277	3370	14.2	44
Upper leg	212	5156	14.8	49.2
HAT	4518	858000	47.6	55
Pelvis	712	8676	9.0	46

Sloth B and another available cadaver were then carefully dissected to aid our functional interpretation of muscle topography. In the identification of muscles we used the criterion of innervation and followed the nomenclature of Evans (1993) in cases of conflicting descriptions in earlier publications (Humphry, 1869; Mackintosh, 1874; Lucae, 1888, Miller, 1935).

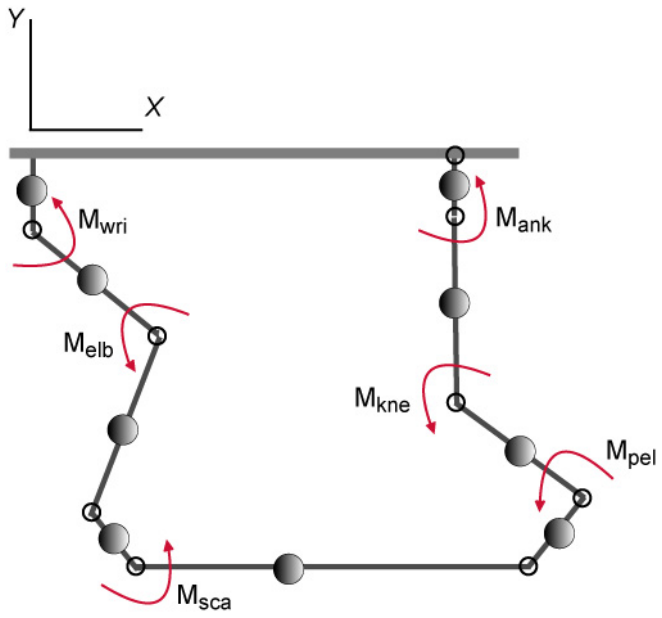

Fig. 6-2: Schematic representation of the link model we used to approximate the locomotor characteristics of *C. didactylus*. A ten-bar mechanism with 6 DoF based on the segment parameters and the moments calculated to produce the kinematics of our 'target' during steady state trot-like locomotion. The link model was subsequently used to calculate the support reaction forces (SRFs) expected to occur in the live animal.

The mechanical link model

The link model was built in Simulink™ (The Mathworks). To calculate inertial properties (i.e. mass, position of CoM, and inertial tensor about the CoM), each model limb element was approximated to circular cylinders (see Preuschoft and Demes, 1984).

To model the movements of our 'target' during steady-state trot-like locomotion, we used a ten-bar mechanism that appears at first sight to match the limb elements and trunk of a two-toed sloth, including hand, lower and upper arm, scapula, trunk including head, pelvis, thigh and lower leg, and foot (Fig. 6-2). The locomotion analysis indicates that the hand remains almost perpendicular to the superstrate during the complete contact phase. Therefore, hand contact was modeled as a weld-joint, which eliminates all possible degrees of freedom (DoF) between this segment and the superstrate. The eight segments left were linked via pin joints. The final configuration takes the form of a closed chain with six DoF. This is the minimum number of independent coordinates necessary to describe the configuration of the system.

Simulation analysis

The equations of motion for a mechanical system represent the relationship between the forces that act on the system and its motion. The simulation analysis was therefore divided into two parts. The first was an inverse dynamic analysis (desired motion is known and the objective is to find unknown forces). Here we seek to find the joint moments acting on each of the six DoF. On the basis of the kinematics of the limbs, and the morphological characteristics, we decided to place the angular drivers in the following joints: wrist, elbow, scapular, pelvic, knee and ankle. The second part was a forward analysis; here the computed moments were applied to each joint of the link model to calculate the SRFs.

For the system to undergo a desired motion, n_{DoF} drivers (six) were described together with their first and second time derivatives as:

$$^{(d)}\Theta = \Theta(q,t) = 0;\ ^{(d)}\dot{\Theta} = \dot{\Theta}(q,t) = 0;\ ^{(d)}\ddot{\Theta} = \ddot{\Theta}(q,t) = 0$$

The functions *f(t)* for the drivers were constructed from the absolute limb element angles and interpolated to obtain 131 points. Simulation started with the positioning

of the model according to the limb element angles measured in our 'target' at initial touch down of the diagonal fore- and hindlimbs (cf. Fig. 6-3).

For the inverse analysis, the general formulation for the equations of motion was stated as:

$$M\ \ddot{q} = h + D'\lambda + {}^{(d)}D'\ {}^{(d)}\lambda$$

where M is the mass matrix, q the array of generalized accelerations, *h* the array of generalized forces, the second and third terms on the right hand side of the equation represent the forces and driver constrains. Here *D* are the Jacobians and λ the Lagrange multipliers. The supra-indices $^{(d)}$ denote those elements related to the drivers. Proper interpretation of the elements of $^{(d)}\lambda$ yields the forces and moments that the driver motors/actuators must provide to produce the desired motion.

For the forward analysis the third term on the right hand side of equation xx vanishes, because moments are introduced via the *h* array. SRF were computed by solving the Lagrange multipliers λ associated with hand and foot contacts.

Inverse and forward analyses were integrated using the ODE3 (bogacki-Shampine) solver (fixed-step size: $1e^{-2}$).

Limitations of the biomechanic link model

The 2D model is restricted to motions in the sagittal plane. This simplified but manageable approach neglects the ab- and adductive motions of the limbs and the lateral bending motion and torsion of the body axis. Out of plane movements, however, lead to a misrepresentation of joint angles projected to the parasagittal plane (Stevens et al., 2006). In this context, limb elements that are moved out of plane appear shortened in a sagittal projection (Fischer and Lehmann, 1998). Thus, the actual 3D motion of live sloths cannot be exhaustively represented in our 2D model, which limits the possibility of adequately matching the kinematic parameters of the model and the 'target'. Small-scale movements of the actual live animal, e.g. the movement of the hand on the support, were also neglected in our model for the sake of simplicity. Another constraint of the approach chosen is that joint moments can only be calculated for the individual DoF in the closed chain. That is to say, torques could not be determined for all limb joints. We chose to determine the torque at the scapular

pivot because the scapula is often neglected as a forelimb element though it is actually very important. For this reason, we cannot present data on the shoulder joint. However, torques at the scapula can be estimated to be very similar to the torques at the shoulder joint (cf. Andrada et al., in press).

Finally, the model comprises just two 'limbs'. The calculated torques and SRFs are thus likely to be smaller in the live sloth when all four limbs have contact to the support, i.e., around touch down and lift off (cf. Nyakatura et al., 2010).

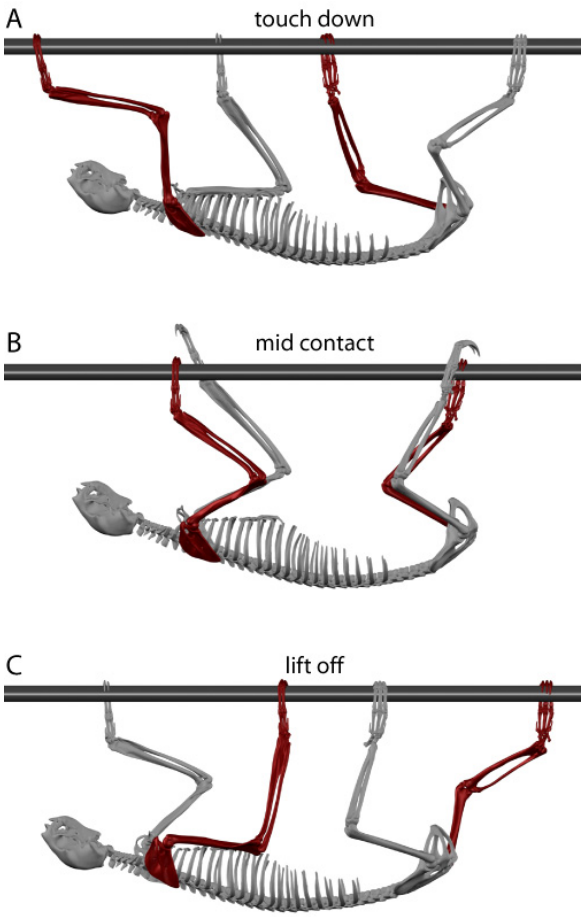

Fig.6-3: Representative illustrations of the skeletal kinematics of *C. didactylus* during the contact phase (highlighted limbs) at touch down (A), mid contact (B), and lift off (C).

RESULTS

Kinematics of the two toed sloth

Although there is some variability in intralimb kinematics during steady-state trot-like locomotion in *C. didactylus,* the following general pattern applies.

The hands and feet are held approximately perpendicular to the support throughout the contact phase, giving the rigid hook-like appendages a secure hold (Fig. 6-3). At touch down the forearm is held almost parallel to the frontal plane, whereas the upper arm is approximately vertical and the shoulder blade is in a protracted position (Fig. 6-3A). The lower leg is oriented in such a way that the distal end is slightly more cranial than the knee. The knee joint is relatively extended, whereas the hip joint is flexed. The thigh is oriented almost parallel to the frontal plane. During the first half of the contact phase the upper arm is retracted, while the shoulder blade maintains its protracted position, i.e., there is much movement in the shoulder joint (Fig. 6-3B). Some flexion also occurs in the elbow joint. The knee joint is increasingly flexed and the hip extended. During the second half of the contact phase there is little movement in the shoulder joint, but the shoulder blade is retracted (i.e., it is rotated about a pivot at the vertebral border that is maintained at a fixed position relative to the trunk). Towards the end of the contact phase the elbow joint extends slightly. This is also true of the knee joint, but hip extension continues until lift off. The kinematic data of the 'target' used to drive our model are reported in Fig. 6-4.

In summary, the motion analysis of the two-toed sloth documented rather conservative overall kinematic patterns when compared to pronograde mammals of a similar size (Nyakatura et al., 2010; Nyakatura and Fischer, 2010).

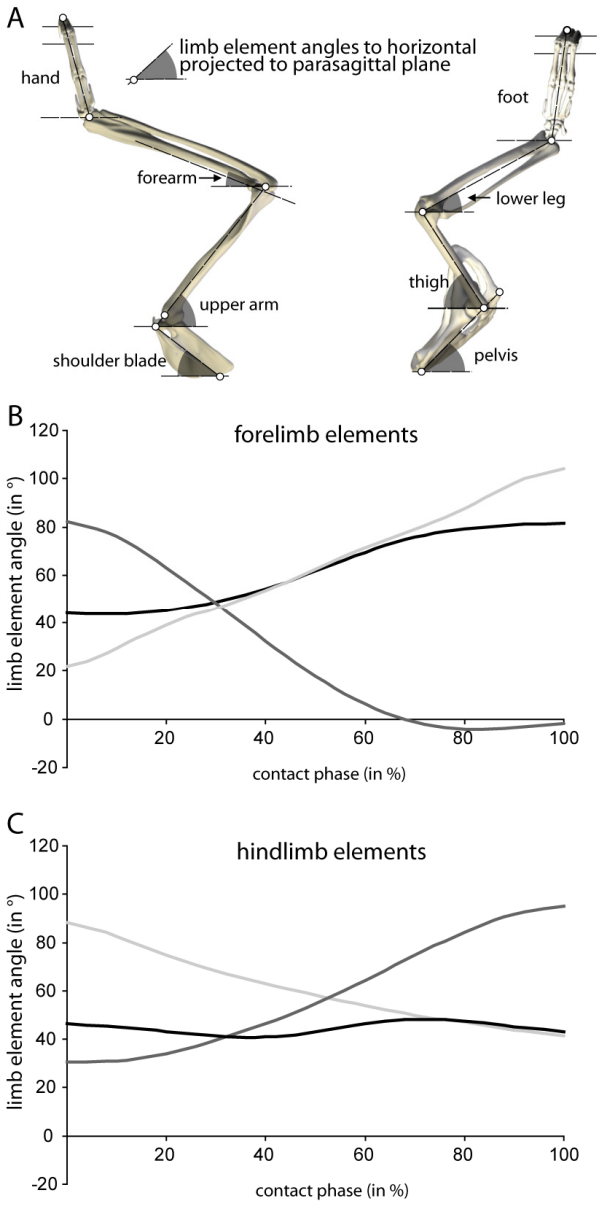

Fig. 6-4: 2D Kinematics of sloth A (n = 20) were used to model the contact phase of the mechanical link model. A: The 2D limb element angles used in this study. B: forelimb element angles (black: scapula; dark gray: upper arm; light gray: lower arm). C: hindlimb element angles (black: pelvis; dark gray: thigh; light gray: lower limb). We observed little movement in the hands and feet and neglected these movements in our model (cf. Nyakatura et al., 2010).

Limb joint torques

The inverse dynamic analysis of the mechanical link model revealed the joint torques necessary to produce the kinematics observed in the live sloth. The greatest overall torque occurs at the wrist (Fig. 6-5). At touch down, a moment of almost 1 Nm per kg flexes the wrist, but then the flexor torques decreases rapidly and an extensor moment acts on the wrist during the last two thirds of the contact phase. A relatively small extensor moment acts on the elbow at touch down. The flexor group at the

elbow then produces a flexor moment of up to 0.7 Nm per kg throughout the remainder of the contact phase. The moment at the scapula first flexes the scapula, i.e., a moment is produced that keeps the scapula protracted. Later on in the contact phase an extensor torque acts on the proximal pivot of the scapula. At the ankle much smaller torques are generated than at the wrist. Here we find a constant extensor torque of around 0.2 Nm per kg. A constant flexor moment of up to 0.5 Nm per kg is produced at the knee. Small constant extensor torques are produced at the hip.

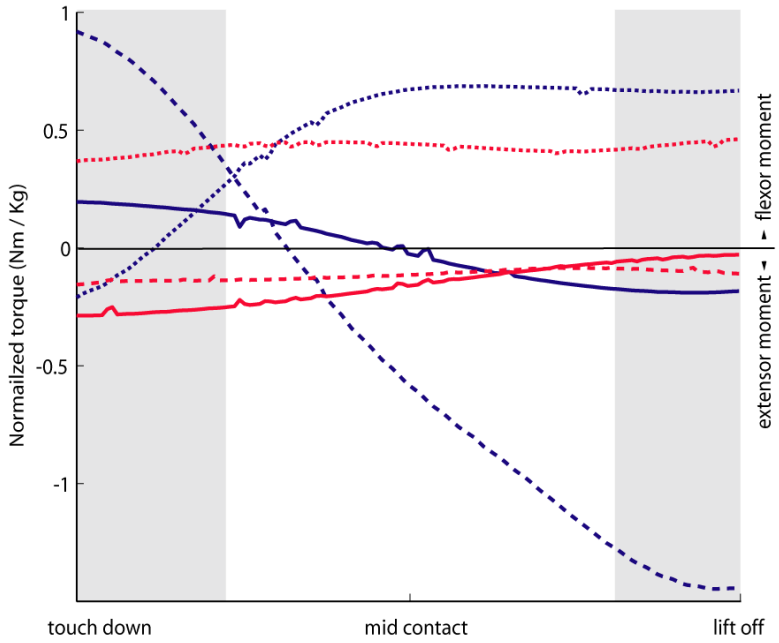

Fig. 6-5: Torques at the joints of the mechanical link model calculated to match the kinematics of the live sloth. Blue line: scapula; blue dotted line: elbow; blue dashed line: wrist; red line: hip; red dotted line: knee; red dashed line: ankle. Gray area: Live sloths have all four limbs in contact with the support and occurring torques are expected to be smaller than in the model.

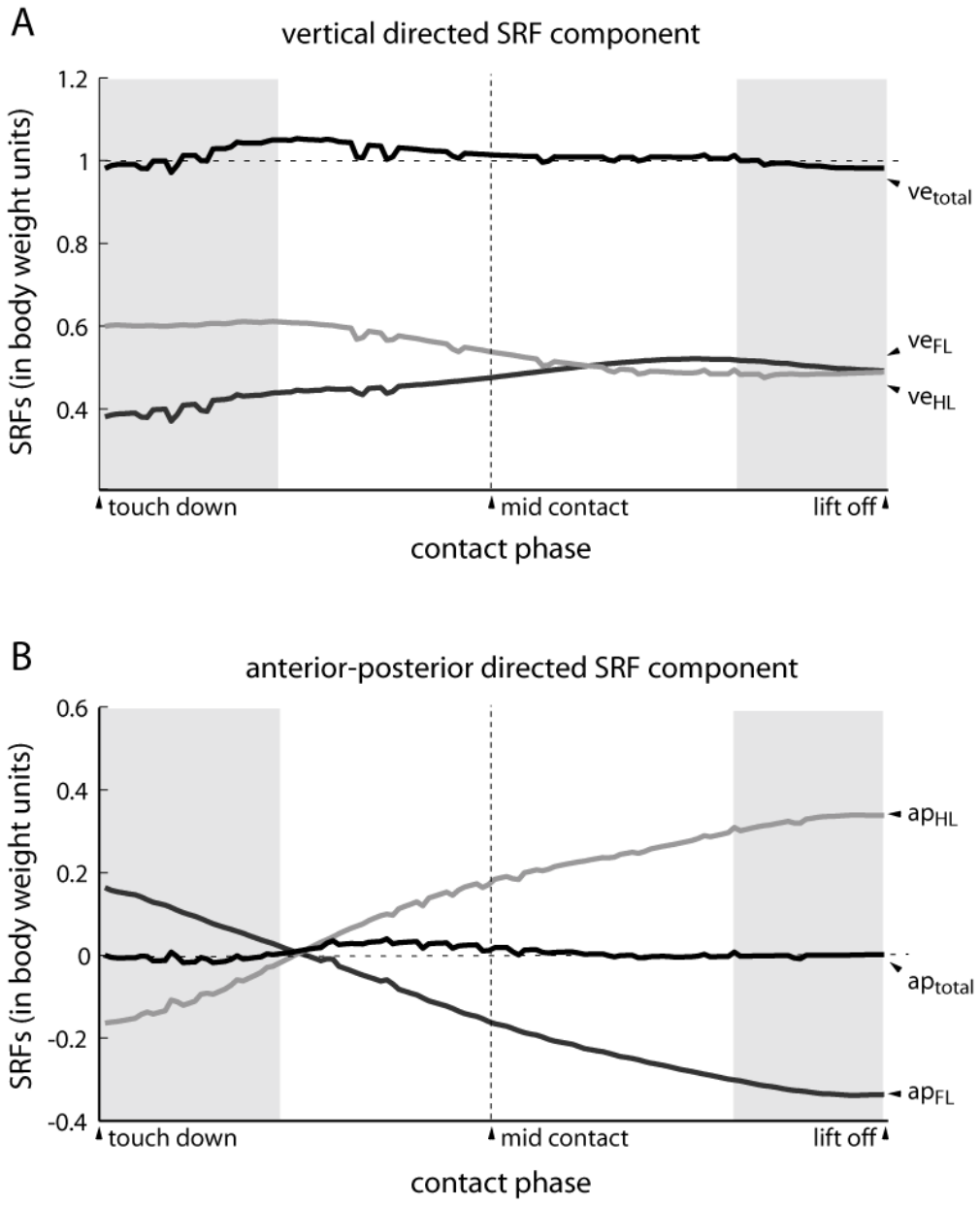

Fig. 6-6: SRFs of fore- and hindlimbs over the course of a contact phase calculated from the mechanical link model. A: vertically directed SRF component; B: anterior-posteriorly directed SRF component. Ve: vertically directed SRF component; ap: anterior-posteriorly directed SRF component; FL: forelimb; HL: hindlimb. Please note the small amplitude of the total exerted inertias to the support (quasistatic locomotion).

Support reaction forces

In our mechanical link model, the majority of the body weight at touch down is carried by the hindlimbs. This amount is reduced when the CoM is moved forward during the contact phase. At lift off, the fore- and the hindlimbs carry approximately half of the

weight each. The anterior-posteriorly directed SRF component shows that the role of the fore- and hindlimbs is reversed. During steady-state locomotion, the braking and propulsive impulses of the fore- and hindlimbs offset each other. This allows the dynamic forces exerted on the support to be controlled enough to vary only very little.
In summary, the total vertical and total anterior-posteriorly directed components of the SRFs differ only slightly from a static situation (Fig. 6-6). Sloth locomotion is therefore quasistatic. Sloths seem to actively minimize dynamic changes in the forces exerted on the supports. In doing so, they sacrifice an energy efficient feature of pendular mechanics.

DISCUSSION

Joint torques during suspensory quadrupedal locomotion

On the basis of the torques calculated as acting on the joints of the mechanical link model, we discuss the likely function of the muscle complexes acting on these joints in the live animals. Since in sloths gravity always pulls the trunk away from the support, we assume that extension of joints is completely passive and that extensors are not recruited for limb extension. However, if the speed of an extension is much slower than would be expected from passive motion due to gravity, the movement is probably the result of an excentric contraction of the flexor muscle, i.e. the activity of the flexor group “permits” the gravity-induced extension of the joint to a certain degree. Furthermore, we assume that limb flexion against the pull of gravity is the concentric contraction of the muscles of the flexor complex.
In sloths, the palm is oriented medially not ventrally when in contact with the support. This makes comparison with other mammals difficult. However, in contrast to the three species analyzed by Witte et al. (2002), the goat studied by Pandy et al. (1988), the horse studied by Clayton et al. (1998) and the pig studied by Thorup et al. (2008), we found that the greatest torque acted on the most distal joint of our model rather than the most proximal one. It is important to note that the highest torques obtained from our model occur close to touch down and lift off. At these instants all four feet of live sloths are in contact with the support, which probably decreases joint torques at individual joints.

At the elbow we calculated a flexor moment for the greater part of the contact phase. As predicted, this is contrary to the extensor torque found in the elbow of pronograde mammals (goat: Pandy et al., 1988; horse: Clayton et al., 1998; small mammals: Witte et al., 2002; pig: Thorup et al., 2008; rat: Andrada et al., subm.). The flexor moment at the scapular pivot of our model in the first half of the contact phase is consistent with muscle activity that keeps the scapular protracted, despite gravity pulling the trunk away from the support. In the second part of the contact phase the scapula is retracted and an extensor moment acts on the scapular pivot. The torque pattern is thus comparable to the pattern found by Witte et al. (2002) in the three species of small mammals.

Sloths have morphological characteristics that are likely linked to their inverse orientation with regard to the force of gravity. For example, the muscular topography of the m. pectoralis is unusual in *C. didactylus*. The posterior slip of the superficial pectoralis (m. pectoralis superficialis posterior: PSP) joins the acromial part of the m. deltoideus and both join the anterior belly of the m. biceps brachii (BB) (Lucae, 1888; Miller, 1935; Nyakatura and Fischer, in prep.). All three muscles have a common insertion on the ulna. In contrast, the deep portions of the pectoralis (m. pectoralis profundus medius et posterior: PP) retain their typical attachment sites at the proximal humerus. The m. latissimus dorsi (LD) also maintains its usual insertion caudal on the proximal humerus.

During suspensory locomotion, the activity of muscles on the flexor side of the limbs counteracts the gravity-induced extension of the limbs. The flexor moments acting on the elbow and shoulder throughout almost the entire contact phase are likely produced by the strong muscles on the flexor side of these joints: the m. brachioradialis at the elbow helped by PSP, BB and the acromial part of the m. deltoideus, and the m. teres major at the shoulder helped by the long head of the m. triceps and the m. dorso-epitrochlearis (Mendel, 1985). The flexor groups at these joints have been hypothesized to take over the ‘anti-gravity role’ during suspensory locomotion in sloths (Mendel, 1985; Nyakatura et al., 2010) and this is confirmed by inverse dynamic analysis (this study). Because the PSP spans several joints, it also flexes the elbow and the shoulder.

The conservative kinematics of the proximal forelimb suggest that the modus of forelimb retraction is also conservative (Nyakatura and Fischer, 2010) and likely to be similar to the forelimb retraction during stance phase of terrestrial mammals (Jenkins and Weijs, 1979; Fischer, 1994). The large m. latissimus dorsi has the topography to pull the proximal humerus caudad and also to effectively retract the scapula, in case of co-activated intrinsic shoulder musculature (mm. subscapularis, infraspinatus et supraspinatus). At the same time, muscles inserting at the vertebral border of the scapula need to maintain the scapular pivot in its position relative to the thorax. This is likely achieved by the combined effect of the cervical part of m. trapezius and the cervical part of m. serratus ventralis. Ventral to the shoulder the posterior part of the m. pectoralis profundus (medial and posterior parts) is also a suitable candidate for retracting the shoulder, given the concerted action of the intrinsic shoulder musculature to fix the shoulder joint. Powerful scapula retraction seemed questionable on the basis of the kinematic analysis alone (Nyakatura and Fischer, 2010), because the inversion with regard to the gravity vector would tend to retract the scapula passively. However, the flexor moment (which leads to scapula protraction) obtained at the scapula pivot in our model must be produced by muscles that actively protract the scapula and maintain its protracted orientation in the first part of the contact phase. After mid contact a retraction moment acts on the scapula pivot, but whether this moment is produced solely by gravity or is actively produced by forelimb retractor muscles remains to be established.

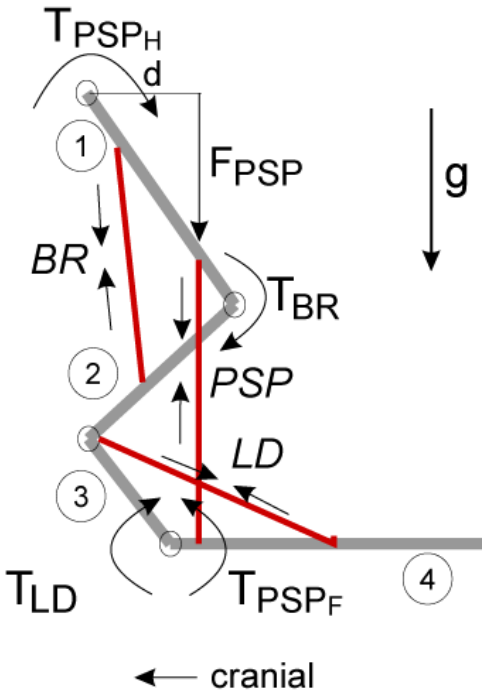

Fig. 6-7: Schematic model for our hypothesis of forelimb function during sloth locomotion. Only selected muscles and the torques produced by these muscles are shown. (1) Forearm, (2) upper arm, (3) shoulder blade, (4) trunk. The contraction of m. brachioradialis (BR) produces a torque (T BR) which flexes the elbow and counteracts the action of gravity (g). The contraction of m. pectoralis superficialis posterior (PSP) produces moments about the wrist joint and the scapular fulcrum of the link model (T PSPh and T PSPf). The latter has to be counteracted by the contraction of the main limb retractors (mainly m. lattisimus dorsi (LD) and m. pectoralis profundus) in order to prevent the trunk and scapula from rotating ventrally (counter-clockwise). Finally, the torque T PSPh remains unbalanced and therefore rotates the sloth cranially, i.e. it produces propulsion.

Due to the morphology of the forelimb, the observed kinematics and the calculated moments at the limb joints, we suggest that the PSP, the BB and the acromial slip of the m. deltoideus together produce an unmatched torque at the wrist that rotates the body cranially (Fig. 6-7.)

The sloth foot is also oriented medially towards the support making comparison with pronograde mammals difficult. The torque at the ankle is much smaller than at the wrist. At the knee, a flexor moment counteracts gravity-induced extension. The moment is likely produced the m. biceps femoris, which extends far out from the knee and thus has an advantageous lever arm. Again, as hypothesized, the torque pattern is an inversion of that of pronograde mammals (cf. goat: Pandy et al. 1988; dog: Dogan et al., 1991; cat: Fowler et al., 1993; small mammals: Witte et al., 2002). However, Thorup et al. (2008) found a small flexor moment at the knee during the first 60% of the stance phase in pigs. A constant extensor moment acts on the hip and retracts the femur, as also found by Pandy et al., 1988; Dogan et al., 1991; Fowler et al., 1993; Witte et al.,

2002; Andrada et al., subm.. However, unlike in pronograde mammals, the hip in sloths does not need to be extended in order to counteract gravity-induced flexion. In the early contact phase at least, gravity will lead to hip extension. Nevertheless, femoral retraction is still the most dominant movement of the hindlimb (Nyakatura et al., 2010). The extensor moment evident in the hip is thus likely to be "permitted" by the excentric work of the hip flexor group (mainly m. iliacus, m. psoas major and m. rectus femoris) to prevent an uncontrolled extension of the hip due to gravity. However, femoral retraction beyond 90 degrees from the horizontal requires the active input of femur retractor muscles such as the m. gluteus.

SRFs during suspensory quadrupedal locomotion

We initially tested whether the locomotion of sloths can be described by a simple connected pendulum. Instead of the expected dynamic fluctuation of vertically directed SRFs we found total vertical SRF to fluctuate only minimally around body weight. That is to say, the transmission of forces to the support is very uniform, at least during steady-state locomotion. This is clearly different to brachiation in gibbons where a dynamic fluctuation of the vertically directed SRF is evident in continuous-contact and ricochetal brachiation (Chang et al., 2000). Dynamic fluctuations of vertical SRFs also occur in the pronograde arboreal quadrupedal locomotion of primates (e.g. Schmitt, 1999; Schmidt, 2005). Moreover, Ishida et al. (1990) compared the upside-down locomotion and pronograde locomotion of Slow Loris, a species characterized by deliberate cautious locomotion similar to that of sloths, and found identical dynamic vertical fluctuation of almost 0.6 BW units in both locomotor modes, in comparison to less than 0.2 BW units in the limbs of sloths.

More generally, during arboreal quadrupedal locomotion on thin branches, primates have been shown to utilize a compliant gait marked by substantial elbow yield, longer contact times, and more pronounced forelimb protraction than when walking on solid ground (Schmitt, 1999). These adjustments lower the peak vertical forces which occur, reduce vertical oscillation of the CoM, and result in a reduction in the oscillation of the support (Schmitt, 1999). The kinematics of the sloth have similar dynamic consequences. As predicted by Schmitt (1999), adjustments to reduce the vertical

oscillation of the CoM should also be observed in other arboreal species and have already been described for chameleons (Peterson, 1984).

During steady-state trot-like suspensory locomotion, sloths mainly produce an accelerating SRF in the forelimbs, which is offset by the braking impulse of the hindlimbs. This means that the forelimbs pull as the hindlimbs brake. Again however, the total anterior-posteriorly directed SRFs of the sloth are not dynamic and the resulting locomotion is very uniform. The forelimbs were also found to have a pulling role in the upside-down quadrupedal locomotion of Slow Loris (Ishida et al., 1990). These authors found that the hindlimbs exerted a net push during pronograde locomotion above the support, whereas the forelimbs exerted a net pull during the contact phase of upside-down locomotion. Our model implies similar dynamics in sloth upside-down locomotion. We suggest that quadrupedal suspensory locomotion is "forelimb dominated" in contrast to the "hindlimb domination" regularly found in pronograde mammals (e.g. Demes et al., 1994).

Conclusions

Inverse dynamic analysis with help of a mechanical link model revealed the joint torques that likely act on the limbs of live sloths during suspensory locomotion and allowed us to determine the SRFs exerted on the support. The "anti-gravity role" of the flexor muscles of the limb joints, rather than the extensor muscles as found in pronograde mammals, was confirmed by the model. Moreover, it was shown that the peculiar morphology of some shoulder muscles is likely related to the generation of propulsion in the forelimbs, where the greatest torques occur at the wrist. Overall, sloths can be characterized as "forelimb dominated" during locomotion.

No simple pendular mechanics apply during steady-state trot-like suspensory locomotion in two-toed sloths. Instead, sloths minimize the fluctuation of the dynamic forces exerted on the support. Why would a suspensory animal not make extensive use of pendular mechanics to effectively progress at low metabolic costs? The locomotor strategy of sloths may be compared to the phenomenon of humans intuitively altering their gait when walking on thin ice. A reduction of the dynamic forces exerted makes the breaking of the support less likely. For a species that is likely unable react quickly enough to a possible break of the support by jumping or

immediately reaching out to a more secure hold, we suggest that this strategy is of adaptive significance in the arboreal habitat. Furthermore, we propose that it also reflects ecological differences between sloths and effective brachiators such as gibbons. The low-energy food resource (predominantly leaves) of sloths is ubiquitous, whereas the high energy food items of brachiating primates are usually harder to find and dispersed over a much larger area (e.g. Geissmann, 2003). We therefore suggest that *C. didactylus* never experienced any significant selective pressure to evolve an energy-efficient locomotor system for long distance travel.

ACKNOWLEDGEMENTS

The authors would like to thank Dr. Dirk Arnold for his assistance during dissections of sloth cadavers and Rommy Petersohn, Sabine Moritz and Lydia Wagner for assistance during the kinematic analysis. We also want to thank Prof. Dr. Holger Preuschoft for insightful discussion. Lucy Cathrow thoroughly edited the language of this manuscript.

- Chapter 7 -

SYNOPSIS

The evolution of obligatory suspensory posture and locomotion in tree sloths – insights from functional morphology

Although this analysis of the musculo-skeletal apparatus and the locomotion of two-toed sloths from the functional perspective cannot answer the question whether quadrupedal suspensory locomotion was already present in the last common ancestor of sloths or not, it provides insight into the evolution of this peculiar locomotor mode.

Whether present or not in the ground pattern, in both scenarios a convergent evolution in the separate lines leading to the two modern genera is most parsimonious (chapter 1; Gaudin and McDonald, 2008). Twice in the natural history of sloths obligatory 'upside-down' posture and locomotion evolved from 'right-side-up' posture and locomotion. The aim of this dissertation is to improve the understanding of the changes associated with this evolution by analyzing the functional morphology of the locomotor apparatus and by studying the locomotion of two-toed sloths and studying aspects the anatomy of two- and three-toed sloths. Since the functional anatomy of the appendages was superbly described in Mendel's publications (cf. Mendel, 1979; 1981a; 1981b; 1985), the focus of the dissertation was laid on the proximal limbs, the pectoral and pelvic girdles, and the body axis.

Methods

Several approaches were used to assess the locomotion and functional morphology of the two-toed sloth. On a general level the methods used can be grouped into anatomical description, motion analysis and biomechanical modeling.

Anatomical description was used to characterize skeletal and muscular properties in both *Choloepus didactylus* and *Bradypus variegatus*. A formal description of the shoulder muscular topography is given, including muscle maps (chapter 4). The comparison of the shoulder anatomy was undertaken in the light of presumably convergent evolution of the 'upside-down' posture and locomotion in order to identify related likely convergent morphological adaptations. The epaxial muscles of *C. didactylus* have also been described (chapter 5). Here not only muscular topography was determined, but also fascicle length and orientation within the epaxial muscles (appendix 1). Each fascicle was digitized with a Microscribe™ to obtain three-

dimensional (3D) information of the internal structure of an individual muscle. Fascicle length and orientation were measured using custom-made software package (developed by H. Stark, Jena). Additionally, histologic properties of the sterno-clavicular articulation were analyzed using differential staining on consecutive cross sections to determine properties of the long ligamentous connection between the clavicle and the sternum in *C. didactylus* (chapter 3).

Motion analysis in this study made use of the benefits of different approaches. First, standard light high-speed videos were recorded in order obtain multiple unrestricted strides with the whole animal within the visible field. These data were used to assess different gait parameters like speed of progression, stride length, interlimb coordination, etc. (chapter 2). Second, biplanar high-speed x-ray motion analysis was used to analyze movements of skeletal elements during unrestrained and steady-state (on a motorized 'tread-pole') locomotion in three study animals. The data was used to evaluate speed-related effects in intralimb coordination by analysis of a comparably large dataset (chapter 2). X-ray analysis was also used to assess maximal in vitro mobility of the spine (appendix 2). Finally, 'scientific rotoscoping' (SR) was chosen to investigate the 3D movements of the shoulder (chapter 3) and the thoraco-lumbar spine (chapter 5). SR combines the biplanar x-ray motion data with a reconstruction of skeletal elements from computer tomography and the experimental scene is virtually rebuilt using a 3D software package (Autodesk Maya™). In SR a hierarchical joint chain is built and anatomical coordinate systems are implemented at each joint. With these coordinate systems the 3D kinematics (six degrees of freedom) of a skeletal element relative to another skeletal element can be assessed with high accuracy (appendix 3).

Biomechanical modeling was used to calculate occurring joint torques and support reaction forces during a contact phase of suspensory quadrupedal locomotion in *C. didactylus* (chapter 6). To this end, a mechanical segment link model was built up and driven by the kinematics measured in a live sloth. The model furthermore incorporated the body segment parameters assessed for the same sloth that was used to drive the model. Inverse dynamic analysis was performed to mathematically calculate the joint torques and support reaction forces of the model as an estimation of the real occurring torques and support reaction forces (not measured here).

Functional morphology and locomotion in two-toed sloths

Anatomical investigation, in-depth locomotion analysis, and biomechanical considerations of this dissertation allow a comprehensive interpretation of the musculo-skeletal apparatus in regard of the obligatory quadrupedal suspensory locomotion from a functional perspective.

In chapter 2 general locomotor characteristics of the two-toed sloth were analyzed. In comparison to published data of pronograde quadrupedal mammals, it was shown that sloths exhibit great variability in interlimb coordination (i.e., gait sequence patterns) and other spatio-temporal gait parameters (like step length, contact phase duration, and speed of progression), whereas the intralimb coordination largely retained the plesiomorphic pattern. An exception to this observation is the tarso-metatarsus element, which is incorporated into the rigid hook-like appendage of the hindlimb and has lost its propulsive role (see below).

Especially for the forelimbs, the similar results of intralimb coordination to pronograde quadrupedal mammals suggest that activation patterns of extrinsic limb muscles during limb protraction and retraction also retained the plesiomorphic pattern. Moreover, in-depth three-dimensional (3D) analysis of shoulder kinematics revealed that even the 3D pattern of shoulder movement is highly comparable to other arboreal species (chapter 3). This is also true for 3D intervertebral movements in the thoraco-lumbar spine and associated pelvic displacements (chapter 5). In particular, the dominant contribution of proximal limb elements to propulsion by exhibiting the greatest effect in cranio-caudal displacement of the appendages, the retention of the zig-zag configuration of the limb (at least in the forelimbs) with pantograph-like movements (cf. Fischer and Blickhan, 2006), 3D motion patterns of the scapula confined by the clavicle and the shape of the thorax, monophasic lateral bending and axial rotation as well as biphasic sagittal bending of the thoraco-lumbar spine during symmetric locomotion, and maximal amplitude of sagittal joint movement at the lumbo-sacral joint in comparison to more cranial intervertebral joints were conserved during the adoption of obligatory suspensory quardupedal locomotion of two-toed sloths. In sum, from the standpoint of the overall kinematics of locomotion there are only subtle differences to the general patterns described for pronograde terrestrial and arboreal species.

Peculiar characteristics of the morphology of two-toed sloths probably rendered possible the retention of these plesiomorphic overall kinematic patterns and thus only subtle differences are apparent in the motion analysis. Intriguingly, specifics of the functional morphology that are probably linked to obligatory suspension in sloths predominantly pertain to the limb elements that were only functionally incorporated as individual propulsive elements into the mammalian limb during the evolution of Theria: The scapula in the forelimb and the tarso-metatarsus in the hindlimb (see Kuznetsov, 1985; Gasc, 2001; Fischer and Blickhan, 2006). (This means, the principle 'last hired – first fired' might not only apply to economics, but could possibly also hold true in sloth limb function.)

In comparison to pronograde mammals of similar size (e.g. dogs and small goats) the motion of the humerus has greater influence on the displacement of the hand (chapter 2). This finding can be attributed to morphologic characteristics that allow effective 3D displacements of the forelimb necessary in a discontinuous habitat for species unable to jump (chapter 3). 3D displacements of the limb are facilitated by complex 3D motions of the scapula relative to the thorax. While the pattern has also been described qualitatively for arboreal quadrupedal primates (Schmidt et al., 2002; Schmidt and Krause, in press), the small-diameter tapered shape of the thorax, the highly mobile sterno-clavicular articulation, and the relatively short scapula increase the medio-lateral displacing effect of scapular movements, while at the same time the cranio-caudal displacing effect is decreased and overall influence of humeral movements is emphasized (chapter 3). An explanation for this finding may lie in the individual developmental program of the scapula that facilitates less constrained modifications in contrast to the linked programs of serially homologous elements of the fore- and hindlimbs as suggested by Schmidt and Fischer (2009).

In contrast, the emphasized influence of femoral movements on the displacing effect of the foot can be attributed to the modification of the distal limb (chapter 2). The tarso-metatarsus element is no longer a functionally independent element, but is completely (re-) integrated into the rigid foot and contributes to form an effective hook-like appendage (Mendel, 1981b). The tarso-metatarsus is usually elongated (similar size as the femur) in quadrupedal therians, the limb is in a zig-zag configuration and the femur and tarso-metatarsus move in matched motion (Kuznetsov, 1985;

Fischer and Blickhan, 2006). In sloths, thus, the hindlimb has only two remaining propulsive elements (when axial movements are neglected), the femur and the lower leg.

Striking differences in the morphology in comparison to pronograde therian mammals are present in the muscular topography of some muscles that connect the trunk and the forelimbs (extrinsic shoulder musculature) of the sloth. For example the m. deltoideus and the m. pectoralis superficialis posterior attach *via* a common tendon with the m. biceps brachii at the lower arm (chapter 4). These muscles do not only support powerful flexion of the elbow, but biomechanical considerations indicate that they are crucial to forelimb movement during contact phase (chapter 6).

Inverse dynamic analysis of a mechanical link model shows that the observed movements cannot be explained by simple pendular mechanics (chapter 6). Instead, the calculated support reaction forces (SRFs) demonstrate the active reduction of dynamic forces that are transmitted to the support. This maybe comparable to a human altering the gait when walking on thin ice, and is proposed to be of adaptive significance in the arboreal setting, because it reduces the risk of breaking the support.

Inverse dynamic analysis was also used to assess torques that act on the limb joints during locomotion (chapter 6). Flexor torques at the limb joints confirm the hypothesis of flexor muscles acting as “anti-gravity” muscles during suspensory locomotion. The biomechanics of two-toed sloth locomotion further indicate that during steady state trot-like locomotion the forelimbs pull the trunk forward, whereas the hindlimbs follow this cranial displacement rather passively and do not push the trunk as in pronograde mammals (chapter 6; reviewed by Demes et al., 1994). “Forelimb driven” locomotion was also found during upside-down locomotion of Slow Loris (Ishida et al., 1990) and probably presents a general difference to pronograde locomotion. The great torque calculated for the wrist joint suggests that especially the lower arm is pulled powerfully during locomotion and is reflected by the acceleration observed in the kinematic analysis (chapter 2). In *Choloepus* the peculiar morphology of the m. pectoralis superficialis posterior and acromial head of the m. deltoideus, which share a common insertion at the lower arm with the anterior belly of the m. biceps brachii, are primed for this task (chapter 4). At the same time the scapular fulcrum needs to be fixed in its position. The m. trapezius and m. serratus ventralis are suitable for this role

(chapter 4). Moreover, the m. deltoideus pars acromialis and the anterior belly of the biceps brachii pull the shoulder joint ventrad to oppose a moment generated by the action of the m. pectoralis superficialis posterior that would further protract the scapula (chapter 6). It is deduced here that the observed scapula retraction is produced by the plesiomorphic pattern of scapular retraction: the shoulder joint is fixed via co-activation of mm. infraspinatus et supraspinatus and m. subscapularis, while the forelimb retractors that attach to the proximal humerus (mainly m. latissimus dorsi and m. pectoralis profundus) pull the whole limb caudal.

The complete absence of asymmetric gaits like bound and gallop in sloths (chapter 2), is mirrored in the morphology of the epaxial back musculature and morphology of the thoraco-lumbar vertebral spine (chapter 5). The processus spinosi are unfavorable for powerful sagittal extension of the vertebral column as necessary during fast asymmetric locomotion. Back musculature is generally thin in the two-toed sloth and the attachment sites of the m. iliocostalis and the m. longissimus reflect the emphasis and lateral bending mobility and effective axial rotation.

The convergent evolution of suspensory quadrupedal locomotion in tree sloths

Due to adopting obligatory 'upside-down' posture sloths evolved an inversed orientation of the body in regard to the force of gravity. Many of the obvious anatomical characteristics of this posture are related to energy effective posture rather than specifically to the locomotion (e.g., the hook-like appendages). As summarized above the solution to the problem of 'upside-down' locomotion and associated changes in the functional demands predominantly relate to minor morphological adjustments in *Choloepus* like the mobilization of the sterno clavicular articulation, reduction of the relative length of the scapula, emphasis on powerful flexion of the limb joints, relocation of attachment sites of certain muscles, etc.. These changes in turn made the retention of plesiomorphic patterns of overall kinematics possible. The retention of kinematic patterns can be hypothesized to also allow the retention of neuro-muscular control for the tasks of limb protraction and retraction.

Functional morphology needs to demonstrate how common phylogenetic heritage might have canalized the spectrum of possibilities that were realized by evolution. The ideal indication of convergent evolution in distantly related organisms to account for

the same functional demands would be presented in form of a morphologically different solution that results in comparable function. Based on knowledge of the overall kinematics (chapter 2) and 3D kinematics (chapter 3) we first deduced the effect of the shoulder muscles in *C. didactylus* and then compared the muscular topography of the two-toed sloth with that of the three-toed sloth (*B. variegatus*) in order to identify convergent morphological solutions to the problem posed by the inverse orientation of the body to the force of gravity (chapter 4).

Many of the identified characteristics that may be related to the inverse orientation of the body to the support are also found in the three-toed sloth. However, these are often realized in the same anatomical manner. It thus remains unclear, whether these traits are simply homoplasic. In tree sloths two factors might disguise convergently evolved morphological traits at the shoulder. First, if early Xenarthrans really had digging adaptations as is suggested by the comparative anatomy (e.g. by the presence of a ischium that is fused to caudal vertebrae and forms a second rigid connection of the pelvis to the spine), strong flexor groups of the forelimbs and long claws probably presented morphological constraints that canalized the evolution of a suspensory lifestyle. It might be noted in this context that *Cyclopes* (the Tiny Anteater) is also capable of suspensory locomotion (Taylor, 1985).

Second, tree sloths, despite their proposed early divergence in the range of 20 to 25 million years ago (Delsuc and Douzery, 2008), are closely related, when compared to taxa that evolved more dramatic examples of convergent evolution (for example wings and active flight in birds and bats) and thus sloths share more phylogentic heritage. Still, the need to effectively pull the forearm, reflected by forelimb kinematics (chapter 2) and great joint torques at the wrist (chapter 6) is met by a few convergently evolved traits of the shoulder musculature (chapter 4). In both sloth genera the m. deltoideus and the m. pectoralis superficialis are connected to the anterior belly of m. biceps brachii, but morphologically different, and might help to effectively pull the forearm in early contact phase (chapters 4 and 6).

Taken together, the evidence gathered in this dissertation somewhat weakens the notion that the obligatory suspensory posture and locomotion in tree sloths is presenting a dramatic example for convergent evolution within mammals (Gaudin,

2004). Only small scale morphological changes are likely to have rendered the retention of plesiomorphic patterns of limb protraction and retraction possible.

Outlook

The question emerges why the kinematic pattern of a limb in zig-zag configuration and pantograph-like behavior is retained in sloths. More comparative data from mammals that evolved different locomotor modes is necessary. Moreover, approaches investigating possible advantages in the neuro-muscular control and developmental analyses might shed light in this seemingly highly conserved pattern of mammalian limb function.

As stated in the introduction, behavioral data from laboratory studies, i.e. from an artificial environment, need to be validated in field studies. A field study was beyond the scope of this dissertation. But, the data gathered here should provide a basis for such an endeavor. For example, it remains unknown in which situations, if ever at all, sloth engage a steady state trot-like locomotion. In any case conclusions on the adaptive significance drawn from observed locomotor characteristics in this lab study should be handled with caution.

Finally, far more extinct sloth species have been identified than extant species have survived until this day. A plio-pleistocene radiation has produced a great variety of different forms including giant species and even forms that have been adapted to an aquatic lifestyle (McDonald and De Iuliis, 2008). The improvement of the understanding of the locomotor apparatus aspired in this dissertation hopefully will also help to make reliable conclusions about the arboreality of fossil sloths.

Summary

The evolution of extant sloths included the transition from a pronograde quadrupedal posture to an obligatory quadrupedal suspensory posture and locomotion at some point in their natural history. Recent phylogenetic analyses suggest only a distant relationship of the two extant genera and imply a convergent evolution of the sloth-like posture and locomotion. Due to the quadrupedal 'upside-down' posture and locomotion and thus inverse orientation of the body in regard of the force of gravity sloths represent a natural experiment to investigate the influence of gravity on the mammalian locomotor apparatus. This dissertation aims to contribute to the understanding of the evolution of the 'upside-down' posture of sloths, and, more generally, to the understanding of the influence of gravity on the mammalian locomotor apparatus.

The dissertation comprises of seven chapters. After a general introduction five chapters follow that are each written to stand on their own, i.e., to be publishable in peer-reviewed journals. Each of these five chapters considers a different aspect of the functional morphology or performance of sloths during active locomotion. The last chapter is a synthesis of the insights gained in the individual analyses.

Several approaches are used to analyze the functional morphology and locomotion of the two-toed sloth. In order to investigate the locomotion of the two toed sloth an in-depth motion analysis is conducted. Spatio-temporal gait parameters and interlimb coordination are obtained from analysis of standard light high-speed video recordings during unrestricted and during steady-state locomotion on a motorized treadmill analogue. Speed related effects of intralimb coordination are assessed from analysis of biplane high-speed x-ray video recordings. Additionally, a new method is used to measure three dimensional (3D) movements the pectoral and pelvic girdles, and intervertebral movements *in vivo* during locomotion. Furthermore the muscular anatomy of the pectoral girdle is studied in two-toed sloths and three-toed sloths to identify possible convergent morphological characterisitcs in both extant sloth genera (*Bradypus* and *Choloepus*). Differential histological staining is used to assess functional characterisitics of the ligamentous connection of the clavicle to the sternum. Finally, a mechanical segment link model is built to perform an inverse dynamic analysis. The analysis is used to assess limb joint torques and support reaction forces.

Spatio-temporal gait parameters and interlimb coordination are very variable in two-sloths but tend to be more uniform during steady-state locomotion at higher speeds. At higher speeds the forelimbs are usually more extended and the sloths utilize a trot-like or a diagonal sequence/ diagonal couplet gait sequence pattern. In contrast, intralimb coordination patterns are less variable and are very similar to those reported for pronograde mammals – especially in the forelimbs, despite the inverse orientation of the body in regard of the gravity vector. By the integration of the tarso-metatarsus into a rigid hook-like foot during the evolution of the obligatory suspensory posture, a formerly propulsive element of the hindlimb is lost. 3D kinematic analysis of shoulder movements revealed that small scaled morphologic changes, such as the relative shortening of the scapula and a smaller thorax diameter, allowed retaining the plesiomorphic kinematic pattern and at the same time maximizes mobility at the shoulder. The histologic properties of the sterno-clavicular articulation indicate a tensile loading regime between thorax and forelimbs and facilitate maximal mobility at this joint.

The ‘upside-down’ posture and locomotion is, amongst others, facilitated by the peculiar topography of some of the shoulder muscles. Based on the kinematic data and knowledge of the muscular anatomy the effect of the shoulder musculature was deduced for the two main roles of the extrinsic shoulder musculature, weight support and locomotion. In line with the kinematic data of the forelimb and the muscular topography of the shoulder, a crucial role of the posterior part of the superficial m. pectoralis, which arises on the sternum and extends to the lower arm, for the generation of propulsion during suspensory quadrupedalism is resulting from the biomechanical analysis. Biomechanics indicate a ‘forelimb drive’ in contrast to the ‘hindlimb drive’ present in most pronograde mammals. The calculation of joint torques confirms the “anti-gravity” role of the limb joint flexor muscles. The determined support reaction forces demonstrate that the two-toed sloths minimize the dynamic fluctuations of forces that are transmitted onto the support. Simple pendular mechanics do not apply for the two-toed sloth.

3D pelvic displacements are similar to those of pronograde mammals and are shown to be almost completely congruent with the summed up intervertebral movements of the six most caudal presacral joints. The absence of a cranio-caudal pattern of maximal

angular defelction along the thoraco-lumbar spine during trot-like quadrupedal suspensory locomotion of the two-toed sloth is consistent with a standing wave of activation that has also been assessed for trotting dogs. Configuration of the intervertebral joints as well as the anatomy of the epaxial musculature is argued to be related to the absence of asymmetric quadrupedalism and reduced need for powerful sagittal flexion in two-toed sloths.

Many morphological traits are realized in the same morphological way in both extant genera. Only few different morphological ‘solutions’ to the problems posed by the adoption of inverse orientation in regard to gravity are identified. In both genera the m. pectoralis as well as the m. deltoideus contributes some fibers to the m. biceps brachii, but it is realized morphologically different.

Taken together strikingly conserved kinematic patterns are found in an aberrant locomotor mode. Morphological changes that are likely related to the adoption of obligatory suspensory posture and locomotion are mostly relating to the muscular topography and small scaled skeletal changes. These changes allowed for the conservation of plesiomorphic patterns during limb movements. Plesiomorphic patterns for limb pro- and retraction, small scaled morphological changes and very similar morphological ‘solutions’ to the problems posed by the new functional demands render the convergent evolution of suspensory quadrupedal posture and locomotion in the tree sloths less unlikely.

ZUSAMMENFASSUNG

Während der Evolution der heutigen Faultiere kam es zu einem Übergang von einer pronograden quadrupeden Körperhaltung und Fortbewegung hin zu einer obligatorisch quadruped-suspensorischen Körperhaltung und Fortbewegung. Neuere phylogenetische Studien legen nahe, dass diese für Faultiere typische Körperhaltung und Fortbewegung zweimalig unabhängig, also konvergent, entstanden ist. Aufgrund der quadruped-suspensorischen Körperhaltung und der damit umgekehrten Ausrichtung des Körpers zur Gravitation, repräsentieren die Faultiere darüber hinaus ein ‚natürliches Experiment', dessen Untersuchung Einblicke in den Einfluss der Gravitation auf den Körper verspricht. Diese Dissertationsschrift hat zum Ziel zum Verständnis der Evolution der quadruped-suspensorischen Körperhaltung und Fortbewegung beizutragen und das Verständnis des Einflusses der Gravitation auf den Bewegungsapparat der Säugetiere zu verbessern.

Die Schrift besteht aus sieben Kapiteln. Nach einer allgemeinen Einleitung folgen fünf Kapitel, die jeweils so geschrieben wurden, dass sie für sich allein stehend in Fachzeitschriften publiziert werden können. Jedes dieser fünf Kapitel beleuchtet einen anderen Aspekt der funktionellen Morphologie und Fortbewegung der Faultiere. Das letzte Kapitel ist eine Synthese der in den Einzelstudien gewonnenen Ergebnisse.

Mehrere methodische Herangehensweisen wurden für die Untersuchung der funktionellen Morphologie und Fortbewegung des Zweifingerfaultieres (*Choloepus didactylus*) gewählt. Eine umfassende Bewegungsanalyse wurde durchgeführt. Metrische Gangparameter sowie Fußfallsequezen wurden mit Hilfe von Hochgeschwindigkeitsvideos für einen großen Bereich durch die Tiere selbst gewählter Fortbewegungsgeschwindigkeiten sowie für kontinuierlich-gleichförmige Fortbewegung auf einer motorisierten Laufstange analysiert. Geschwindigkeitsabhängige Effekte der Beinkinematik wurden mittels biplanarer Röntgenkinematographie dokumentiert. Zusätzlich wurde ein neuer Ansatz genutzt, um die dreidimensionale (3D) Bewegung der Elemente des Schultergürtels, des Beckens sowie 3D intervertebral Bewegung *in vivo* während der Fortbewegung zu messen. Des Weiteren wurde die Muskeltopographie für je einen Vertreter der Gattungen *Choloepus* und *Bradypus* formal dokumentiert, um eventuelle konvergente Charakteristika in der Schultermuskulatur zu identifizieren. Histologische Färbungen

auf Schnittserien wurden angefertigt, um die funktionellen Eigenschaften der ligamentösen Verbindung zwischen der Clavicula und dem Sternum zu untersuchen. Schließlich wurde ein biomechanisches Modell erstellt anhand dessen eine invers dynamische Analyse durchgeführt wurde, um an den Gliedmaßengelenken angreifende Drehmomente sowie Superstratreaktionskräfte zu ermitteln.

Die metrischen Gangparameter erwiesen sich als sehr variabel zeigten aber Tendenz in den höheren Geschwindigkeitsbereichen weniger variabel zu sein. Die untersuchten Zweifingerfaultiere bedienten sich bei höherer Geschwindigkeit einheitlich einer Trab-ähnlichen oder diagonalen Fußfallsequenz. Im Gegensatz dazu waren die Parameter der Beinkinematik für alle Geschwindigkeitsbereiche einheitlich. Zudem unterschied sich die Beinkinematik des Zweifingerfaultieres nur wenig von der Beinkinematik pronograd-quadrupeder Säugetiere ähnlicher Körpergröße. Dies trifft vor allem auf die Vorderextremitäten zu. Die Analyse zeigt weiterhin, dass die Integration des Tarso-Metatarsus-Elements in einen versteiften Fuß den Verlust eines propulsiven Elementes in der Hinterextremität darstellt. Die 3D-Analyse der Schulterkinematik zeigte, dass kleinere morphologische Veränderungen, wie etwa die relative Verkürzung der Scapula oder ein kleinerer Durchmesser des Thorax, die Beibehaltung des plesiomorphen Bewegungsmusters der Schulter ermöglicht haben und darüber hinaus die Beweglichkeit der Schulter maximiert haben. Die histologischen Eigenschaften der ligamentösen sterno-clavicularen Artikulation weisen auf eine herrschende Zugspannung zwischen den Vorderextremitäten und dem Thorax.

Die quadruped-suspensorische Fortbewegung wird auch durch die besondere Topographie der Schultermuskulatur ermöglicht. Basierend auf den Kenntnissen zur 3D Kinematik der Schulter sowie der ausführlichen Dokumentation der muskulären Topographie wurde die Wirkung der Schultermuskulatur in Bezug auf ihre vorrangigen Aufgaben, nämlich Aufhängung des Thorax zwischen den Vorderextremitäten und Erzeugung von Beinbewegung, deduziert.

In Übereinstimmung mit den kinematischen und anatomischen Daten wurde auch durch die biomechanische Analyse die besondere Bedeutung des M. pectoralis superficialis posterior herausgestellt. Dieser Muskel erstreckt sich vom Sternum bis zum Unterarm. In diesem Zusammenhang zeigte die biomechanische Analyse weiterhin, dass im Faultier vorrangig die Vordergliedmaßen für die Propulsion des

Körpers verantwortlich sind, während dies in pronograd-quadrupeden Säugetieren in der Regel die Hintergliedmaßen sind. Die Berechnung der in den Gliedmaßengelenken angreifenden Drehmomente bestätigt die zuvor postulierte ‚anti-Gravitationswirkung' der Flexoren. Die berechneten Superstratreaktionskräfte belegen, dass Faultiere aktiv die dynamisch bedingten Schwankungen, welche auf das Superstrat während der Fortbewegung übertragen werden, minimieren und eine vermeintlich energieeffiziente Pendelmechanik keine Rolle spielt.

Die 3D Bewegung des Beckens (welche additiv durch die intervertebrale Bewegung der präsakralen Wirbelsäule erzeugt wird) stimmt in wesentlichen Punkten mit der Bewegung pronograd-quadrupeder Säugetiere überein. Die Abwesenheit eines cranio-caudalen Musters entlang der thoraco-lumbalen Wirbelsäule während Trab-ähnlicher Fortbewegung steht in Übereinstimmung mit einer stehenden Welle der Muskelaktivierung, die bei Hunden im Trab gemessen wurde. Die Konfiguration der intervertebralen Gelenke der präsakralen Wirbelsäule sowie die Topographie der epaxialen Rückenmuskulatur, werden als Hinweis auf eine fehlende Notwendigkeit kraftvolle sagittale Flexion zu erzeugen gedeutet, da bei Faultieren asymmetrische Gangarten nicht vorkommen.

Viele Merkmale sind in beiden rezenten Gattungen in gleicher Weise morphologisch realisiert. Es ist daher nicht zu unterscheiden, ob es sich bei diesen Merkmalen um Plesiomorphien handelt oder ob diese Merkmale konvergent entstanden sind. Nur wenige Merkmale wurden identifiziert, die bei gleicher angenommener Funktion, auf unterschiedliche Art und Weise morphologisch realisiert wurrden. Als Beispiel seien die unterschiedlich konfigurierten M. pectoralis und M. deltoideus genannt, welche aber sowohl bei *Choloepus* als auch bei *Bradypus* Fasern zum M. biceps brachii beisteuern, was hier als funktionell bedeutsam gewertet wurde.

Zusammenfassend kann ausgesagt werden, dass eine im Vergleich zu pronograd-quadrupeden Säugetieren auffallend ähnliche Kinematik bei der quadruped-suspensorischen Fortbewegung der Zweifingerfaultiere festgestellt wurde. Morphologische Veränderungen, welche im Zusammenhang mit der umgekehrten Orientierung des Körpers zur Gravitation stehen, betreffen vorrangig die muskuläre Topographie and kleinere skelettale Veränderungen. Die Veränderungen erlaubten aber auch die Beibehaltung der plesiomorphen Bewegungsmuster. Plesiomorphe

Kinematik, die kleineren morphologischen Veränderungen, sowie die große Übereinstimmung der morphologischen ‚Lösungen', welche für die durch die veränderte Körperhaltung hervorgerufenen neuen funktionellen Anforderungen durch die Evolution gefunden wurden, lassen die konvergente Evolution quadruped-suspensorischer Körperhaltung und Fortbewegung weniger unwahrscheinlich erscheinen.

References

Alexander RMcN. 1981. The gaits of tetrapods: adaptations for stability and economy. *Symp Zool Soc Lond* 48, 269-287.

Andrada E, Schmidt A, Mämpel J, Fischer MS, Witte H. In press. The effect of substrate inclination on torque and power patterns in rats. *Robot Auton Syst*.

Apfelbach R, Grzimek B. 1997. *Grzimek's encyclopedia of mammals* (in German). Leipzig: Brockhaus.

Ashley-Ross M. 1994. Hindlimb kinematics during terrestrial locomotion in a salamander (*Dicamptodon tenebrosius*). *J Exp Biol* 193, 255-283.

Ashton EH, Oxnard CE. 1964. Locomotor patterns in primates. *Proc Zool Soc, Lond* 142, 1-28.

Beebe W. 1926. The three-toed sloth. *Bradypus cucullinger cucullinger* Wagler. *Zoologica* 7, 1-67.

Benninger MI, Seiler GS, Robinson LE, Ferguson SJ, Bonél HM, Busato AR, Lang J. 2004. Three-dimensional motion pattern of the caudal lumbar and lumbosacral portions of the vertebral column of dogs. *Am J Vet Res* 65, 544-552.

Benninger MI, Seiler GS, Robinson LE, Ferguson SJ, Bonél HM, Busato AR, Lang J. 2006. Effects of anatomic conformation on three-dimensional motion of the caudal lumbar and lumbosacral portions of the vertebral column of dogs. *Am J Vet Res* 67, 43-50.

Benjamin M, Ralphs JR. 1998. Fibrocartilage in tendons and ligaments – an adaptation to compressive load. *J Anat*, 193,481-494.

Bock WJ. 1980. The definition and recognition of biological adaptation. Amer Zool, 20,217-227.

Boczek-Funcke A, Kuhtz-Buschbeck JP, Illert M, 1996. Kinematic analysis of the cat shoulder girdle during treadmill locomotion: an x-ray study. *Europ J Neurosci* 8, 261-272.

Boszczyk BM, Boszczyk AA, Putz R. 2001. Comparative and functional anatomy of the mammalian lumbar spine. *Anat Rec* 264, 157-168.

Brainerd EL, Baier DB, Gatesy SM, Hedrick TL, Metzger KA, Gilbert SL, Crisco JJ. 2010. X-ray reconstruction of moving morphology (XROMM): Precision, Accuracy and Applications in Comparative Biomechanics research. *J Exp Zool* 313A, 262-279.

Britton SW. 1941. Form and function in the sloth. *Quart Rev Biol* 16, 13-34.

Buchholtz EA, Stepien CC. 2009. Anatomical transformation in mammals: developmental origin of aberrant cervical anatomy in tree sloths. *Evol Develop* 11, 69-79.

Carrier DR, Deban SM, Fischbein, T. 2006. Locomotor function of the pectoral girdle 'muscular sling' in trotting dogs. *J Exp Biol* 209, 2224-2237.

Carrier DR, Deban SM, Fischbein T. 2008. Locomotor function of the forelimb protractor and retractor muscles of dogs: evidence of strut-like behavior at the shoulder. *J Exp Biol* 211, 150-162.

Cartmill M. 1985. Climbing. In: Hildebrand, M., Bramble, D.M., Liem, K.F., Wanke, D.B. (Ed.), Functional vertebrate morphology. The Belknap Press of Harvard University Press, Cambridge, London, pp. 73-88.

Cartmill M, Lemelin P, Schmitt D. 2002. Support polygons and symmetrical gaits in mammals. *Zool J Linn Soc* 136, 401-420.

Cartmill M, Lemelin P, Schmitt D. 2007. Understanding the adaptive value of diagonal sequence gaits in primates: a comment on Shapiro and Raichlen, 2005. *Am J phys Anthrop* 133, 822-825.

Chan LK. 2007 Glenohumeral mobility in primates. *Folia Primatol* 78,1-18.

Chan LK. 2008. The range of passive arm circumduction in primates: do hominins really have more mobile shoulders? *Am J Phys Anthropol* 136,265-277.

Chang YH, Bertram JEA, Lee DV. 2000. External forces and torques generated by the brachiating white-handed gibbon (*Hylobates lar*). *Amer J phys Anthropol* 113, 201-216.

Cheng J, Stein RB, Jovanic K, Yoshida K, Bennet DJ, Han Y. 1998. Identification, localization, and modulation of neural networks for walking in the mudpuppy (*Necturus maculatus*) spinal cord. *J Neurosci* 18, 4295-4304.

Clayton HM, Lanovaz JL, Schamhardt HC, Willemen MA, Colborne GR. 1998. Net joint moments and powers in the equine forelimb during the stance phase of the trot. *Equine Vet J* 30, 384-389.

Courtine G, Roland RR, Hodgson J, McKay H, Raven J, Zhong H, Yang H, Tuszynski MH, Edgerton VR. 2005. Kinematic and EMG determinants in quadrupedal locomotion of a

non-human primate (Rhesus). *J Neurophysiol* 93, 3127-3145.

Curtis DJ. 1995. Functional anatomy of the trunk musculature in the Slow Loris (*Nycticebus coucang*). *Am J Phys Anthropol* 97, 367-379.

Cuvier GLSFD. 1798. Tableau elementaire de l'histoire naturelle des animaux (in French). JB Bailliére, Paris, pp. 1-711.

Davis DD. 1949. The shoulder architecture of bears and other carnivores. *Fieldiana Zoology* 81, 285-305.

Day LM, Jayne BC. 2007. Interspecific scaling of the morphology and posture of the limbs during the locomotion of cats (Felidae). *J Exp Biol* 210, 642-654.

Delsuc F, Douzery EJP. 2008. Recent advances and future prospects in xenarthran molecular phylogenetics. In: Vizcaíno, S.F., Loughry, W.J. (Ed.), The Biology of the Xenarthra. University Press of Florida, Gainesville, pp. 11-23.

Delsuc F, Catzeflis FM, Stanhope MJ, Douzery EJP. 2001. The evolution of armadillos, anteaters and sloths depicted by nuclear and mitochondrial phylogenies: implications for the status of the enigmatic fossil *Eurotamandua*. *Proc R Soc Lond B* 268, 1605-1615.

Demes B, Jungers WL, Nieschalk U. 1990. Size and speed-related aspects of quadrupedal walking in Slender and Slow Lorises. In: Jouffroy, F.K., Stack, M.H., Niemitz, C. (Ed.), Gravity, posture and locomotion in primates. Editrice Il Sedicesimo, Firenze,.pp. 175-198.

Demes B, Larson SG, Stern JT, Jungers WL, Biknevicius AR, Schmitt D. 1994. The kinetics of primate qadrupedalism: „hindlimb drive" reconsidered. *J Hum Evol* 26, 353-374.

Dogan S, Manley PA, Vanderby R, Kohles SS, Hartman LM, BcBeath AA. 1991. Canine intersegmental hip joint forces and moments before and after cemented total hip replacement. J Biomech 28, 753-758.

Eaton jr. TH. 1944. Modifications of the shoulder girdle related to reach and stride in mammals. *J Morph* 75, 167-171.

Endo H, Komiya T, Kawada S, Hayashida A, Kimura J, Itou T, Koie H, Sakai T. 2009. Three-dimensional reconstruction of the xenarthrous process of the thoracic and lumber vertebrae in the giant anteater. *Mammal Study* 34, 1-6.

Engelmann GF. 1985. The phylogeny of the xenarthra. In: Montgomery, G.G. (Ed.), The evolution and ecology of armadillos, sloths, and vermilinguas. Smithonian Institution Press, Washington, London, pp. 51-64.

English AWM. 1978. An electromyographic analysis of forelimb muscles during overground stepping in the cat. *J exp Biol* 76, 105-123.

Evans HE. 1993. Miller's anatomy of the dog. WB Sauders, 1113 pp.

Faber, M., Schamhardt, H., van Weeren, R., Johnston, C., Roepstorff, L. and Barneveld, A. (2000). Basic three-dimensional kinematics of the vertebral column of horses walking on a treadmill. *Am. J. Vet. Res.* 61, 399-406.

Federative Committee on Anatomical Terminology (FCAT). (2008). *Terminologica Anatomica*, pp. 1-292. Stuttgart: Thieme Verlag.

Fischer MS. 1994. Crouched posture and high fulcrum, a principle in the locomotion of small mammals: the example of the rock hyrax (*Procavia capensis*) (Mammalia: Hyracoidea). *J hum Evol* 26, 501-524.

Fischer MS. 1998. Die Lokomotion von Procavia Capensis (Mammalia, Hyracoidea): Zur Evolution des Bewegungssystems bei Säugetieren. *Abhandlungen des Naturwissenschaftlichen Vereins in Hamburg* 33, 1-188. (in German).

Fischer MS. 1999. Kinematics, EMG, and inverse dynamics of the therian forelimb – a synthetical approach. *Zool Anz* 238, 41-54.

Fischer MS, Lehmann R. 1998. Application of cineradiography for metric and kinematic study of in-phase gaits during locomotion of the pika (*Ochotona rufescens*, Mammalia: Lagomorpha). *Zoology* 101, 148-173.

Fischer MS, Witte H. 1998. The functional morphology of the three-segmented limb of mammals and its specialities in small to medium-sized therian mammals. *Proc Europ Mech Coll Biol Technol Walk* 375, 10-17.

Fischer MS, Blickhan R. 2006. The tri-segmented limbs of therian mammals: kinematics, dynamics, and self-stabilization – a review. *J Exp Zool* 305A, 935-952.

Fischer MS, Krause C, Lilje K. 2010. Evolution of chameleon locomotion, or how to become arboreal as a reptile. *Zoology* 113, 67-74.

Fischer MS, Schilling N, Schmidt M, Haarhaus D, Witte H. 2002. Basic limb kinematics of small therian mammals. *J Exp Biol* 205, 1315-1338.

Fleagle JG. 1974. Dynamics of a brachiating simang [*Hylobates* (*Symphalangus*) *syndactylus*]. *Nature* 248, 259-260.

Fleagle JG. 1976. Locomotion and posture of the Malayan Siamang and implications for hominoid evolution. *Folia Primatol* 26, 245-269.

Flower WH. 1882. On the mutual affinities of the animals composing the order Edentata. *Proc Zool Soc* 1882, 50:358-367.

Fowler EG, Gregor RJ, Hodgson JA, Roy RR. 1993. Relationship between ankle muscle and joint kinetics during the stance phase of locomotion in the cat. *J Biomech* 26, 465-483.

Frolich LM, Biewener AA. 1992. Kinematic and electromyographic analysis of the functional role of the body axis during terrestrial and aquatic locomotion in the salamander *Ambystoma Tigrinum*. *J Exp Biol* 162, 107-130.

Gasc JP. 1993. Asymmetrical gait of the saharian rodent *Meriones shawi shawi* (Duvernoy, 1842) (Rodentia, Mammalia): a high-speed cineradiographic analysis. *Can J Zool* 71, 790-798.

Gasc JP. 2001. Comparative aspects of gait, scaling and mechanics in mammals. *Comp Biochem Physiol* A 131, 121-133.

Gatesy SM, Baier DB, Jenkins FA, Dial KP. 2010. Scientific rotoscoping: a morphology-based method of 3D-motion analysis and visualization. *J Exp Zool*, 313A:280-298.

Gaudin TJ, Biewener AA. 1992. The functional morphology of xenarthrous vertebrae in the armadillo *Dasypus novemcinctus* (Mammalia, Xenarthra). *J Morph* 214, 63-81.

Gaudin TJ. 2004. Phylogenetic relationships among sloths (Mammalia, Xenarthra, Tardigrada): The craniodental evidence. *Zool J Linn Soc* 140, 255-305.

Gaudin TJ, McDonald HG. 2008. Morphology-based investigations of the phylogenetic relationships among extant and fossil xenarthrans. In: Vizcaíno, S.F., Loughry, W.J. (Ed.), The Biology of the Xenarthra. University Press of Florida, Gainesville, pp. 24-36.

Geissmann T. 2003. Vergleichende Primatologie. Springer, Berlin, Heidelberg, pp. 1-357.

Goldfinch AJ, Molnar RE. 1978. Gait of the Brush-tailed Possum (*trichosurus vulpecula*). *Austr Zool* 19, 277-289.

Goffart M. 1971. Function and form in the sloth. Pergamon Press, Oxford. 225 pp.

Goslow GE, Reinking RM, Stuart DG. 1973. The cat step cycle: hind limb joint angles and muscle lengths during unrestrained locomotion. *J. Morphol.* 141, 1-42.

Goslow GE, Seeherman HJ, Taylor CR, McCutchin MN, Heglund NC. 1981. Electrical activity and relative length changes of dog limb muscles as a function of speed and gait. *J. Exp. Biol.* 94, 15-42.

Gould SJ, Lewontin RC. 1979. The spandrels of San Marco and the panglossian paradigm: a critique of the adaptationist programme. *Proc R Soc Lond B* 205. 581-598.

Gradner G, Bockstahler B, Peham C, Henninger W, Podbregar I. 2007. Kinematic study of back movement in clinically sound malinois dogs with consideration of the effect of radiographic changes in the lumbosacral junction. *Vet Surg* 36, 472-481.

Grand TI. 1972. A mechanical interpretation of terminal branch feeding. *J Mammal* 53, 198-201.

Greenwood AD, Castresana J, Feldmeier-Fuchs G, Pääbo S. 2001. A molecular phylogeny of two extinct sloths. *Mol Phylogenet and Evol* 18, 94-103.

Hackert, R., Schilling, N., Fischer, M.S., 2006. Mechanical self-stabilization, a working hypothesis for the study of the evolution of body proportions in terrestrial mammals? *C r Palevol* 5, 541-549.

Haussler KK, Bertram JEA, Gellman K, Hermanson JW. 2001. Segmental in vivo vertebral kinematics at the walk, trot and canter: a preliminary study. *Equine Vet J Suppl* 33, 160-164.

Heglund NC, Taylor RC. 1981. Speed, stride frequency and energy cost per stride: how do they change with body size and gait? *J Exp Biol* 138, 301-318.

Herbin M, Gasc JP, Renous S. 2004. Symmetrical and asymmetrical gaits in the mouse: patterns to increase velocity. *J Comp Physiol A* 190, 895-906.

Higurashi Y, Hirasaki E, Kumakura H. 2009. Gaits of Japanese macaques (*Macaca fuscata*) on a horizontal ladder and arboreal stability. *Am J Phys Anthropol* 138, 448-457.

Hildebrand M. 1966. Analysis of the symmetrical gaits of tetrapods. *Folia Biotheoret* 6, 9-22.

Hildebrand M. 1967. Symmetrical gaits of primates. *Am J phys Anthrop* 26, 119-130.

Hildebrand M., 1977. Analysis of asymetrical gaits. *J Mammal* 58, 131-156.

Höss M, Dilling A, Currant A, Pääbo S. 1996. Molecular phylogeny of the extinct ground sloth *Mylodon darwinii*. *Proc natl Acad Sci* 93, 181-185.

Howell AB. 1944. Speed in animals. University of Chicago press, Chicago.

Huang R, Zhi Q, Patel K, Wilting J, Christ B. 2000. Dual origin and segmental organization of the avian scapula. *Development* 127:3789-3794.

Humphry GM. 1869. The mycology of the limbs of the Unau, the Ai, the two-toed anteater, and the Pangolin. *J Anat Physiol* 3, 2-78.

Hutchinson JR, Schwerda D, Famini DJ, Dale RHI, Fischer MS, Kram R. 2006. The locomotor kinematics of Asian and African elephants: changes with speed and size. *J Exp Biol* 209, 3812-3827.

Ishida H, Jouffroy FK, Nakano Y. 1990. Comparative dynamics of pronograde and upside down horizontal auadrupedalism in the Slow Loris (*Nyctecebus coucang*). In: Jouffroy, F.K., Stack, M.H., Niemitz, C. (Ed.), Gravity, posture and locomotion in primates. Editrice Il Sedicesimo, Firenze, pp. 209-220.

Jenkins FA. 1974. The movement of the shoulder in claviculate and aclaviculate mammals. *J Morph* 144, 71-84.

Jenkins FA, Camazine SM. 1977. Hip structure and locomotion in ambulatory and cursorial carnivores. *J Zool Lond* 181, 351-370.

Jenkins FA, Weijs WA. 1979. The functional anatomy of the shoulder in the Virginia Opossum (*Didelphis virginiana*). *J Zool Lond* 188, 379-410.

Jenkins FA, Goslow GE. 1983. The functional anatomy of the shoulder of the savannah monitor lizard (*Varanus exanthematicus*). J Morphol 175, 195-216.

Jenkins FA, Dombrowski PJ, Gordon EP. 1978. Analysis of the shoulder in brachiating spider monkeys. *Am J Phys Anthropol* 48, 65-76.

Jouffroy FK, Petter A. 1990. Gravity-related kinematic changes in lorisine horizontal locomotion in relation to position of the body. In: Jouffroy, F.K., Stack, M.H., Niemitz, C. (Ed.), Gravity, posture and locomotion in primates. Editrice Il Sedicesimo, Firenze, pp. 199-208.

Jouffroy FK, Stern JT. 1990. Telemetered EMG Study of the Antigravity versus Propulsive Actions of Knee and Elbow Muscles in the Slow Loris. In: Jouffroy, F.K., Stack, M.H., Niemitz, C. (Ed.), Gravity, posture and locomotion in primates. Editrice Il Sedicesimo, Firenze, pp. 209-220.

Jouffroy FK, Lessertisseur J, Vassal P. 1962. Particularites musculaires des Extremites du Bradype ai (*Bradypus tridactylus* L.) dans leur rapports avec la suspension arhoricole. *Bull Assoc Anatom* 11*,* 392-400.

Jungers WL, Stern JT. 1981. Preliminary electromyographical analysis of brachiation in gibbon and spider monkey. *Int J Primatol* 2, 19-33.

Jungers WL, Godfrey LR, Simons EL, Chatrath PS, Rakotosamimanana B. 1991. Phylogenetic and functional affinities of *Babakotia* (Primates), a fossil lemur from northern Madagascar. *Proc natl Acad Sci* 88, 9082-9086.

Jungers, W.L., Godfrey, L.R., Simons, E.L., Chatrath, P.S., 1997. Phalangeal curvature and positional behaviour in extinct sloth lemurs (Primates, Paleopropithecidae). *Proc natl Acad Sci* 94, 11998-12001.

Kafkafi N, Golani I. 1998. A traveling wave of lateral movement coordinates both turning and forward walking in the ferret. *Biol Cybern* 78, 441-453.

Kagaya M, Ogihara N, Nakatsukasa, M. 2008. Morphological study of the anthropoid thoracic cage: scaling of thoracic width and analysis of rib curvature. *Primates* 49, 89-99.

Kell DB, Oliver SG. 2003. Here is the evidence, now what ist he hypothesis? The complementary roles of inductive and hypothesis-driven science in the post-genomic era. *BioEssays* 26, 99-105.

Konstant W, Stern JT, Fleagle JG, Jungers WL. 1982. Function of subclavius muscle in a ninhuman primate, the spider monkey (*Ateles*). *Folia Primatol* 38, 170-182.

Kraft R. 1995. Xenarthra. *Handbuch der Zoologie* (in German). Volume 8 (Mammalia), pp. 1-79..

Kummer B. 1970. Die Beanspruchung des Armskeletts beim Hangeln. Ein Beitrag zum Brachiatorenproblem (in German). *Anthropol Anz* 32, 74-82.

Kuznetsov AN. 1985. Comparative functional analysis of the fore- and hind limbs in mammals (in Russian). *Zool J Moscow* 64, 1862–1867.

Kuznetsov AN. 1995. Energetical profit of third segment in parasagittal legs. *J theoret Biol* 172, 95-105.

Lammers AR, Gauntner T. 2008. Mechanics of torque generation during quadrupedal arboreal locomotion. *J Biomech* 41, 2388-2395.

Larson SG, Stern JT. 1989. The role of propulsive muscles of the shoulder during quadrupedalism in vervet monkeys (Cercopithecus aethiops): implications for neural control of locomotion. *J motor Bahav* 21, 457-472.

Larson SG, Stern JT. 2007. Humeral retractor EMG during quadrupedal walking in primates. *J Exp Biol 210*, 1204-1215.

Lauder GV. 1981. Form and function: structural analysis in evolutionary morphology. *Paleobiology* 7, 430-442.

Lemelin P, Schmitt D, Mackenzie A, George G, Cartmill M. 2007. The effects of substrate type and size on the locomotion of Kinkajous. Abstract. *Integr and Comp Biol* 47, e71.

Licka TF, Peham C, Zohmann E. 2001. Treadmill study of the range of back movement at the walk in horses without back pain. *Am J Vet Res* 62, 1173-1179.

Lucae JCG. 1882. The muscles and the skeleton of the black lemur and the sloth (*Lemur macaco* and *Choloepus didactylus*) (in German). Mahlau and Waldschmidt Verlag, Senckenbergische Naturforschende Gesellschaft, Frankfurt am Main. 84 pp.

Maes LD, Herbin M, Hackert R, Bels VL, Abourachid A. 2008. Steady locomotion in dogs: temporal and associated spatial coordination patterns and the effect of speed. *J Exp Biol* 211, 138-149.

Mackintosh HW. 1873. On the myology of the genus *Bradypus*. *Proc R Irish Acad* Bg1, 517-529.

Mackintosh HW. 1874. On the muscular anatomy of *Choloepus didactylus*. *Proc R Irish Acad* Bg1, 66-79.

Manter JT. 1938. The dynamics of quadrupedal walking. *J Exp Biol* 15, 522-540.

Mayr E. 1983. How to carry out the adaptationist program? *Amer Naturalist* 121, 324-334.

McDonald HG. 2007. Biomechanical inferences of locomotion in ground sloths: integrating morphological and track data. In: Lucas, S.G., Spielmann, J.A., Lockley, M.G. (Ed.), Cenozoic vertebrate track and traces. New Mexico Museum of Nat. Hist. and Sci. Bull. 42, pp. 201-208.

McDonald HG, DeIuliis G. 2008. Fossil history of sloths. In: Vizcaíno, S.F., Loughry, W.J. (Ed.), The Biology of the Xenarthra. University Press of Florida, Gainesville, pp. 39-55.

McDonald HG, Vizcaíno SF, Bargo MS. 2008. Skeletal anatomy and the fossil history of the vermilingua. In: Vizcaíno, S.F., Loughry, W.J. (Ed.), The Biology of the Xenarthra. University Press of Florida, Gainesville, pp. 64-78.

Meincke F. 1911. Morphologische Untersuchungen über die Myologie an den Extremitäten bei *Bradypus tridactylus* (in German). Morph Jahrb H2, 311-358.

Mendel FC. 1979. The wrist joint of two-toed sloths and its relevance to brachiating adaptations in the Hominoidea. *J Morphol* 162, 413-424.

Mendel FC. 1981a. Foot of two-toed sloths: its anatomy and potential uses to size of support. *J Morphol* 170, 357-372.

Mendel FC. 1981b. The hand of two-toed sloths (*Choloepus*): its anatomy and potential uses relative to size of support. *J Morphol* 169, 1-19.

Mendel FC. 1981c. Use of hands and feet of two-toed sloths (*Choloepus hoffmanni*) during climbing and terrestrial locomotion. *J Mammal* 62, 413-421.

Mendel FC. 1985a. Adaptations for suspensory behavior in the limbs of two-toed sloths. In: Montgomery, G.G. (Ed.), The evolution and ecology of armadillos, sloths, and vermilinguas. Smithonian Institution Press, Washington, London, pp. 151-162.

Mendel FC. 1985b. Use of hands and feet of three-toed sloths (*Bradypus variegatus*) during climbing and terrestrial locomotion. *J Mammal* 66, 359-366.

Miles SS: The shoulder anatomy of the armadillo. *J Mammal* 1941, 22:157-169.

Miller RA. 1935. Functional adaptations in the forelimb of the sloths. *J Mammal* 16, 38-51.

Miller S, van der Meché FGA. 1975. Movements of the forelimbs of the cat during stepping on a treadmill. *Brain Res* 91, 255-270.

Nicolopoulos-Stournaras S, Iles JF. 1984. Hindlimb muscle activity during locomotion in the rat (*Rattus norvegicus*)(Rodentia: Muridae). *J Zool Lond* 203, 427-440.

Nielsen R. 2009. Adaptionism – 30 years after Gould and Lewontin. *Evolution* 63, 2487-2490.

Muybridge E. 1887. Animals in motion (reprint). Dover publishing incorporation, New York.

Nyakatura JA, Fischer MS. 2010. Three dimensional kinematic analysis of the pectoral girdle during upside-down locomotion of the two-toed sloth (Choloepus didactylus, Xenarthra). *Front Zool* 7, Art. No. 21.

Nyakatura JA, Fischer MS. 2010. Functional morphology and three-dimensional kinematics of the thoraco-lumbar region of the spine of the two-toed sloth. *J Exp Biol* 213, 4278-4290.

Nyakatura JA, Heymann EW. 2010. Effects of support size and orientation on symmetric gaits of free-ranging tamarins of Amzonian Peru: implications for the functional significance ofait sequence patterns. *J Hum Evol* 58, 242-251.

Nyakatura JA, Klinge A, Fischer MS, Schmidt M. 2007. Locomotion on sloped arboreal substrates: a comparison of gait parameters in cotton-top tamarins and an arboreal australodelphid marsupial. Abstract. *J Morphol* 268, 1112.

Nyakatura JA, Fischer MS, Schmidt M. 2008. Gait parameter adjustments of cotton-top tamarins (*Saguinus oedipus*, Callitrichidae) to locomotion on inclined arboreal substrates. *Am J phys Anthrop* 135, 13-26.

Nyakatura JA, Petrovitch A, Fischer MS.2010. Limb kinematics during locomotion in the two-toed sloth (*Choloepus didactylus*, Xenarthra) and its implications for the evolution of the sloth locomotor apparatus. *Zoology* 113, 221-234.

Owen R. 1842. Description of the skeletal on an extinct gigantic sloth, Mylodon robustus Owen, with observations on the osteology, natural affinities, and probable habits of the megatheroid quadrupeds in general. R and J Taylor, London. 176 pp.

Pandy MG, Kumar V, Berme N, Waldron KJ. 1988. The dynamics of quadrupedal locomotion. *J Biomech Eng* 110, 230-237.

Patel BA, Carlson KJ. 2008. Apparent density patterns in subchondral bone of the sloth and anteater forelimb. *Biol Lett* 4, 486-489.

Pauwels F, 1960. A new theory for the influence of mechanical stimuli on the differentiation of supporting tissue (in German). *Anat and Embryol* 121, 478-515.

Pennycuick CJ. 1975. On the running of the gnu (*Connochaetes taurinus*) and other animals. *J Exp Biol* 63, 775-779.

Peterson JA. 1984. The locomotion of *Chameleo* (Reptilia: Sauria) with particular reference to the forelimb. *J Zool Lond* 202, 1-42.

Poinar H, Kuch M, McDonald HG, Martin P, Pääbo S. 2003. Nuclear Gene Sequences from a Late Pleistocene Sloth Coprolite. *Curr Biol* 13, 1150-1152.

Preuschoft H, Demes B. 1984. Biomechanics of brachiation. In: The lesser Apes: Evolutionary and Behavioural Biology (Ed. H Preuschoft, DJ Chivers, WY Brockelman, N Creel). Edinburgh Unversity Press, Edinburgh, pp. 96-118.

Preuschoft H. 2002. What does "arboreal locomotion" mean exactly and what are the relationships between "climbing", environment and morphology? *Z Morph Anthrop* 83, 171-188.

Pridmore PA 1992. Trunk movements during locomotion in the marsupial *Mondelphis domestica* (Didelphidae). *J Morph* 211, 137-146.

Pridmore PA. 1994. Locomotion of *Dromiciops australis* (Marsupialia: Microbiotheriidae). *Austr J Zool* 42, 679-699.

Pujos F, DeIuliis G, Argot C, Werdelin L. 2007. A peculiar climbing Megalonychidae from the pleistocene of Peru and its implication for sloth history. *Zool J Linn Soc* 149, 179-235.

Ralphs JR, Benjamin M. 1994. The joint capsule: structure, composition, aging and disease. *J Anat* 184, 503-509.

Rasmussen S, Chan AK, Goslow GE. 1978. The cat step cycle: electromyographic patterns for hindlimb muscles during posture and unrestrained locomotion. *J Morphol* 155, 253-270.

Reilly PC, Wainwright, SM. 1994. Conclusion: Ecological morphology and the power of integration. In: Ecological Morphology (Ed. PC Wainwright, Reilly SM). The university of Chicago press, Chicago, pp. 339-354.

Reilly SM, Delancey MJ. 1997. Sprawling locomotion in the lizard Sceloporus clarkia: the effects of speed on gait, hindlimb kinematics, and axial bending during walking. *J Zool Lond* 241, 417-433.

Ritter DA, Nassar PN, Fife M, Carrier DR. 2001. Epaxial muscle function in trotting dogs. *J Exp Biol* 204, 3053-3064.

Robert C, Valette JP, Degueurce C, Denoix JM. 1999. Correlation between surface electromyography and kinematics of the hindlimb of horses at trot on a treadmill. *Cells Tissues Organs* 165, 113-122.

Robilliard JJ, Pfau T, Wilson AM. 2007. Gait characterization and classification in horses. *J Exp Biol* 210, 187-197.

Rocha-Barbosa O, Renous S, Gasc JP. 1996. Comparison of the fore and hind limb kinematics in the symmetrical and asymmetrical gait of a caviomorph rodent, the domestic guinea pig, *Cavia procellus* (Linné, 1758) (Rodentia, Caviidae). *Annl Sci nat Zool Paris 13e Série* 17, 149-165.

Rocha-Barbosa O, de Castro Loguercio MF, Renous S, Gasc JP. 2005. Limb joint kinematics and their relation to increasing speed in the

guinea pig *Cavia porcellus* (Mammalia: Rodentia). *J Zool Lond* 266, 293-305.

Rockwell H, Evans FG, Pheasant HC. 1938. The comparative morphology of the vertebrate spinal column. Its form as related to function. *J Morph* 63, 87-117.

Rollinson J, Martin RD. 1981. Comparative aspects of primate locomotion, eith special reference to arboreal cercopithecines. *Symp Zool Soc Lond* 48, 377-427.

Rubenson J, Lloyd DG, Besier TF, Heliams DB, Fournier PA. 2007. Running in ostriches (*Struthio camelus*): three-dimensional joint axes alignment and joint kinematics. *J Exp Biol* 210, 2548-2562.

Sarich VM. 1985. Xenarthran systematics: albumin immunological evidence. In: Montgomery, G.G. (Ed.), The evolution and ecology of armadillos, sloths, and vermilinguas. Smithonian Institution Press, Washington, London, pp. 77-82.

Schendel MJ, Dekutoski MB, Ogilvie JW, Olsewski JM, Wallace LJ. 1995. Kinematics of the canine intervertebral joints. An *in vivo* study before and after adjacent instrumentation. *Spine* 20, 2555-2564.

Schilling N, Fischer MS. 1999. Kinematic analysis of treadmill locomotion of tree shrews, *Tupaia glis* (Scandentia: Tupaiidae). *Z Säugetierk* 64, 129-153.

Schilling N, Carrier DR. 2009. Function of the epaxial muscles during trotting. *J Exp Biol* 212, 1053-1063.

Schilling N, Carrier DR. 2010. Function of the epaxial muscles in walking, trotting and galloping dogs: implications for the evolution of epaxial muscle function in tetrapods. *J Exp Biol* 213, 1490-1502.

Schilling N, Fischbein T, Yang EP, Carrier DR. 2009. Function of the intrinsic hindlimb muscles in trotting dogs. *J Exp Biol* 212, 1036-1052.

Schmidt M. 2005. Hind limb proportions and kinematics: are small primates different from other small mammals? *J Exp Biol* 208, 3367-3383.

Schmidt M. 2005. Quadrupedal locomotion in squirrel monkeys (Cebidae: *Saimiri sciureus*) – a cineradiographic study on limb kinematics and related substrate reaction forces. *Am J Phys Anthropol* 128, 359-370.

Schmidt M. 2008. Forelimb proportions and kinematics: are small primates different from other small mammals? *J Exp Biol* 211, 3775-3789.

Schmidt M, Fischer MS. 2000. Cineradiographic study of forelimb movements during quadrupedal walking in the Brown Lemur (*Eulemur fulvus*, Primates: Lemuridae). *Am J Phys Anthropol* 111, 245-262.

Schmidt M, Fischer MS. 2009. Morphological integration in mammalian limb proportions: dissociation between function and development. *Evolution* 63, 749-766.

Schmidt M, Krause C. in press. Scapula movements and their contribution to three-dimensional forelimb excursions in quadruped primates. In: D'Aout, K., Vereecke, E.E. (Ed.), Primate Locomotion: Linking in situ and ex situ Research. Springer press, New York, Berlin.

Schmidt M, Schilling N. 2007. Fiber type distribution in the shoulder muscles of the tree shrew, the cotton-top tamarin, and the squirrel monkey related to shoulder movements and forelimb loading. *J Hum Evol* 52, 401-419.

Schmidt M, Voges D, Fischer MS. 2002. Shoulder movements during quadrupedal locomotion in arboreal primates. *Z Morph Anthrop* 83, 235-242.

Schmitt D. 1999. Compliant walking in primates. *J Zool Soc Lond* 248, 149-160.

Schmitt D, Lemelin P. 2002. Origins of primate locomotion: gait mechanics of the woolly opossum. *Am J phys Anthrop* 118, 231-238.

Schmitt D, Larson SG, Stern JT. 1994. Serratus ventralis function in vervet monkeys (*Cercopithecus aethiops*): are primate quadrupeds unique? *J Zool Lond* 232, 215-230.

Schön Ybarra MA, Schön MA. 1987. Positional behavior and limb bone adaptations in red howling monkeys (*Alouatta seniculus*). Folia Primatol 49, 70-89.

Scholle HC, Schumann NP, Biedermann F, Stegeman, Graßme R. Roeleveld K, Schilling N, Fischer MS. 2001. Spatiotemporal surface EMG characteristics from rat triceps brachii muscle during treadmill locomotion indicate selective recruitment of functionally distinct muscle regions. *Exp Brain Res* 138, 26-36.

Seilacher A. 1970. Arbeitskonzept zur Konstruktions-Morphologie. *Lethaia* 3, 393-396.

Seyfarth A, Günther M, Blickhan R. 2001. Stable operation of an elastic three-segment leg. *Biol Cybernetics* 84, 365-382.

Shapiro LJ, Raichlen DA. 2007. A response to Cartmill et al.: primate gaits and arboreal stability. Am J phys Anthrop 133, 825-827.

Shapiro LJ, Demes B, Cooper J. 2001. Lateral bending of the lumbar spine during quadrupedalism in strepsirhines. *J. Hum. Evol*. 40, 231-259.

Slijper EJ. 1946. Comparative biologic-anatomical investigations on the vertebral column and spinal musculature of mammals. *Kan Ned Akad Wet Verh* (Tweede Sec.) 42, 1-128.

Sokal RR, Rohlf FJ. 1985. Biometry. W.H. Freeman and company, New York.

Stern JT, Wells JP, Jungers WL, Vangor AK, Fleagle JG. 1980. An electromyographic study of the pectoralis major in the Atelines and Hylobates, with special reference to the evolution of a Pars Clavicularis. *Am J Phys Anthropol* 52, 13-25.

Stevens NJ. 2003. The influence of substrate size, orientation and compliance upon prosimian arboreal quadrupedalism. Ph.D. Dissertation, Stony Brook, University.

Stevens NJ. 2006. Stability, limb coordination and substrate type: the ecorelevance of gait sequence pattern in primates. *J exp Zool* 305A, 953-963.

Stevens NJ, Schmitt DO, Cole TM, Chan LK. 2006. Technical note: out-of-plane angular correction based on a trigonometric function for use in two-dimensional kinematic studies. *Am J phys Anthropol* 129, 399-402.

Strauss WL, Wislocki GB. 1932. On certain similarities between sloths and slow lemurs. *Bull Mus Comp Zool Harvard College* 74, 45-56.

Sudhaus W. 2006. Die Notwendigkeit morphologischer Analysis zur Rekonstruktion der Stammesgeschichte. *Species Phylogeny Evolution* 1, 17-32.

Superina M, Miranda F, Plese T. 2008. Maintenance of xenarthra in captivity. In: Vizcaíno, S.F., Loughry, W.J. (Ed.), The Biology of the Xenarthra. University Press of Florida, Gainesville, pp. 232-243.

Swartz SM. 1989. Pendular mechanics and the kinematics and energetics of brachiating locomotion. *Int J Primatol* 10, 387-418.

Taylor BK. 1978. The anatomy of the forelimb in the anteater (*Tamandua*) and its functional implications. *J Morph* 157, 347-368.

Taylor BK. 1985. Functional anatomy of the forelimb in vermilinguas (anteaters). In: Montgomery, G.G. (Ed.), The evolution and ecology of armadillos, sloths, and vermilinguas. Smithonian Institution Press, Washington, London, pp. 151-162.

Thorup VM, Laursen BR. 2007. Net joint kinetics in the limbs of pigs walking on concrete floor in dry and contaminated conditions. *J Anim Sci* 86, 992-998.

Tokuriki M. 1973a. Electromyographic and joint-mechanical studies in quadrupedal locomotion. I. Walk. Jap J vet Sci 35, 433-446.

Tokuriki M. 1973b. Electromyographic and joint-mechanical studies in quadrupedal locomotion. II. Trot. Jap J vet Sci 35, 525-533.

Tokuriki M. 1974. Electromyographic and joint-mechanical studies in quadrupedal locomotion. III. Gallop. Jap J vet Sci 36, 121-132.

Tomita M. 1967. A study on the movement patterns of four limbs in walking. 1. Observation and discussion on the two types of the movement order of four limbs seen in mammals while walking. *J Anthrop Soc Nippon* 75, 120-146.

Turnquist JE, Schmitt D, Rose MD, Cant JGH. 1999. Pendular motion in the brachiation of captive Lagothrix and Ateles. *Am J Primatol* 48, 263-281.

Van de Graaff KM, Harper J, Goslow GE. 1982. Analysis of posture and gait selection during locomotion in the Striped Skunk (Mephitis mephitis). *J Mammal* 63, 582-590.

Vassal PA, Jouffroy FK, Lessertisseur J. 1962. Musculature de la main et du pied du Paresseux Ai (*Bradypus tridactylus* L.) (in French). *Folia Clinica et Biologica* 31, 142-153.

Vilensky JA. 1983. Gait characteristics of two macaques, with emphasis on relationships with speed. *Am J phys Anthrop* 61, 255-265.

Vilensky JA, Larson SG. 1989. Primate locomotion: utilization and control of symmetrical gaits. *Annu Rev Anthropol* 18, 17-35.

Vilensky JA, Moore A, Libii J. 1994. Squirrel monkey locomotion on an inclined treadmill: implications for the evolution of gaits. *J Hum Evol* 26, 375-386.

Voisin JL. 2006. Clavicle, a neglected bone: morphology and relation to arm movements and shoulder architecture in primates. *Anat Rec* 288A, 944-953.

Wallace IJ, Demes B. 2008. Symmetrical gaits of *Cebus apella*: implications for the functional significance of diagonal sequence gait in primates. *J Hum Evol* 54, 783-794.

Webb SD. 1985. The interrelationships of tree sloths and ground sloths. In: Montgomery, GG (Ed.), The evolution and ecology of armadillos,

sloths, and vermilinguas: Smithonian Institution Press, Washington, London, pp. 105-112.

Wennerstrand J, Johnston C, Roethlisberger-Holm K, Erichsen C, Eksell P, Drevemo S. 2004. Kinematic evaluation of the back in the sport horse with back pain. *Equine Vet J* 36, 707-711.

Wetzel RM. 1985. The identification and distribution of recent Xenarthra (=Edentata). In: Montgomery, G.G. (Ed.), The evolution and ecology of armadillos, sloths, and vermilinguas. Smithonian Institution Press, Washington, London, pp. 5-22.

White JL. 1993. Indicators of locomotor habits in xanarthrans: evidence for locomotor heterogeneity among fossil sloths. *J Vert Paleontol* 13, 230-242.

Whitehead PF, Larson SG. 1994. Shoulder motion during quadrupedal walking in *Cercopithecus aethiops*: integration of cineradiographic and electromyographic data. *J hum Evol* 26, 525-544.

Windle BCA, Parsons FG. 1899. On the myology of the Edentata. *Proc Zool Soc Lond* 1899, 990-1017.

Wislocki GB. 1928. Observations on the gross and microscopic anatomy of the sloths (*Bradypus griseus griseus* Gray and *Choloepus hoffmanni* Peters). *J Morphol Physiol* 46, 317-397.

Witte H, Biltzinger J, Hackert R, Schilling N, Schmidt M, Reich C, Fischer, MS. 2002. Torque patterns of the limbs of small therian mammals during locomotion on flat ground. *J Exp Biol* 205, 1339-1353.

Wood KB, Schendel MJ, Pashman RS, Butterman GR, Lewis JL, Ogilvie JW, DS Bradford. 1992. In vivo analysis of canine intervertebral and facet motion. *Spine* 17, 1180-1186.

Yamamoto, I., Panjabi, M. M., Crisco, T. and Oxland, T. (1989). Three-dimensional movements of the whole lumbar spine and lumbosacral joint. *Spine* 14, 1256-1260.

Young JW, Patel BA, Stevens NJ. 2007. Body mass distribution and gait mechanics in fat-tailed dwarf lemurs (*Chirogaleus medius*) and patas monkeys (*Erythrocebus patas*). *J Hum Evol* 53, 26-40.

APPENDIX 1

Quantification of fascicle length and pennation angle of the epaxial muscles

To quantify fascicle length and pennation angle to the sagittal plane of the epaxial musculature at the thoraco-lumbar spine we prepared a 3-D reconstruction of muscle fascicle orientation within the epaxial musculature. The method was developed by Heiko Stark to determine functional consequences of muscle architecture (Stark et al., 2008). Back muscles were stepwise dissected. The cadaver was tied immobile to the table during the whole procedure of data aquisition. After careful removal of skin and superficial connective tissue we glued small metal beads on several spinal processes as well as on other points of the body (pelvis, both knees, occiput) using two component glue (Henkel™ Central and Eastern Europe GmBH, Vienna, Austria) for calibration purposes. Calibration was undertaken before and after each session. To assess fascicle characteristics we digitized the spatial position of several points along each fascicle from end to end using a Microscribe™. The individual data points from each fascicle were transformed to line objects, smoothed with customized software (program "cloud" by H. Stark, www.stark-jena.de), and finally exported into 3-D software (Blender, www.blender.org). Fascicle characteristics were also obtained in "cloud". After measurement of a layer of fascicles the layer was carefully removed to enable access to the subjacent more profound fascicles. All fascicles, aponeuroses and tendons of the left body part of the m. iliocostalis, m. longissimus and the transversospinal system were measured from the 7th thoracic vertebra to the pelvis or sacrum, respectively. In Blender the fascicles (n = 621) were fit onto a CT reconstructed skeleton for visualization.

Results

M. iliocostalis. The average pennation angle of fascicles of the m. iliocostalis to the sagittal plane increases slightly in caudal direction at the lumbar spine, whereas the fascicles run more uniformly in cranio-lateral direction at the thorax (Fig A1). Fascicle length at the thoraco-lumbar region is comparable to a completely thoracic region (measured from vertebral level of TH15 to TH20), but a little more variable. Fascicles of the m. iliocostalis usually span three vertebral levels.

M. longissimus dorsi. The pennation angle of the few most caudal fascicles of m. longissumus dorsi is directed laterally but the average pennation angle is uniformly at about 15° in cranio-lateral direction at the thorax and more cranial lumbar spine. Fascicle length at the lumbar spine is much more variable than at the thorax, where individual fascicles almost exclusively span two vertebral levels.

Transversospinal system. Mean pennation angle to the sagittal plane increases from almost parallel to the vertebral column near the lumbo-sacral joint to similar values as the other epaxial muscles at the thorax. But, it is important to point out that the general orientation of most fascicles is cranio-medial instead of cranio-lateral. Fascicle lengths of the transversospinal system are very variable reflecting its composition of different muscles. Lengths vary from fascicles that span only one vertebral level (e.g. mm. rotatores breves) to fascicles that span the complete lumbar spine and directly attach to thoracic vertebrae (m. semispinalis, m. multifidus).

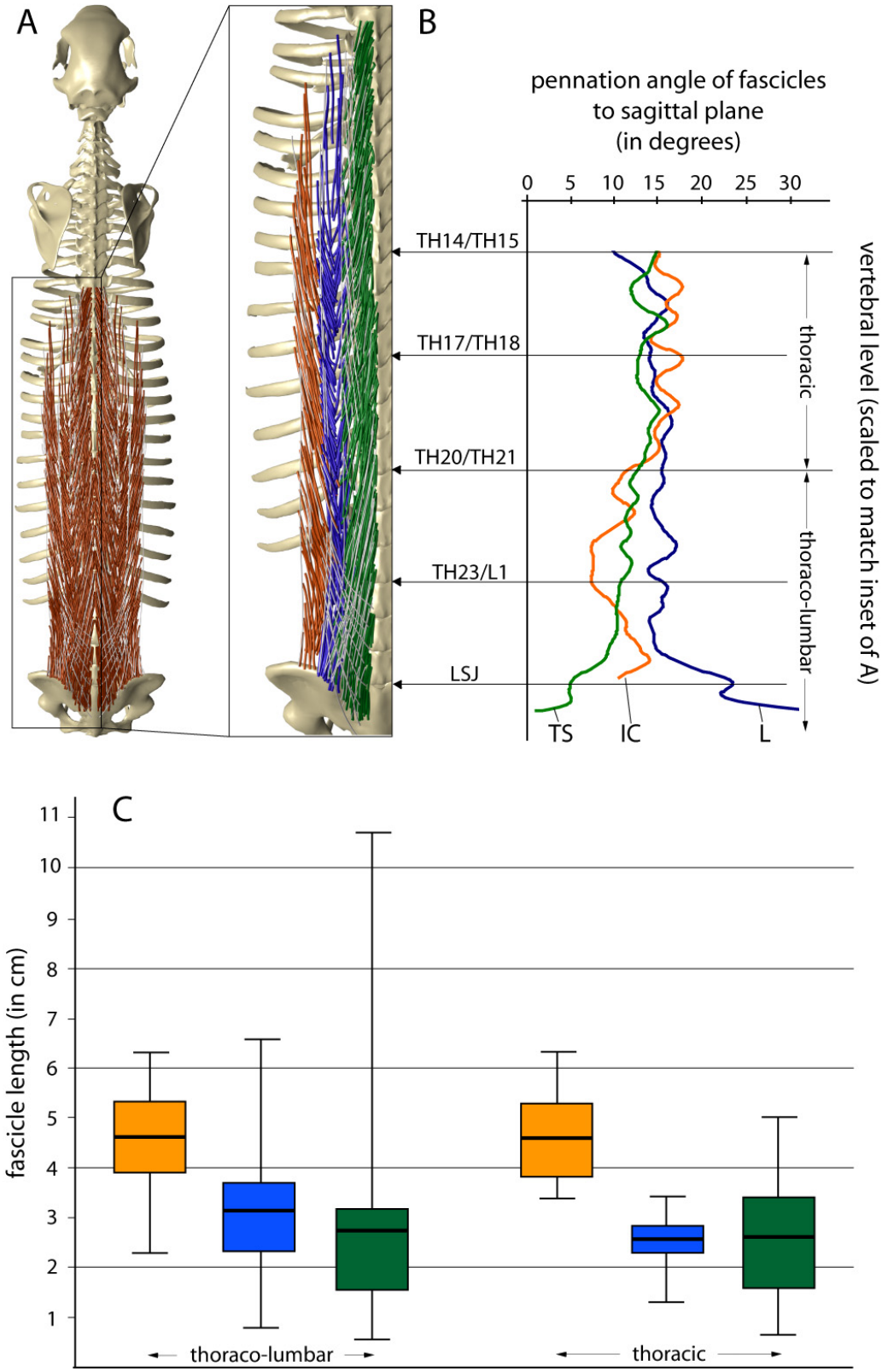

Fig. A1: Characteristics of epaxial muscles. A: dorsal aspect of a *C. didactylus* axial skeleton with reconstructed fascicles and aponeuroses mapped on. B: Pennation angles of fascicles of the m. iliocostalis (orange), m. longissimus dorsi (blue), and transversospinal system (green) from vertebral level of thoracic vertebra 15 to pelvis. Graph is scaled to match vertebral level of inset of A. C: Box-and-whisker plots of fascicle length of epaxial muscles in the thoraco-lumbar region (level TH21 to sacrum) and a thoracic region (TH15 to TH 20).

APPENDIX 2

In vitro bending to assess maximal mobility of the spine

The pelvis of a formalin fixated cadaver of *Choloepus didactylus* was fixed at a table and the cadaver was objected to saggital bending, lateral bending and torsion. At the thoraco-lumbar spine no hyperextension is possible due to the configuration of the laminae arcus vertebrae which can be compared to roofing tiles (see chapter 5).

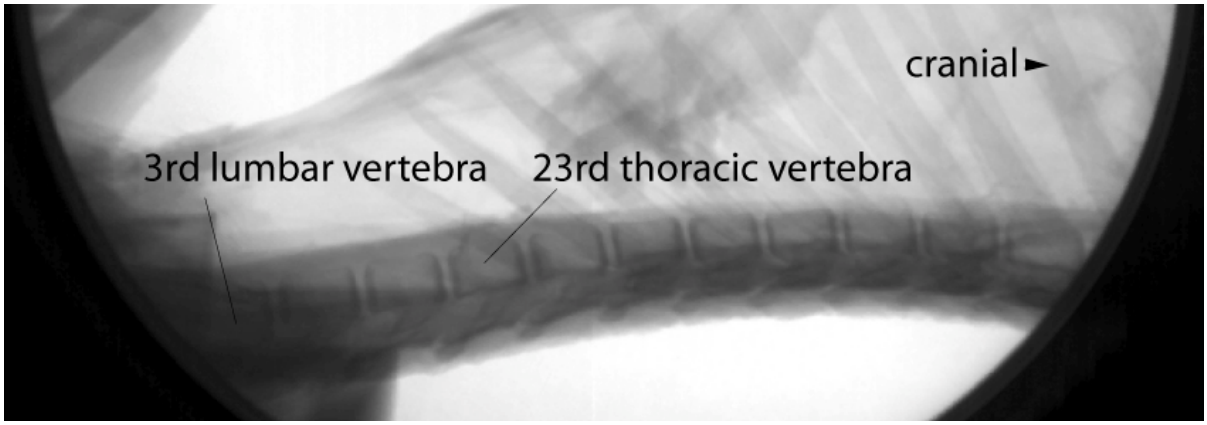

Fig. A2: X-ray image of a cadaver of C. didactylus objected to maximal possible saggital bending. No hyperextension of the thoraco-lumbar spine is possible.

APPENDIX 3

Accuracy of the 3D scene for 'scientific rotoscoping' within Maya™

General accuracy for optimal conditions was measured by comparing the known opening of a vernier caliper (150 mm) to the measured opening following the approach used in this study (Fig. A3). We determined the opening to be 150.705 mm within Maya™; i.e., a deviation of less then one millimeter.

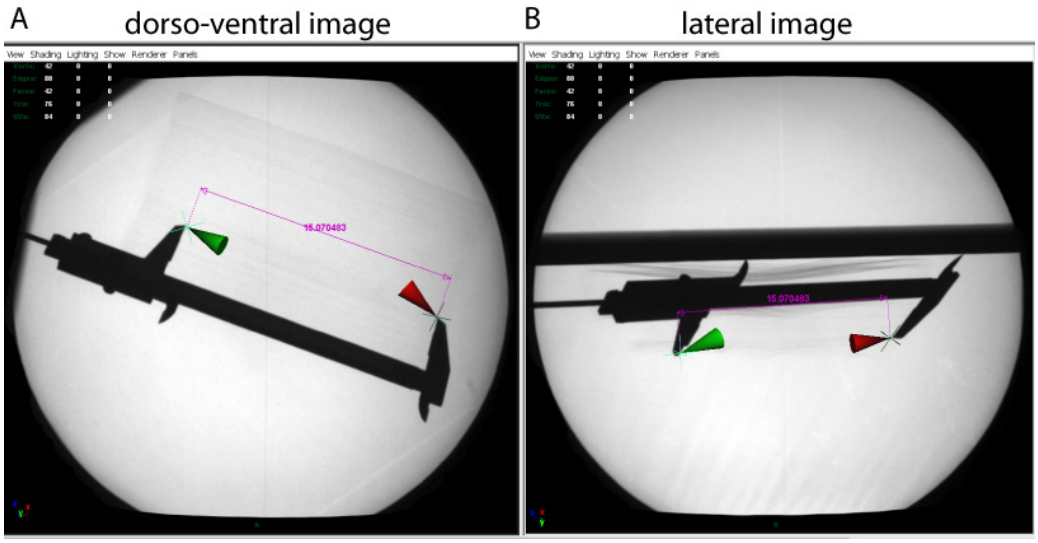

Fig. A3: Maya™ screenshot of assessment of accuracy in measurements with re-created x-ray cameras. Outside jaws of a vernier caliper were opened to exactly 150 mm. The caliper was randomly positioned within the visible field of both x-ray cameras. X-ray data was processed in the same manner as the sloth recordings of this study (i.e., un-distortion of images, calibration of 3-D space, and recreation of x-ray cameras in Maya™). Then, two cones were created and the tips of the cones were oriented in 3-D space to virtually touch the tips of the outside jaws of the caliper in both projections. The distance between the tips of the cones was finally measured using the distance measurement tool of Maya™.

APPENDIX 4

Identification of muscles at the shoulder by using the criterion of innervation

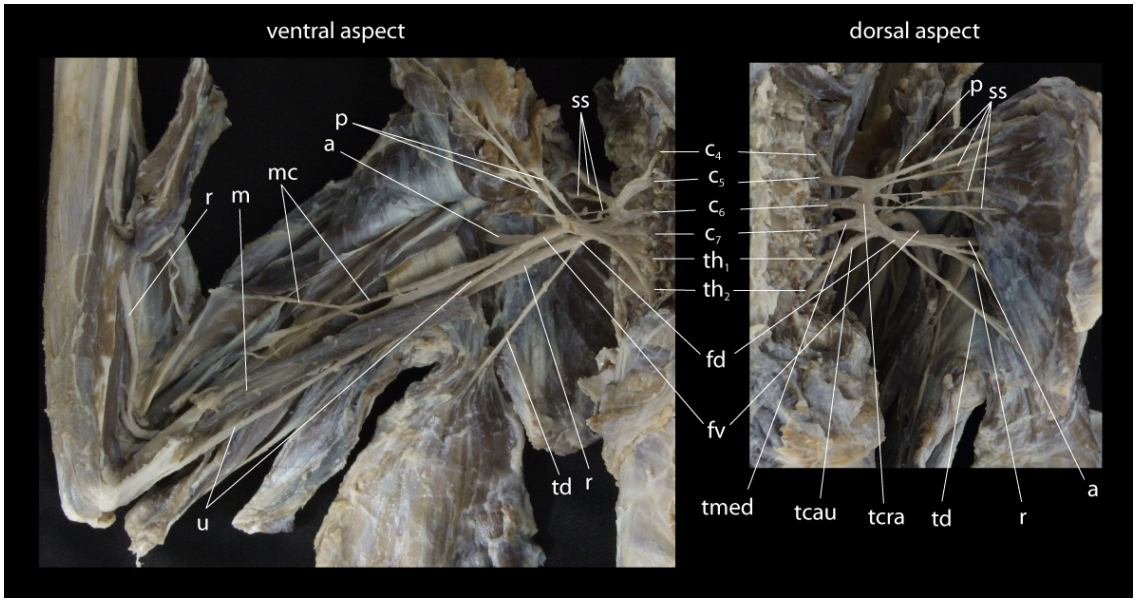

Fig. A4: Preparation of the plexus brachialis and its offbranching nerves allowed identification of the shoulder muscles by using the criterion of innervation.

c_4-th_2: spinal nerves. The 7th cervical spinal nerve exits posterior to the 6th cervical vertebra.
tcra: truncus cranialis
tmed: truncus medialis
tcau: truncus caudalis

The plexus brachialis pars infraclavicularis
fv: fasciculus ventralis. Branching off are:
- m: n. medianus. Innervating the majority of the flexors at the lower arm and hand as well as the skin of the palmar surface.
- mc: n. musculocutaneus. Innervating the flexors of the upper arm (m. biceps brachii and m. brachialis)
- u: n. ulnaris. Innervating the ulnar flexors at the lower arm and hand.

fd: Fasciculus dorsalis. Branching off are:
- a: n. axilaris. Innervating the m. deltoideus and m. teres minor.
- r: n. radialis. innervating the extensors at the upper arm (m. triceps brachii, m. dorso epitrochlearis), lower arm and hand.
- td: n. thoracodorsalis. Innervating the m. latissimus dorsi.

p: n. pectoralis. Two branches (lateral and medial) innervating the m. pectoralis.
ss: n. subscapularis. Innervating the m. subscapularis and m. teres major.

Plexus brachialis pars supraclavicularis (not shown)
Branches that innervate the mm. rhomboideus, levator scapulae, serratus anterior, supraspinatus et infraspinatus.

Eigenständigkeitserklärung

Hiermit erkläre ich, dass ich die vorliegende Arbeit selbständig und nur unter Verwendung der angegeben Hilfsmittel und Literatur verfasst habe. An der Erstellung der in der vorliegenden Arbeit verwendeten Originalarbeiten haben Co-Autoren mitgewikt. Mein Eigenanteil ist in der Arbeit ausgewiesen. Die Promotionsordnung der Biologisch-Pharmazeutischen Fakultät der Friedrich-Schiller-Universität Jena ist mir bekannt.

Ort, Datum John A. Nyakatura

Erklärung zur Bewerbung

Hiermit erkläre ich, dass ich mich mit der vorliegenden Arbeit an keiner anderen Hochschule um den akademischen Grad Dr. rer. nat. beworben habe und dass ich weder früher noch gegenwärtig die Eröffnung eines Verfahrens zum Erwerb des oben genannten Grades an einer anderen Hochschule beantragt habe.

Ort, Datum John A. Nyakatura